Remediation of aquaculture wastewater using wetland plants

by

Nicholas C. Blandford

A Thesis submitted to the Faculty of Graduate Studies of

The University of Manitoba

in partial fulfilment of the requirements of the degree of

MASTER OF SCIENCE

Department of Biosystems Engineering

University of Manitoba

Winnipeg, Manitoba, Canada

Copyright © 2024 by Nicholas C. Blandford

ABSTRACT

The aquaculture industry is among the fastest growing food production sectors globally. Land-based aquaculture operations discharge aquaculture wastewater (AWW) high in nitrogen and phosphorus, which require effective management to mitigate environmental impacts. Constructed wetlands (CWs) are treatment technologies used for the remediation of nutrient-rich wastewaters, while nitrogenous wastes like ammonia and urea in AWW are viable fertilizers for biomass production in flooded soils. This research involved a series of four studies evaluating the performance of CW systems treating AWW. Model CW systems were constructed in mesocosms (~1500 L of water) and had a gradient of nutrient loading treatments applied through repeated AWW additions. In the first study, cattail (*Typha* spp.) CWs achieved >95% total phosphorus (TP) removal from water within 33 days of treatment, although elevations of TP (>0.2 mg L^{-1}) occurred for 3–4 weeks under TP loadings of 1.02–1.64 mg m^{-2} d^{-1}. The second, third, and fourth studies utilized CWs planted with northern wild rice (*Zizania palustris* L.) and emulated established wetlands, managed natural stands, and flooded paddies, respectively. In the second study, TP concentrations increased to >0.25 mg L^{-1} under TP loadings of 4.66–9.25 mg m^{-2} d^{-1}, whereas biofilm growth dominated at 14.46 mg m^{-2} d^{-1} and resulted in the removal of TP from the water column. In the third study, low wild rice biomass resulted in fewer plant nutrient sinks, facilitating algal growth. The fourth study achieved a 70% TP reduction in CW water within the first 27 days. However, among higher TP loadings (>54.63 mg m^{-2} d^{-1}), water quality degradations occurred throughout the subsequent 42 days. Wild rice biomass in flooded paddies contributed to ~3.8 g m^{-2} of phosphorus uptake over 90 days. These findings provide insights into the operational timelines of cattail and wild rice CW systems treating AWW. The discharge of CW effluents should be coordinated with periods of low TP concentrations. Further

assessments could evaluate the effectiveness of various fertilizer regimes, explore strategies for optimizing different biomass production systems, and investigate the practical integration of agronomy systems into a circular economy model.

ACKNOWLEDGEMENTS

I would like to express my gratitude to all who have supported me throughout this degree. First of all, I would like to thank my supervisors, Dr. Vince Palace and Dr. Nazim Cicek, for cultivating an environment that provided me the freedom to learn and the ability to explore my interests. Thank you to my committee member, Dr. Richard Grosshans, for your encouraging and knowledgeable feedback. Thank you to Kenton McCorquodale-Bauer for your help with laboratory work and your valuable input throughout the research process. Thank you to Braedon Humeniuk for your help establishing field studies for this project. This project would not have been feasible without the help of two Really Awesome Teammates (RATs), Leah Dickenson and Krista Robertson. Working with RATs has made this experience all the more rewarding and I am fortunate to have worked alongside such talented and encouraging individuals.

Funding for this research was primarily provided by our funding partners, Myera Group and the IIISD – Experimental Lakes Area. Additional funding was provided by the University of Manitoba's Faculty of Graduate Studies, Faculty of Agricultural and Food Sciences, and Department of Biosystems Engineering, as well as through an NSERC Canada Graduate Scholarship – Master's.

Finally, a special thank you is owed to my family, without whom none of this would have been possible. Your belief in me has been a constant source of motivation. To our Miniature Schnauzer, Rosie: you have been by my side (quite literally) more than anyone throughout the writing process. Your snoring quickly became the soundtrack to which this thesis was drafted, and your presence has been a comfort I will always cherish.

TABLE OF CONTENTS

ABSTRACT ii
ACKNOWLEDGEMENTS iv
LIST OF TABLES ix
LIST OF FIGURES xiii
CHAPTER 1: GENERAL INTRODUCTION 1
1.0 Introduction 1
2.0 The Aquaculture Industry 2
3.0 Wild Rice 6
4.0 Constructed Wetlands for Wastewater Remediation 13
5.0 Fish-rice Agronomy Systems 15
6.0 Objectives 16
CHAPTER 2: REMOVAL OF NUTRIENTS FROM AQUACULTURE WASTEWATER USING CATTAIL (*Typha* spp.) CONSTRUCTED WETLANDS 20
Preface 20
Contribution of Authors 20
1.0 Introduction 21
2.0 Materials and Methods 22
2.1 Constructed Wetland Mesocosms 22
2.2 Collection of Aquaculture Wastewater and Experimental Design 24
2.3 Water Quality Analyses 25
2.4 Cattail Growth and Biomass Measurements 25
2.5 Calculations and Statistical Analyses 26
3.0 Results and Discussion 28
3.1 Nutrients in Aquaculture Wastewater 28
3.2 Cattail Growth and Nutrient Content 30
3.3 Water Quality Responses in Constructed Wetland Mesocosms 36
4.0 Conclusion 46
CHAPTER 3: NORTHERN WILD RICE (*Zizania palustris* L.) CONSTRUCTED WETLANDS FOR AQUACULTURE WASTEWATER REMEDIATION 48
Preface 48
Contribution of Authors 48
1.0 Introduction 49

2.0 Materials and Methods 52
2.1 Constructed Wetland Mesocosms and Field Site Details 52
2.2 Aquaculture Wastewater Collection 54
2.3 Experimental Design 55
2.4 Mesocosm Sampling and Sample Analysis 58
2.4.1 Aquaculture Wastewater Additions 58
2.4.2 Water Quality 59
2.4.3 Biofilm Tiles 62
2.4.4 Soil 64
2.4.5 Microbial 65
2.4.6 Plant Tissues and Algal Mats 66
2.4.7 Mesocosms Water Volume and Surface Area Estimations 67
2.5 Nutrient Loading Calculations 67
2.6 Constructed Wetland Performance Parameters 68
2.7 Mass Balance Analysis 71
2.8 Statistical Analysis 72
2.8.1 Water Quality 72
2.8.2 Biofilm Growth Curves 75
2.8.3 Other Endpoints 75
3.0 Results and Discussion 76
3.1 Aquaculture Wastewater Chemistry 76
3.2 Resultant Nutrient Loadings in Mesocosms 80
3.3 Response of Constructed Wetland Systems to Aquaculture Wastewater 85
3.3.1 Established Wetland Systems 86
3.3.1.1 Temperature and Light Data Loggers 86
3.3.1.2 Phosphorus in Mesocosm Water 89
3.3.1.3 Nitrogen in Mesocosm Water 93
3.3.1.4 Biofilm and Phytoplankton 97
3.3.1.5 Performance of Constructed Wetlands for Phosphorus Treatment 103
3.3.1.6 Modelling and Interaction Analysis 106
3.3.1.7 Microbial Activity 109
3.3.1.8 Soil Nutrient Content 110
3.3.1.9 Plant and Algal Biomass 112
3.3.1.10 Phosphorus Mass Balance 117

3.3.2 New Stand Systems 123
3.3.2.1 Temperature and Light Data Loggers 123
3.3.2.2 Phosphorus in Mesocosm Water 124
3.3.2.3 Nitrogen in Mesocosm Water 128
3.3.2.4 Biofilm and Phytoplankton 130
3.3.2.5 Performance of Constructed Wetlands for Phosphorus Treatment 134
3.3.2.6 Modelling and Interaction Analysis 138
3.3.2.7 Microbial Activity 141
3.3.2.8 Soil Nutrient Content 142
3.3.2.9 Plant and Algal Biomass 144
3.3.2.10 Phosphorus Mass Balance 148
3.3.3 Comparison of Constructed Wetland Systems 154
4.0 Conclusion 157
CHAPTER 4: RESPONSES OF NORTHERN WILD RICE (*Zizania palustris* L.) FLOODED PADDIES FERTILIZED WITH AQUACULTURE WASTEWATER 159
Preface 159
Contribution of Authors 159
1.0 Introduction 160
2.0 Materials and Methods 163
2.1 Constructed Paddy Mesocosms and Field Site Details 163
2.2 Aquaculture Wastewater Collection 164
2.3 Experimental Design 164
2.4 Mesocosm Sampling and Sample Analysis 166
2.4.1 Aquaculture Wastewater Additions 167
2.4.2 Water Quality 167
2.4.3 Biofilm Tiles 168
2.4.4 Soil 168
2.4.5 Microbial 168
2.4.6 Plant Tissues 168
2.4.7 Mesocosms Water Volume and Surface Area Estimations 169
2.5 Nutrient Loading Calculations 169
2.6 Flooded Paddy Performance Parameters 169
2.7 Mass Balance Analysis 170
2.8 Statistical Analysis 170
3.0 Results and Discussion 171

3.1 Aquaculture Wastewater Chemistry 171
3.2 Resultant Nutrient Loadings in Mesocosms 174
3.3 Response of Constructed Wetland Systems to Aquaculture Wastewater 178
3.3.1 Temperature and Light Data Loggers 178
3.3.2 Phosphorus in Mesocosm Water 180
3.3.3 Nitrogen in Mesocosm Water 185
3.3.4 Biofilm and Phytoplankton 190
3.3.5 Performance of Constructed Wetland for Phosphorus Treatment 196
3.3.6 Modelling and Interaction Analysis 199
3.3.7 Microbial Activity 202
3.3.8 Soil Nutrient Content 203
3.3.9 Plant and Algal Biomass 205
3.3.10 Phosphorus Mass Balance 209
4.0 Conclusion 215
CHAPTER 5: GENERAL CONCLUSIONS 216
1.0 Summary and Overview 216
2.0 Chapter 2 Summary 217
3.0 Chapter 3 Summary 217
4.0 Chapter 4 Summary 218
5.0 Comparison of Treatment Systems 220
6.0 Conclusion 222
REFERENCES 224
APPENDIX 266
Appendix Tables 266
Appendix Figures 274

LIST OF TABLES

Table 1. Mean (± SD) concentrations of total N (TN) and total P (TP) in aquaculture wastewater (AWW) added to mesocosms throughout the study. Duplicate samples were analyzed at each time point to account for potential heterogeneity in AWW solutions. The study day column indicates the day that AWW was sampled, analyzed, and applied to mesocosms. 29

Table 2. Cattail shoot N:P ratios on study days 20 and 53. Different mesocosm treatments are expressed as total phosphorus (TP) and total nitrogen (TN) loadings resulting from aquaculture wastewater additions. 36

Table 3. Performance of cattail constructed wetlands treating phosphorus in aquaculture wastewater (AWW). The maximum anticipated total phosphorus (TP) concentration in mesocosm water (C_{max}) was calculated assuming no phosphorus elimination occurred during the study. The final TP concentration in mesocosm water (C_f) represents the TP concentration measured at the end of the study (i.e. day 33). Hydraulic loading rate (HLR) was calculated for the 28-day period of AWW additions, while concentration reduction (CR) and total phosphorus load removal (PLR) were calculated for the 33-day treatment period. 44

Table 4. Study design details for the UM site mesocosms. Treatments are expressed as the nominal volume of aquaculture wastewater (AWW) applied to mesocosms on a biweekly basis. A total of 6 AWW addition events occurred over a period of 69 days. 56

Table 5. Calculation details for performance parameters of constructed wetlands (CWs) implemented in the treatment of total phosphorus (TP) in aquaculture wastewater (AWW). Initial (i) and final (f) measurements refer to study days -1 and 69, respectively. 70

Table 6. Mean (± SD) total phosphorus (TP), total ammonia nitrogen (TAN), total Kjeldahl nitrogen (TKN), density, and pH in aquaculture wastewater (AWW) added to UM site mesocosms. Samples were analyzed at room temperature (20–25°C). 77

Table 7. Nominal volumes of aquaculture wastewater (AWW) added to UM site mesocosms with the corresponding mesocosm surface area, and the resulting total phosphorus (TP), total ammonia nitrogen (TAN), and total Kjeldahl nitrogen (TKN) loadings. Additions of AWW occurred over a period of 69 days. Unique labels for reference mesocosms are included in the TP loading column. 81

Table 8. Total phosphorus (TP) loadings in UM site mesocosms with an estimate of fish quantities required to produce equivalent TP loadings. Fish waste TP production was assumed to occur at a rate of 9.55 kg t $fish^{-1}$ yr^{-1} (Hennessy et al., 1996). 85

Table 9. Calculated and measured parameters relating to the performance of EW systems removing total phosphorus (TP) from aquaculture wastewater (AWW). 105

Table 10. Summary of statistically significant results for different endpoints assessed in EW mesocosm soil during day 0 (background) and day 100 (final) samples, and the difference between background and final samples (change). Endpoints were assessed using general linear models and indicated in the table if a statistically significant result was detected. The directionality of the relationship is indicated in parentheses as either positive (+) or negative (-). 111

Table 11. Summary of results for different endpoints assessed in EW mesocosm biomass tissues at the end of the study. Endpoints were assessed using general linear models and indicated in the table if a statistically significant result was detected. The directionality of the relationship is indicated in parentheses as either positive (+) or negative (-). 117

Table 12. Calculated and measured parameters relating to the performance of NS systems removing total phosphorus (TP) from aquaculture wastewater (AWW). 137

Table 13. Pairwise contrast test results for water quality parameters with statistically significant interaction terms in fitted linear mixed models for the NS mesocosms. The difference in estimated marginal means (estimate) is reported with standard error (SE). 139

Table 14. Summary of statistically significant results for different endpoints assessed in NS mesocosm soil during day 0 (background) and day 100 (final) samples, and the difference between background and final samples (change). Endpoints were assessed using general linear models and indicated in the table if a statistically significant result was detected. The directionality of the relationship is indicated in parentheses as either positive (+) or negative (-). 144

Table 15. Summary of results for different endpoints assessed in NS biomass tissues at the end of the study. Endpoints were assessed using general linear models and indicated in the table if a statistically significant result was detected. The directionality of the relationship is indicated in parentheses as either positive (+) or negative (-). 147

Table 16. Study design details for the RL site mesocosms. Treatments are expressed as the nominal volumes of aquaculture wastewater (AWW) applied to the mesocosms on a biweekly basis. A total of 5 AWW addition events occurred over a period of 60 days. The fourth and fifth addition events involved the addition of twice the nominal AWW volume applied during the first three addition events. 165

Table 17. Mean (± SD) or range (min–max) of total phosphorus (TP), total ammonia nitrogen (TAN), total Kjeldahl nitrogen (TKN), density, and pH of aquaculture wastewater (AWW) sources added to mesocosms. The mean is reported for the first AWW collection event and the range is reported for the second, based on the corresponding sample size. Samples were analyzed at room temperature (20–25°C). 172

Table 18. Nominal volumes of aquaculture wastewater (AWW) added to mesocosms with resulting total phosphorus (TP), total ammonia nitrogen (TAN), and total Kjeldahl nitrogen (TKN) loadings. Additions of AWW occurred over a period 60 days at

the RL site. Unique labels for reference mesocosms are also included in the TP loading column. 175

Table 19. Total phosphorus (TP) loadings in RL site mesocosms with an estimate of fish quantities required to produce equivalent TP loadings. Fish waste TP production was assumed to occur at a rate of 9.55 kg t fish^{-1} yr^{-1} (Hennessy et al., 1996). 177

Table 20. Calculated and measured parameters relating to the performance of FP systems removing total phosphorus (TP) from aquaculture wastewater (AWW). 198

Table 21. Pairwise contrast test results for water quality parameters with statistically significant interaction terms in fitted linear mixed models for the FP mesocosms. The difference in estimated marginal means (estimate) is reported with standard error (SE). 200

Table 22. Summary of statistically significant results for different endpoints assessed in FP mesocosm soil during day 0 (background) and day 98 (final) samples, and the difference between background and final samples (change). Endpoints were assessed using general linear models and indicated in the table if a statistically significant result was detected. The directionality of the relationship is indicated in parentheses as either positive (+) or negative (-). 204

Table 23. Summary of results for different endpoints assessed in RL biomass tissues on day 49 and 77. Endpoints were assessed using general linear models and indicated in the table if a statistically significant result was detected. The directionality of the relationship is indicated in parentheses as either positive (+) or negative (-). 209

Table A - 1. Water quality parameters of source water used in UM site mesocosms. 266

Table A - 2. Soil quality parameters of source soil used in UM site mesocosms. Results are reported on a dry mass basis, where applicable. 267

Table A - 3. Parameters of logistic growth models fit to biofilm tile chlorophyll *a* data. P_0 = initial chl *a* concentration, K = carrying capacity, r = growth rate, df = degrees of freedom, σ = goodness of fit, t_{mid} = time where half K is reached. 267

Table A - 4. Results from fitted linear mixed models (LMMs) for water quality parameters. Instances where response variables were $\log_{10}$-transformed to meet model assumptions are indicated. 268

Table A - 5. Results from general linear models for soil quality parameters. Response variables were analyzed in units of mg kg^{-1} (on a dry mass basis) with the exception of pH (unitless), EC (mS cm^{-1}), OM (%), and CEC (mg per 100 g). Predictor variables were calculated by adding a unique constant for each mesocosm type (C) to the total phosphorus (TP) loading from aquaculture wastewater additions. Values for C were as follows: EW = 89.6, NS = 42.9, FP = 285.2 269

Table A - 6. Results from general linear models for plant tissue nutrient parameters at the UM field site. Response variables were analyzed in units of mg kg^{-1} (on a dry mass basis). 270

Table A - 7. Parameters of logistic growth models fit to biofilm tile chlorophyll *a* data for NS mesocosms. P_0 = initial chl *a* concentration, K = carrying capacity, r = growth rate, df = degrees of freedom, σ = goodness of fit, t_{mid} = time where half K is reached. 271

Table A - 8. Water quality parameters of source water used in RL site mesocosms (i.e. pond water). Concentrations of nutrients are reported as mg L^{-1} with phosphorus parameters reported as PO_4–P..... 271

Table A - 9. Soil quality parameters of source soil used in RL site mesocosms. Results are reported on a dry mass basis, where applicable. 271

Table A - 10. Water quality parameters of water used to maintain water levels in RL site mesocosms (i.e. RM of Carman water). Concentrations of nutrients are reported as mg L^{-1} with phosphorus parameters reported as PO_4–P. Results are reported as the mean (± SD) of two samples collected at the middle and end of the 2022 summer..... 272

Table A - 11. Parameters of logistic growth models fit to biofilm tile chlorophyll *a* data for FP mesocosms. P_0 = initial chl *a* concentration, K = carrying capacity, r = growth rate, df = degrees of freedom, σ = goodness of fit, t_{mid} = time where half K is reached. 272

Table A - 12. Results from general linear models for plant tissue nutrient parameters at the RL field site. Response variables were analyzed in units of mg kg^{-1} (on a dry mass basis). 273

LIST OF FIGURES

Figure 1. Historical wild rice crop production (left axis) and price (right axis) in Manitoba. Data provided by Manitoba Agriculture (personal communication, September 5, 2024). Used with permission. 12

Figure 2. Schematic of a cattail constructed wetland mesocosm complete with soil, water, and cattail plants. Dimensions indicated in the figure are approximate. 23

Figure 3. Density of cattail shoots in mesocosms. Aquaculture wastewater (AWW) additions are indicated with vertical dashed lines. Prior to the additions of AWW, a single tally of plants was recorded. After AWW additions began, then mean of three tallies is plotted with ±1 standard deviation of the mean. Different mesocosm treatments are expressed as total phosphorus (TP) loadings resulting from AWW additions. 31

Figure 4. Cattail shoot height in mesocosms. Aquaculture wastewater (AWW) additions are indicated with vertical dashed lines. The mean shoot height is plotted with ±1 standard deviation of the mean. Different mesocosm treatments are expressed as total phosphorus (TP) loadings resulting from AWW additions. 32

Figure 5. Estimates for total cattail shoot biomass (top panels) and total cattail shoot P content (bottom panels) in mesocosms on study day 20 (left-side panels) and day 53 (right-side panels). Linear models (black lines) are displayed with 95% confidence intervals (shaded regions). Different mesocosm treatments are expressed as the total phosphorus (TP) loadings resulting from aquaculture wastewater additions with a $\log_{10}(TP + 1)$ transformation. Data are reported on a dry mass basis. 34

Figure 6. Concentrations of total ammonia nitrogen (TAN), nitrite nitrogen (NO_2–N), and nitrate nitrogen (NO_3–N) in cattail constructed wetland mesocosm water. Weekly additions of aquaculture wastewater (AWW) are indicated by vertical dashed lines. Shaded panels over each graphic indicate mesocosm treatments with the numerical values representing total nitrogen (TN) loading resulting from AWW additions in units of mg m^{-2}. 38

Figure 7. Concentrations of total dissolved nitrogen in cattail constructed wetland mesocosm water. Weekly additions of aquaculture wastewater (AWW) are indicated by vertical dashed lines. Shaded panels over each graphic indicate mesocosm treatments with the numerical values representing total nitrogen (TN) loading resulting from AWW additions in units of mg m^{-2}. 39

Figure 8. Concentrations of total (TP), total dissolved (TDP), and soluble reactive phosphorus (SRP) detected in cattail constructed wetland mesocosm water. Weekly additions of aquaculture wastewater (AWW) are indicated with vertical dashed lines. Shaded panels over each graphic indicate mesocosm treatments with the numerical values representing TP loading resulting from AWW additions in units of mg m^{-2}. 40

Figure 9. Comparison between the total mass of phosphorus added to cattail constructed wetland mesocosms over a 28-day period from aquaculture wastewater (TP from AWW) and the quantity of phosphorus remaining in mesocosm water on day 33 (TP in water column). Reference A (REF-A), reference B (REF-B), and unplanted reference (UP-REF) mesocosms received no AWW throughout the study. 45

Figure 10. Schematic of a wild rice constructed wetland mesocosm with soil, water, and wild rice plants. Dimensions indicated in the figure are approximate. 54

Figure 11. Photos of different constructed wetland systems at the UM site with different forms of biomass observed throughout the study. (A): EW mesocosm; (B): NS mesocosm (C): hornwort observed in an EW mesocosms; (D): algal mats observed in a NS mesocosm. 57

Figure 12. Timeline of sampling events at the UM field site. The first addition of aquaculture wastewater (AWW) to mesocosms is used to indicate the beginning of the study (i.e. study day 0). Vertical dashed lines indicate additions of AWW. 58

Figure 13. Homemade floating containers (left) which held ceramic tiles used to quantify biofilm growth (right). 62

Figure 14. Logarithmic total phosphorus (TP) loadings from aquaculture wastewater additions evenly distributed for each mesocosm type (i.e. EW, NS). Constants used in data transformations were derived from the y-intercept of the line-of-best fit (solid blue lines). 74

Figure 15. Temperature and light intensity data from loggers placed outside of mesocosms (UM air) and in select EW mesocosms. Loggers were set to record data every 20 min. Each graphical panel presents the data from one logger with the total phosphorus loading from aquaculture wastewater indicated in units of mg m^{-2} where applicable. 87

Figure 16. Total (TP), total dissolved (TDP), and soluble reactive (SRP) phosphorus concentrations in EW mesocosm water. Each graphical panel represents a mesocosm with the TP loading from aquaculture wastewater (AWW) additions indicated in units of mg m^{-2}. Vertical dashed lines indicate AWW addition events. 89

Figure 17. Total dissolved (TDN), total ammonia (TAN), nitrite (NO_2–N), and nitrate (NO_3–N) nitrogen concentrations in EW mesocosm water. Each graphical panel represents a mesocosm with the total phosphorus loading from aquaculture wastewater (AWW) additions indicated in units of mg m^{-2}. Vertical dashed lines indicate AWW addition events. 94

Figure 18. Biofilm tile chlorophyll *a* (chl *a*) concentrations in EW mesocosms. Measured data (points) are included with fitted logistic growth curves (solid lines). Note that different y-axis scales are used across the graphical panels. Each graphical panel represents a mesocosm with the total phosphorus loading from aquaculture wastewater (AWW) additions indicated in units of mg m^{-2}. Vertical dashed lines indicate AWW addition events. 98

Figure 19. Biofilm tile ash-free dry mass (AFDM) in EW mesocosms. Replicates were pooled on day 6, while the mean (± SD) of three replicates is presented on day 63. Each graphical panel represents a mesocosm with the total phosphorus loading from aquaculture wastewater (AWW) additions indicated in units of mg m^{-2}. Vertical dashed lines indicate AWW addition events. 100

Figure 20. Chlorophyll *a* (chl *a*) concentrations in EW mesocosm water. Each graphical panel represents a mesocosm with the total phosphorus loading from aquaculture wastewater (AWW) additions indicated in units of mg m^{-2}. Vertical dashed lines indicate AWW addition events. 102

Figure 21. Comparison of total phosphorus (TP) concentrations in EW mesocosm water during initial (day -1) and final (day 69) timepoints of the performance period. General linear models (solid lines) were fit to measured data (points) with 95% confidence intervals (shaded regions). Predictor variables were calculated by adding a constant (89.6) to the TP loading from aquaculture wastewater additions. 104

Figure 22. Phosphorus load reduction (PLR) for total phosphorus (TP) in EW mesocosm water during the 70-day performance period. A general linear model (solid line) was fit to calculated data (points) with a 95% confidence interval (shaded region). Predictor variables were calculated by adding a constant (89.6) to the TP loading from aquaculture wastewater additions. 106

Figure 23. Interaction plots of estimated marginal means based on the fitted linear mixed models for total (TP), total dissolved (TDP), and particulate (PP) phosphorus of the interaction between treatment and time for the EW mesocosms. Predictor variables were calculated by adding a constant (89.6) to the TP loading from aquaculture wastewater additions. 108

Figure 24. Microbial activity as total ATP (tATP) in EW mesocosm water (left) and wild rice roots (right). General linear models (solid lines) were fit to measured data (points) with 95% confidence intervals (shaded regions). Predictor variables were calculated by adding a constant (89.6) to the total phosphorus (TP) loading from aquaculture wastewater additions. 110

Figure 25. Background (day 0), final (day 100) soil Olsen phosphorus (OP) in EW mesocosms. General linear models (solid lines) were fit to measured data (points) with 95% confidence intervals (shaded regions). Predictor variables were calculated by adding a constant (89.6) to the total phosphorus (TP) loading from aquaculture wastewater additions. 111

Figure 26. Biomass in EW mesocosms at the end of the study period reported on a dry mass basis. General linear models (solid lines) were fit to measured data (points) with 95% confidence intervals (shaded regions). Predictor variables were calculated by adding a constant (89.6) to the total phosphorus (TP) loading from aquaculture wastewater additions. 113

Figure 27. Mean length of wild rice plants in EW mesocosms at the end of the study period. A general linear model (solid line) was fit to measured data (points) with a 95% confidence interval (shaded region). Predictor variables were calculated by

adding a constant (89.6) to the total phosphorus (TP) loading from aquaculture wastewater additions. 114

Figure 28. Quantities of different types of biomass in EW mesocosms at the end of the study period reported on a dry mass basis. The total phosphorus (TP) nutrient loadings from aquaculture wastewater are indicated with numerical values or the appropriate reference label. 114

Figure 29. Total phosphorus (TP) content of different forms of biomass in EW mesocosms at the end of the study period. General linear models (solid lines) were fit to measured data (points) with 95% confidence intervals (shaded regions). TP content is reported on a dry mass basis. Predictor variables were calculated by adding a constant (89.6) to the total phosphorus (TP) loading from aquaculture wastewater additions. 116

Figure 30. Quantities of total (TP), total dissolved (TDP), and soluble reactive (SRP) phosphorus in EW mesocosm water. Each graphical panel represents a mesocosm with the TP loading from aquaculture wastewater (AWW) additions indicated in units of mg m^{-2}. Vertical dashed lines indicate AWW addition events. 118

Figure 31. Total quantities of phosphorus (P) in different matrices during initial and final timepoints in EW mesocosms. Wild rice plants are presented as either aboveground (AG; seeds and shoots) or belowground (BG; roots) plant tissues. The total P (TP) nutrient loadings from aquaculture wastewater are indicated with numerical values or the appropriate reference label. 119

Figure 32. Relative proportions of phosphorus (P) in different matrices during initial and final timepoints in EW mesocosms. Wild rice plants are presented as either aboveground (AG; seeds and shoots) or belowground (BG; roots) plant tissues. The total P (TP) nutrient loadings from aquaculture wastewater are indicated with numerical values or the appropriate reference label. 120

Figure 33. Change in quantity of phosphorus (ΔP) in different matrices between initial and final timepoints in EW mesocosms. Positive values represent increases of P with time while negative values represent decreases of P with time. Wild rice plants are presented as either aboveground (AG; seeds and shoots) or belowground (BG; roots) plant tissues. The total P (TP) nutrient loadings from aquaculture wastewater are indicated with numerical values or the appropriate reference label. 121

Figure 34. Comparison between the change in total quantity of phosphorus (ΔP) in EW mesocosms between initial and final timepoints (grey bars) and the total quantity of P added through aquaculture wastewater (AWW) additions (blue points). Positive values represent an increase of P with time while negative values represent a decrease of P with time. The total P (TP) nutrient loadings from AWW are indicated with numerical values or the appropriate reference label. 122

Figure 35. Temperature and light intensity data from loggers in select NS mesocosms. Loggers were set to record data every 20 min. Each graphical panel presents the

data from one logger with the total phosphorus loading from aquaculture wastewater indicated in units of mg m^{-2}. 123

Figure 36. Total (TP), total dissolved (TDP), and soluble reactive (SRP) phosphorus concentrations in NS mesocosm water. Each graphical panel represents a mesocosm with the TP loading from aquaculture wastewater (AWW) additions indicated in units of mg m^{-2}. Vertical dashed lines indicate AWW addition events. 125

Figure 37. Total dissolved (TDN), total ammonia (TAN), nitrite (NO_2–N), and nitrate (NO_3–N) nitrogen concentrations in NS mesocosm water. Each graphical panel represents a mesocosm with the total phosphorus loading from aquaculture wastewater (AWW) additions indicated in units of mg m^{-2}. Vertical dashed lines indicate AWW addition events. 129

Figure 38. Biofilm tile chlorophyll *a* (chl *a*) concentrations in NS mesocosms. Measured data (points) are included with fitted logistic growth curves (solid lines). Note that different y-axis scales are used across the graphical panels. Each graphical panel represents a mesocosm with the total phosphorus loading from aquaculture wastewater (AWW) additions indicated in units of mg m^{-2}. Vertical dashed lines indicate AWW addition events. 132

Figure 39. Biofilm tile ash-free dry mass (AFDM) in NS mesocosms. Replicates were pooled on day 6, while the mean (± SD) of three replicates is presented on day 63. Each graphical panel represents a mesocosm with the total phosphorus loading from aquaculture wastewater (AWW) additions indicated in units of mg m^{-2}. Vertical dashed lines indicate AWW addition events. 133

Figure 40. Chlorophyll *a* (chl *a*) concentrations in NS mesocosm water. Each graphical panel represents a mesocosm with the total phosphorus loading from aquaculture wastewater (AWW) additions indicated in units of mg m^{-2}. Vertical dashed lines indicate AWW addition events. 134

Figure 41. Comparison of total phosphorus (TP) concentrations in NS mesocosm water during initial (day -1) and final (day 69) timepoints of the performance period. General linear models (solid lines) were fit to measured data (points) with 95% confidence intervals (shaded regions). Predictor variables were calculated by adding a constant (42.9) to the TP loading from aquaculture wastewater additions. 136

Figure 42. Phosphorus load reduction (PLR) for total phosphorus (TP) in NS mesocosm water during the 70-day performance period. A general linear model (solid line) was fit to calculated data (points) with a 95% confidence interval (shaded region). Predictor variables were calculated by adding a constant (42.9) to the TP loading from aquaculture wastewater additions. 138

Figure 43. Interaction plots of estimated marginal means based on the fitted linear mixed models for total dissolved phosphorus (TDP), total dissolved nitrogen (TDN), and pH of the interaction between treatment and time for the NS mesocosms. Predictor variables were calculated by adding a constant (42.9) to the total phosphorus loading from aquaculture wastewater additions. 140

Figure 44. Microbial activity as total ATP (tATP) in NS mesocosm water (left) and wild rice roots (right). General linear models (solid lines) were fit to measured data (points) with 95% confidence intervals (shaded regions). Predictor variables were calculated by adding a constant (42.9) to the total phosphorus (TP) loading from aquaculture wastewater additions. 142

Figure 45. Background (day 0), final (day 100) soil Olsen phosphorus (OP) in NS mesocosms. General linear models (solid lines) were fit to measured data (points) with 95% confidence intervals (shaded regions). Predictor variables were calculated by adding a constant (42.9) to the total phosphorus (TP) loading from aquaculture wastewater additions. 143

Figure 46. Biomass in NS mesocosms at the end of the study period reported on a dry mass basis. General linear models (solid lines) were fit to measured data (points) with 95% confidence intervals (shaded regions). Predictor variables were calculated by adding a constant (42.9) to the total phosphorus (TP) loading from aquaculture wastewater additions. 145

Figure 47. Mean length of wild rice plants in NS mesocosms at the end of the study period. A general linear model (solid line) was fit to measured data (points) with a 95% confidence interval (shaded region). Predictor variables were calculated by adding a constant (42.9) to the total phosphorus (TP) loading from aquaculture wastewater additions. 145

Figure 48. Quantities of different types of biomass in NS mesocosms at the end of the study period reported on a dry mass basis. The total phosphorus (TP) nutrient loadings from aquaculture wastewater are indicated with numerical values or the appropriate reference label. 146

Figure 49. Total phosphorus (TP) content of different forms of biomass in NS mesocosms at the end of the study period. General linear models (solid lines) were fit to measured data (points) with 95% confidence intervals (shaded regions). Predictor variables were calculated by adding a constant (42.9) to the total phosphorus (TP) loading from aquaculture wastewater additions. 147

Figure 50. Quantities of total (TP), total dissolved (TDP), and soluble reactive (SRP) phosphorus in NS mesocosm water. Each graphical panel represents a mesocosm with the TP loading from aquaculture wastewater (AWW) additions indicated in units of mg m^{-2}. Vertical dashed lines indicate AWW addition events. 149

Figure 51. Total quantities of phosphorus (P) in different matrices during initial and final timepoints in NS mesocosms. Wild rice plants are presented as either aboveground (AG; seeds and shoots) or belowground (BG; roots) plant tissues. The total P (TP) nutrient loadings from aquaculture wastewater are indicated with numerical values or the appropriate reference label. 150

Figure 52. Relative proportions of phosphorus (P) in different matrices during initial and final timepoints in NS mesocosms. Wild rice plants are presented as either aboveground (AG; seeds and shoots) or belowground (BG; roots) plant tissues.

The total P (TP) nutrient loadings from aquaculture wastewater are indicated with numerical values or the appropriate reference label. 151

Figure 53. Change in quantity of phosphorus (ΔP) in different matrices between initial and final timepoints in NS mesocosms. Positive values represent increases of P with time while negative values represent decreases of P with time. Wild rice plants are presented as either aboveground (AG; seeds and shoots) or belowground (BG; roots) plant tissues. The total P (TP) nutrient loadings from aquaculture wastewater are indicated with numerical values or the appropriate reference label. 152

Figure 54. Comparison between the change in total quantity of phosphorus (ΔP) in NS mesocosms between initial and final timepoints (grey bars) and the total quantity of P added through aquaculture wastewater (AWW) additions (blue points). Positive values represent an increase of P with time while negative values represent a decrease of P with time. The total P (TP) nutrient loadings from AWW are indicated with numerical values or the appropriate reference label. 153

Figure 55. Timeline of sampling events at the RL field site. The first addition of aquaculture wastewater (AWW) to mesocosms is used to indicate the beginning of the study (i.e. study day 0), which is a unique date for each field site. Vertical dashed lines indicate additions of AWW. 166

Figure 56. Logarithmic total phosphorus (TP) loadings from aquaculture wastewater additions evenly distributed for flooded paddy (FP) mesocosms. The constant used in data transformations was derived from the y-intercept of the line-of-best fit (solid blue line). 170

Figure 57. Temperature and light intensity data from loggers placed outside of mesocosms (RL air) and in select FP mesocosms. Loggers were set to record data every 20 min. Each graphical panel presents the data from one logger with the total phosphorus loading from aquaculture wastewater indicated in units of mg m^{-2} where applicable. 179

Figure 58. Total (TP), total dissolved (TDP), and soluble reactive (SRP) phosphorus concentrations in FP mesocosm water. Each graphical panel represents a mesocosm with the TP loading from aquaculture wastewater (AWW) additions indicated in units of mg m^{-2}. Vertical dashed lines indicate AWW addition events. The final two AWW addition events (dark dashed lines) were made with a different AWW source and twice the nominal volume of the first three addition events (light dashed lines). 181

Figure 59. Total dissolved (TDN), total ammonia (TAN), nitrite (NO_2–N), and nitrate (NO_3–N) nitrogen concentrations in FP mesocosm water. Each graphical panel represents a mesocosm with the total phosphorus loading from aquaculture wastewater (AWW) additions indicated in units of mg m^{-2}. Vertical dashed lines indicate AWW addition events. The final two AWW addition events (dark dashed lines) were made with a different AWW source and twice the nominal volume of the first three addition events (light dashed lines). 187

Figure 60. Biofilm tile chlorophyll *a* (chl *a*) concentrations in FP mesocosms. Measured data (points) are included with fitted logistic growth curves (solid lines). Note that different y-axis scales are used across the graphical panels. Each graphical panel represents a mesocosm with the total phosphorus loading from aquaculture wastewater (AWW) additions indicated in units of mg m^{-2}. Vertical dashed lines indicate AWW addition events. The final two AWW addition events (dark dashed lines) were made with a different AWW source and twice the nominal volume of the first three addition events (light dashed lines). 192

Figure 61. Biofilm tile ash-free dry mass (AFDM) in FP mesocosms. The mean (± SD) of three replicates is presented for each sampling event. Each graphical panel represents a mesocosm with the total phosphorus loading from aquaculture wastewater (AWW) additions indicated in units of mg m^{-2}. Vertical dashed lines indicate AWW addition events. The final two AWW addition events (dark dashed lines) were made with a different AWW source and twice the nominal volume of the first three addition events (light dashed lines). 193

Figure 62. Chlorophyll *a* (chl *a*) concentrations in FP mesocosm water. Each graphical panel represents a mesocosm with the total phosphorus loading from aquaculture wastewater (AWW) additions indicated in units of mg m^{-2}. Vertical dashed lines indicate AWW addition events. The final two AWW addition events (dark dashed lines) were made with a different AWW source and twice the nominal volume of the first three addition events (light dashed lines). 195

Figure 63. Comparison of total phosphorus (TP) concentrations in FP mesocosm water during initial (day -1) and final (day 69) timepoints of the performance period. General linear models (solid lines) were fit to measured data (points) with 95% confidence intervals (shaded regions). Predictor variables were calculated by adding a constant (285.2) to the TP loading from aquaculture wastewater additions. 197

Figure 64. Phosphorus load reduction (PLR) for total phosphorus (TP) in FP mesocosm water during the 70-day performance period. A general linear model (solid line) was fit to calculated data (points) with a 95% confidence interval (shaded region). Predictor variables were calculated by adding a constant (285.2) to the TP loading from aquaculture wastewater additions. 199

Figure 65. Interaction plots of estimated marginal means based on the fitted linear mixed models for total phosphorus (TP), soluble reactive phosphorus (SRP), particulate phosphorus (PP), soluble reactive silica (SRSi), and specific conductance (SPC) of the interaction between treatment and time for the FP mesocosms. Predictor variables were calculated by adding a constant (285.2) to the TP loading from aquaculture wastewater additions. 201

Figure 66. Microbial activity as total ATP (tATP) in FP mesocosm water (left) and wild rice roots (right). General linear models (solid lines) were fit to measured data (points) with 95% confidence intervals (shaded regions). Predictor variables were calculated by adding a constant (285.2) to the total phosphorus (TP) loading from aquaculture wastewater additions. 202

Figure 67. Background (day 0), final (day 98) soil Olsen phosphorus (OP) in FP mesocosms. General linear models (solid lines) were fit to measured data (points) with 95% confidence intervals (shaded regions). Predictor variables were calculated by adding a constant (285.2) to the total phosphorus (TP) loading from aquaculture wastewater additions. 203

Figure 68. Wild rice biomass in FP mesocosms at the end of the study period reported on a dry mass basis. A general linear model (solid line) was fit to measured data (points) with a 95% confidence interval (shaded region). Predictor variables were calculated by adding a constant (285.2) to the total phosphorus (TP) loading from aquaculture wastewater additions. 205

Figure 69. Mean length of wild rice plants in FP mesocosms at the end of the study period. A general linear model (solid line) was fit to measured data (points) with a 95% confidence interval (shaded region). Predictor variables were calculated by adding a constant (285.2) to the total phosphorus (TP) loading from aquaculture wastewater additions. 206

Figure 70. Total phosphorus (TP) content of different portions of wild rice biomass in FP mesocosms study days 49 and 77. Nutrient content is reported on a dry mass basis. General linear models (solid lines) were fit to measured data (points) with 95% confidence intervals (shaded regions). Predictor variables were calculated by adding a constant (285.2) to the TP loading from aquaculture wastewater additions. Note that wild rice seeds were not evaluated for TP content on study day 49. 208

Figure 71. Quantities of total (TP), total dissolved (TDP), and soluble reactive (SRP) phosphorus in FP mesocosm water. Each graphical panel represents a mesocosm with the TP loading from aquaculture wastewater (AWW) additions indicated in units of mg m^{-2}. Vertical dashed lines indicate AWW addition events. The final two AWW addition events (dark dashed lines) were made with a different AWW source and twice the nominal volume of the first three addition events (light dashed lines). 210

Figure 72. Total quantities of phosphorus (P) in different matrices during initial and final timepoints in FP mesocosms. Wild rice plants are presented as either aboveground (AG; seeds and shoots) or belowground (BG; roots) plant tissues. The total P (TP) nutrient loadings from aquaculture wastewater are indicated with numerical values or the appropriate reference label. 212

Figure 73. Relative proportions of phosphorus (P) in different matrices between initial and final timepoints in FP mesocosms. Wild rice plants are presented as either aboveground (AG; seeds and shoots) or belowground (BG; roots) plant tissues. The total P (TP) nutrient loadings from aquaculture wastewater are indicated with numerical values or the appropriate reference label. 212

Figure 74. Change in quantity of phosphorus (ΔP) in different matrices between initial and final timepoints in FP mesocosms. Positive values represent increases of P with time while negative values represent decreases of P with time. Wild rice

plants are presented as either aboveground (AG; seeds and shoots) or belowground (BG; roots) plant tissues. The total P (TP) nutrient loadings from aquaculture wastewater are indicated with numerical values or the appropriate reference label. 213

Figure 75. Comparison between the change in total quantity of phosphorus (ΔP) in FP mesocosms between initial and final timepoints (grey bars) and the total quantity of P added through aquaculture wastewater (AWW) additions (blue points). Positive values represent an increase of P with time while negative values represent a decrease of P with time. The total P (TP) nutrient loadings from AWW are indicated with numerical values or the appropriate reference label. 214

Figure A - 1. Nutrient content, density, and pH of aquaculture wastewater (AWW) applied to mesocosms throughout the 2022 field studies. The second AWW collection was used only at the RL field site. Nutrient content analysis of AWW included total phosphorus (TP), total ammonia nitrogen (TAN), total Kjeldahl nitrogen (TKN). 274

Figure A - 2. Total phosphorus (TP) in EW mesocosm water. Graphical panels indicate total phosphorus loadings (as mg m^{-2}). Vertical dashed lines indicate aquaculture wastewater additions. 275

Figure A - 3. Total dissolved phosphorus (TDP) in EW mesocosm water. Graphical panels indicate total phosphorus loadings (as mg m^{-2}). Vertical dashed lines indicate aquaculture wastewater additions. 275

Figure A - 4. Soluble reactive phosphorus (SRP) in EW mesocosm water. Graphical panels indicate total phosphorus loadings (as mg m^{-2}). Vertical dashed lines indicate aquaculture wastewater additions. 276

Figure A - 5. Total dissolved nitrogen (TDN) in EW mesocosm water. Graphical panels indicate total phosphorus loadings (as mg m^{-2}). Vertical dashed lines indicate aquaculture wastewater additions. 276

Figure A - 6. Total ammonia nitrogen (TAN) in EW mesocosm water. Graphical panels indicate total phosphorus loadings (as mg m^{-2}). Vertical dashed lines indicate aquaculture wastewater additions. 277

Figure A - 7. Nitrite nitrogen (NO_2–N) in EW mesocosm water. Graphical panels indicate total phosphorus loadings (as mg m^{-2}). Vertical dashed lines indicate aquaculture wastewater additions. 277

Figure A - 8. Nitrate nitrogen (NO_3–N) in EW mesocosm water. Graphical panels indicate total phosphorus loadings (as mg m^{-2}). Vertical dashed lines indicate aquaculture wastewater additions. 278

Figure A - 9. Particulate phosphorus (PP) in EW mesocosm water. Graphical panels indicate total phosphorus loadings (as mg m^{-2}). Vertical dashed lines indicate aquaculture wastewater additions. 278

Figure A - 10. Soluble reactive silica (SRSi) in EW mesocosm water. Graphical panels indicate total phosphorus loadings (as mg m^{-2}). Vertical dashed lines indicate aquaculture wastewater additions. 279

Figure A - 11. Total alkalinity (Alk) in EW mesocosm water. Graphical panels indicate total phosphorus loadings (as mg m^{-2}). Vertical dashed lines indicate aquaculture wastewater additions. 279

Figure A - 12. Dissolved organic carbon (DOC) in EW mesocosm water. Graphical panels indicate total phosphorus loadings (as mg m^{-2}). Vertical dashed lines indicate aquaculture wastewater additions. 280

Figure A - 13. Temperature in EW mesocosm water. Graphical panels indicate total phosphorus loadings (as mg m^{-2}). Vertical dashed lines indicate aquaculture wastewater additions. 280

Figure A - 14. Dissolved oxygen (DO) in EW mesocosm water. Graphical panels indicate total phosphorus loadings (as mg m^{-2}). Vertical dashed lines indicate aquaculture wastewater additions. 281

Figure A - 15. pH in EW mesocosm water. Graphical panels indicate total phosphorus loadings (as mg m^{-2}). Vertical dashed lines indicate aquaculture wastewater additions. 281

Figure A - 16. Specific conductance (SPC) in EW mesocosm water. Graphical panels indicate total phosphorus loadings (as mg m^{-2}). Vertical dashed lines indicate aquaculture wastewater additions. 282

Figure A - 17. Total phosphorus (TP) in NS mesocosm water. Graphical panels indicate total phosphorus loadings (as mg m^{-2}). Vertical dashed lines indicate aquaculture wastewater additions. 282

Figure A - 18. Total dissolved phosphorus (TDP) in NS mesocosm water. Graphical panels indicate total phosphorus loadings (as mg m^{-2}). Vertical dashed lines indicate aquaculture wastewater additions. 283

Figure A - 19. Soluble reactive phosphorus (SRP) in NS mesocosm water. Graphical panels indicate total phosphorus loadings (as mg m^{-2}). Vertical dashed lines indicate aquaculture wastewater additions. 283

Figure A - 20. Total dissolved nitrogen (TDN) in NS mesocosm water. Graphical panels indicate total phosphorus loadings (as mg m^{-2}). Vertical dashed lines indicate aquaculture wastewater additions. 284

Figure A - 21. Total ammonia nitrogen (TAN) in NS mesocosm water. Graphical panels indicate total phosphorus loadings (as mg m^{-2}). Vertical dashed lines indicate aquaculture wastewater additions. 284

Figure A - 22. Nitrite nitrogen (NO_2–N) in NS mesocosm water. Graphical panels indicate total phosphorus loadings (as mg m^{-2}). Vertical dashed lines indicate aquaculture wastewater additions. 285

Figure A - 23. Nitrate nitrogen (NO_3–N) in NS mesocosm water. Graphical panels indicate total phosphorus loadings (as mg m^{-2}). Vertical dashed lines indicate aquaculture wastewater additions. 285

Figure A - 24. Particulate phosphorus (PP) in NS mesocosm water. Graphical panels indicate total phosphorus loadings (as mg m^{-2}). Vertical dashed lines indicate aquaculture wastewater additions. 286

Figure A - 25. Soluble reactive silica (SRSi) in NS mesocosm water. Graphical panels indicate total phosphorus loadings (as mg m^{-2}). Vertical dashed lines indicate aquaculture wastewater additions. 286

Figure A - 26. Total alkalinity (Alk) in NS mesocosm water. Graphical panels indicate total phosphorus loadings (as mg m^{-2}). Vertical dashed lines indicate aquaculture wastewater additions. 287

Figure A - 27. Dissolved organic carbon (DOC) in NS mesocosm water. Graphical panels indicate total phosphorus loadings (as mg m^{-2}). Vertical dashed lines indicate aquaculture wastewater additions. 287

Figure A - 28. Temperature in NS mesocosm water. Graphical panels indicate total phosphorus loadings (as mg m^{-2}). Vertical dashed lines indicate aquaculture wastewater additions. 288

Figure A - 29. Dissolved oxygen (DO) in NS mesocosm water. Graphical panels indicate total phosphorus loadings (as mg m^{-2}). Vertical dashed lines indicate aquaculture wastewater additions. 288

Figure A - 30. pH in NS mesocosm water. Graphical panels indicate total phosphorus loadings (as mg m^{-2}). Vertical dashed lines indicate aquaculture wastewater additions. 289

Figure A - 31. Specific conductance (SPC) in NS mesocosm water. Graphical panels indicate total phosphorus loadings (as mg m^{-2}). Vertical dashed lines indicate aquaculture wastewater additions. 289

Figure A - 32. Total phosphorus (TP) in FP mesocosm water. Graphical panels indicate total phosphorus loadings (as mg m^{-2}). Vertical dashed lines indicate aquaculture wastewater (AWW) additions. The final two AWW addition events (dark dashed lines) were made with a different AWW source and twice the nominal volume of the first three addition events (light dashed lines). 290

Figure A - 33. Total dissolved phosphorus (TDP) in FP mesocosm water. Graphical panels indicate total phosphorus loadings (as mg m^{-2}). Vertical dashed lines indicate aquaculture wastewater (AWW) additions. The final two AWW addition events (dark dashed lines) were made with a different AWW source and twice the nominal volume of the first three addition events (light dashed lines). 291

Figure A - 34. Soluble reactive phosphorus (SRP) in FP mesocosm water. Graphical panels indicate total phosphorus loadings (as mg m^{-2}). Vertical dashed lines indicate aquaculture wastewater (AWW) additions. The final two AWW addition

events (dark dashed lines) were made with a different AWW source and twice the nominal volume of the first three addition events (light dashed lines). 292

Figure A - 35. Total dissolved nitrogen (TDN) in FP mesocosm water. Graphical panels indicate total phosphorus loadings (as mg m^{-2}). Vertical dashed lines indicate aquaculture wastewater (AWW) additions. The final two AWW addition events (dark dashed lines) were made with a different AWW source and twice the nominal volume of the first three addition events (light dashed lines). 293

Figure A - 36. Total ammonia nitrogen (TAN) in FP mesocosm water. Graphical panels indicate total phosphorus loadings (as mg m^{-2}). Vertical dashed lines indicate aquaculture wastewater (AWW) additions. The final two AWW addition events (dark dashed lines) were made with a different AWW source and twice the nominal volume of the first three addition events (light dashed lines). 294

Figure A - 37. Nitrite nitrogen (NO_2–N) in FP mesocosm water. Graphical panels indicate total phosphorus loadings (as mg m^{-2}). Vertical dashed lines indicate aquaculture wastewater (AWW) additions. The final two AWW addition events (dark dashed lines) were made with a different AWW source and twice the nominal volume of the first three addition events (light dashed lines). 295

Figure A - 38. Nitrate nitrogen (NO_3–N) in FP mesocosm water. Graphical panels indicate total phosphorus loadings (as mg m^{-2}). Vertical dashed lines indicate aquaculture wastewater (AWW) additions. The final two AWW addition events (dark dashed lines) were made with a different AWW source and twice the nominal volume of the first three addition events (light dashed lines). 296

Figure A - 39. Particulate phosphorus (PP) in FP mesocosm water. Graphical panels indicate total phosphorus loadings (as mg m^{-2}). Vertical dashed lines indicate aquaculture wastewater (AWW) additions. The final two AWW addition events (dark dashed lines) were made with a different AWW source and twice the nominal volume of the first three addition events (light dashed lines). 297

Figure A - 40. Soluble reactive silica (SRSi) in FP mesocosm water. Graphical panels indicate total phosphorus loadings (as mg m^{-2}). Vertical dashed lines indicate aquaculture wastewater (AWW) additions. The final two AWW addition events (dark dashed lines) were made with a different AWW source and twice the nominal volume of the first three addition events (light dashed lines). 298

Figure A - 41. Total alkalinity (Alk) in FP mesocosm water. Graphical panels indicate total phosphorus loadings (as mg m^{-2}). Vertical dashed lines indicate aquaculture wastewater (AWW) additions. The final two AWW addition events (dark dashed lines) were made with a different AWW source and twice the nominal volume of the first three addition events (light dashed lines). 299

Figure A - 42. Dissolved organic carbon (DOC) in FP mesocosm water. Graphical panels indicate total phosphorus loadings (as mg m^{-2}). Vertical dashed lines indicate aquaculture wastewater (AWW) additions. The final two AWW addition events (dark dashed lines) were made with a different AWW source and twice the nominal volume of the first three addition events (light dashed lines). 300

Figure A - 43. Temperature in FP mesocosm water. Graphical panels indicate total phosphorus loadings (as mg m^{-2}). Vertical dashed lines indicate aquaculture wastewater (AWW) additions. The final two AWW addition events (dark dashed lines) were made with a different AWW source and twice the nominal volume of the first three addition events (light dashed lines). 301

Figure A - 44. Dissolved oxygen (DO) in FP mesocosm water. Graphical panels indicate total phosphorus loadings (as mg m^{-2}). Vertical dashed lines indicate aquaculture wastewater (AWW) additions. The final two AWW addition events (dark dashed lines) were made with a different AWW source and twice the nominal volume of the first three addition events (light dashed lines). 302

Figure A - 45. pH in FP mesocosm water. Graphical panels indicate total phosphorus loadings (as mg m^{-2}). Vertical dashed lines indicate aquaculture wastewater (AWW) additions. The final two AWW addition events (dark dashed lines) were made with a different AWW source and twice the nominal volume of the first three addition events (light dashed lines)..... 303

Figure A - 46. Specific conductance (SPC) in FP mesocosm water. Graphical panels indicate total phosphorus loadings (as mg m^{-2}). Vertical dashed lines indicate aquaculture wastewater (AWW) additions. The final two AWW addition events (dark dashed lines) were made with a different AWW source and twice the nominal volume of the first three addition events (light dashed lines)..... 304

CHAPTER 1: GENERAL INTRODUCTION

1.0 Introduction

In Canada, the annual production of wild rice is highly variable and undergoes substantial fluctuations in yield (Aiken et al., 1988). Several factors impact crop success, including changes in water quality, fluctuating water levels, competition from other aquatic plants, and anthropogenic activities such as damming and altering waterways (Aiken et al., 1988; Archibold, 2003; Moodie, 1991). Demand for wild rice is high, especially with the development of new wild rice products such as soups and blended rice, which have gained popularity since their introduction (Nelson & Dahl, 1986; Oelke & Boedicker, 2000). The marketing of wild rice beyond North America and into Europe, Australia, and Japan has further contributed to growing demand (Oelke & Boedicker, 2000).

While the production of wild rice in Canada occurs predominately in lakes and rivers, paddy farming, which is mainly practiced in the United States, is the primary method of wild rice cultivation globally (Hayes et al., 1989; Nelson & Dahl, 1986). The development of paddy farming in Minnesota and California has intensified wild rice production by allowing for better control over environmental conditions, leading to increased yields and more consistent grain production (Aiken et al., 1988; Oelke & Boedicker, 2000; Oelke et al., 1982). However, producing wild rice in paddies presents conflicting issues. Specifically, the application of fertilizers is required to ensure optimum yields, but, this practice leads to the discharge of excess fertilizer into the surrounding environment through runoff and discharge when paddies are drained prior to harvest (Oelke et al., 1982). Therefore, the water quality of the effluent

discharged from wild rice paddies must be considered to ensure the protection of aquatic ecosystems.

Wild rice plants have a high demand for nitrogen and only ammonia-based fertilizers are viable for use in paddy farming because of their stability in flooded soils (Oelke et al., 1997). Similarly, wild rice plants have a high requirement for phosphorus. As a result, wild rice plants can grow successfully in water high in nitrogen, phosphorus and potassium (Oelke et al., 1982). Meanwhile, aquaculture waste consists of solid wastes in the form of feces and uneaten feed, as well as dissolved wastes primarily in the form of metabolic products (Naylor et al., 1999). In fact, the main nitrogenous metabolic wastes excreted by finfish are ammonia and urea, representing 80–90% and 10–15% of dissolved nitrogen waste outputs, respectively (Bureau, 2004; Ip & Chew, 2010). Therefore, both the high concentrations of nitrogen and phosphorus in aquaculture waste and the high proportion of ammonia-based nitrogen can be used as an effective organic fertilizer for wild rice. Before exploring the potential for aquaculture to be paired with wild rice production, each sector is reviewed individually below.

2.0 The Aquaculture Industry

Aquaculture serves as a sustainable alternative to conventional capture fisheries, addressing the decline in wild fish stocks and the increasing demand for fish and fisheries products (Little et al., 2016). Consequently, the aquaculture industry is currently among the fastest growing food production sectors globally (FAO, 2024). Contrary to capture fisheries which have plateaued in production since 1990 and are not anticipated to increase further, the production of aquatic animals via aquaculture has risen in recent years, helping meet the global need for food in a

growing population (FAO, 2024; Subasinghe et al., 2009). In the past 50 years, several countries have undergone a “blue revolution”, characterized by the rapid and expansive development of their aquaculture industries (Garlock et al., 2020). Between 1990 and 2010, worldwide aquaculture production grew at an average annual rate of 7.8%, ultimately achieving the current scenario where approximately half of all fish consumed worldwide are now produced via aquaculture (FAO, 2024; Troell et al., 2014). In fact, in the year 2022, the production of farmed aquatic animals (94.4 million tonnes) exceeded the production of captured aquatic animals (91.0 million tonnes) for the first time in history (FAO, 2024). Global aquaculture production in 2022 was dominated by the production of finfish (47.1% or 61.6 million tonnes), algae (27.9% or 36.5 million tonnes), molluscs (14.4% or 18.9 million tonnes), and crustaceans (9.7% or 12.8 million tonnes) (FAO, 2024).

The aquaculture industry directly contributes to improvements in global food security through the production of a local food source, and indirectly through the socioeconomic opportunities provided by the industry, particularly employment opportunities in rural areas (Bhari, 2018; FAO, 2024). Many of the production practices implemented in modern aquaculture help achieve the United Nations’ Sustainable Development Goals (SDGs), specifically SDG 14 which aims to conserve and sustainably use marine resources (Yarkina & Logunova, 2022). Environmental sustainability is viewed as a crucial requirement for a successful aquaculture industry and significant public pressure has been applied to reduce the environmental impacts associated with the aquaculture sector (Boyd & Schmittou, 1999; Subasinghe et al., 2009). Despite these efforts, the effects of climate change reflected in changing temperatures, weather, water quality, and water supply continue to represent a potential constraint on the aquaculture industry (Subasinghe

et al., 2009). In response, intensive systems have been developed which utilize contained, controlled, recirculating designs to minimize potential impacts on aquatic ecosystems and provide greater control over environmental variables (Ahmed & Turchini, 2021).

With the adoption of novel production systems, inland aquaculture has undergone significant growth in recent decades (FAO, 2024). In 2022, inland aquaculture accounted for 62.6% of global aquaculture production with finfish representing 89.7% of the total inland aquaculture production (FAO, 2024). In China, where inland aquaculture is prolific, common production practices include pond culture, rice-fish culture, pen culture, cage culture, and culture-based fisheries (Li et al., 2018). Meanwhile in Canada, which ranks 25th in world aquaculture production, inland aquaculture production is primarily associated with land-based fish farms rearing salmonid species (Noakes, 2018). In response to growing concerns surrounding coastal environments, North America has adopted land-based aquaculture systems in an effort to mitigate the risks posed to aquatic ecosystems by conventional aquaculture practices (Bartley, 2022). Land-based aquaculture facilities provide a controlled environment for the rearing of aquatic species, allowing for continuous, year-round production (Drengstig & Bergheim, 2013; Tian & Dong, 2023). Furthermore, land-based aquaculture systems offer the ability to manage water quality, control diseases, and ensure food safety (Tian & Dong, 2023). However, land-based aquaculture facilities discharge wastewater, raising environmental concerns (Tom et al., 2021). Aquaculture wastewater (AWW) contains high quantities of nutrients, such as nitrogen and phosphorus, which can pose a threat of eutrophication in receiving environments and threaten the health of aquatic ecosystems (Ahmad et al., 2022; Troell et al., 2013). While nutrient enrichment is the primary environmental concern following the discharge of AWW (Walker et

al., 2003), compliance with sustainable production practices requires further considerations regarding the utilization of water, feed, and energy throughout the rearing process (Avnimelech et al., 2008; Y. Liu et al., 2016; Troell et al., 2013). Improving the ability to recycle water in land-based aquaculture systems and reducing the quantity of nutrients discharged in AWW can help achieve sustainable production (Tom et al., 2021).

North American governments have demonstrated support for the expansion of the aquaculture industry, leading to plans, policies, and legislation to support economic growth (Olin et al., 2012). Canada advantageously possesses an abundance of inland resources, strong regulatory frameworks, and access to markets which can further industry development (Olin et al., 2012). Achieving the desired growth of the aquaculture industry in Canada will require complementing policies and regulations which consider both economic interests and environmental sustainability. Research has demonstrated that land-based fish farms are capable of producing market size fish, further supporting the expansion of the fish farming industry into inland regions (Crouse et al., 2021; Davidson et al., 2016). Additionally, under optimal conditions, land-based aquaculture facilities have been found to be economically viable, offering lower production costs when compared to marine systems (Bennich, 2015). The diversification of North America's aquaculture industry has led to novel and innovative designs for the rearing of a variety of fresh and saltwater aquatic species in land-based systems (Cross et al., 2017). These advancements enable a greater variety of aquaculture products to be available for consumers with fewer geographic limitations on where production can occur.

3.0 Wild Rice

Wild rice (*Zizania* spp.) refers to species of annual aquatic grasses. The genus *Zizania* is comprised of four species: northern wild rice (*Z. palustris* L.), found in shallow lakes and streams in the Great Lakes and Boreal regions of North America; southern wild rice (*Z. aquatica* L.), found in marshes, swamps, rivers, streams, and lakes along the Atlantic and Gulf Coast, as well as in the St. Lawrence River and southern Great Lakes region; Texas wild rice (*Z. texana* Hitchc.), found in a small region of central Texas; and Manchurian wild rice (*Z. latifolia* (Griseb.) Turcz. ex Stapf), found in wetlands and rivers throughout East Asia (Terrell et al., 1997). Two well-supported clades exist between North American and East Asian wild rice, indicative of the genetic separation of *Z. latifolia* from the North American species (Lu et al., 2022).

When taxonomic distinctions for the genus *Zizania* were made in the seventh edition of *Gray's Manual of Botany* (1908), the names for the two distinct annual wild rice species (i.e. northern wild rice and southern wild rice) were reversed (Aiken et al., 1988; Fassett, 1924; Robinson & Fernald, 1908). This error, which was subsequently corrected in the eighth edition of *Gray's Manual of Botany* (1950), has resulted in confusion surrounding records, texts, and specimens from this time period (Aiken et al., 1988; Bean, 1950). To further complicate matters, a lack of consensus also existed as to whether northern and southern wild rice should be considered distinct species. For example, Fassett (1924) recognized *Z. aquatica* as the only species of annual wild rice, with four varieties (Fassett, 1927). Modern genetic analyses have demonstrated that northern wild rice and southern wild rice are distinct species and it is now widely accepted that four species comprise the genus *Zizania* (Xu et al., 2015). Confusion surrounding the taxonomy

of the genus *Zizania* was exacerbated by an error in an important manual and an overall lack of consensus regarding classification. These issues led to misidentification and incorrect species records in historical texts and specimens, complicating efforts to accurately determine the ecology of wild rice species and continue to present challenges when interpreting the results of earlier research (Aiken et al., 1988).

Northern wild rice is the species of North American wild rice most commonly consumed, cultivated, and harvested because of its larger grain, greater abundance and broader geographic distribution (Archibold, 2003; Porter, 2019). Across the Canadian Prairie Provinces (i.e. Alberta, Saskatchewan, and Manitoba) and Northwestern Ontario, northern wild rice grows in lakes and rivers; extensive stands of northern wild rice are also found in southern Canada, ranging as far east as Nova Scotia and as far south as northern United States (Aiken et al., 1988). Wild rice is an aquatic grass which grows in optimum water depths of 30–60 cm, and severe changes in water depth can negatively impact the success of the plant (Aiken et al., 1988). In aquatic ecosystems, wild rice plants provide habitat and food for a variety of aquatic species including fish, waterfowl, and invertebrates (Catling & Small, 2001; Hansen, 2008). Dense stands of wild rice help stabilize sediments and improve water quality through reductions in turbidity and uptake of nutrients (Drewes & Silbernagel, 2012).

Wild rice follows an annual life cycle, which begins with germination in the spring after seeds have spent several months in cold water (Oelke et al., 1982). A detailed description of wild rice plant development is provided by Oelke et al. (1982). Briefly, following germination the plant develops submerged leaves and grows upwards, towards the water's surface. Then, the plant

enters a floating leaf stage, characterized by the development of ribbon-like leaves that float on the surface of the water. These early life stages develop from May to June, are particularly vulnerable, and can be uprooted if water levels increase suddenly (Aiken et al., 1988). As the plant continues to mature, stems extend above the water surface and aerial leaves develop, and then the plant begins tillering (Marcum, 2007). Plant stems elongate and produce inflorescences in mid to late July (Oelke et al., 1982). Wild rice is monoecious, with staminate flowers located at the lower portion of the inflorescence and pistillate flowers at the top (Oelke et al., 1982). The pollen produced by staminate flowers is windborne, and plants usually cross-pollinate, although self-pollination is possible (Oelke et al., 1982). Approximately four weeks following fertilization, caryopses have developed, elongated, ripened, and are ready for harvest in late August to early September (Oelke et al., 1982).

Wild rice has been a staple food source for centuries and has significant historical, cultural, and spiritual meaning among Indigenous communities across North America (Archibold, 2003; Vennum, 1988). The Ojibwe word for wild rice, *manoomin*, is believed to translate to “good berry” or “good seed”, reflecting the importance of the plant in Ojibwe culture (Vennum, 1988). Traditional harvesting methods involve paddling canoes through wild rice stands in the fall, bending the plants over the canoe and striking them with sticks to knock ripe grains into the boat (Aiken et al., 1988). The annual wild rice harvest serves as a cultural tradition that brought communities together in cooperative camps for the labour-intensive process of gathering, processing, and preserving wild rice (Raster & Hill, 2017). The wild rice harvest not only provided vital subsistence but also reinforced cultural identity, social bonds, and provided an opportunity for education and knowledge sharing (Raster & Hill, 2017; Vennum, 1988; Walker

& Doerfler, 2009). Many Ojibwe villages were established near wild rice stands to manage the crop and ensure a reliant food supply (Jenks, 1899). As Ojibwe peoples migrated westward and northward, wild rice grains collected from previous harvests were sowed among the new regions they inhabited, either encouraging plant growth or introducing wild rice to regions where it did not exist previously (Moodie, 1991). Management strategies were implemented which involved monitoring water levels, removing competing plants, trapping animals which consume wild rice, and encouraging the presence of predators which prey upon grain-eating animals (Jenks, 1899; Moodie, 1991; Raster & Hill, 2017; Walker & Doerfler, 2009). For example, weeding was performed to remove plants that compete with wild rice for nutrients, muskrats were trapped and removed from wild rice stands, and bundles of wild rice were used to form perches which hawks could then utilize to prey upon blackbirds and other pests which could negatively impact the success of the crop (Moodie, 1991).

The propagation methods and management strategies implemented in wild rice stands facilitated and intensified the production of wild rice across a broader range, enabling both the Ojibwe and Dakota to produce wild rice in excess of their own requirements (Moodie, 1991; Vennum, 1988). Wild rice became a key part of the North American economy and was traded heavily with Europeans during the fur trade era (Taube, 1951). Maintaining the right to Indigenous food sovereignty has been affirmed in treaties within both the United States (e.g. the White Pine Treaty of 1837) and Canada (e.g. The Numbered Treaties [1871-1921]), with specific mention of retaining rights and access to wild rice stands (e.g. the White Pine Treaty, the Paypom Treaty [1873]) (Daugherty, 1986; Kinew, 1995; Luby, 2023). Despite treaty provisions, issues

surrounding Indigenous food sovereignty remain, highlighting the need for just and sustainable food systems in the modern context (Grey & Patel, 2015; Kamal et al., 2015; Matties, 2016).

The commercialization and industrialization of wild rice began within the past century, and the first attempts at domestication began in the 1950s in Minnesota using paddy systems (Archibold, 2003; Hayes et al., 1989; Kinew, 1995). Paddy-based wild rice farming involves the cultivation of the crop in constructed fields that have undergone substantial preparation prior to flooding whereas natural stand production involves managing stands of wild rice growing in natural aquatic environments, such as lakes and rivers, which are inherently more susceptible to changes in environmental conditions (Aiken et al., 1988; Oelke et al., 1997; Oelke et al., 1982). Paddy-based systems are designed to facilitate the collection of grains using a mechanical harvester such as a combine (Oelke et al., 1982). Differing beliefs surrounding the cultural and religious significance of wild rice have resulted in varying degrees of commercial activity and approaches to cultivation in certain regions (Hayes et al., 1989). For instance, Indigenous groups in the Whiteshell Provincial Park in Manitoba have historically opposed mechanical harvesting of wild rice in natural stands (Aiken et al., 1988), while others have expressed concerns surrounding the paddy production of wild rice (Raster & Hill, 2017).

Developments into nonshattering cultivars of wild rice allow for better retention of the grain on the panicle even when ripe, reducing grain losses and allowing for crops to be more easily harvested via combine in paddy systems, which ultimately results in increased yields (Archibold, 2003). Natural stands of wild rice yield an average of 0.02–0.14 t ha^{-1} and are largely dependent on the growing conditions of a given year whereas the paddy-farmed rice in Minnesota and

California provide much more consistent yields of 0.53 and 1.4 t ha^{-1}, respectively (Hayes et al., 1989). By 1985, the total world production of wild rice was 15,200 t and paddy production accounted for >95% of this figure (Hayes et al., 1989; Nelson & Dahl, 1986). Meanwhile, the natural stands in Saskatchewan, Manitoba, and Ontario accounted for 143, 283, and 16 t of wild rice production, respectively (Hayes et al., 1989; Nelson & Dahl, 1986). While Statistics Canada currently collects industry statistics relating to grain farming, the data related to wild rice farming is grouped with and collected alongside other grain farming (e.g. barley, buckwheat, oat) and therefore individual production quantities for wild rice cannot be determined in the federally-collected database (Statistics Canada, personal communication, March 8, 2024). The production of wild rice in natural stands in Canada is subject to extreme year-to-year variation in yield (Aiken et al., 1988). Historical provincial data in Manitoba indicates that the production of wild rice ranged from 20,412 to 1,088,600 kg between 1970 and 2011, with a relatively stable price for the grain within this time period (Figure 1).

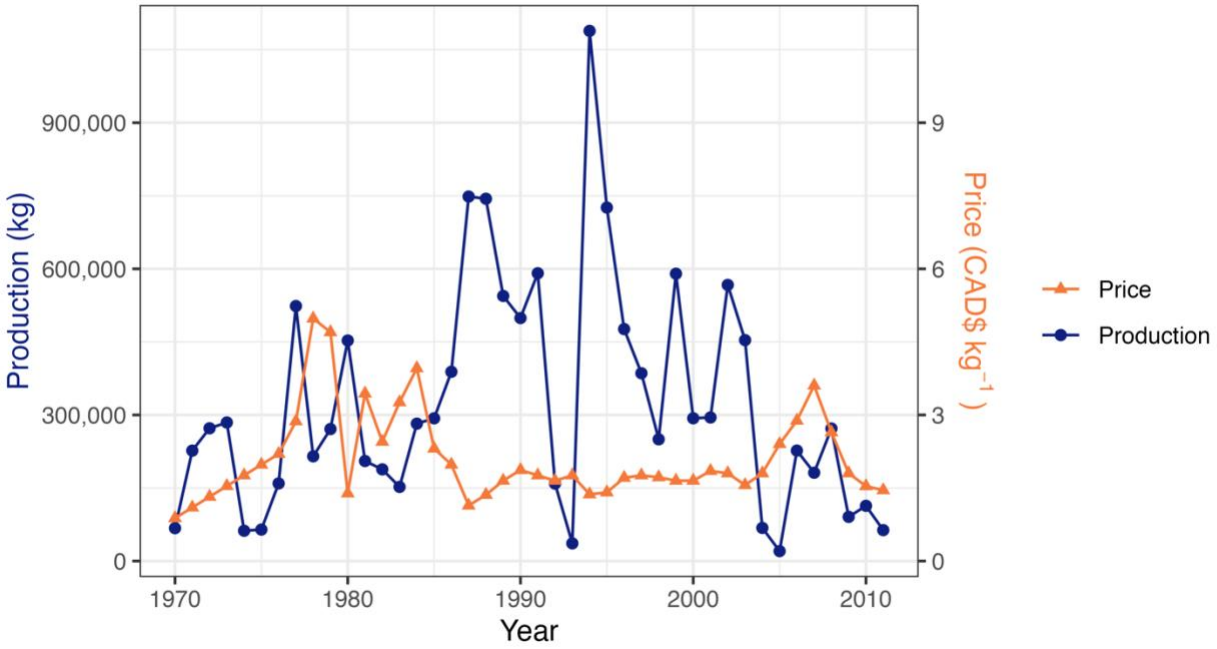

Figure 1. Historical wild rice crop production (left axis) and price (right axis) in Manitoba. Data provided by Manitoba Agriculture (personal communication, September 5, 2024). Used with permission.

The grain produced by wild rice plants is of high nutritional quality, and contains minerals, vitamins, protein, and dietary fibre (Surendiran et al., 2014). Wild rice is also a whole grain that contains high quantities of antioxidants (Qiu et al., 2009), and a diet comprised of wild rice can help reduce oxidative stress, inflammation, hyperlipidemia, and cardiovascular disease (Surendiran et al., 2013; Zhang & Zhai, 2016). Alongside these nutritional benefits, wild rice possesses a unique nutty flavour and texture, ultimately generating consumer interest and market demand for wild rice products (Catling & Small, 2001; Hauser, 2014; Johnson & Percich, 1992; Winchell & Dahl, 1984). Wild rice had been adopted into gourmet cuisines and is often sold and marketed in blended products where wild rice is mixed with other grains such as white and brown rice (Hauser, 2014; Winchell & Dahl, 1984). An opportunity exists for commercial expansion of the Canadian wild rice industry, which can enhance agricultural crop diversity in

the country, improve food security, and provide a variety of socioeconomic benefits (Ahmed et al., 2021; Porter, 2019). As consumer demand for high-quality, healthy, and functional food products continues to rise (Baker et al., 2022), food systems undergo transformations to supply sustainably produced, nutritious foods within culturally-accepted diets (Brouwer et al., 2021). Increasing wild rice production can help meet demand in local and global food markets and establish the crop among these emerging agricultural ideals.

4.0 Constructed Wetlands for Wastewater Remediation

Wetlands are ecosystems which are either entirely covered or saturated with water and are valuable assets which contribute several ecological functions such as flood control, nutrient cycling, water purification, erosion control, and habitat provision (Barbier, 2011). Constructed wetlands (CWs) are engineered systems which aim to mimic the natural remediation capabilities of wetlands and have been implemented in the treatment of municipal, industrial, and agricultural wastewaters (Hammer, 1989; Sundaravadivel & Vigneswaran, 2001). While wild rice can either be grown in natural stands or flooded paddies, both approaches involve managing a system where water, plants, and soil or sediment interact. These methods are similar to those implemented in CWs which utilize the natural processes and abilities of a wetland ecosystem for beneficial water management. The implementation of wild rice in CWs can emulate the conditions in which the crop is normally produced while providing the additional benefits offered by CWs for remediation.

Two primary types of CW systems exist: free water surface (FWS) where water flows over the CW substrate through wetland vegetation and is exposed to the atmosphere, and subsurface flow

(SSF) where water flows through the CW substrate beneath the surface in contact with plant roots and associated microbial communities (Norton, 2007; Vymazal, 2010). A variety of processes contribute to the removal of contaminants in CWs; physical processes include filtration and settling of particles, biological processes include direct plant uptake of nutrients as well as nutrient cycling performed by microbial communities associated with rhizomes and CW substrates (e.g. soil), and chemical processes include sorption, photodegradation, and volatilization (DeBusk, 1999; Norton, 2007).

Uptake of nutrients by CW plants often serves only as temporary storage for nutrients because plants will release nutrients during decay (Kadlec & Wallace, 2008). However, harvesting plant biomass can be an effective means to remove nutrients from the CW system and reduce the risk of eutrophication among downstream environments that receive CW effluents (Grosshans et al., 2011; Kamilya et al., 2022). In CWs receiving lighter loads of nutrients, plant uptake can represent the major mechanism of nutrient removal, accounting for more than half of the removed nitrogen and phosphorus (Vymazal, 2020).

The type of macrophytes implemented in CWs will impact the treatment process and therefore plant selection is a crucial component of CW design (Gorgoglione & Torretta, 2018; Vymazal, 2013). In North America, cattail (*Typha* spp.) plants are the most commonly used vegetation in CW systems (Rozema, VanderZaag, et al., 2016). Cattail plants have extensive root systems which improve treatment through direct uptake of nutrients and by providing surface area for microbial communities which play crucial roles in the removal of pollutants (Gorgoglione & Torretta, 2018). Although many FWS CWs contain multiple plant species, when cattail are

present they will often out-compete other plants (Gorgoglione & Torretta, 2018). Wild rice plants are not among the most commonly used plant species in CWs, but have been implemented with success in the past (Brix, 2003; Gorgoglione & Torretta, 2018). Wild rice has a significant nutrient demand and therefore uptakes nutrients from water and soil (Sims et al., 2012). Additionally, northern wild rice is an annual plant, allowing for CW vegetation to be removed from the system each year, avoiding a release of nutrients which would occur following decay of plant matter.

5.0 Fish-rice Agronomy Systems

The concept of integrating fish farming within wild rice ecosystems is described by Ahmed et al. (2021) and involves utilizing available wild rice habitat for the rearing of fish, with netting or fencing to contain fish during the rearing process. This concept of farming follows the traditional model of fish culture in rice fields in Asia, where fish production occurs within, or in connection to rice agronomy systems (Hambrey et al., 2008; Ottinger et al., 2016). Wild rice wetlands in North America serve as habitat for species such as fathead minnow (*Pimephales promelas*), lake whitefish (*Coregonus clupeaformis*), northern pike (*Esox lucius*), walleye (*Sander vitreus*), white sucker (*Catostomus commersonii*), and yellow perch (*Perca flavescens*) (Ahmed et al., 2021). Ahmed et al. (2021) suggest the fish species implemented in the wild rice-fish farming system be native, naturally occurring, hardy, and desired for human consumption.

Meanwhile, other circular economy concepts have been proposed which utilize CWs for the reclamation of wastewater from fish farming operations (Rousseau et al., 2008; Staudenmann & Junge-Berberovic, 2003). This approach couples AWW treatment and wastewater reclamation

with the production of biomass, such as plants or algae, which can be harvested for human consumption or for use in other products. Nutrient recycling from AWW has been used in the production of vegetables and fruits (Enduta et al., 2011; Graber & Junge, 2009), microalgae (Guo et al., 2013; Viegas et al., 2021), and other various forms of plant biomass (Blandford et al., 2024; Lin et al., 2002; Paolacci et al., 2022). While harvested food products can be directly consumed by humans, other forms of cultivated biomass can be used as animal feed in other production systems (Sherwood, 2020). The integration of food production systems with wastewater treatment contributes to sustainable agriculture practices where waste reductions are achieved, environmental resources are conserved, beneficial water management practices can be implemented, and circular economy concepts can be realized. For instance, the circular economy loop can be completed through the utilization of AWW produced during fish farming for the production of microalgae which can in turn be used as aquafeed (Ansari et al., 2021; Nagarajan et al., 2021). In wild rice agronomy systems paired with fish farming operations, wastewater generated during the rearing of fish can be applied to the wild rice CW systems. The AWW functions as a fertilizer, increasing production of wild rice and algae within the CW. While wild rice can be harvested as an output, algae can be recycled as feed in the aquaculture system, achieving a circular economy.

6.0 Objectives

Aquaculture is among the fastest growing food production sectors in the world and the adoption of land-based aquaculture systems which discharge wastewater high in nutrients is of environmental concern. Meanwhile, modern agriculture practices aim to develop and implement sustainable methods of livestock and crop production which can reduce wastes, introduce new

economic opportunities, and ultimately improve the footprint of the agronomy system. The primary objective of this thesis is to understand how CWs can be implemented in the remediation of AWW. Through the use of model CWs constructed in mesocosms, the performance and operation timeline of CWs treating AWW was assessed through nutrient evaluation in CW water, soil, and plant tissues.

The overall objectives of this thesis were to:

1. Assess the performance of cattail CWs treating AWW (Chapter 2)
2. Assess the performance of wild rice CWs treating AWW (Chapter 3)
3. Assess the performance of wild rice flooded paddies treating AWW (Chapter 4)
4. Assess the potential for AWW to be utilized as a fertilizer for biomass production (Chapters 2, 3, and 4)
5. Determine the potential for AWW to be used within a circular economy system which involves biomass production (Chapters 2, 3, and 4)

The main objectives of Chapter 2 were to determine how AWW additions impacted water quality in cattail CWs. The growth of plants was monitored and plant tissue samples were collected as a potential nutrient sink, however the primary focus was monitoring temporal variations in water quality among cattail CWs amended with a gradient of nutrient loading conditions. The hypothesis that nitrogen and phosphorus can be eliminated from CW water was tested and nutrient removal performance was predicted to be related to nutrient inputs (i.e. nutrient loading conditions). The remediation capacity of cattail CWs was assessed in relation to the observed changes in water quality.

In Chapter 3, two studies were conducted using wild rice. The objective of the first study was to determine the performance of wild rice wetlands treating AWW. The objective of the second study was to determine the performance of newly established wild rice stands treating AWW. Mesocosms were constructed and seeded with a natural variety of wild rice. Management practices emulated those commonly used in managed natural stands of wild rice. The effects of AWW loadings upon water quality, soil quality, and biomass production were evaluated in relation to nutrient loading treatments. For both studies, the hypothesis that nutrients in AWW can be treated by wild rice CW systems was tested and predicted to be related to nutrient loading. Among high nutrient loadings, a deterioration in water quality was predicted to occur that would negatively impact CW performance. Established wetland systems were predicted to contain greater abundances of algae and therefore be more susceptible to water quality deteriorations than the newly established wild rice stands.

In Chapter 4, a study was conducted to determine the performance of wild rice flooded paddy systems treating AWW. Management practices emulated those commonly used in commercial flooded paddies of wild rice. The effects of AWW loadings upon water quality, soil quality, and biomass production were evaluated and related to nutrient loading. The hypothesis that nutrients in AWW can be a beneficial fertilizer for flooded wild rice paddies without causing deteriorations in water quality was tested and predicted to be feasible among the mid to low end of the evaluated nutrient loadings. Under greater nutrient loading conditions, water quality was predicted to deteriorate in response to rapid growth of algae. Among lower nutrient loadings, direct uptake of nutrients by plants was predicted to be a major contributor to nutrient removal

while other mechanisms such as sorption to soil and uptake by other forms of biomass (e.g. algae) were predicted to be minor.

CHAPTER 2: REMOVAL OF NUTRIENTS FROM AQUACULTURE WASTEWATER USING CATTAIL (*Typha* spp.) CONSTRUCTED WETLANDS

Preface

A version of this study has been published in the Journal of Environmental Quality (Blandford et al., 2024). Wiley permits the authors of published articles to include the published work as part of a thesis or dissertation. The original article can be found here:

Blandford, N. C., McCorquodale-Bauer, K., Grosshans, R., Hardy, B., Cicek, N., & Palace, V. (2024). Removal of nutrients from aquaculture wastewater using cattail (*Typha* spp.) constructed wetlands. *Journal of Environmental Quality 53*(5), 767-775. https://doi.org/10.1002/jeq2.20608.

A modified version of the published manuscript is presented here including additional details surrounding methodology, as well as an expanded presentation and discussion of results.

Contribution of Authors

The author contributor roles taxonomy (CRediT) statement for the published manuscript is as follows:

Nicholas C. Blandford (University of Manitoba): Conceptualization; formal analysis; funding acquisition; investigation; methodology; project administration; visualization; writing–original draft. **Kenton McCorquodale-Bauer** (University of Manitoba): Conceptualization; investigation; methodology; writing–review and editing. **Richard Grosshans** (International

Institute for Sustainable Development): Conceptualization; investigation; methodology; resources. **Bruce Hardy** (Myera Group): Conceptualization; funding acquisition; resources. **Nazim Cicek** (University of Manitoba): Conceptualization; funding acquisition; methodology; resources; supervision; writing–review and editing. **Vince Palace** (International Institute for Sustainable Development – Experimental Lakes Area): Conceptualization; funding acquisition; methodology; project administration; resources; supervision; writing–review and editing.

1.0 Introduction

In response to concerns surrounding the sustainability of wild fisheries, aquaculture has emerged as an alternative method for fish production and is now a significant contributor to global food production (FAO, 2020; Garlock et al., 2020). In particular, inland aquaculture operations have experienced substantial growth in the past two decades and accounted for over 60% of the world's total farmed fish in 2018 (FAO, 2020; Naylor et al., 2021). However, land-based aquaculture facilities discharge nutrient-rich wastewaters which have the potential to create eutrophic conditions in receiving waters, threatening the health of aquatic ecosystems (Dodds & Smith, 2016; Nora'aini et al., 2005). Constructed wetlands (CWs) are a cost-effective, low-energy wastewater treatment technology used to reduce nutrient content in various types of wastewater, including aquaculture wastewater (AWW) (Lin et al., 2002; Vymazal, 2010). These systems are particularly beneficial in remote locations where there is limited access to conventional wastewater treatment methods (Wu et al., 2015). Cattail (*Typha* spp.) are abundant and broadly distributed aquatic macrophytes that have been implemented in CWs to treat wastewater (Ciria et al., 2005). In cattail wetlands, the production of biomass is directly related to the uptake of nutrients such as N and P (Dubbe et al., 1988). Therefore, biomass harvesting of

cattail can be an effective approach to remove nutrients from a system, helping reduce the risk of eutrophication in polluted environments (Grosshans et al., 2011). Previous research has identified seasonal variations of P uptake in cattail wetlands (Ciria et al., 2005; Dubbe et al., 1988). However, the intricacies of P dynamics within CW systems treating AWW, their impacts on the trophic status of the CW, and the concerns regarding the nutrient content of discharged CW effluents remain unresolved. It is the aim of the present study to provide an analysis of CW nutrient removal for AWW to evaluate the potential use of CWs for the direct treatment of land-based AWW effluents. Further, the present study aims to determine how cattail CWs perform in the late summer and early fall in northern climates when overall plant growth has begun to decline. In this manner, the feasibility of employing cattail CWs for AWW treatment for a prolonged duration can be determined with the potential to enhance overall treatment capacity. The performance of CW systems for the removal of N and P was assessed across a gradient of nutrient loading conditions achieved through the weekly addition of AWW for 5 weeks. The optimum conditions (i.e. AWW loading rates) for effective nutrient treatment under northern growing conditions were then considered in response to CW performance and corresponding water quality alterations.

2.0 Materials and Methods

2.1 Constructed Wetland Mesocosms

Seven cattail CWs were established in mesocosms (Figure 2; 2.56 m diameter, 0.57 m height) at the Prairie Wetland Research Facility at the University of Manitoba, Winnipeg, MB, Canada (49° 48’ 35.9” N, 97° 07’ 33.0 W”). Mesocosms consisted of circular low-density polyethylene stock tanks (ACE Rotomolds; Hospers, IA, USA) and were amended with 20 cm of organic

topsoil and 30 cm of water (City of Winnipeg; ~1,500 L). The water and soil sources used in mesocosms were analyzed for nutrient content (see Appendix; Table A - 1, Table A - 2). Mesocosms were closed systems from which water was replenished or removed when warranted, allowing for a controlled input and output of nutrients. In June 2021, each CW was planted with 15 individual cattail plants 1.0–1.5 m in length collected from Oak Hammock Marsh (Stonewall, MB, Canada). An additional 8th mesocosm was constructed to serve as an unplanted reference (UP-REF). The UP-REF mesocosm had no plants or AWW added, measured 1.75 m in diameter and 0.4 m in height, and was established with 10 cm of soil and 15 cm of water.

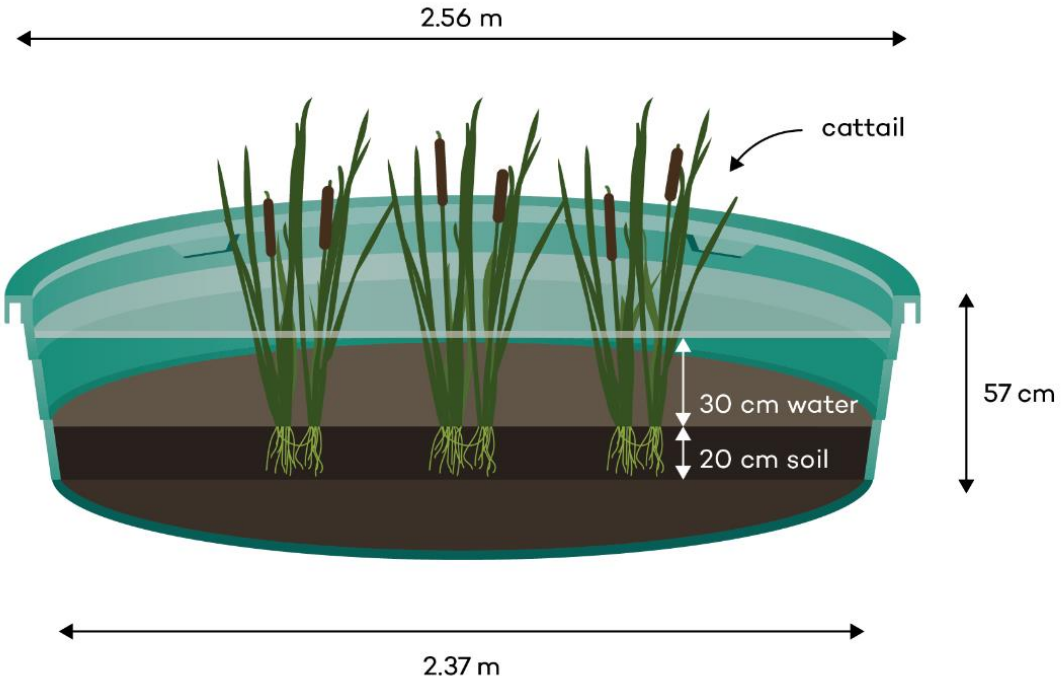

Figure 2. Schematic of a cattail constructed wetland mesocosm complete with soil, water, and cattail plants. Dimensions indicated in the figure are approximate.

Once established, CWs were allowed to acclimate and proliferate for a period of 40 days prior to beginning AWW additions. Water levels were maintained in mesocosms by adding water as

needed throughout the duration of the study. Mesocosm water volumes were approximated using the geometric formula for a truncated cone. The mean of 20 depth measurements collected across the area of the mesocosm was used to determine an initial water depth and establish a reference depth location from which subsequent measures were taken at least once per week. The surface area of each mesocosm was calculated by measuring the diameter of the soil surface of each mesocosm.

2.2 Collection of Aquaculture Wastewater and Experimental Design

All AWW was collected from 600-gallon (~2,270 L) circular tanks used for lake trout (*Salvelinus namaycush*) rearing at the University of Manitoba's Biological Sciences Animal Holding facility. Collection of AWW occurred twice per week in the mornings, ~24 h after fish were fed. To facilitate the transport of AWW into the field, a slurry of solids and liquid totaling 60 L in volume was collected each week. Five CWs were randomly selected to receive AWW, while two were randomly selected to receive no AWW (i.e. reference treatment; REF-A and REF-B). The 60 L of collected AWW was distributed across these five CWs following a regression design in which the nominal treatment volume (i.e. weekly AWW volume) followed an exponential trend; weekly AWW additions of 1.0, 2.0, 4.5, 7.5, or 15.0 L were applied to CWs for a total of 5 weeks, achieving total nominal AWW addition volumes of 5.0, 10.0, 22.5, 37.5, and 75.0 L. The beginning of AWW additions on August 5th, 2021, was used to indicate the start of the study (i.e. study day 0). Subsequent additions of AWW occurred on study days 8, 14, 21, and 28. Using the mean concentration of total N (TN) and total P (TP) in AWW (see Section 3.1; Table 1), the total nutrient loadings achieved in CWs over 28 days were 13.7, 34.5, 76.9, 130.5, 209.2 and 3.01, 7.59, 16.90, 28.67, and 45.97 mg m^{-2}, for TN and TP, respectively.

2.3 Water Quality Analyses

Water samples were collected from mesocosms on study days -2, 7, 12, 20, 26, and 33; each week, water samples were collected 1–2 days prior to AWW additions. Grab samples were collected 10 cm below the water surface using 500 mL Nalgene bottles, stored in a dark cooler, and processed in the laboratory within 2 h of collection. Total nutrients were assessed in an unfiltered aliquot, while dissolved nutrients were analyzed after filtration through a 0.45 µm nylon syringe filter (Mandel Scientific; Guelph, ON, Canada). Total phosphorus (TP), total dissolved phosphorus (TDP), soluble reactive phosphorus (SRP), and total dissolved nitrogen (TDN) were measured spectrophotometrically with HACH kits (HACH; Loveland, CO, USA). Filtered water samples were stored at 4ºC for <48 h prior to analysis for total ammonia nitrogen (TAN), nitrite-nitrogen (NO_2–N), and nitrate-nitrogen (NO_3–N) on study days -2, 7, 12, and 20 using a flow injection analyzer (Lachat QuickChem 8500, HACH) following standard methods (Rice et al., 2012).

2.4 Cattail Growth and Biomass Measurements

Cattail shoots were manually counted a total of seven times between study days -40 and 33. Prior to day 0, a single tally of shoots was recorded. After day 0, CWs had proliferated extensively and therefore the mean of three tallies was taken. A plateau in stem density was observed after day 0 (see Section 3.2; Figure 3), and therefore the stem density estimates required for biomass calculations made on day 53 were assumed to be equal to the stem densities recorded on day 33. Mean shoot height was recorded a total of six times throughout the study as the mean of 10 shoots evenly distributed across the surface area of the mesocosm.

Plant tissue samples were collected on study days 20 and 53 by cutting cattail shoots at the soil-water interface. A single sample consisted of three aboveground shoots harvested in close proximity. A total of three samples were collected from each CW during each sampling event. Minimal flowering was observed across all CWs and therefore flowering stalks were excluded from biomass samples. Samples were dried at 25 ºC for 3 weeks in drying room and submitted to a commercial laboratory (Farmers Edge Laboratories; Winnipeg, MB, Canada) for nutrient content analysis. Dried samples were ground, digested with acid in a microwave system, and analyzed by inductively couple plasma optical emission spectroscopy (ICP-OES). Further details on commercial laboratory methodology is available upon request of the laboratory. The mean of the three bundles was used to represent the nutrient content of plant tissue and used in combination with the number of shoots counted in each CW to provide an estimate of total cattail shoot biomass.

2.5 Calculations and Statistical Analyses

All data were processed in R version 4.1.1 (R Core Team, 2021) with tidy data approaches (Wickham et al., 2019). Data visualizations were performed using ggplot2 (Wickham, 2016). Nominal AWW treatment volumes were converted to TP loadings (expressed as mg PO_4–P per wetland m^2), and a $\log_{10}(x + 1)$ transformation was applied for use as the predictor variable in linear regression models. TP loading was chosen as a predictor variable in growth models because additions of P, but not N, are known to impact the growth of cattail plants (Craft et al., 1995; Miao et al., 2000). However, TP and total nitrogen (TN) loadings were highly correlated ($R^2 > 0.999$). The residuals of all fitted models were inspected to verify model assumptions. For all statistical analyses, an alpha of 0.05 was used.

The performance of CWs was assessed by evaluating the hydraulic loading rate (HLR), total phosphorus concentration reduction (CR), and total phosphorus load reduction (PLR) using modified versions of the equations detailed in Kadlec (2016). Briefly, HLRs were calculated using the total volume of AWW applied to CWs over a 28-day period while CR and PLR were calculated by comparing the sum of TP added via AWW additions and background TP in mesocosm water to the final TP concentration measured in mesocosms on day 33. The modified equations were as follows:

$$HLR = \frac{\bar{q}}{A}$$

Equation 1

$$CR = \frac{\left(\frac{(\overline{C_{AWW}})(V_{AWW}) + (C_{source})(V_{final})}{V_{final}}\right) - C_f}{\left(\frac{(\overline{C_{AWW}})(V_{AWW}) + (C_{source})(V_{final})}{V_{final}}\right)}$$

Equation 2

$$PLR = \frac{\left((\overline{C_{AWW}})(V_{AWW}) + (C_{source})(V_{final})\right) - (C_f)(V_{final})}{(A)(0.090349\ yr)}$$

Equation 3

where HLR: hydraulic loading rate, m week^{-1}; $\bar{q}$: mean flow of aquaculture wastewater (AWW) additions, m^3 week^{-1}; A: wetland surface area, m^2; CR: fractional total P concentration reduction; $\overline{C_{AWW}}$: mean total P concentration in AWW, mg L^{-1}; V_{AWW}: total volume of AWW added, L; C_{source}: total P concentration in water source, mg L^{-1}; V_{final}: final (day 33) mesocosm water

volume, L; C_f: final (day 33) total P concentration in mesocosm water, mg L^{-1}; PLR: total P load reduction, mg m^{-2} yr^{-1}. Note that the treatment period of 33 days was converted to years for use in the PLR calculation.

3.0 Results and Discussion

3.1 Nutrients in Aquaculture Wastewater

The mean (± SD) concentration of TN and TP in AWW for the five addition events was 13.4 ± 4.3 mg L^{-1} and 2.94 ± 0.85 mg L^{-1}, respectively (Table 1). The mean (±SD) N:P ratio of AWW was 4.9 ± 2.2. In the literature, N:P ratios of 28.9 (Hawrot-Paw et al., 2019), 12.0 (Han et al., 2020), 6.9, and 6.6 (Tossavainen et al., 2019) have been reported in AWW. Although AWW was stored in a sealed bucket, it is possible that denitrification could occur under the storage conditions of the present study, resulting in a lower N:P ratio relative to literature values. However, both the concentrations and relative proportions of nutrients detected in AWW can be highly variable, and are largely dependent on site characteristics (e.g. flushing rates) and farming practices (e.g. type of feed, species, stocking density) (Walker et al., 2003). In a summary of 14 different land-based aquaculture effluents, Lalonde et al. (2015) reported concentration ranges of 0.28–4.73 mg L^{-1} and 0.005–0.727 mg L^{-1} for TN and TP, respectively. These results are indicative of the broad range of nutrient concentrations and ratios that can exist in AWW. The AWW collection methods used in the present study were designed to maximize the quantity of collected nutrients while minimizing the volume of water collected. These methods facilitated the transportation of AWW to the field site while also providing sufficient time to elapse to ensure a substantial collection of nutrients could be collected from fish tanks.

Table 1. Mean (± SD) concentrations of total N (TN) and total P (TP) in aquaculture wastewater (AWW) added to mesocosms throughout the study. Duplicate samples were analyzed at each time point to account for potential heterogeneity in AWW solutions. The study day column indicates the day that AWW was sampled, analyzed, and applied to mesocosms.

Study day	TN (mg L^{-1})	TP (mg L^{-1})
0	13.6 (1.6)	3.73 (0.05)
8	11.1 (0.4)	1.90 (0.05)
14	9.6 (1.0)	2.68 (0.04)
21	11.8 (2.1)	3.90 (0.51)
28	20.7 (1.8)	2.47 (0.16)
Study mean	13.4 (4.3)	2.94 (0.85)

Hennessy et al. (1996) reported waste loadings ranges from two fish farms of 20.3–39.3 and 9.1–10 kg t $fish^{-1}$ yr^{-1} for TAN and TP, respectively, which were similar to the waste loadings of other fish farms. The total AWW loadings applied in the present study (outlined in Section 2.2) achieved loading rates of 2.4–35.8 and 0.5–7.9 mg d^{-1} for TN and TP, respectively. Therefore, when applying the mean waste loading rate reported by Hennessy et al. (1996) for TP (i.e. 9.55 kg t $fish^{-1}$ yr^{-1}), the AWW additions of the present were equivalent (on a nutrient quantity basis) to the waste produced by 19.2–302.7 g of fish. The low-end surface area of large-scale CWs treating wastewater is approximately 40–250 ha in size (Kadlec, 2016). Therefore, if the cattail CW system utilized here was constructed with a surface area of 100 ha and identical AWW loadings conditions were applied, the up-scaled CW would be treating the waste produced by 4–79 t of fish, assuming no other treatment strategies are implemented alongside the CW.

3.2 Cattail Growth and Nutrient Content

Linear regression did not reveal a relationship between TP loading and overall change in shoot density ($t = 0.915$, $p = 0.402$), or overall change in wetland height ($t = -0.306$, $p = 0.772$) for the 5-week study period. High variability was observed between REF-A and REF-B mesocosms, however, the removal of references from the regression models did not alter statistical significance for the overall change in shoot density ($t = 2.435$, $p = 0.093$) or for the overall change in wetland height ($t = -0.392$, $p = 0.711$). Cattails in CWs proliferated extensively in the 40 days prior to AWW additions, indicated by a rapid increase in shoot density (Figure 3). However, after study day 0, new shoots were no longer being rapidly produced and existing shoots were no longer increasing in height (Figure 4). Shoot counts were highly variable, negatively impacting statistical power. Future studies may wish to enhance methods for collecting shoot counts to better detect differences in CW shoot densities. This could include working with lower plant density CWs, dividing CWs into sections which are easier to count, or implementing new remote sensing or automated count technologies.

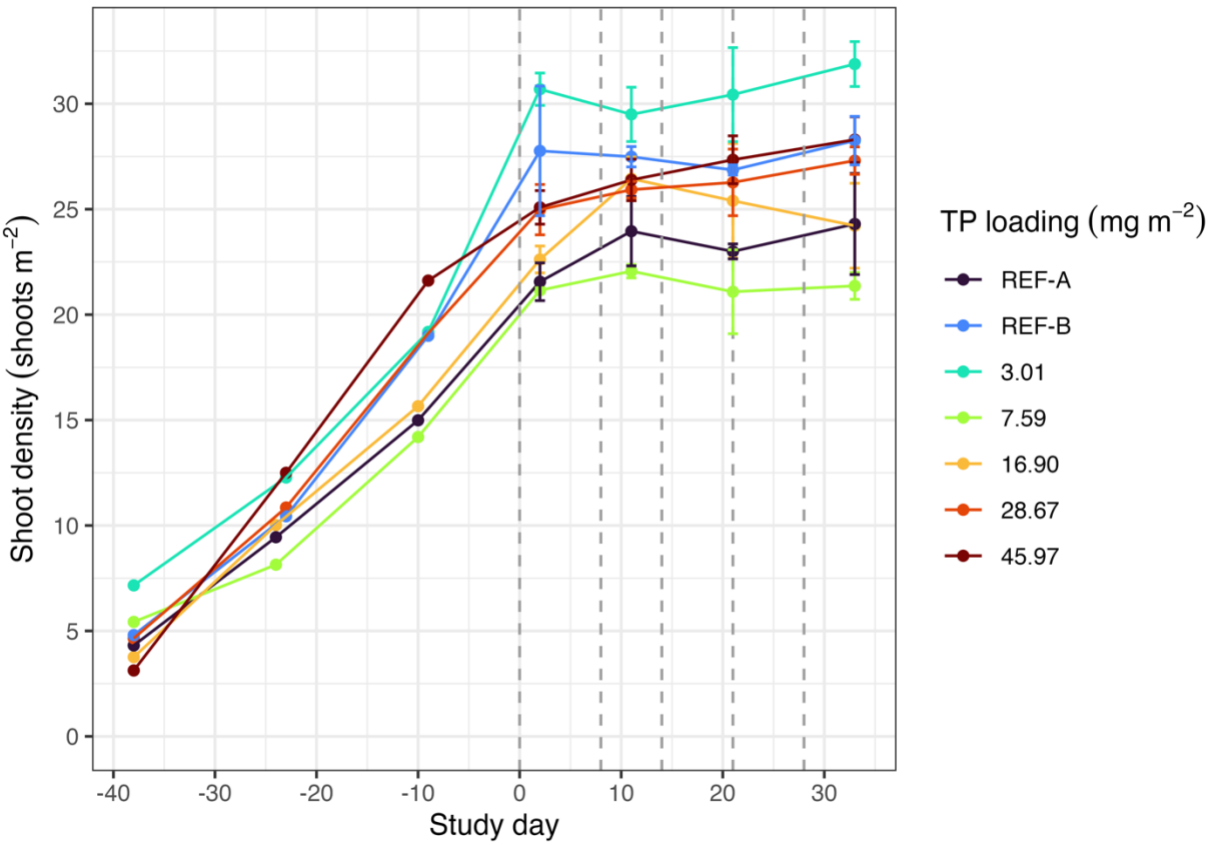

Figure 3. Density of cattail shoots in mesocosms. Aquaculture wastewater (AWW) additions are indicated with vertical dashed lines. Prior to the additions of AWW, a single tally of plants was recorded. After AWW additions began, then mean of three tallies is plotted with ±1 standard deviation of the mean. Different mesocosm treatments are expressed as total phosphorus (TP) loadings resulting from AWW additions.

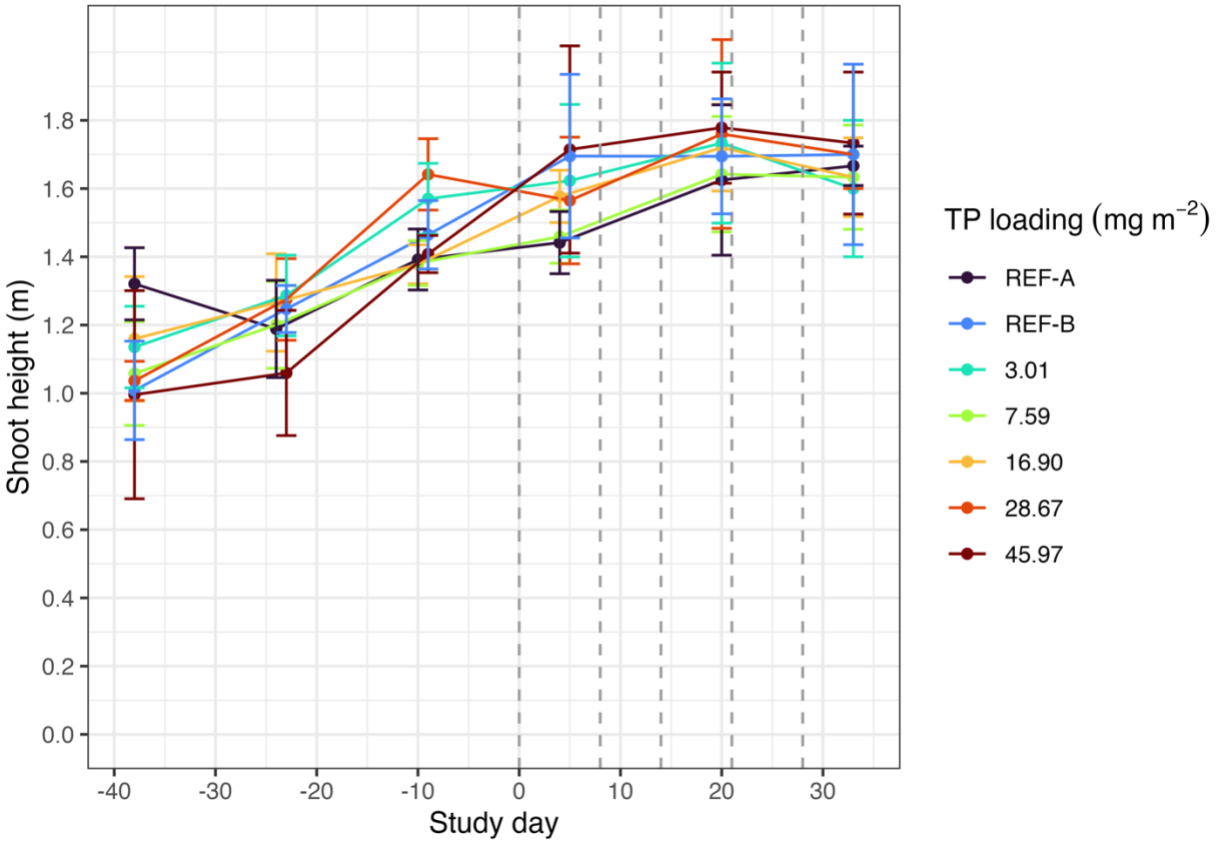

Figure 4. Cattail shoot height in mesocosms. Aquaculture wastewater (AWW) additions are indicated with vertical dashed lines. The mean shoot height is plotted with ±1 standard deviation of the mean. Different mesocosm treatments are expressed as total phosphorus (TP) loadings resulting from AWW additions.

Linear regression revealed that TP loading was not a statistically significant predictor of shoot biomass on day 20 ($t = 1.589$, $p = 0.173$) or day 53 ($t = 0.925$, $p = 0.397$), nor was it a statistically significant predictor of aboveground plant tissue P content on day 20 ($t = 1.847$, $p = 0.124$) or day 53 ($t = 1.019$, $p = 0.355$) (Figure 5). Aboveground plant tissue P content and shoot biomass were strongly correlated ($R^2 = 0.929$) on day 20, and therefore followed nearly identical trends. The mean (± SD) shoot biomass of all CWs on day 20 (6.62 ± 1.88 Mg ha^{-1}) was compared to the mean shoot biomass on day 53 (4.72 ± 0.66 Mg ha^{-1}), and a statistically significant difference was observed (paired t-test; $t = 2.955$, $df = 6$, $p = 0.025$). Cattail shoot

biomass production reaches a plateau in early September, at which point nutrients are allocated to belowground tissues and stored until the following growing season (Dubbe et al., 1988; Linde et al., 1976; Sojda & Solberg, 1993). However, total cattail biomass continues to increase into the late summer with substantial nutrient uptake of N and P occurring in rhizomes (Dubbe et al., 1988). Future studies should compare nutrient uptake and storage capacity for both aboveground and belowground plant tissues. Direct measures of rhizome tissues would provide a more comprehensive representation of the potential response of cattail CWs to AWW and the remediation capacity of these systems.

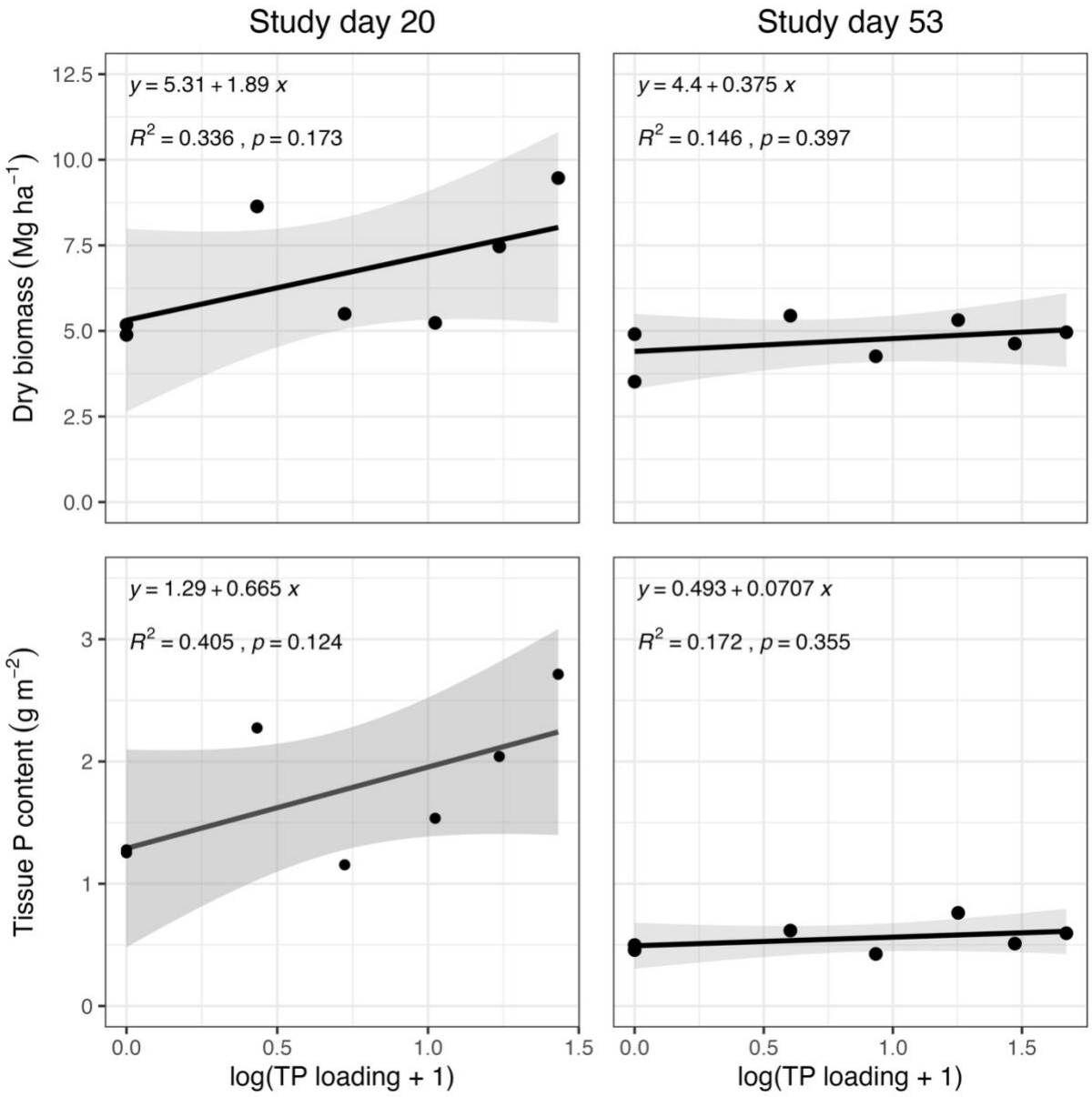

Figure 5. Estimates for total cattail shoot biomass (top panels) and total cattail shoot P content (bottom panels) in mesocosms on study day 20 (left-side panels) and day 53 (right-side panels). Linear models (black lines) are displayed with 95% confidence intervals (shaded regions). Different mesocosm treatments are expressed as the total phosphorus (TP) loadings resulting from aquaculture wastewater additions with a $\log_{10}(TP + 1)$ transformation. Data are reported on a dry mass basis.

The N:P ratios of aboveground plant tissue are a useful diagnostic tool to detect nutrient limitations in wetlands (Koerselman & Meuleman, 1996). Koerselman and Meuleman (1996) conducted a review of freshwater wetland fertilization studies and determined that N:P ratios >16 indicate P limitations, while N:P ratios <14 indicate N limitations. The N:P ratios of cattail plants on day 20 were <14, suggesting N limitations in all CWs (Table 2). On day 53, N:P ratios increased slightly, suggesting N limitations were somewhat alleviated and/or P limitations were introduced. Inspection of mesocosm water quality revealed low quantities of TAN, NO_2–N, NO_3–N (see Section 3.3; Figure 6). One potential explanation for the N limitations observed in the present study is that uptake from, and/or removal of nitrogen from the water column exceed the inputs from AWW additions. Nitrogen species in AWW are primary ammonia and urea, which are readily available for biological uptake and sorption processes (Walker et al., 2003). The N limitations observed here and corresponding low concentrations of N species in CW water imply a greater capacity for N loading in cattail CW systems, either through the application of greater volumes of AWW, or by way of an AWW source with a higher N:P ratio, such as those often seen in the literature (Han et al., 2020; Hawrot-Paw et al., 2019; Tossavainen et al., 2019). If the former method is used to achieve higher N loadings, additional concerns around phosphorus are warranted.

Table 2. Cattail shoot N:P ratios on study days 20 and 53. Different mesocosm treatments are expressed as total phosphorus (TP) and total nitrogen (TN) loadings resulting from aquaculture wastewater additions.

TP loading (mg m^{-2})	TN loading (mg m^{-2})	N:P ratio	
		Study day 20	Study day 53
REF-A	REF-A	9.16	17.24
REF-B	REF-B	8.64	12.10
3.01	13.7	8.12	12.25
7.59	34.5	9.01	17.12
16.90	76.9	8.17	10.73
28.67	130.5	8.68	13.18
45.97	209.2	8.33	12.22

3.3 Water Quality Responses in Constructed Wetland Mesocosms

The N generated by land-based aquaculture operations is primarily dissolved and in the form of ammonia and urea (Walker et al., 2003). Elevations in TN and ammonia have been observed downstream of AWW discharge points, posing a risk of eutrophication and ammonia toxicity in the receiving environment (Boaventura et al., 1997; Lalonde et al., 2015). Ammonia is particularly toxic in the aquatic environment, and has been the focus of toxicity tests involving zooplankton (Sarma et al., 2003), fish (Randall & Tsui, 2002), and aquatic macrophytes (Nimptsch & Pflugmacher, 2007). Additions of AWW had minor impacts on inorganic N species (Figure 6) and TDN (Figure 7) in CW water throughout the duration of the study. In the literature, CWs have demonstrated the ability to remove >95% of total inorganic nitrogen (TIN) with excellent (>82%) removal of individual inorganic N species (Lin et al., 2002). These findings align with the results presented here, which demonstrate that TAN and NO_2–N concentrations were similar among CWs that received AWW and CWs that did not (i.e.

reference treatment). However, minor elevations in NO_3–N were observed in AWW-dosed CWs relative to reference conditions, which could contribute to increased algal growth and eutrophication with extended CW usage (Figure 6). Overall, high elimination of the inorganic N species added via AWW is evident when comparing relative concentrations of TIN species (Figure 6) to TDN (Figure 7). Therefore, we suspect the TDN detected in wetland water is comprised predominately of organic N originating from mesocosm soil. In the long term, TDN could physically settle, biodegrade, and/or be taken up by plants and algae (Healy et al., 2007; Näsholm et al., 2009; Neilson & Larsson, 1980). An increase in NO_3–N was observed among all mesocosms on day 20. While this sampling event may have captured an elevation in NO_3–N prior to the assimilation of nitrate by plants, this is unlikely as an NO_3–N elevation is also observed in UP-REF. Therefore, the increase in NO_3–N appears to have occurred regardless of the presence/absence of plants. Elevations in nutrient could have implications for the overall long-term functinaility of CWs and warrant further investigation. Varying nutrient loading conditions may impact the long-term nutrient reduction capabilities of CW systems treating AWW and should be optimized to sustain perfromance over time. While greater N loadings should be considered in future studies to capitalize on the ability of cattail CWs to effectively eliminate N species from CW water, the long-term response of CWs must be considered along with the corresponding short and long-term response of P species. It is critical to assess the risk of P overloading and to determine which nutrient (N or P) is in excess when optimizing maximum nutrient loading rates in CWs.

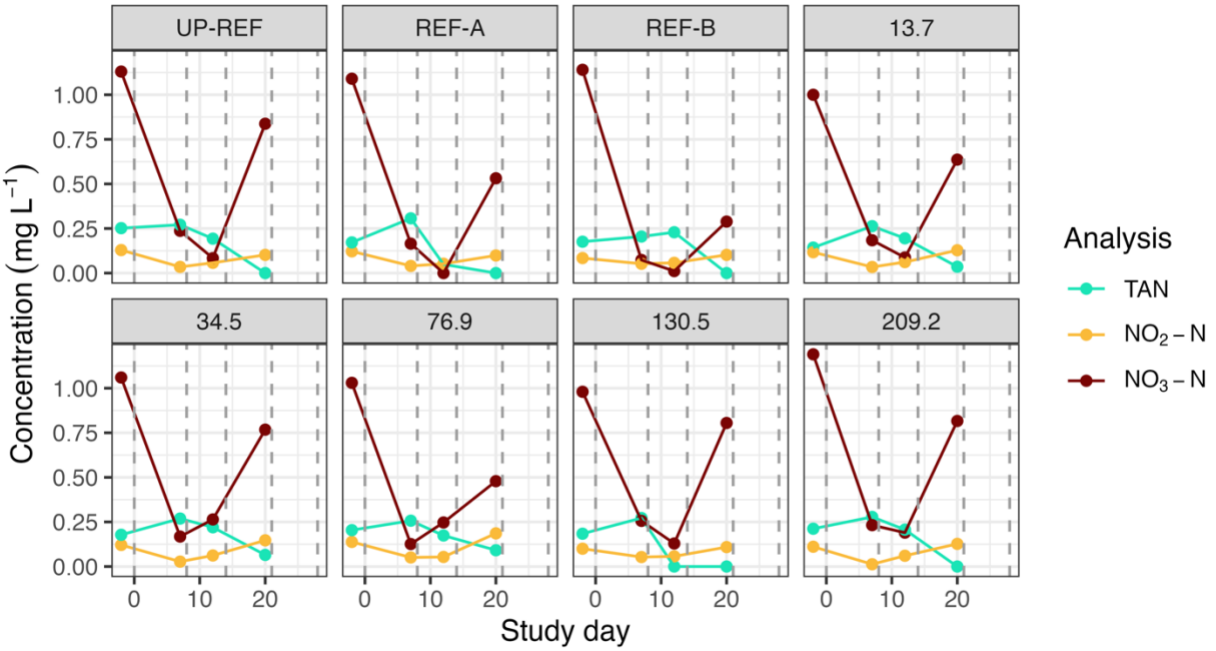

Figure 6. Concentrations of total ammonia nitrogen (TAN), nitrite nitrogen (NO_2–N), and nitrate nitrogen (NO_3–N) in cattail constructed wetland mesocosm water. Weekly additions of aquaculture wastewater (AWW) are indicated by vertical dashed lines. Shaded panels over each graphic indicate mesocosm treatments with the numerical values representing total nitrogen (TN) loading resulting from AWW additions in units of mg m^{-2}.

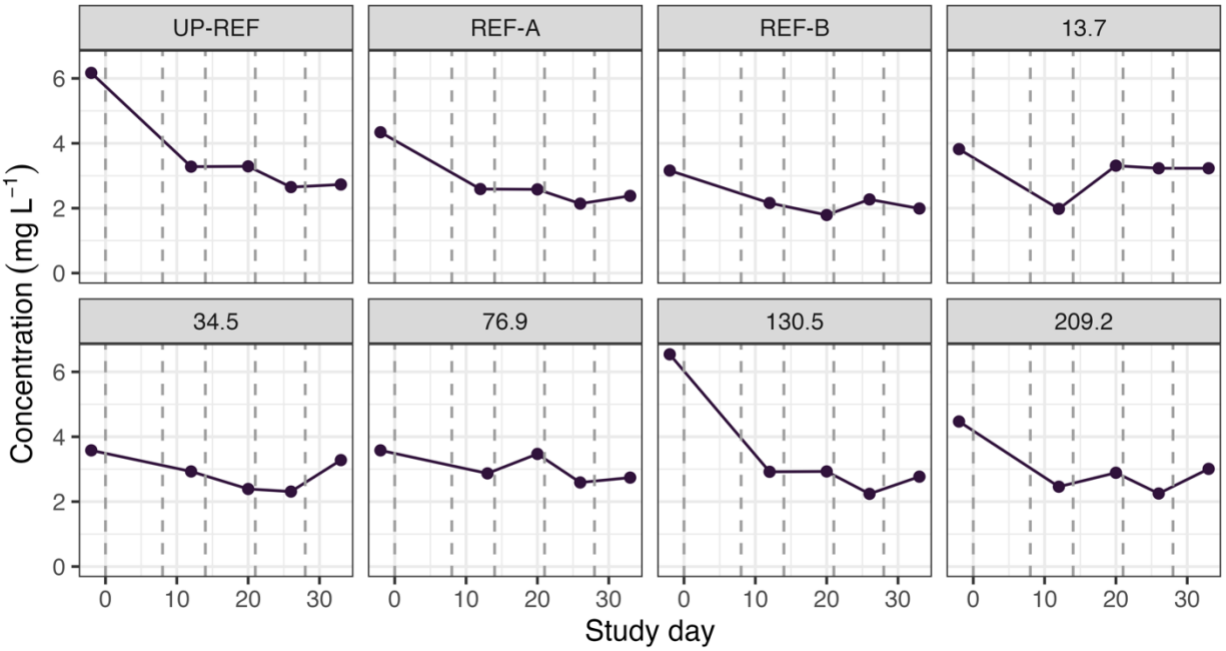

Figure 7. Concentrations of total dissolved nitrogen in cattail constructed wetland mesocosm water. Weekly additions of aquaculture wastewater (AWW) are indicated by vertical dashed lines. Shaded panels over each graphic indicate mesocosm treatments with the numerical values representing total nitrogen (TN) loading resulting from AWW additions in units of mg m^{-2}.

Prolonged elevations in P were observed among the CWs which received greater quantities of AWW (Figure 8) While background P concentrations were elevated among REF-B and the 3.01 mg m^{-2} treatment, concentrations decreased notably by the second sampling event. Meanwhile, the high-loading treatments (i.e. 28.67 and 45.97 mg m^{-2}) had high background P concentrations, which persisted for several weeks. This finding suggests that among low-loading treatments, P removal from water exceeded loading from AWW, whereas in high-loading treatments, CWs acted as buffers, preventing rapid P level increases but allowing P to persist for 3–4 weeks in CW water before its elimination. Note that difference in background P concentrations among all mesocosms likely resulted during the CW establishment period, prior to AWW additions. Further investigation into soil dynamics and algae production would be valuable to elucidate the cause of these discrepancies.

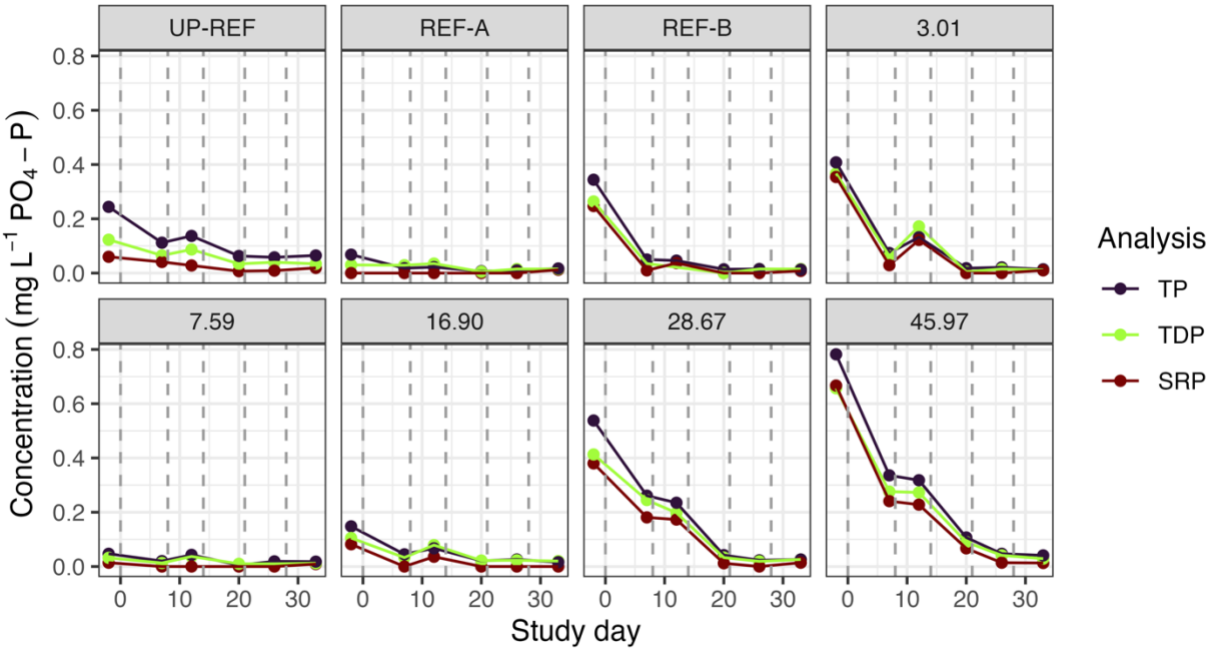

Figure 8. Concentrations of total (TP), total dissolved (TDP), and soluble reactive phosphorus (SRP) detected in cattail constructed wetland mesocosm water. Weekly additions of aquaculture wastewater (AWW) are indicated with vertical dashed lines. Shaded panels over each graphic indicate mesocosm treatments with the numerical values representing TP loading resulting from AWW additions in units of mg m^{-2}.

During an 8-week period between early July and early September, cattail stands exhibit peak nutrient uptake during which approximately two-thirds of the total seasonal biomass production occurs (Dubbe et al., 1988). By day 0 of the present study, CWs were no longer undergoing substantial increases in cattail density (Figure 3) or height (Figure 4). Therefore, in all likelihood peak biomass production had already been reached by the time AWW additions began, and the P elimination observed here occurred outside of this rapid production phase. The bulk of P elimination from CW water observed in Figure 8 therefore occurred during this end-of-season period. The potential for extended usage of CWs for AWW treatment beyond the rapid growth period in the summer months is of particular interest in northern, cold climates where wastewater treatment can be substantially limited during the winter months (Werker et al., 2002). The P

elimination observed in Figure 8 suggests that continued usage of cattail CWs for AWW treatment into the fall end-of-season growing conditions is plausible. These results improve an understanding of the overall treatment capacity of cattail CW systems and could help improve overall CW performance by providing insight to cattail CW operators working in northern climates.

SRP comprised a substantial fraction of the TP detected in mesocosm water (Figure 8). Extended periods of elevated P content, specifically SRP, are concerning as it is the only form of P that is assimilated by bacteria and algae (Correll, 1998). Although particulate and dissolved organic forms of P can be converted to SRP under the proper conditions, readily available SRP can contribute to the growth and development of algae, resulting in eutrophic conditions in affected CWs. Here we observe that this window of opportunity is narrow because after 20–26 days of treatment, excess P species are eliminated from CW water. Throughout the study, differences in the quantity of TP and TDP were small, indicating that suspended algae and other forms of particulate P comprised a minor fraction of P species at any given time, regardless of loading conditions. This finding suggests that SRP uptake into water column algae was not substantial. Future studies could include direct measures of particulate P, chlorophyll *a*, and dissolved oxygen in CW water to further elaborate on algal growth and trophic status in CW systems.

Some discrepancies between TP and TDP observed Figure 8 are noteworthy. There were some instances where quantities of TDP slightly exceeded TP. For example, slightly greater quantities of TDP are measured in REF-A on days 12 and 20. Variation among TP samples can be attributed to the heterogeneous nature of samples, while variation in both TP and TDP can be

attributed to varying efficiency of the digestion of the method for P determination and other sources of variation arising in the laboratory (e.g. instrumental, human). Care was taken to ensure that samples were properly mixed prior to conducting analyses for TP and TDP, however duplicate or triplicate analyses were not systematically performed on mesocosm water samples because of time and cost limitations. In cases where TDP > TP, it can be assumed that these values are approximately equal and the small observed discrepancies in Figure 8 arose from methodology variation between samples.

After 33 days of treatment, TP concentrations in all planted CWs were below 0.05 mg L^{-1}, indicating cattail CWs were highly effective in eliminating TP from wetland water (Table 3). These effluents were compliant with the recommended limits outlined in the Water Protection Act of Manitoba (Manitoba Water Stewardship, 2011). The TP concentrations of the second-highest (28.67 mg m^{-2}) and highest (45.97 mg m^{-2}) P loading treatments are notably greater than other CWs, suggesting some residual P originating from AWW remains after 33 days of treatment. Wetlands are known to be robust to eutrophication as they can retain and filter significant quantities of nutrients (Sánchez-Carrillo et al., 2011). With TP concentrations <0.05 mg L^{-1}, the risk of eutrophication occurring within the CW system is less concerning and emphasis should be placed upon the current trophic state of the receiving environment and its sensitivity to P inputs from CW effluents (Li et al., 2008). When comparing the total quantity of TP added to mesocosms via AWW additions to the total quantity of TP remaining in mesocosm water on day 33, high removal of TP was observed (Figure 9). In fact, the quantities of P in all AWW-dosed CWs were equivalent to reference conditions. Therefore, TP loadings of up to 45.97 mg m^{-2} over 28 days were effectively treated by cattail CWs after 33 days. The mechanism

for P removal could include uptake by cattails, adsorption to soils, or precipitation. With low concentrations of TP observed in wetland water on day 33, CW effluent could be discharged without major environmental concerns surrounding the quantity of P released into the receiving environment. However, the reflooding of CWs has the potential to release additional P from soil into the water column, posing a risk of water quality deterioration and eutrophication with continued CW usage (Olila et al., 1997). Thus, it is particularly important to understand the mechanism for the observed P removal from CW water and assess for potential P accumulation in soils in future studies. Once soils are P-saturated, CW performance may be reduced (i.e. lower CR and PLR) without soil adsorption as a possible mechanism for P elimination from CW water. Note that the observed differences between the CR of planted mesocosms and UP-REF in Table 3 are indicative of the impact that the presence of plants has upon P elimination from mesocosm water.

Table 3. Performance of cattail constructed wetlands treating phosphorus in aquaculture wastewater (AWW). The maximum anticipated total phosphorus (TP) concentration in mesocosm water (C_{max}) was calculated assuming no phosphorus elimination occurred during the study. The final TP concentration in mesocosm water (C_f) represents the TP concentration measured at the end of the study (i.e. day 33). Hydraulic loading rate (HLR) was calculated for the 28-day period of AWW additions, while concentration reduction (CR) and total phosphorus load removal (PLR) were calculated for the 33-day treatment period.

TP loading ($mg\ m^{-2}$)	AWW additions ($L\ week^{-1}$)	HLR ($mm\ week^{-1}$)	C_{max} ($mg\ L^{-1}$)	C_f ($mg\ L^{-1}$)	CR (%)	PLR ($mg\ m^{-2}\ yr^{-1}$)
UP-REF	0	0	0.440	0.065	85.2	456.6
REF-A	0	0	0.440	0.017	96.1	591.7
REF-B	0	0	0.440	0.013	97.0	792.7
3.01	1.0	0.257	0.472	0.014	97.0	477.5
7.59	2.0	0.646	0.492	0.018	96.3	766.6
16.90	4.5	1.439	0.543	0.016	97.1	955.0
28.67	7.5	2.441	0.667	0.026	96.1	869.9
45.97	15.0	3.914	1.023	0.041	96.0	856.8

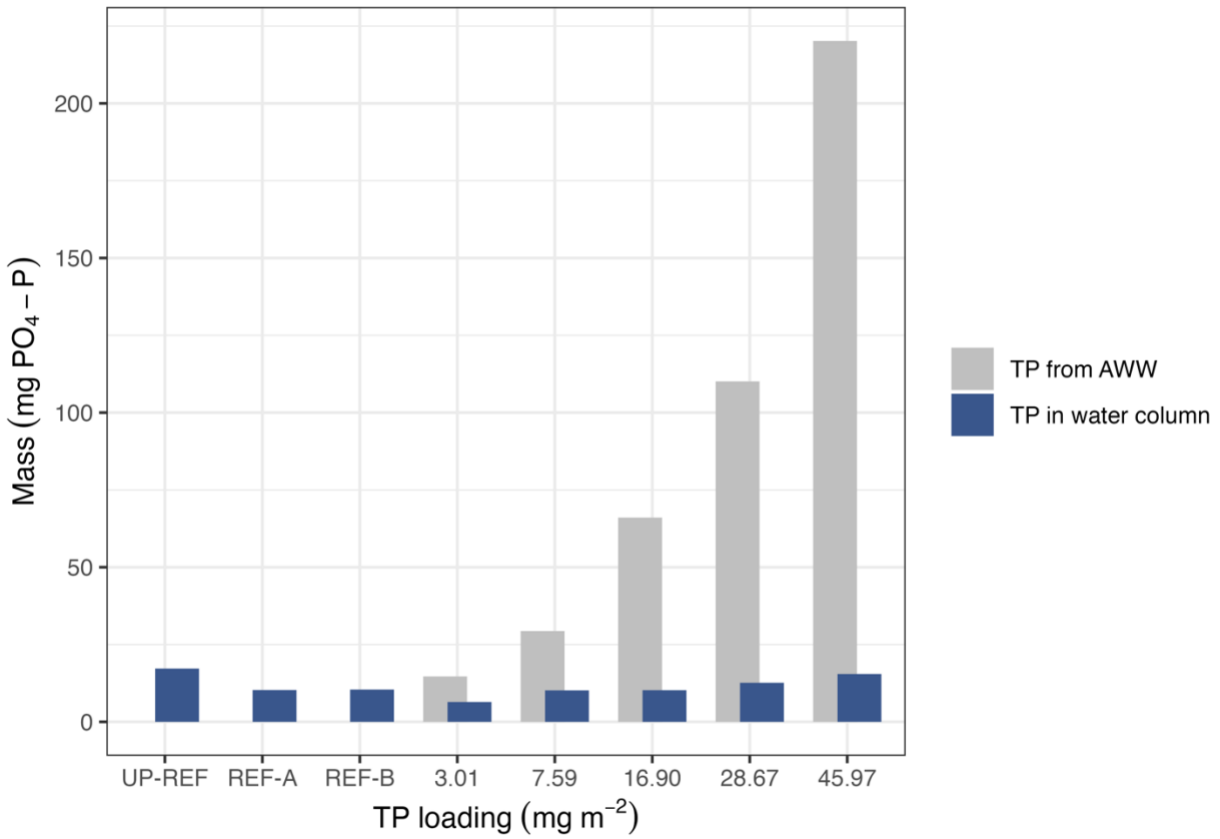

Figure 9. Comparison between the total mass of phosphorus added to cattail constructed wetland mesocosms over a 28-day period from aquaculture wastewater (TP from AWW) and the quantity of phosphorus remaining in mesocosm water on day 33 (TP in water column). Reference A (REF-A), reference B (REF-B), and unplanted reference (UP-REF) mesocosms received no AWW throughout the study.

Cattail CWs achieved excellent TP CR, with TP concentrations reduced by 95% or greater in all mesocosms after 33 days of treatment (Table 3). While high CR is partly related to the use of low HLR (Kadlec, 2016), cattail plants appear to be effective in removing P. Furthermore, a relationship was observed between PLR and TP loading where the three highest TP loading treatments displayed greater PLR relative to the reference and two lowest TP loading treatments. Greater nutrient loading applications could result in even greater PLR. Therefore, the overall treatment capacity of cattail CW systems for AWW could be expanded through the implementation of greater nutrient loadings than those utilized in the present study. While the

maximum capacity for cattail CWs was likely not reached here, water quality alterations were observed at TP loadings of 28.67 and 45.97 mg m^{-2}, which have the potential to limit functionality of CW systems (Figure 8). However, the systematically high CR and the manner in which PLR was elevated among high P loading treatments demonstrate the high performance of cattail CWs in the elimination of P from AWW. Kadlec (2016) conducted a review of CW performance and found median TP effluent concentrations of 0.038 mg L^{-1} and PLR of 770 mg m^{-2} yr^{-1}, similar to the values reported in Table 3.

4.0 Conclusion

This study demonstrates the ability of cattail CWs to treat AWW. The applied gradient of nutrient loadings did not cause a detectable difference in plant growth; however, low quantities of P remained in CW water after 33 days of treatment. Cattail CWs buffered the impacts of P loadings; increases of P species in CW water were prevented; however, prolonged elevations in P were detected for approximately 3–4 weeks among high-loading treatments. Excess P was eventually reduced in CW water, and TP concentrations were reduced below 0.05 mg L^{-1} after 33 days of treatment. Although no TDN increases were evident in CW water, NO_3–N elevations of approximately 0.25 mg L^{-1} were observed relative to reference conditions. Further investigation into how elevated NO_3–N can impact CW performance is warranted. To minimize impacts on the receiving environment, management strategies could coordinate CW effluent release with reduced N and P levels in CW water. Additionally, cattail CWs demonstrate the potential to accommodate AWW loadings into the late summer and early fall as P elimination was observed after aboveground plant growth had reached a plateau. Detailed analysis of nutrient content in CW soils and belowground plant tissues can help elucidate the mechanisms of nutrient removal

in these systems. The nutrient removal potential of cattail CWs is particularly useful in the treatment of N and P in AWW and could be implemented in other forms of wastewater high in nutrients.

CHAPTER 3: NORTHERN WILD RICE (*Zizania palustris* L.) CONSTRUCTED WETLANDS FOR AQUACULTURE WASTEWATER REMEDIATION

Preface

A version of this study is currently in preparation for publication. A modified version of the manuscript in preparation is presented here, with additional details surrounding methodology and an expanded discussion of results. This chapter presents the results of two studies conducted concurrently at the same field site using identical methodology. The Results and Discussion section is divided into two subsections, each dedicated to presenting the findings of its respective study.

Contribution of Authors

The author contributor roles taxonomy (CRediT) statement for the manuscript in preparation is as follows:

Nicholas C. Blandford (University of Manitoba): Conceptualization; formal analysis; funding acquisition; investigation; methodology; project administration; visualization; writing–original draft. **Leah Dickenson** (University of Manitoba): Conceptualization; investigation; methodology; writing–review and editing. **Krista Robertson** (University of Manitoba): Conceptualization; investigation; methodology; writing–review and editing. **Richard Grosshans** (International Institute for Sustainable Development): Conceptualization; methodology; resources; writing–review and editing. **Bruce Hardy** (Myera Group): Conceptualization; funding acquisitions; resources. **Nazim Cicek** (University of Manitoba): Conceptualization; funding acquisition; methodology; resources; supervision; writing–review and editing. **Vince Palace**

(International Institute for Sustainable Development – Experimental Lakes Area): Conceptualization; funding acquisition; methodology; project administration; resources; supervision; writing–review and editing.

1.0 Introduction

Aquaculture is a major food production sector which has experienced remarkable growth in recent years (Garlock et al., 2020). In 2022, total global aquaculture reached a record-high production of 130.9 million tonnes (USD 312.8 billion), with inland aquaculture accounting for 62.6% of the total (FAO, 2024). Inland aquaculture systems are the primary means of finfish production, and were responsible for the production of 89.7% of the total global inland aquaculture production in 2022 (FAO, 2024). Finfish provide high-quality protein and essential nutrients for proper nutrition, and strong links have been established between fish consumption and improved cardiovascular health (Allison, 2011; Ruxton, 2011). The growth of the aquaculture industry has directly improved the food security of millions of people through the production of a nutritious food product which can be consumed locally while also indirectly improving food security through the generation of income sources in rural communities (Béné, 2006; Béné et al., 2015).

High feed conversion ratios have resulted in fish farming becoming a globally adopted sustainable alternative to conventional fisheries and terrestrial animal production systems, which typically have higher carbon footprints (FAO, 2022; Hall et al., 2011). In particular, land-based aquaculture facilities offer improvements over issues that are inherent among cage-based systems such as competition with wild population, control of diseases and parasites, and water

quality management (Heller, 2017). However, land-based aquaculture operations generate wastewater high in nutrients (i.e. nitrogen and phosphorus), raising environmental concerns for surrounding aquatic ecosystems (Ahmad et al., 2022; Cripps & Bergheim, 2000; Tom et al., 2021; Troell et al., 2013). Environmental impacts resulting from aquaculture wastewater (AWW) can vary substantially depending on farming practices and characteristics of the receiving environment. However, the most commonly observed impact is nutrient enrichment (Walker et al., 2003). Inputs of phosphorus can drive eutrophication among receiving environments, threatening the health of the aquatic ecosystem (Benoy et al., 2016; Hozumi et al., 2018; Kurniawan et al., 2021; Schindler et al., 2012). Nitrogen species such as ammonia and nitrate are also major components of AWW, which are known to be toxic to aquatic species and can contribute to cyanobacteria production (Camargo et al., 2005; Jing et al., 2021; John et al., 2020; Randall & Tsui, 2002; Yang et al., 2017). It is crucial to manage nutrient loadings from aquaculture operations to minimize the risk of eutrophication and preserve the health of receiving environments.

Constructed wetlands (CWs) are an engineered wastewater treatment technology which aim to simulate natural wetlands and have been employed in the treatment of municipal, industrial, and agricultural wastewaters (Hammer, 1989; Sundaravadivel & Vigneswaran, 2001). In CWs, water can be treated by physical (e.g. sedimentation, UV exposure), chemical (e.g. precipitation, adsorption, volatilization), and biological (e.g. microbial degradation, plant uptake) processes (Vymazal, 2011a). Wetland plants can uptake nutrients from within the CW system, and the subsequent harvesting of standing biomass can be a highly effective strategy for achieving nutrient remediation, accounting for greater than 50% of N and P removal in wastewater

(Vymazal, 2020). Circular economy concepts have been proposed which utilize CWs for the reclamation of AWW (Rousseau et al., 2008; Staudenmann & Junge-Berberovic, 2003). The nutrients in AWW can be used to fuel production of algal or plant biomass which can in turn be incorporated into aquaculture feed (Nagarajan et al., 2021), or used in other applications, such as feedstock for bioenergy (Cicek et al., 2006; Grosshans & Grieger, 2013; Nagarajan et al., 2021), as fibres for use as reinforcement materials in composites (Shadhin et al., 2021; Sharma et al., 2023), or as fertilizers after composting (Kouki et al., 2016).

Wild rice (*Zizania* spp.) refers to a genus of rooted emergent aquatic macrophytes which often grow in dense stands in freshwater marshes, rivers, streams and lakes (Terrell et al., 1997). Northern wild rice (*Zizania palustris* L.) is an annual plant, and the species of wild rice found in the Canadian Prairie Provinces, and the Great Lakes region in North America (Ahmed et al., 2021; Aiken et al., 1988). Northern wild rice is a staple food and has been a valuable resource for centuries, and has significant historical, cultural and spiritual meaning among Indigenous communities across North America (Archibold, 2003; Raster & Hill, 2017; Vennum, 1988). Managed natural stands are the primary means of wild rice harvesting in Canada, while paddy-based farming serves as the main method of production in the USA (Archibold, 1995; Hayes et al., 1989; Oelke & Schreiner, 2007). The grain produced by wild rice plants is a nutritious product and provides many essential nutrients to consumers (Surendiran et al., 2014).

Wild rice plants are not among the most commonly used plants in CWs (Brix, 2003; Vymazal, 2011b), however there are instances where they have been utilized with success (Waki et al., 2015; Ye & Li, 2009). Wild rice plants require significant quantities of nutrients and can

stimulate microbial communities, helping to further improve water quality through nutrient cycling processes (Atkins et al., 1992; Jorgenson, 2013; McMillian, 2021; Sims et al., 2012). Ammonia-based fertilizers, such as urea, are stable in flooded soils and are therefore the only viable N fertilizers in wild rice wetlands (Oelke et al., 1997). The ability of wild rice to uptake N and P and the high proportion of ammonia in AWW makes it an ideal candidate for implementation in CW systems designed for the treatment of AWW.

In this study, the potential for northern wild rice to be implemented in CW systems treating AWW was investigated. A natural variety of wild rice was established in CW systems, AWW was applied, and treatment performance was evaluated. The integration of wild rice plants into CW systems provides an opportunity to develop circular economies which involve the fertilization of wild rice with fish waste (Ahmed et al., 2021). Instead of discharging AWW into a receiving environment, the waste produced during fish farming can be used as a fertilizer by wild rice CW systems, which can in turn produce a promising, high-value crop. Rice fields in Asia have been well-utilized as aqua-ecosystems that include fish production, or that are connected to agronomy systems (Hambrey et al., 2008; Ottinger et al., 2016). A similar ecosystem approach to wild rice-fish cultivation has been proposed in North America as many commercially relevant fish species have a preference for wild rice habitats (Ahmed et al., 2021).

2.0 Materials and Methods

2.1 Constructed Wetland Mesocosms and Field Site Details

Wild rice CWs were established in mesocosms (Figure 10; 2.56 m diameter, 0.57 m height) consisting of circular low-density polyethylene stock tanks (ACE Rotomolds; Hospers, IA,

USA). Mesocosms were amended with 20 cm of organic topsoil (Reimer Soils; Winnipeg, MB, Canada), 30 cm (~1,500 L) of tap water (City of Winnipeg; Winnipeg, MB, Canada), and planted with a natural variety of northern wild rice (Floating Leaf; Sunnyside, MB, Canada) at a rate of 10 g m^{-2}. Mesocosms were constructed at the University of Manitoba (UM) field site, situated at the Prairie Wetland Research Facility at the University of Manitoba, Winnipeg, MB, Canada (49° 48’ 35.9” N, 97° 07’ 33.0 W”). The UM site mesocosms emulated natural wild rice stands. These mesocosms were established in the fall of 2021, at which point they were seeded with wild rice and underwent an overwintering period, simulating the stratification period required to break dormancy that is achieved in the natural environment throughout the winter prior to germination in the spring (Kovach & Bradford, 1992). The source water and soil used in mesocosms were analyzed for their nutrient content (see Appendix; Table A - 1, Table A - 2). Zooplankton and fathead minnows (*Pimephales promelas*) were added to mesocosms and served as components of a broader research project which evaluated the impacts of AWW on aquatic ecosystems, and aimed to assess the feasibility of wild rice and fish co-culture (Dickenson, *in preparation*; Robertson, *in preparation*). While endpoints relating to zooplankton and fathead minnows are not discussed here, the present study was designed with consideration for these other research components and together with the results presented here, inform on the broader objectives of the research project.

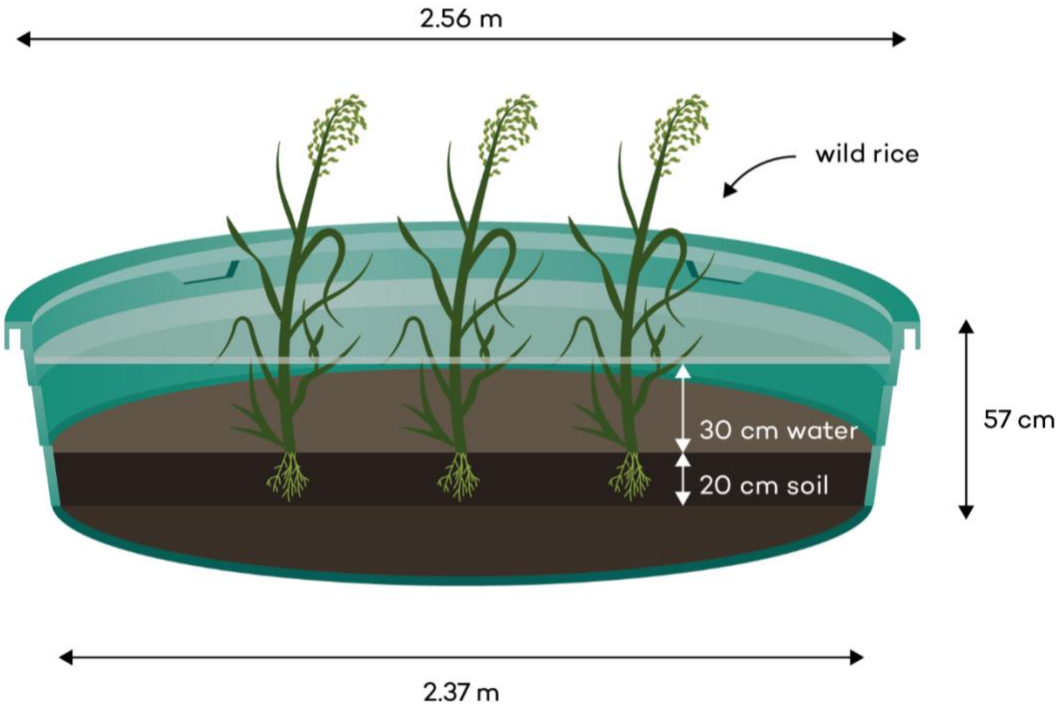

Figure 10. Schematic of a wild rice constructed wetland mesocosm with soil, water, and wild rice plants. Dimensions indicated in the figure are approximate.

2.2 Aquaculture Wastewater Collection

All AWW was collected from a local commercial aquaculture facility (Ridgeland Aquafarms; Anola, MB, Canada) rearing Arctic char (*Salvelinus alpinus*). Using a two-inch diameter pump, AWW was collected from a solid waste settling tank adjacent to the aquaculture facility. The collected AWW was a mixture comprised of both solid and liquid wastes. Collected AWW was transported to the field site where it was stored outdoors in the shade in a closed 1,000 L container. Prior to making additions of AWW to mesocosms, the AWW stock was mixed, a grab sample was collected, and submitted to a commercial laboratory (Farmers Edge Laboratories; Winnipeg, MB, Canada) for nutrient analysis. Further details surrounding the methodology used by Farmer's Edge Laboratories for the various samples analyzed as part of this manuscript are available upon request of the laboratory.

2.3 Experimental Design

The UM site consisted of 18 mesocosms, which were further divided into two types of treatment systems that were studied simultaneously (Table 4). The first type of mesocosm, referred to herein as an established wetland (EW) system, consisted of 7 mesocosms which had been previously planted with cattail (*Typha* spp.) and subjected to AWW loadings during the summer of 2021 (see Chapter 2). The second type of mesocosm, referred to herein as a new stand (NS) system, consisted of 10 mesocosms which had fresh soil added at the time of establishment in fall 2021. An additional 18th mesocosm was deployed to serve as an unplanted reference (UP-REF) that contained no wild rice and received no AWW. The UP-REF mesocosm was used to identify potential aerial sources of nutrient deposition into the mesocosms at the UM field site and to the evaluate the impacts of plants on nutrient elimination from CW water. The UP-REF mesocosm varied in its dimensions and water and soil content; it measured 1.75 m in diameter and 40 cm in height and was established with 10 cm of soil and 15 cm of water. The UP-REF mesocosm was initially established alongside the EW mesocosms and is therefore presented alongside this series of mesocosms in figures and tables, where applicable. Planted references (i.e. mesocosms that contained wild rice but received no AWW) are labelled with the corresponding type of CW system (i.e. EW or NS), a reference label (i.e. REF), and assigned a letter in alphabetical order, with the three labels separated by dashes (e.g. EW-REF-A).

Table 4. Study design details for the UM site mesocosms. Treatments are expressed as the nominal volume of aquaculture wastewater (AWW) applied to mesocosms on a biweekly basis. A total of 6 AWW addition events occurred over a period of 69 days.

Mesocosm type	Nominal biweekly addition volume (L)
Unplanted	0 (UP-REF)
EW	0 (EW-REF-A)
	0 (EW-REF-B)
	2.5
	3.9
	6.1
	9.6
	15.0
NS	0 (NS-REF-A)
	0 (NS-REF-B)
	0 (NS-REF-C)
	1.0
	1.6
	2.5
	3.9
	6.1
	9.6
	15.0

The NS mesocosms were randomly assigned to treatments, while the EW mesocosms were assigned to treatments reflective of the loadings applied in Chapter 2 in the previous year; the applied gradient of nutrient loadings ranging from low to high volumes of AWW was preserved, although a different AWW source and different nominal volumes were utilized, resulting in different nutrient loading conditions. A total of 6 AWW addition events occurred at the UM site which took place on a biweekly basis over a period of 69 days. Nominal volumes of AWW applied to mesocosms were selected to target nutrient loadings which encompassed the low end of the ranges of fertilizer additions commonly applied to wild rice in similar settings (Atkins et al., 1992; Day & Lee, 1990; Day, 1988; Kaiser & Piotrowski, 2023).

All cattail plants and other debris were removed from the EW mesocosms upon conclusion of the Chapter 2 study and were seeded with wild rice during fall 2021. However, because of their prior establishment, these mesocosms differed substantially in their appearance and contents during the summer 2022 (Figure 11). Most notably, substantial growth of hornwort (*Ceratophyllum* sp.) was observed among EW mesocosms, while the growth of filamentous algal mats was more predominate among NS mesocosms. Therefore, distinctions were made between these two types of CW systems.

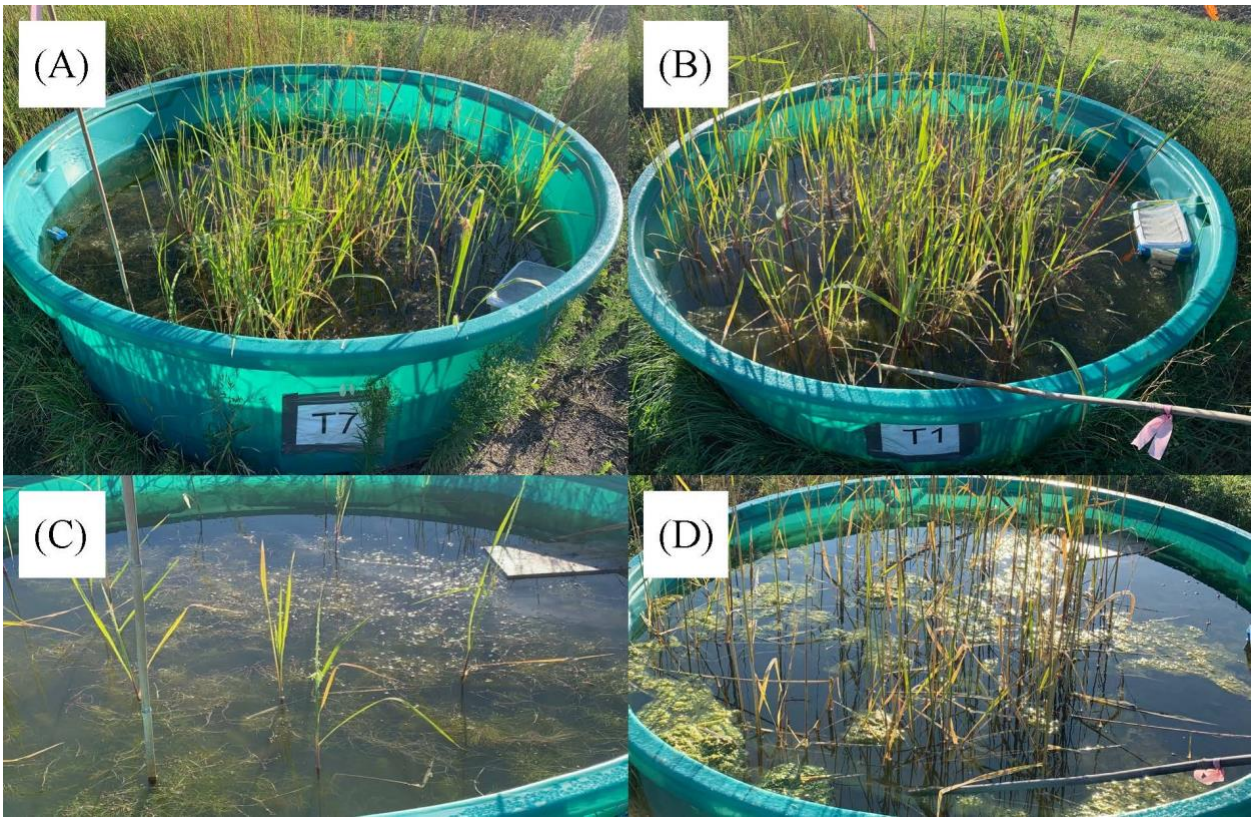

Figure 11. Photos of different constructed wetland systems at the UM site with different forms of biomass observed throughout the study. (A): EW mesocosm; (B): NS mesocosm (C): hornwort observed in an EW mesocosms; (D): algal mats observed in a NS mesocosm.

2.4 Mesocosm Sampling and Sample Analysis

Sampling in mesocosms was scheduled at regular intervals and identical sampling schedules were used for both EW and NS studies. Study days are defined with the start of the study period (i.e. day 0) beginning when initial AWW additions occurred. Important dates pertaining to the sampling of mesocosms are presented in Figure 12, with AWW additions indicated by vertical dashed lines. Initial AWW additions (i.e. day 0) occurred on June 22nd, 2022.

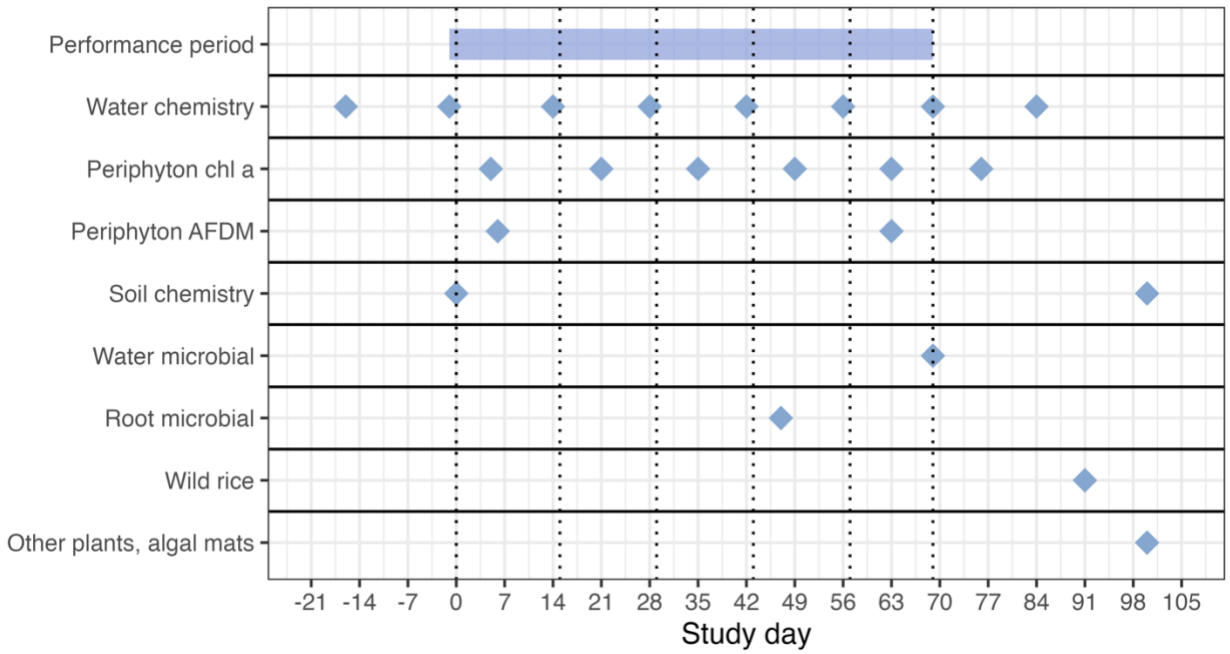

Figure 12. Timeline of sampling events at the UM field site. The first addition of aquaculture wastewater (AWW) to mesocosms is used to indicate the beginning of the study (i.e. study day 0). Vertical dashed lines indicate additions of AWW.

2.4.1 Aquaculture Wastewater Additions

Additions of AWW occurred on study days 0, 15, 29, 43, 57, and 69. Throughout the process of adding AWW to mesocosms, a large bucket containing AWW stock was stirred continuously to ensure that the aliquots distributed to mesocosms were of consistent composition (i.e. solids were

not allowed to settle). Treatment volumes of AWW were measured using a graduated cylinder and AWW was added to mesocosms by pouring the measured volume evenly across the surface area of the mesocosm. A grab sample was collected in a 250 mL polyethylene bottle from the stirred stock solution and submitted for nutrient analysis at a commercial laboratory (Farmers Edge Laboratories). An additional grab sample was collected in a 50 mL conical tube and stored at 4°C for a maximum of 72 h in the event that the 250 mL grab sample spoiled or commercial laboratory analysis was unavailable. This occurred twice for the AWW additions on day 0 and 57. For these instances, the nutrient content of AWW was determined using the 50 mL sample which was analyzed using the same methods applied to mesocosm water samples (see Section 2.4.2).

2.4.2 Water Quality

Water samples were collected on study days -16, -1, 14, 28, 42, 56, 69, and 84 (Figure 12). Water samples were collected 0–1 days prior to a corresponding addition of AWW. Throughout the study period, frequent in situ measurements of basic water quality parameters (i.e. temperature, pH, dissolved oxygen, conductivity) were taken using a handheld probe (YSI ProQuatro; Yellow Springs Instruments; Yellow Springs, OH, USA). The YSI probe was calibrated weekly for pH and specific conductance (SPC), while dissolved oxygen (DO) was calibrated in the field prior to each use. In general, measurements were collected in the morning (08:30-11:00). Temperature and light data loggers (Onset HOBO MX2202 Pendant Wireless Data Logger; Onset; Bourne, MA, USA) were installed in the centre of mesocosms, positioned 10 cm above the soil-water interface, and set to log every 20 min. The EW and NS systems had a total of 3 and 4 loggers randomly assigned to mesocosms, respectively. An additional logger was

placed at the UM field site in an open area to record light intensity without any obstruction or shade resulting from plants, soil, or the sides of mesocosms.

Water samples consisted of grab samples collected from ~10 cm below the water surface using two 500 mL Nalgene bottles. To avoid collecting excess debris, water samples were pre-screened at the time of sample collection through a 1 mm mesh secured over the mouth of sampling bottles. Sample bottles were stored on ice in a cooler in the dark and processed in the laboratory on the same day as collection. Aliquots of unfiltered samples were taken for corresponding analyses (i.e. total nutrient analyses, soluble reactive silica [SRSi]), while the remaining sample was filtered through a Whatman grade GF/C glass microfibre filter (1.2 µm effective pore size; Cytiva; Marlborough, MA, USA) and filtrate was collected for corresponding analyses (i.e. dissolved nutrient analyses). Unfiltered and filtered samples were stored in 50 mL polypropylene conical tubes at 4°C prior to further analysis, with the exception of SRSi which was stored in a 30 mL polyethylene container at room temperature. Filters for chlorophyll *a* (chl *a*) analysis were folded in half using forceps, wrapped in aluminum foil, and stored at -20°C prior to further analysis. Filters for particulate phosphorus (PP) analysis were rolled using forceps, inserted into a glass vials, and stored at room temperature prior to analysis. It should be noted that on study day 97, additional samples were collected for chl *a* and PP, but no other water chemistry endpoints were assessed and therefore this sampling event is not indicated on the timeline in Figure 12.

Total phosphorus (TP), total dissolved phosphorus (TDP), total dissolved nitrogen (TDN), and total alkalinity (Alk) were measured spectrophotometrically at University of Manitoba

laboratories with HACH kits (HACH; Loveland, CO, USA). In all cases, TP was analyzed within 8 h of sample collection. In most cases, TDP and TDN were analyzed alongside TP, however in instances where this was not possible, filtered water samples were stored at 4°C and analyses were conducted within 36 h of sample collection. Filtered water samples were also assessed at University of Manitoba laboratories for total ammonia nitrogen (TAN), nitrite-nitrogen (NO_2–N), nitrate-nitrogen (NO_3–N), and soluble reactive phosphorus (SRP) using a flow injection analyzer (Lachat QuickChem 8500, HACH) following standard methods (Rice et al., 2012). Filtered samples were stored at 4°C for a maximum of 48 h prior to analysis. Dissolved organic carbon (DOC), PP, SRSi, and chl *a* were analyzed following standard methodology (Stainton et al., 1977). DOC was analyzed using a Shimadzu total organic carbon analyzer (Shimadzu TOC-VCPH; Shimadzu, Kyoto, Japan), PP and SRSi were analyzed using a Shimadzu UV-1800 scanning spectrophotometer, and chl *a* was analyzed using a Trilogy benchtop fluorometer equipped with a chlorophyll *a* non-acidification fluorescence module (Turner Designs, San José, CA, USA). Samples collected for PP, SRSi, and chl *a* were preserved and archived throughout the study period and subsequently analyzed in the fall at the International Institute for Sustainable Development – Experimental Lakes Area (IISD-ELA) chemistry lab in northwestern Ontario, Canada. For chl *a* analysis, an extraction solution consisting of 68% methanol, 27% acetone, and 5% deionized water was used in place of the extraction solution described by Stainton et al. (1977). This modified extraction solution is implemented in the IISD-ELA chemistry laboratory for improvement of chl *a* extraction from glass microfibre filters; further details of the methodology are available upon request of the IISD-ELA chemistry lab. Any analyte concentrations measured below detection limits were set at half the laboratory limit of detection.

2.4.3 Biofilm Tiles

Each mesocosm contained unglazed ceramic tiles (1 x 1 inch) which provided a surface for biofilm growth throughout the study. A total of 50 biofilm tiles were placed in homemade floating containers which were constructed in a manner that allowed tiles to rest ~5 cm below the water surface of mesocosms (Figure 13). Homemade floating containers were made from polypropylene containers (32 x 17 x 11 cm) which had rectangles (24 x 5 cm) cut from two sides and replaced with 1 mm mesh. The mesh allowed mesocosm water to continually access the tiles while debris and other biological organisms were excluded. The centre of the floating container lids were removed and replaced with mosquito mesh which excluded debris but did not impede sunlight. Small pieces of pool noodles were fixed to the corners of the containers to provide the buoyancy required for the desired submergence of tiles below the mesocosm water surface.

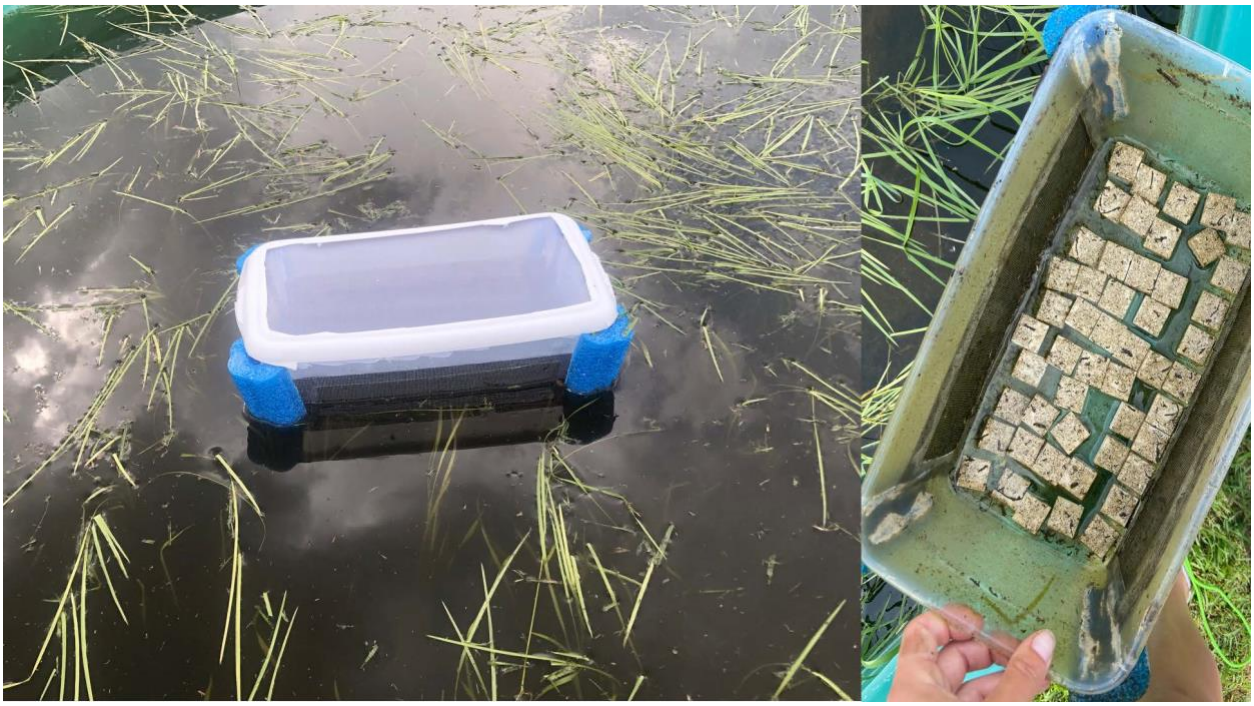

Figure 13. Homemade floating containers (left) which held ceramic tiles used to quantify biofilm growth (right).

Biofilm tiles were assessed for chl *a* on study days 5, 21, 35, 49, 63, and 76 (Figure 12). Three tiles were randomly selected from floating containers for analysis at each sampling event. The selected tiles were placed directly into a 50 mL conical tube filled with 15 mL of extraction solution (68% methanol, 27% acetone, 5% deionized water) and stored in the dark at 4°C for 24 h prior to spectroscopic analysis. Additionally, three tiles were randomly collected from floating containers for ash-free dry mass (AFDM) analysis on days 6 and 63 (Figure 12). The selected tiles were placed into Whirlpaks, transported back to the laboratory, scraped with cell lifters, and rinsed with deionized water. The biofilm removed from tiles through scraping and rinsing was frozen and stored at -20°C prior to analysis.

Biofilm chl *a* was analyzed using different instrumentation than chl *a* in water because of the need for rapid analysis of biofilm tiles; biofilm chl *a* was analyzed using an Ultrospec 4300 pro spectrophotometer based on standard methods (Jeffrey & Humphrey, 1975; Lichtenthaler & Buschmann, 2001; Wellburn, 1994). However, the following modified equation was used in the determination of chl *a* concentration:

$$\text{chl } a = 16.5(\mathrm{A}_{665} - \mathrm{A}_{700}) - 8.3(\mathrm{A}_{650} - \mathrm{A}_{700})$$

Equation 4

where chl *a* is the concentration of chl *a* in µg L^{-1}, A_{665} is the absorbance at 665 nm, A_{700} is the absorbance at 700 nm, A_{650} is the absorbance at 650 nm.

Equation 4 was implemented here to maintain consistency between the biofilm chl *a* (analyzed at the University of Manitoba laboratories) and water column chl *a* (analyzed at the IISD – ELA

chemistry laboratory). Equation 4 is used for the spectrophotometric determination of chl *a* in stock and standard solutions in the IISD-ELA chl *a* gross fluorescence method. Here, this equation was implemented in the determination of chl *a* content of biofilm tile extracts. More information on the chlorophyll *a* gross fluorescence method is available upon request of the IISD-ELA chemistry lab.

Frozen AFDM tile contents were thawed, filtered through pre-ashed (400°C for 10 h) and pre-weighed Whatman GF/C filters. The retained biomass was rinsed with deionized water, dried in an oven at 105°C for 24 h, weighed, ignited at 500°C for 12 h in a muffle furnace, and then weighed again (Rice et al., 2012). The sample AFDM was then calculated as the difference between the mass of the dry filter before ignition and the mass of the filter after ignition. Final results were expressed relative to surface area by dividing the AFDM by the surface area of a biofilm tile (i.e. 1 square inch, or 6.45 cm^2). Tiles collected at the beginning of the experiment (i.e. day 5) contained very little biofilm and therefore three tiles were pooled to achieve sufficient sample mass for the gravimetric analysis.

2.4.4 Soil

Background soil samples were collected prior to AWW additions on day 0 (Figure 12). Additionally, soil samples were collected several weeks after AWW additions had ended, on day 100. Composite soil samples for each mesocosm were made by combining grab samples collected from the top 10 cm of soil at 10 locations evenly distributed across the surface area of the mesocosm. Samples were freeze-dried for a minimum of 48 h to remove water, then submitted to a commercial laboratory for nutrient analysis (Farmer's Edge Laboratories).

2.4.5 Microbial

Microbial samples of mesocosm water were collected on day 69 (Figure 12). A 500 mL grab sample of mesocosm water was collected from ~10 cm below the surface, stored on ice in a dark cooler and transported back to the laboratory. A 200 mL aliquot of the water sample was filtered (Whatman GF/C) within 2 h of sample collection. Filtrate was discarded and filters were immediately placed into extraction buffer for analysis. Total adenosine triphosphate (tATP) in samples was measured using 2nd generation ATP testing (LuminUltra, 2023). Deposit & Surface Analysis (DSA) test kits (LuminUltra; Fredericton, NB, Canada) were used according to the manufacturer's instructions for biofilm collectors (LuminUltra, 2017) and fluorescence was measured using a PhotonMaster luminometer (EQP-PAC-PMT, LuminUltra).

Root microbial samples were collected on day 47 (Figure 12). A total of three plants were randomly selected from each mesocosm and one root was removed from each plant, for a total of three samples. Roots were placed directly into extraction buffer for analysis. Between samples, equipment was cleaned with 70% ethanol and rinsed with deionized water. Samples were stored in the dark, transported to the laboratory, and analyzed within 2 h of sample collection. The tATP in samples was measured using DSA test kits following the manufacturer's instructions for measured deposits (LuminUltra, 2017). However, rather than weighing samples prior to analysis, roots were removed from sample tubes using forceps and fresh weight was collected after the analysis was completed. The mean tATP of the three root samples was taken for use in statistical analyses.

2.4.6 Plant Tissues and Algal Mats

Plant tissue samples of wild rice plants were collected on day 91 (Figure 12). A total of 20 plants were collected from each mesocosm; plants were carefully pulled from mesocosm soil, and divided up into aboveground (AG; i.e. shoots and leaves) and belowground (BG; i.e. roots) portions. Collected BG portions were rinsed in mesocosm water to remove excess soil. Prior to bundling, the length of AG shoots was recorded. In instances where fewer than 20 plants could be collected, the total number of plants in the mesocosm was recorded and all of the plants in the mesocosm were collected as a representative sample. Plant bundles were weighed, dried at 25°C for 3 weeks in a drying room, then weighed again. Dried bundles were submitted to a commercial laboratory (Farmer's Edge Laboratory) where they were homogenized by grinding prior to nutrient content analysis.

Decommissioning of mesocosms occurred on day 100. This involved the removal of all remaining plants and algal mats from the mesocosms. Wild rice plants were removed from soil with roots still attached, rinsed in mesocosm water to remove excess soil, combined, and fresh weight was recorded. Mesocosms also contained algal mats and hornwort, which were removed from mesocosms, squeezed to remove excess water, and then weighed. Mesocosms were raked by hand to collect any additional remaining plant or algal biomass. Subsamples of hornwort and algal mats collected from the mesocosms were processed and analyzed for nutrient content in an identical manner to wild rice plant bundles.

2.4.7 Mesocosms Water Volume and Surface Area Estimations

To account for variations in both the physical dimensions and water depths of mesocosms in mass-based analyses, mesocosm water volumes were estimated using the geometric formula for a cylinder alongside measured concentrations of analytes. An initial water depth was determined by taking the mean of 25 depth measurements evenly distributed across the surface area of the mesocosm. The diameter of each mesocosm was also measured to account for potential size variations. The upper (measured at the water surface) and lower (measured at the soil-water interface) diameters were verified to be in agreement (within 1.5%) and therefore the geometric formula for the volume of a cylinder was applied. A reference water depth location was established in each mesocosm that was measured routinely throughout the duration of the study. The depth at this reference location was mathematically related to water volume, allowing for estimates of water volume in each mesocosm to be made. The water depths in all mesocosms were maintained at ~30 cm by adding water as needed throughout the duration of the study. The upper diameter of mesocosms measured as part of this process were used to determine CW surface area with the geometric formula for the area of a circle. Two styles of mesocosms were used for planted mesocosms which resulted in two possible values for upper diameter: 2.19 or 2.46 m. The surface areas of CWs is presented in the Results and Discussion (see Section 3.2; Table 7).

2.5 Nutrient Loading Calculations

Nutrient concentrations in AWW were determined by multiplying the raw reported concentrations (reported on a mass basis in mg kg^{-1}) by the density of the sample. Nutrient concentrations in AWW were then multiplied by the nominal volume of AWW added to

mesocosms to determine nutrient loadings. There were two instances where TKN was not measured in AWW samples (i.e. days 0 and 57). For these samples, the mean TKN concentration of the AWW source was used in the determination of nutrient loadings. Total nutrient loadings for a given nutrient parameter were calculated as the sum of all masses added via AWW additions and normalized to the surface area of the mesocosm, and are expressed in units of mg m^{-2}.

2.6 Constructed Wetland Performance Parameters

To assess CW performance, a 70-day period referred to herein as the "performance period" was defined during which TP data was analyzed in mesocosm water (Figure 12). The performance period spanned from study days -1 to 69. The final AWW addition event (i.e. the 6th addition) made on day 69 was not considered in calculations because no mesocosm water TP data was available for the subsequent sampling event on day 84. Therefore, the nutrient loadings values for the performance period (which were subsequently used for the analysis of CW performance) differed from the total nutrient loadings for the entire study period. Both values (i.e. nutrient loadings for the performance period and the nutrient loadings for the entire study period) are included in the presentation of CW performance results to avoid confusion in the interpretation of results and to facilitate comparison with other endpoints. All CW performance parameters were assessed over the 70-day performance period using the calculated TP concentrations in mesocosm water if no elimination was achieved (C_{max}), final TP concentration measured in mesocosm water on day 69 (C_f), concentration reduction (CR) of TP, phosphorus load removal (PLR), and hydraulic loading rate (HLR). A summary of the CW performance parameters

including the equations used in the calculations is presented in Table 5. Performance parameters were derived and modified from those presented by Kadlec (2016).

Table 5. Calculation details for performance parameters of constructed wetlands (CWs) implemented in the treatment of total phosphorus (TP) in aquaculture wastewater (AWW). Initial (i) and final (f) measurements refer to study days -1 and 69, respectively.

Parameter	Parameter Abbreviation	Equation	Equation details
Calculated concentration of TP if no elimination was achieved	C_{max}	$\frac{\text{mass TP}_{\text{water,i}} + \text{mass TP}_{\text{AWW}}}{V_f}$	V = mesocosm water volume
Final measured concentration of TP	C_f		Directly measured; no equation
Concentration reduction	CR	$\frac{C_{max} - C_f}{C_{max}}(100\%)$	Reported on a percentage basis
Phosphorus load reduction	PLR	$\frac{(\text{mass TP}_{\text{water,i}} + \text{mass TP}_{\text{AWW}}) - (\text{mass TP}_{\text{water,f}})}{(A)(70\ \text{d})}$	A = CW surface area 70 d = duration of performance period
Hydraulic loading rate	HLR	$\frac{\text{AWW loading rate}}{A}$	AWW loading rate = mean volume of AWW applied to CW per unit time A = CW surface area

2.7 Mass Balance Analysis

Mass balance calculations were made by multiplying the estimated volume or mass of a given matrix (i.e. soil, water, plant, algal mat) by the measured concentration of TP. However, depending on the matrix, additional considerations were required.

Water volume estimates were made at each sampling event (details described previously in Section 2.4.7) and were multiplied by the corresponding measured concentration value for TP to determine the total mass of TP in mesocosm water.

Soil volumes were approximated by collecting 10 measurements of soil depth across the surface area of the mesocosm. The mean of the 10 measurements was used to estimate volume with the geometric formula for the volume of a cylinder (in a similar manner to how water volumes were estimated). Additionally, soil nutrient chemistry was reported on a dry mass basis and therefore the soil density was empirically derived for both wet and dry soil (see Appendix; Table A - 2). The mass of wet soil in mesocosms was estimated using the wet soil density and the wet soil volume derived through the 10 depth measurements. A dry mass equivalent of soil was then calculated using the moisture content measured in soil. The dry mass estimate of soil was then multiplied by nutrient concentrations to determine the total mass of TP in mesocosm soil.

For wild rice plants, an estimate of the AG:BG biomass ratio was made using the collected bundles of AG and BG wild rice tissues. This ratio was then applied to the total fresh biomass of wild rice measured during the decommissioning of mesocosms to provide an estimate for the total AG and total BG fresh wild rice biomass. Corresponding estimates for wild rice dry

biomass were then made using the measured moisture content of plant bundles. Hornwort and algal mats were also analyzed in a similar manner except no delineations were required between AG and BG biomass. In other words, the moisture content of collected subsamples was applied to the total fresh biomass measured during takedown to provide an estimate of total dry biomass for hornwort and algal mats. The TP content measured in dry biomass was then multiplied by the corresponding dry biomass estimate to determine the total TP of biomass in mesocosms.

2.8 Statistical Analysis

All statistical analyses were performed in R version 4.1.1 (R Core Team, 2021) with tidy data approaches (Wickham et al., 2019). Data visualizations were performed using ggplot2 (Wickham, 2016). A significance level (alpha) of 0.05 was used for all statistical tests and data are presented as mean ± standard deviation (SD) where applicable, unless otherwise stated.

2.8.1 Water Quality

The differences in water quality endpoints among treatments over time were assessed using linear mixed models (LMMs) with the following model structure: y ~ Treatment + Time + Treatment x Time + (1|Mesocosm), where y was a water quality endpoint (the response variable), Treatment and Time were the fixed effects, Treatment x Time was the interaction effect, and (1|Mesocosm) was the random effect accounting for the repeated sampling of each mesocosm over time. Treatment was defined as a continuous predictor for the total TP loading applied to the mesocosms via AWW additions (in units of mg m^{-2}), Time was defined as a continuous predictor for study day, and Mesocosm was defined as a categorical factor according to an assigned arbitrary label for each mesocosm. By design, AWW loadings followed a

logarithmic scale, and therefore treatments were always $\log_{10}$ transformed to help meet the assumption of linearity in fitted models. Additionally, a constant was added prior to the $\log_{10}$ transformation of treatment to address the zero values for nutrient loading among reference mesocosms. In the interest of preserving a common model specification for a given CW system, a constant was identified for each CW type and systematically applied to all fitted models for that CW type. Constants were derived from the y-intercept of the line-of-best-fit generated from the linear regression of treatment loadings evenly distributed in logarithmic space (Figure 14). The constants generated from this procedure were compared to other common practices (e.g. half the smallest nonzero value) and found to offer improvements in meeting model assumptions, particularly the assumption of linearity. The resulting constants applied to TP loadings prior to log-transformation were 89.6 and 42.9 for the EW and NS systems, respectively. LMMs were fit using the nlme package for R (version 3.1-158; Pinheiro & Bates, 2000; Pinheiro et al., 2022) and the residuals of fitted models were inspected to verify model assumptions. In cases where model assumptions were not satisfied, a $\log_{10}$ transformation was applied to the response variable and model assumptions were rechecked.

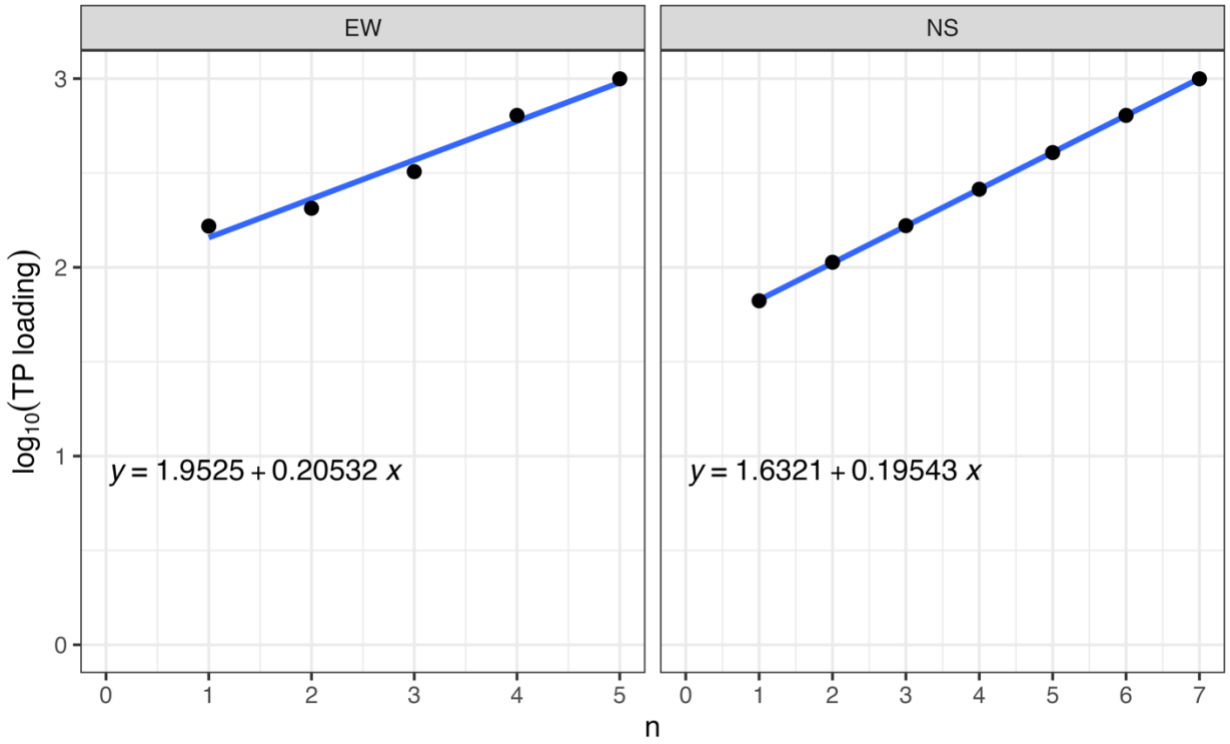

Figure 14. Logarithmic total phosphorus (TP) loadings from aquaculture wastewater additions evenly distributed for each mesocosm type (i.e. EW, NS). Constants used in data transformations were derived from the y-intercept of the line-of-best fit (solid blue lines).

The Treatment-Time interaction effect was of primary interest and included in all LMMs where applicable (Paine, 1996). When significant results were detected for the interaction term (i.e. Treatment x Time), a post hoc interaction analysis was conducted using the emmeans package in R (version 1.7.5; Lenth, 2022). For this analysis, study day (Time) was treated as a factor and the covariate trend was assessed at each level of the factor. A pairwise contrast of covariate trends for each study day was performed with a Tukey adjustment for multiple comparisons using the emmeans and emtrends functions of the emmeans package. Statistically significant interactions were visualized using interaction plots generated with the emmip function of the emmeans package. Temperature, DO, pH, and SPC were all measured with much greater frequency than other water quality endpoints, resulting in a large number of pairwise contrasts. Therefore, these

endpoints had the mean value of consecutive groupings reported in instances where three or more statistically significant contrasts occurred in succession.

2.8.2 Biofilm Growth Curves

Biofilm chl *a* was modelled using logistic growth curves with the growthcurver package in R (version 0.3.1; Sprouffske, 2020). Growth curve parameters were optimized among fitted logistic growth curves following a standard logistic growth equation:

$$P_t = \frac{P_0 K}{P_0 + (K - P_0)e^{-rt}}$$

Equation 5

where P_t is the biofilm chl *a* concentration at time t, P_0 is the initial biofilm chl *a* concentration, K is the carrying capacity, and r is the growth rate.

Additionally, the goodness of fit of the parameters in the logistic growth equation (σ) and the time where half-K was reached (t_{mid}; i.e. the inflection point) were also calculated using the growthcurver package.

2.8.3 Other Endpoints

General linear models were used to assess soil quality endpoints (i.e. Olsen P [OP], K, S, Ca, Mg, Na, B, Cu, Fe, Mn, Zn, Cl, pH, electrical conductivity [EC], organic matter [OM], cation exchange capacity [CEC]) and plants tissue endpoints (i.e. TN, NO_3–N, K, total S [TS], Ca, Mg, B, Cu, Fe, Mn, Zn). In an identical manner to LMMs (described previously in Section 2.6.1), the predictor variable used in general linear models involved a $\log_{10}$ transformation of TP loadings

with the addition of the unique constant for each mesocosm type. Model assumptions were verified by inspecting the residuals of fitted models. When required, $\log_{10}$ transformations were applied to response variables to meet model assumptions.

3.0 Results and Discussion

3.1 Aquaculture Wastewater Chemistry

Concentrations of TP, TAN, and total Kjeldahl nitrogen (TKN) as well as density and pH were consistent throughout the use of collected AWW (Figure A - 1). The mean (± SD) values for TP, TAN, TKN, density, and pH are presented for the AWW collection throughout its usage in Table 6. The TKN analysis does not include nitrite or nitrate, and therefore a sample of AWW was analyzed on three occasions for TAN, NO_2–N, and NO_3–N and was found to contain mean (± SD) concentrations of 267.917 ± 34.011, 2.975 ± 0.254, and 10.383 ± 1.406 mg L^{-1}, respectively. In other words, NO_2–N and NO_3–N concentrations in AWW were approximately 1% and 4% the corresponding TAN value, respectively. Therefore, it can be assumed that TKN ≈ TN, an assumption that has been made in other aquaculture studies (Lekang et al., 2000).

Table 6. Mean (± SD) total phosphorus (TP), total ammonia nitrogen (TAN), total Kjeldahl nitrogen (TKN), density, and pH in aquaculture wastewater (AWW) added to UM site mesocosms. Samples were analyzed at room temperature (20–25°C).

Number of samples	TP (mg L^{-1})	TAN (mg L^{-1})	TKN (mg L^{-1})	Density (g mL^{-1})	pH
9	43.0 (5.8)	229.2 (44.6)	296.2 (132.6)*	0.998 (0.001)	7.58 (0.09)*

*A reduced sample size (n = 6) was used to calculate mean and standard deviation because of missing data

When considering TAN concentrations and nutrient loadings, it is important to consider the equilibrium between the unionized form (ammonia; NH_3) and the ionized form (ammonium; NH_4^+) of ammonia nitrogen. This equilibrium is a key consideration in ecological risk assessments (Constable et al., 2003; Wang et al., 2020) and in the management of aquaculture systems (Rogers & Klemetson, 1985; Tomasso, 1994) because of how ammonia nitrogen, particularly unionized ammonia, is toxic to aquatic biota (Eddy, 2005; Mummert et al., 2003; Neil et al., 2005). For instance, water quality standards of <0.02 mg L^{-1} NH_3 and <1.0 mg L^{-1} TAN have been established in aquaculture systems to maintain the health of rearing fish (Lawson, 1995). As pH and temperature increase, ammonia toxicity rises because of the equilibrium shifting to favour the presences of additional unionized ammonia (Wurts, 2003). In fact, within the pH range suitable for most freshwater fish, an increase in pH by one unit corresponds to a ten-fold increase in unionized ammonia concentrations (Thurston et al., 1981). However, relative to the total water volume in CWs, the volume of AWW applied to CWs was small. Therefore, substantial dilution of AWW occurred following additions into CWs and the resultant pH in the mesocosm water dictated the chronic exposure conditions to which the

resident biota of the CW mesocosms were subjected. However, for example, at 20°C and a pH of 7.6, a 1.55% fraction of TAN in AWW would exist in the unionized form (Durborow et al., 1997; Emerson et al., 1975). With very high TAN concentrations (often >200 mg L^{-1}) measured in AWW, corresponding unionized ammonia concentrations would be >3.1 mg L^{-1}. In the short term, the additions of high quantities of unionized ammonia could contribute to acute toxicity. In smaller volume systems without the capacity for dilution or in scenarios where AWW effluents are being discharged on a continual or semi-continual basis (e.g. in open or semi-closed aquaculture systems; Lawson, 1995) there exists greater potential for ammonia toxicity in the receiving environment. Among all AWW samples, TAN, and not organic nitrogen, was the major fraction comprising TKN. The mean organic nitrogen concentration in AWW (i.e. the difference between TKN and TAN) was 67.0 mg L^{-1}. Throughout the use of the AWW, TAN generally comprised upwards of 75% of the corresponding TKN value. Therefore, ammonia loading into CWs was substantial, creating a risk of ammonia toxicity for resident biota.

The nutrient content of aquaculture effluents can be highly variable and is largely impacted by site-specific processes (e.g. flushing rates, production scale, management practices) and the considerations for discharged effluents vary with the assimilative capacity of the receiving environment (Fernandes et al., 2001; Walker et al., 2003). In a survey of land-based fish farm effluents in Atlantic Canada, Lalonde et al. (2015) sampled effluents from 14 different aquaculture facilities (including one facility raising arctic char) and found ranges of 0.005–0.727 mg L^{-1} for TP, 0.28–4.73 mg L^{-1} for TN, 0.015–2.776 mg L^{-1} for ammonia, and 5.5–7.7 for pH. Effluent characterizations of facilities rearing Arctic char are limited, however Lekang et al. (2000) reported TP concentrations of 3.300 mg L^{-1} and TN concentrations of 2.5 mg L^{-1} in the

initial untreated wastewater of a land-based char farm, and Snow (2007) sampled AWW from a facility rearing Arctic char in Atlantic Canada and reported TP, SRP, TAN, NO_2–N, and NO_3–N concentrations of 6.30, 4.49, 2.08, 1.27, and 21.64 mg L^{-1}, respectively. Meanwhile, Eikebrokk and Ulgenes (1993) investigated TP and TN concentrations of untreated effluents from an Atlantic salmon (*Salmo salar*) farm. Their results demonstrated how nutrient concentrations in the untreated AWW increased when tank flushing was used due to the sudden release of accumulated organic matter within the tanks. Compared to tanks under normal operation – when water is flowing continuously through tanks without any flushing – the concentrations of nutrients that resulted from tank flushing were elevated and more variable. Tank flushing was found to remove as much as 97, 84, and 86% of the suspended solids (SS), chemical oxygen demand (COD), and TP from tanks, respectively. For example, at one sampling timepoint the mean TP, TN, SS, and total organic carbon (TOC) in untreated AWW from tanks operating normally was 0.13, 0.65, 4.4, and 3.4 mg L^{-1}, respectively. Meanwhile, in tanks where flushing was performed, mean TP, TN, SS, and TOC concentrations were 2.73, 5.02, 58, and 7.3 mg L^{-1}, respectively. Ultimately, the release of nutrients from fish farm tanks into AWW can be as high as 80–90% during periods of flushing (Eikebrokk & Ulgenes, 1993).

With broad ranges of nutrient concentrations in AWW arising from different farming practices, sampling methods, and wastewater treatment strategies, it is difficult to compare the AWW of the present study to literature values. However, it should be noted that AWW used in the present study was collected focusing on solids that could have increased the quantity of nutrients per unit volume. This method facilitated the transport of AWW to field sites and avoided cumbersome additions of large nominal volumes of AWW to achieve desired nutrient loadings. The

assessment of nutrient content of AWW sources in Table 6 is not intended to be representative of the nutrient concentrations of discharged effluent from a fish farm. Instead, it is used for the determination of nutrient loadings applied to CW mesocosms.

3.2 Resultant Nutrient Loadings in Mesocosms

The study designs for both studies, including both nominal volumes of AWW and the resulting total nutrient loading rates, are presented in Table 7. A correlation matrix comparing the TP, TAN, and TKN nutrient loadings in Table 7 was computed for each mesocosm type (i.e. EW and NS) and nutrient loadings were highly correlated ($R^2 > 0.999$) in all cases. For simplicity in model fitting, presentation of results, and comparisons between various analyses, the TP nutrient loading was applied as a representative indicator of treatment and used as a predictor variable in fitted models and data visualizations. Unless otherwise stated, nutrient loading treatments are referred to by, and presented as, the total TP nutrient loading (in units of mg m^{-2}) resulting from AWW additions throughout the study period with the exception of reference mesocosms which follow the alphabetical labelling system previously described in Section 2.3.

Table 7. Nominal volumes of aquaculture wastewater (AWW) added to UM site mesocosms with the corresponding mesocosm surface area, and the resulting total phosphorus (TP), total ammonia nitrogen (TAN), and total Kjeldahl nitrogen (TKN) loadings. Additions of AWW occurred over a period of 69 days. Unique labels for reference mesocosms are included in the TP loading column.

Mesocosm type	Total AWW added (L)	Surface area (m^2)	TP (mg m^{-2})	TAN (mg m^{-2})	TKN (mg m^{-2})
EW	0.0	4.753	0.0 (EW-REF-A)	0.0	0.0
	0.0	4.753	0.0 (EW-REF-B)	0.0	0.0
	15.0	3.767	165.4	945.1	1383.5
	23.4	4.753	205.5	1123.2	1521.1
	36.6	4.753	321.5	1756.7	2379.2
	57.6	3.767	638.4	3488.4	4724.3
	90.0	3.767	997.5	5450.6	7381.8
NS	0.0	3.767	0.0 (NS-REF-A)	0.0	0.0
	0.0	3.767	0.0 (NS-REF-B)	0.0	0.0
	0.0	3.767	0.0 (NS-REF-C)	0.0	0.0
	6.0	3.767	66.5	363.4	492.1
	9.6	3.767	106.4	581.4	787.4
	15.0	3.767	166.3	908.4	1230.3
	23.4	3.767	259.4	1417.1	1919.3
	36.6	3.767	405.7	2216.6	3001.9
	57.6	3.767	638.4	3488.4	4724.3
	90.0	3.767	997.5	5450.6	7381.8
Unplanted	0.0	2.138	0.0 (UP-REF)	0.0	0.0

In a greenhouse study, Walker et al. (2010) subjected individual wild rice plants to fertilizer applications of 0, 2.39, 4.78, 9.55, and 14.33 g m^{-2} N and 0, 0.87, 1.74, 3.47, 5.21 g m^{-2} P. Meanwhile in natural settings, Atkins et al. (1992) fertilized small quadrats of a wild rice stand with treatments ranging from 0-420 kg ha^{-1} N (0-42000 mg m^{-2} N) and 0-210 kg ha^{-1} P (0-21000 mg m^{-2} P) to determine the optimum fertilization rate considering costs and the resulting plant densities. However, when the optimum rate of 210 kg ha^{-1} N (21000 mg m^{-2} N) and 105 kg ha^{-1} (10500 mg m^{-2}) was applied to large plots of wild rice stands in a whole-lake setting, severe plant mortalities occurred. In other fertilization trials simulating natural wild rice stands, Day and Lee (1990) used N additions of either 200 or 800 kg ha^{-1} N (20000 or 80000 mg m^{-2} N), and P additions of either 30, 67, 120, or 268 kg ha^{-1} P (3000, 6700, 12000, or 26800 mg m^{-2} P). Melanson and Payne (1988) conducted a multiyear nutrient enrichment study in a freshwater lake in Nova Scotia, Canada. The experimental areas were fertilized with urea and phosphate at a 10:1 N to P ratio, targeting concentrations of 2 mg L^{-1} in the lake. Wild rice was introduced into the lake one year after fertilizations began and plants were successfully established in fertilized areas (mean TP concentration of 0.214 mg L^{-1}), but did not survive in the unfertilized control areas (mean TP concentration of 0.011 mg L^{-1}). The use of large P application rates in these fertilization studies was intentional to prevent potential P limitations and optimize biomass production. The environmental impacts of these fertilizer application rates were not evaluated. Additionally, these studies often utilized flocculant sediments which are known to be unproductive and require additions of phosphorus to rectify deficiencies and achieve suitable wild rice production (Day, 1988). Future research suggestions reflect the need to assess the environmental effects of fertilizing wild rice systems with high quantities of nutrients (Atkins et al., 1992; Day & Lee, 1990).

Concerns surrounding water quality apply to both wild rice producers and regulatory agencies; water quality will determine the suitability of wild rice production, and high-nutrient water discharged from wild rice systems can have detrimental ecotoxicological effects (Oelke et al., 1982). The excessive N and P generated from agricultural activities are widely recognized for their significant contribution to nutrient enrichment in receiving environments, ultimately leading to eutrophication which can threaten the health of aquatic ecosystems (Benoy et al., 2016; Daniel et al., 1998; Schindler et al., 2012). Meanwhile, further nutrient release from sediments is influenced by the decomposition of organic matter (Sain, 1984; Twilley et al., 1985), turbulent mixing (Boström, 1984), and microbial processes (Johnston, 1991). For instance, in eutrophic lakes that support high macrophyte biomasses, sediments can be reduced and release P over time, resulting in large P fluxes from the littoral zone (Carpenter & Lodge, 1986). Similarly, organic soils in wild rice fields can release substantial quantities of nutrients into the water column, resulting in both economic losses of fertilizer and adverse environmental impacts (Oelke et al., 1982). The top dressing of P through fertilizer applications facilitates its entry into the water column and therefore recommendations highlight the benefits of incorporating fertilizer into soils and the need to calibrate fertilizer additions according to initial soil nutrient content (Oelke et al., 1982).

A primary objective of the present study was to evaluate the feasibility of pairing wild rice production with fish farming. Surface applications of AWW were used to simulate the direct application of effluents from land-based fish farming facilities. In response to the high nutrient concentrations and density in source soil (Table A - 2), and in consideration for the overall objectives of the project, AWW was not incorporated into soil prior to seeding. Moreover,

incorporation of AWW throughout the growing season would not be feasible without causing major disturbance to the plants and the entire CW system. To minimize the potential impacts that may accompany non-incorporated fertilizer additions (e.g. eutrophication) while still applying fertilizer for enhancing wild rice production, lower nutrient loading treatments were applied to EW and NS systems. To contextualize the loadings applied in the present study, a comparison was made to the common waste loading of fish farms rates reported by Hennessy et al. (1996) (Table 8). The mean waste loading rate reported by Hennessy et al. (1996) for TP was 9.55 kg t $fish^{-1}$ yr^{-1}. Utilizing this rate, the range of AWW additions of the EW and NS studies achieved equivalent nutrient loadings to the waste produced by 344.1–2075.7 g and 138.4–2075.7 g of fish, respectively. Large-scale CWs utilized for the treatment of phosphorus are often >50 ha in size (Kadlec, 2016), which equates to over 100,000 times to size of the CWs utilized here (surface area of 3.767–4.75 m^2; Table 7). These results indicate that upscaling the treatment systems and study design implemented here could effectively treat the waste loadings from several tonnes of fish produced on a commercial scale.

Table 8. Total phosphorus (TP) loadings in UM site mesocosms with an estimate of fish quantities required to produce equivalent TP loadings. Fish waste TP production was assumed to occur at a rate of 9.55 kg t fish^{-1} yr^{-1} (Hennessy et al., 1996).

Mesocosm type	TP loading (mg m^{-2})	TP loading rate (mg d^{-1})	Mass of fish (g)
EW	0.0 (EW-REF-A)	0.0	0.0
	0.0 (EW-REF-B)	0.0	0.0
	165.4	9.0	344.1
	205.5	14.2	539.7
	321.5	22.1	844.1
	638.4	34.9	1328.4
	997.5	54.5	2075.7
NS	0.0 (NS-REF-A)	0.0	0.0
	0.0 (NS-REF-B)	0.0	0.0
	0.0 (NS-REF-C)	0.0	0.0
	66.5	3.6	138.4
	106.4	5.8	221.4
	166.3	9.1	345.9
	259.4	14.2	539.7
	405.7	22.1	844.1
	638.4	34.9	1328.4
	997.5	54.5	2075.7
Unplanted	0.0 (UP-REF)	0.0	0.0

3.3 Response of Constructed Wetland Systems to Aquaculture Wastewater

Individual subsections are presented below for each CW system. While an independent presentation of results is included for each CW system, to avoid redundancy in the discussion, subsequent sections often reference explanations from earlier sections. A final concluding section (Section 3.3.3) provides a comparison of EW and NS systems.

Plots of individual parameters not presented here are included in the Appendix. The response of main phosphorus species (TP, TDP, SRP), nitrogen species (TDN, TAN, NO_2-N, NO_3-N), and algal species (as chl *a*) throughout the study were of particular interest for an assessment of water quality responses, evaluation of CW performance, and determination of treatment capacity.

However, assessments of other parameters such as temperature and light conditions in CWs were also made. The subsequent sections provide visualizations and discussions of these key water quality parameters, as well as present the results from LMMs and interaction analyses. In instances where multiple parameters were plotted simultaneously (e.g. main phosphorus species), plots for each individual parameter is also included in the Appendix to provide more detail into trends associated with water quality parameters, ensuring trends are discernible when viewed collectively and in isolation.

3.3.1 Established Wetland Systems

3.3.1.1 Temperature and Light Data Loggers

Results from data loggers which measured water temperature and light intensity in mesocosms are plotted in Figure 15. Diurnal changes in water temperature are evident in Figure 15 with a mean daily change in temperature of 7.0°C. Mesocosms were situated aboveground and had a large surface area exposed to the surrounding environment. Systems with large surface areas relative to their total water volume are particularly susceptible to temperature fluctuations arising from changing air temperatures in the surrounding environment. Meanwhile the UM air logger, which was placed on the edge of the UP-REF mesocosm, experienced extreme fluctuations with daily changes in temperature often >20°C. The surface temperature of the mesocosm material appears to have resulted in inaccurately high measurements for air temperature. However, the primary purpose of the UM air logger was to characterize light conditions at the field site, rather than ambient air temperature.

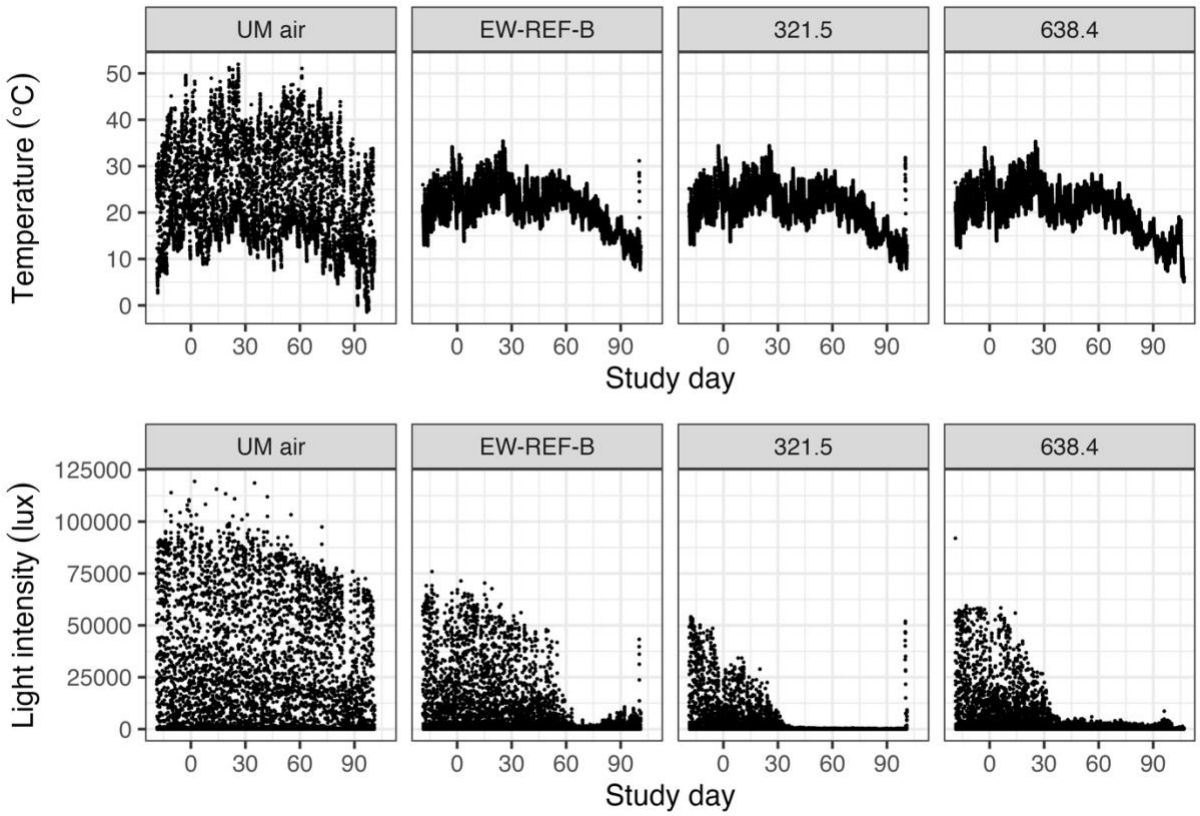

Figure 15. Temperature and light intensity data from loggers placed outside of mesocosms (UM air) and in select EW mesocosms. Loggers were set to record data every 20 min. Each graphical panel presents the data from one logger with the total phosphorus loading from aquaculture wastewater indicated in units of mg m^{-2} where applicable.

A decline in water temperature was observed after day 70 (i.e. August 31st, 2022; Figure 15). Data loggers provided additional resolution and an extended monitoring period not represented by YSI measurements for water temperature (Figure A - 13). In CWs, seasonal variations in temperature impact plant-mediated processes which can impact performance (Stein & Hook, 2005). Wild rice growth is known to be impacted by water temperature (Lee & Stewart, 1981) and the production of biomass is directly related to nutrient removal in CWs, as has been demonstrated in other studies (Abbasi et al., 2019; Kyambadde et al., 2005; Vymazal, 2020).

Data loggers inside mesocosms were positioned ~10 cm above the soil-water interface. In addition to the mesocosm walls themselves, various forms of biomass proliferated in EW systems and contributed to shading. In particular, hornwort proliferated substantially throughout the water column (see Section 3.3.1.9; Figure 28) and obstructed light loggers. A steep decline in light intensity corresponds to the proliferation of hornwort (Figure 15); in the 321.5 and 638.4 mg m^{-2} treatments, very little to no light intensity was recorded from day 40 onward, while in EW-REF-B very little to no light intensity was recorded from day 60 onward. Shading can substantially impact algal growth in mesocosms (Li et al., 2011) and while excessive algal growth can negatively impact CW functionality, healthy biofilms can act to improve CW performance (Badhe et al., 2014). Periphyton and phytoplankton communities directly impact P cycling in CWs which can have beneficial impacts for wastewater treatment (Vymazal, 2007). Despite the low light intensity recorded by loggers in CWs, notable biofilm (Section 3.3.1.4) and algal mat (Section 3.3.1.9) growth was observed, suggesting light conditions at the air-water interface or in the upper portions of the water column were able to support algal growth.

When nutrient limitations are resolved, full sunlight can increase the production of total wild rice biomass (Sims et al., 2012). In the present study, mesocosms were positioned in an open area without shading from nearby obstacles and therefore the UM air logger received full sunlight. During the early development of wild rice when plants are below (i.e. emergence stage), or just above, the surface of the water (i.e. floating leaf stage), light conditions for plants may have been impacted by the surrounding mesocosms walls and by turbidity in the water column. When comparing light conditions at the start of the study period prior to biomass proliferation, the difference in light intensity between the UM air logger and loggers within mesocosms suggests

that some reductions in light intensity occurred (Figure 15). However, the observed growth throughout the study suggests that these impacts did not substantially impact biomass production.

3.3.1.2 Phosphorus in Mesocosm Water

The concentrations of main P species (i.e. TP, TDP, SRP) in mesocosm water are presented in Figure 16. To facilitate comparisons between different P analyses, all results are reported and discussed as PO_4–P. Generally, TP concentrations were below 0.1 mg L^{-1}, with the exception of the 321.5 and 638.4 mg m^{-2} treatments where TP and TDP concentrations were generally 0.25-0.30 mg L^{-1} during the second half of the study period (Figure 16).

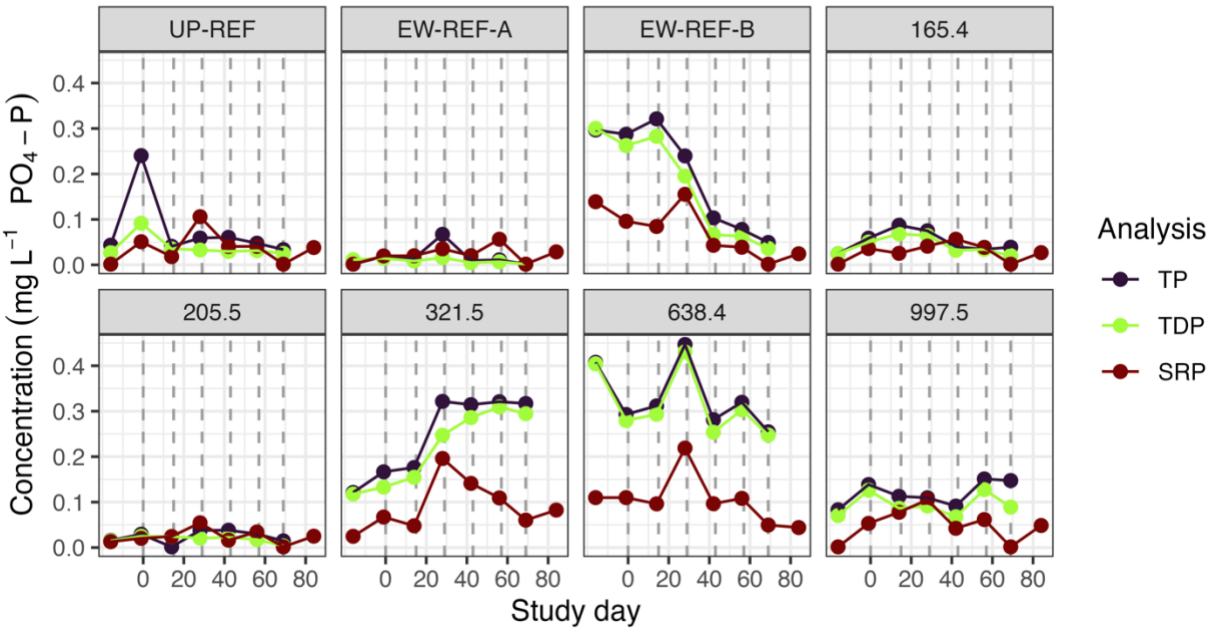

Figure 16. Total (TP), total dissolved (TDP), and soluble reactive (SRP) phosphorus concentrations in EW mesocosm water. Each graphical panel represents a mesocosm with the TP loading from aquaculture wastewater (AWW) additions indicated in units of mg m^{-2}. Vertical dashed lines indicate AWW addition events.

Similar trends were observed for TP, TDP, and SRP in each mesocosm (Figure 16). At low concentrations, SRP comprised a significant fraction of the TP in mesocosm water. At higher concentrations, SRP represented approximately one-third of the corresponding TP concentration. One exception was observed for the 321.5 mg m^{-2} treatment where SRP concentrations decreased from day 28 to 69 but TP concentrations remained constant. While no algal mats were found in the 321.5 mg m^{-2} treatment (see Section 3.3.1.9; Figure 28), a doubling of biofilm chl *a* concentrations was observed between study days 21 and 35 (see Section 3.3.1.4; Figure 18) and elevated microbial activity was observed in mesocosm water (see Section 3.3.1.7; Figure 24). This might explain a reduction in SRP during this period; SRP is the form of P that is assimilated by bacteria and algae (Correll, 1998). The assimilation of P into bacteria and algae is not necessarily indicative of remediation as a subsequent release of SRP from degraded cells can occur (Chen et al., 2018; Zhu et al., 2013). Note that samples for TP and TDP on study day 84 were spoiled and therefore not included in Figure 16. However, after the final AWW addition event on day 69, concentrations of SRP remained relatively constant on day 84 and therefore a similar trend would be expected for TP and TDP.

Minor differences between TP and TDP were observed throughout the study period (Figure 16), indicating that P species in CW water consisted of significant fractions of dissolved organic P (DOP). This finding is further supported by low concentrations in PP samples; PP concentrations in the 0-30 µg L^{-1} range were observed for the majority of samples (Figure A - 9). An elevation in PP was observed on study day -1 in UP-REF which agrees with the large difference between TP and TDP in Figure 16. Notable elevations in PP were also observed on day 69 for the 165.4 mg m^{-2} treatment and on day 56 and 69 for the 997.5 mg m^{-2} treatment, but did not correspond

with the differences between TP and TDP observed in Figure 16. For each water sampling event, two 500 mL sampling bottles were collected. Care was taken to ensure TP, TDP, and SRP were all analyzed from the same sampling bottle. However, depending on the remaining sample volume available, other analyses were conducted using water from the second sampling bottle. While sampling methods were identical for both bottles, some degree of variability is inevitable with these methods. For instance, if the collection process for the first sampling bottle disturbed soil in the mesocosm, elevated PP concentrations could be observed in the second bottle if small soil particles which were able to pass through initial screening were captured. Similarly, if solids settled in a sampling bottle and the sampling bottle was not completely mixed in the laboratory before removing aliquots for TP, TDP, and SRP analyses, then particulate matter could be concentrated in the remaining sample volume. It is unlikely that these examples had a substantial impact on results because the difference between TP and TDP generally agrees with PP results, however they may have been responsible for the few instances where discrepancies were observed.

Elevated TP and TDP concentrations were observed in the highest (997.5 mg m^{-2}) treatment throughout the study period, however the elevated concentrations ranged from 0.10–0.15 mg L^{-1}, approximately half that of the concentrations observed among the second-highest (638.4 mg m^{-2}) and third-highest (321.5 mg m^{-2}) treatment mesocosms. These results are indicative of a threshold among high loading treatments beyond which P elevations in CW water were not observed to the same extent. Substantial quantities of hornwort were present in all treatments with no evident relationship to nutrient loading conditions (see Section 3.3.1.9; Figure 28). Meanwhile, the greatest quantities of both algal mat and wild rice biomass were observed in the

997.5 mg m^{-2} treatment. In the 997.5 mg m^{-2} treatment, excess P from AWW additions was assimilated into algal mats and wild rice plants, contributing to the removal of P species from CW water. Meanwhile, the lower nutrient loading treatments (i.e. EW-REF-A, 165.4, 205.5 mg m^{-2}) all had low concentrations of P in CW water throughout the study. The EW-REF-B mesocosm had high background concentrations of P (i.e. >0.25 mg L^{-1}), however P was eliminated throughout the study and was below 0.1 mg L^{-1} after 72 days of treatment, indicative of the nutrient removal capabilities of EW systems under background conditions (i.e. no AWW loadings). Upon substantial nutrient loading via AWW additions, EW systems experienced elevations in P which persisted for a period of >5 weeks (for the 321.5 mg m^{-2} treatment) or >9 weeks (for the 638.4 mg m^{-2} treatment). Under greater nutrient loading conditions (i.e. 997.5 mg m^{-2}), the P species input via AWW additions did not reside in CW water to the same extent and instead appear to have stimulated the production of algal and wild rice biomass. Effectively, reference and low nutrient loading treatments were able to effectively eliminate P species from CW water while high nutrient loadings resulted in elevations and/or persistence of P species in CW water. At the highest nutrient loading treatment evaluated (997.5 mg m^{-2}), responses were instead observed in biofilm, algal mats, and wild rice plants which were able to assimilate excess nutrient inputs from AWW additions and eliminate P from CW water. Future considerations for CW operations must consider the release of P from algae and plant litter which arises upon decay and cell degradation of organic matter.

Under the nutrient gradient evaluated, EW systems effectively accommodated AWW loadings up to 205.5 mg m^{-2} TP over a period of 69 days (i.e. 2.978 mg m^{-2} d^{-1}). For the 321.5 mg m^{-2} treatment (i.e. 4.659 mg m^{-2} d^{-1}) and the 638.4 mg m^{-2} treatment (i.e. 9.252 mg m^{-2} d^{-1}),

elevations of P species in CW water occurred. Such elevations appear to lead to the production of biomass because under nutrient loading rates of 997.5 mg m^{-2} (14.457 mg m^{-2} d^{-1}), elevations in algal and plant biomass were observed instead of elevations of P in CW water. Nutrient loadings of 205.5 mg m^{-2} allow for the sustainable management of P, sustained CW performance, and continued usage of EW systems. If more intensive management practices were employed which could involve the physical removal of algal mats and other biomass, greater nutrient loadings in EW systems could be feasible.

3.3.1.3 Nitrogen in Mesocosm Water

The concentrations of the main nitrogen species (TDN, TAN, NO_2-N, NO_3–N) in mesocosm water are presented in Figure 17. An overall increase in TDN was observed among all mesocosms, including reference treatments (Figure 17). However, day 84 TDN concentrations were highest (>2 mg L^{-1}) in EW-REF-B and 321.5, 638.4, and 997.5 mg m^{-2} treatments. These four treatments displayed the largest increases in TDN concentration (≥1 mg L^{-1}) among planted mesocosms between study day -1 and 84. A large increase in TDN was observed on day 28 in the EW-REF-B mesocosm that was not observed in other mesocosms, and ultimately resulted in high TDN in EW-REF-B throughout the second half of the study. With the exception of elevated TAN observed in all mesocosms on day 69, TAN concentrations were below, equal to, or slightly greater than limits of detection throughout the study period (Figure 17; Figure A - 6). Constant concentrations of NO_2–N were also observed in CW water which were within 0.05-0.15 mg L^{-1} for the majority of the study (Figure 17; Figure A - 7).

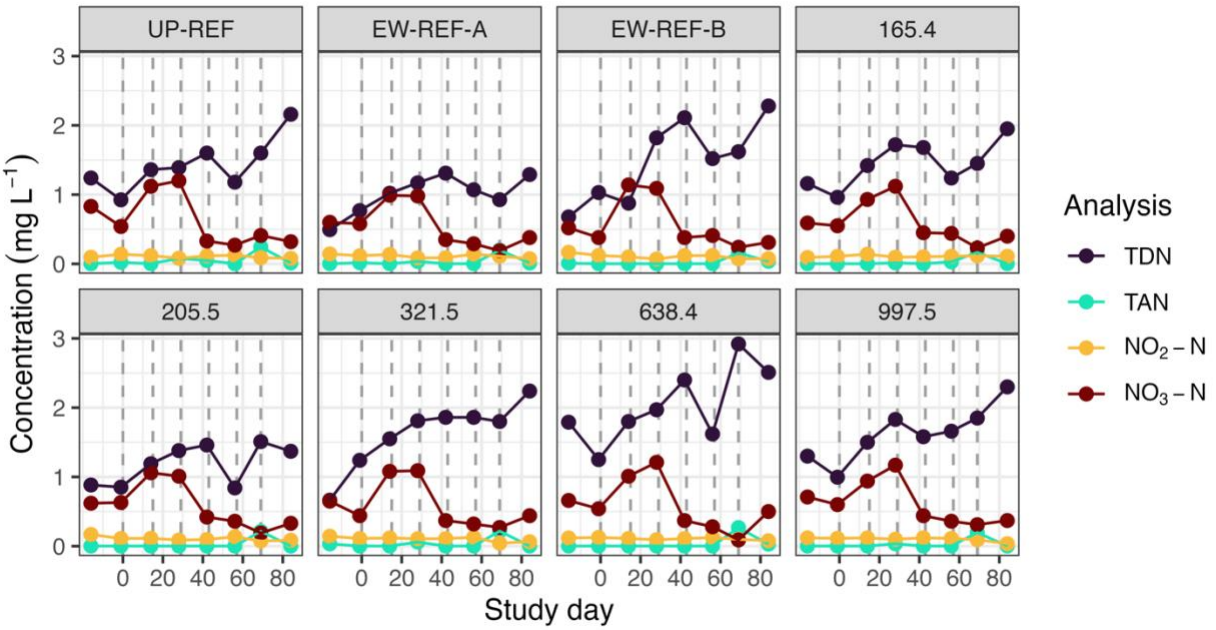

Figure 17. Total dissolved (TDN), total ammonia (TAN), nitrite (NO_2–N), and nitrate (NO_3–N) nitrogen concentrations in EW mesocosm water. Each graphical panel represents a mesocosm with the total phosphorus loading from aquaculture wastewater (AWW) additions indicated in units of mg m^{-2}. Vertical dashed lines indicate AWW addition events.

During the first four sampling events (i.e. from day -16 to 28), NO_3–N comprised a significant portion (>50%) of TDN in mesocosm water (Figure 17). High concentrations of NO_3–N in source water (Table A - 1) were responsible for high background concentrations in mesocosm water. In natural systems where background NO_3–N is abundant, inputs of TAN and NO_2–N from fish farms effluents will have no substantial impact on the total inorganic N (TIN) concentration in the receiving environment (Carr & Goulder, 1990). From day 42 onward, a significant decrease in NO_3–N occurred across all treatments, ultimately reaching a scenario where NO_3–N was no longer the major component of TDN. The removal of N in CW systems can be associated to some combination of assimilation by plants or algae and accumulation or immobilization in soils, but denitrification is often responsible for the majority of N removal (Poe et al., 2003; Reinhardt et al., 2006). Moreover, the removal of NO_3–N via denitrification is

expected to increase throughout the study period as other nutrient sinks are filled (Poe et al., 2003). A general decline in DO was also observed among mesocosms (Figure A - 14), suggesting that anaerobic conditions necessary for denitrification bacteria reactions may have occurred, especially near the end of the study period (Snow et al., 2012). Algae can rapidly assimilate NO_3–N (Taziki et al., 2015), and the decrease in NO_3–N concentrations on day 42 precedes the period where the most rapid biofilm growth was observed (see Section 3.3.1.4; Figure 18). Therefore, both denitrification and uptake by algae appear to have contributed to the elimination of NO_3–N from CW water in EW systems. Similar trends in NO_3–N concentrations were observed in both planted and unplanted (UP-REF) mesocosms (Figure 17), confirming that the presence of plants was not a major contributor to NO_3–N elimination during this period.

The impact of AWW additions on N species appears minor, with slight elevations of TDN observed among the highest nutrient loading treatments. The divergence between TDN and NO_3–N concentrations throughout the study are evident, particularly from day 42 onward (Figure 17). Continued loading of AWW provided substantial quantities of organic N to CW water. During the second half of the study, high TDN concentrations were observed alongside low relative concentrations of TIN species, indicating that TDN in CW water was primarily in the form of dissolved organic N (DON). However, a substantial increase in TDN was also observed in UP-REF which contained no plants and received no AWW, suggesting that either N release from soils, atmospheric inputs of N, or inputs from further additions of tap water to mesocosms were substantial (Figure 17). DON fluxes from soils and sediments are complex processes capable of contributing substantial quantities of DON to the water column (Burdige & Zheng, 1998). The inclusion of TN analyses in addition to TDN could be utilized in future studies to

better represent phytoplankton and bacteria that are removed during filtration and therefore not represented in TDN measurements. Uptake by phytoplankton and bacteria are among the main sinks for DON and are not entirely represented in the dissolved fraction of nutrient analyses (Berman & Bronk, 2003). While atmospheric inputs of organic N can contribute substantially to N deposition (around 30% of water soluble N), inputs of multiple inorganic N species would be expected (Cape et al., 2011). While increases in TDN were observed in Figure 17, they were not accompanied by increases in TIN, suggesting that either atmospheric inputs were not substantial, or atmospherically-deposited TIN species were rapidly converted to organic forms of N and/or eliminated from CW water through biological and chemical processes. In a similar manner, tap water additions to mesocosms also represent a significant contribution to TDN, with elevations of inorganic N species expected to accompany increases in TDN. If inorganic N species were quickly assimilated by organisms or converted by processes within the mesocosms, then organic N could dominate the nitrogen pool, leading to the observed increase in TDN without corresponding increases in inorganic N. Greater sampling resolution could be implemented in future studies to better resolve such trends and potentially capture time periods when N fluxes and conversions occur.

Under the nutrient gradient evaluated in the present study, minor alterations in N species in EW water were observed at nutrient loadings above 321.5 mg m^{-2} TP (corresponding loadings of 1756.7 mg m^{-2} TAN and 2379.2 mg m^{-2} TKN; Table 7) over a period of 69 days (i.e. TP, TAN, and TKN nutrient loading rates of 4.659, 25.459, 34.481 mg m^{-2} d^{-1}, respectively). Responses of N species in CW water appear to be limited to minor increases in TDN in the form of DON. The response of algae to DON inputs should be considered. In laboratory experiments, organic N

compounds were shown to support similar algal growth yields as inorganic N compounds (Neilson & Larsson, 1980). In fact, Neilson and Larsson (1980) demonstrated that urea achieved similar algal growth yields as nitrate and ammonia, and both N atoms of the urea molecule were utilized by algae. Urea and TAN are the primary forms of N excretion in fish and therefore comprise a predominant fraction of organic N in AWW (Dalsgaard et al., 2015; Kajimura et al., 2004). The discharge of effluents containing high concentrations of DON compounds from CWs remains an environmental concern. The potential for algae to utilize nutrients present in AWW provides an interesting opportunity for the integration of algae culture within, or adjacent to CW systems. Algae production has been beneficial in the treatment of land-based AWW effluents (Castine et al., 2013; Lawton et al., 2013) and by pairing microalgae production with AWW treatment, functional fish feeds for aquaculture can be produced, promoting a circular economy approach to fish farming that offers both economic and environmental benefits (Ansari et al., 2021; Ansari et al., 2017; Han et al., 2019).

3.3.1.4 Biofilm and Phytoplankton

Biofilm tile chl *a* concentrations and fitted logistic growth models are plotted in Figure 18. Key model parameters associated with growth curves are found in the Appendix (Table A - 3). Growth curves were fit without major issues with the exception of the 321.5 mg m^{-2} treatment, which had very large K and t_{mid} values because of the high chl *a* concentrations observed on day 5 (Figure 18, Table A - 3). Therefore, the logistic growth curve fit for the 321.5 mg m^{-2} treatment does not accurately represent biofilm growth and is not considered in the discussion of results, and serves as a representation of the difficulties and high variability that often accompanies field data (Hill et al., 1994).

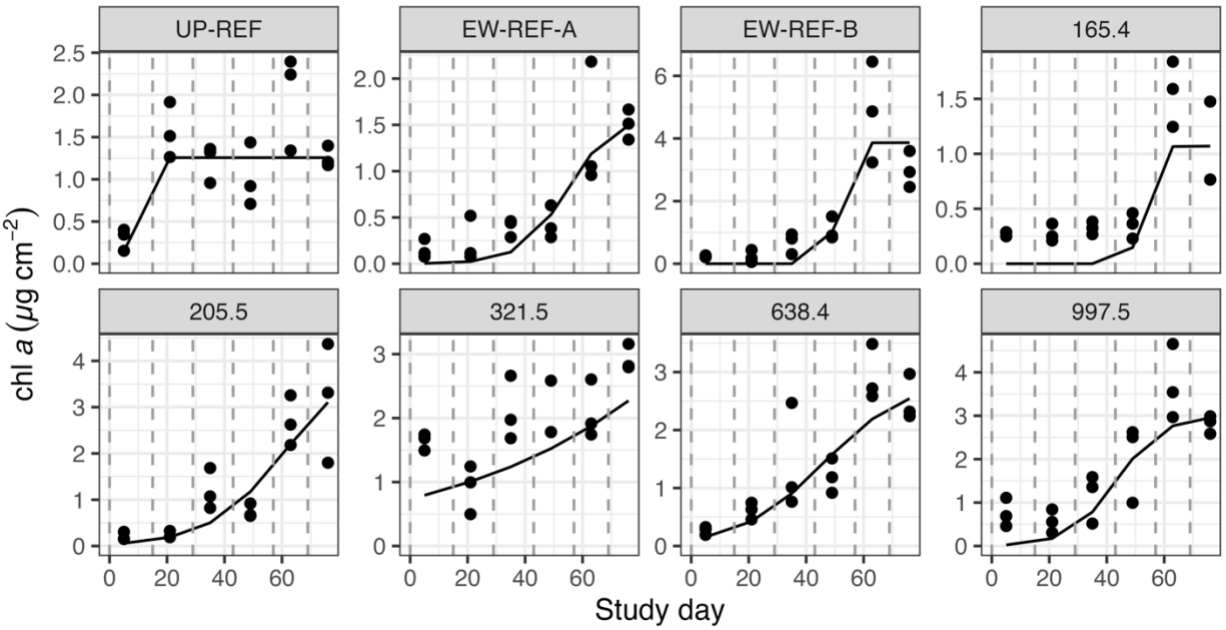

Figure 18. Biofilm tile chlorophyll *a* (chl *a*) concentrations in EW mesocosms. Measured data (points) are included with fitted logistic growth curves (solid lines). Note that different y-axis scales are used across the graphical panels. Each graphical panel represents a mesocosm with the total phosphorus loading from aquaculture wastewater (AWW) additions indicated in units of mg m^{-2}. Vertical dashed lines indicate AWW addition events.

Biofilm chl *a* concentrations were generally lower during the first four sampling events and a notable increase in chl *a* was observed during the final two sampling events (Figure 18). Mean (± SD) K values of 2.93 ± 0.11 µg cm^{-2} and 2.67 ± 1.56 µg cm^{-2} were observed for the two-highest nutrient loading treatments (i.e. 638.4 and 997.5 mg m^{-2}) and for the four-lowest nutrient loading treatments (i.e. EW-REF-A, EW-REF-B, 165.4 mg m^{-2}, 205.5 mg m^{-2}), respectively (Table A - 3). However, high variability was observed among the latter group. The two-highest nutrient loading treatments also had a lower mean t_{mid} value (44.66 ± 1.83 d) than the low nutrient loading treatments (54.77 ± 4.60 d). Biofilms appear to have responded to AWW additions, but responses were only evident at nutrient loadings of 638.4 mg m^{-2} or greater. Under such conditions, biofilm blooms in EW systems occurred sooner (lower t_{mid}) and greater yields were observed (greater K). However, growth rates (r values) were variable with no treatment-based

trends evident. Carr and Goulder (1990) found greater periphyton chl *a* concentrations downstream of fish farm effluents than upstream, indicating that nutrient enrichment from AWW can increase periphytic algal growth. In CWs, periphyton play crucial roles in P removal and retention (Dodds, 2003). The potential for periphyton and associated biofilm growth to be implemented in wild rice CW systems should be investigated further alongside considerations for management practice such as the removal of biofilm biomass.

No treatment-based trends in AFDM were observed among the EW mesocosms (Figure 19). Biofilm responses of chl *a* are known to be more responsive to nutrient additions than AFDM, and Lang et al. (2012) hypothesize that such a finding could result from an increase in the chlorophyll content per unit biomass of photoautotrophs, or an increase in the ratio of photoautotrophic biomass to nonphotoautrophic biomass that does not substantially impact the total periphyton biomass. The periphyton taxonomic composition of biofilms could be evaluated in future studies to determine periphyton community structure and diversity within CW treatment systems treating AWW.

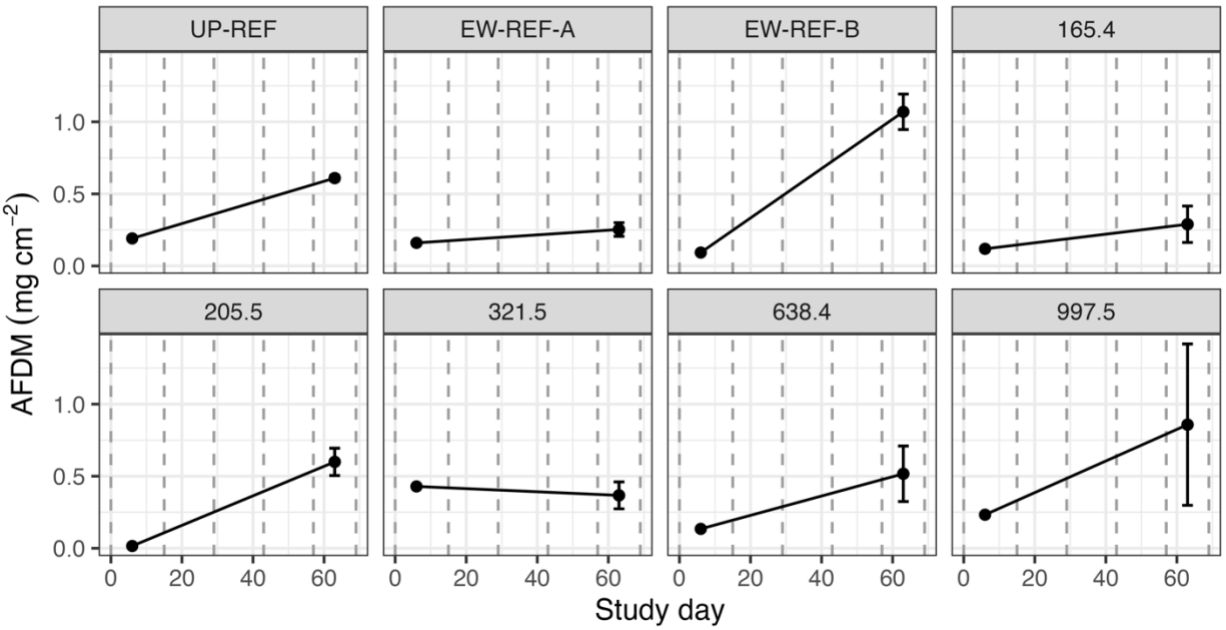

Figure 19. Biofilm tile ash-free dry mass (AFDM) in EW mesocosms. Replicates were pooled on day 6, while the mean (± SD) of three replicates is presented on day 63. Each graphical panel represents a mesocosm with the total phosphorus loading from aquaculture wastewater (AWW) additions indicated in units of mg m^{-2}. Vertical dashed lines indicate AWW addition events.

Biofilm tiles implemented in the present study provided a substrate of known surface area upon which biofilm could proliferate. In larger scale CWs, periphytic biofilms can contribute substantially to N and P removal and CWs can either have artificial substrates added to facilitate their growth, or can be left to form plant-periphyton complexes with CW plants (Gao et al., 2019). In the present study, biofilm growth was also observed on the surface of soil, plants, and mesocosm walls. Differences in periphyton productivity are known to exist across different surfaces (Cronk & Mitsch, 1994), and therefore variations in chl *a* and AFDM may exist for biofilms growing on different surfaces in CWs. Further, light and nutrient conditions are both known to have an impact on periphyton community structure (McCall et al., 2017). To optimize AWW treatment capacity, future studies should investigate differences in biofilm productivity

between artificial and natural substrates in wild rice CW systems and evaluate the influence of environmental variables on biofilm growth.

In the water column, chl *a* concentrations were generally below 5 µg L^{-1} among EW mesocosms for the duration of the study period (Figure 20). An exception was observed for the 997.5 mg m^{-2} treatment where concentrations of 24.63 and 22.02 µg L^{-1} were measured on days 69 and 84, respectively. However, by day 97 concentrations were equivalent to baseline levels (3.83 µg L^{-1}). The increase and subsequent decrease in chl *a* may have been related to seasonal dynamics of phytoplankton surrounding periods of maximum phytoplankton growth as similar increases and decreases were also observed in UP-REF, EW-REF-A, EW-REF-B, and the 165.4 mg m^{-2} treatment (Nõges et al., 2010). Despite a partial decrease on day 56, EW-REF-B had elevated chl *a* concentrations from day 28 onward, with values in the 5-15 µg L^{-1} range. A high quantity of both biofilm (Figure 18, Figure 19) and phytoplankton (Figure 20) were observed in EW-REF-B which corresponded to a reduction of high P in CW water between study days 14 and 42 (discussed previously in Section 3.3.1.2; Figure 16).

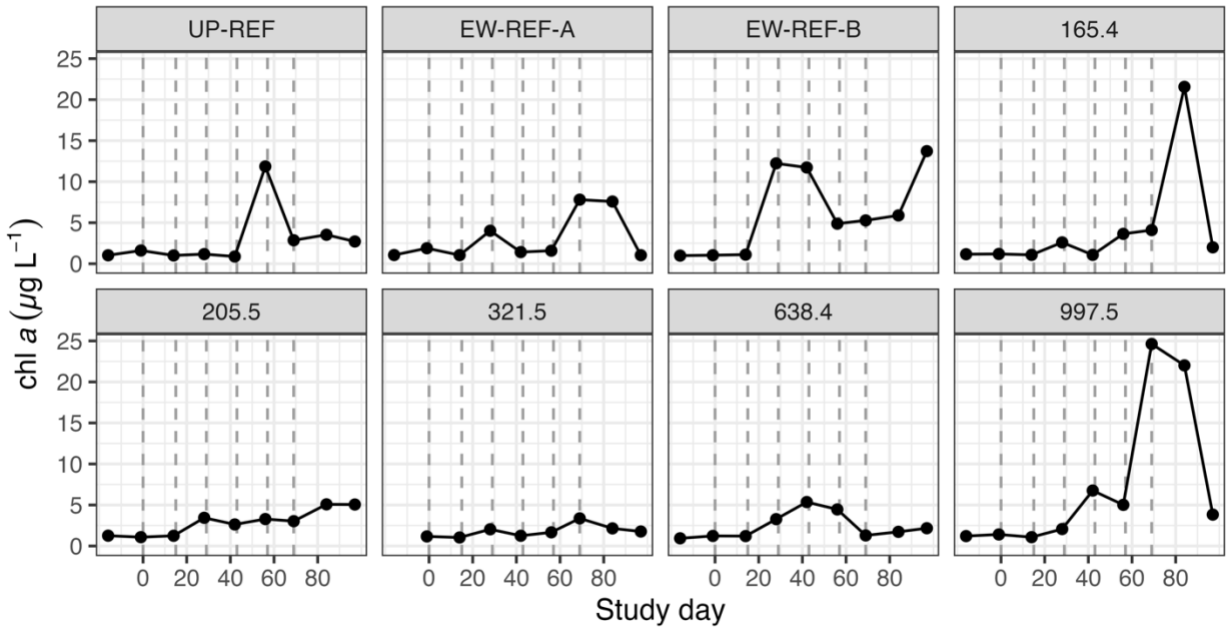

Figure 20. Chlorophyll *a* (chl *a*) concentrations in EW mesocosm water. Each graphical panel represents a mesocosm with the total phosphorus loading from aquaculture wastewater (AWW) additions indicated in units of mg m^{-2}. Vertical dashed lines indicate AWW addition events.

Concentrations of chl *a* in surface waters have been widely used as an ecological indicator for trophic status in surface waters and often algal abundance (measured as chl *a*) represents the beginning of water quality degradation resulting from eutrophication (Bricker et al., 1999; Ptacnik et al., 2008). Elevated concentration of N and P in the water column are not necessarily indicators of eutrophication because of the wide range of assimilative capacities than can exist among aquatic ecosystems (Bricker et al., 1999). For example, wetlands are known to be robust to eutrophication because of their ability to retain and filter significant quantities of nutrients (Sánchez-Carrillo et al., 2011). Despite high P concentrations in CW water for the 321.5 and 638.4 mg m^{-2} treatments (Figure 16), no substantial elevations of chl *a* in CW water were observed (Figure 20). Meanwhile, the 997.5 mg m^{-2} treatment did not exhibit the same P elevations in CW water but underwent major increases in chl *a* concentrations. In terms of algae,

nutrient loadings up to 638.4 mg m^{-2} did not result in serious phytoplankton blooms in EW systems unless background P species in CW water were high. High chl *a* in water of the 997.5 mg m^{-2} treatment was consistent with the previously discussed results (Section 3.3.1.2) where P elevations in CW water were observed for the 321.5 and 638.4 mg m^{-2} treatments, but not for the 997.5 mg m^{-2} treatment. Together, the elevated phytoplankton and biofilm observed for the 997.5 mg m^{-2} treatment and the water quality data discussed previously (Section 3.3.1.2) suggests that at nutrient loadings of 321.5 and 638.4 mg m^{-2}, water quality responses occur in the form of elevated P species but at 997.5 mg m^{-2}, algal responses become the predominate indicators of water quality degradation.

3.3.1.5 Performance of Constructed Wetlands for Phosphorus Treatment

The performance of CW systems was evaluated by assessing the elimination of P from CW water throughout the performance period (i.e. from day -1 to 69; Figure 12). Initial and final TP concentrations in CW water were approximately equal among the high nutrient loading treatments and diverged slightly among the low nutrient loading treatment with lower TP in final samples (Figure 21). Details and parameters related to CW performance are presented in Table 9. Despite the potential for serious water quality degradation if no P species were eliminated from CW water (C_{max}), CWs were able to effectively eliminate TP reflected by C_f and CR values in Table 9. With the exception of one instance (for the 321.5 mg m^{-2} treatment), the CR in all CWs that received AWW was greater than the mean CR of reference treatments (85.3%), however no treatment based trend in CR was observed among AWW-treated mesocosms. High CR is related the use of low HLR (Kadlec, 2016) and here greater PLR was also observed with increasing nutrient loadings, indicating that CW systems were able to progressively accommodate AWW

loadings. An exponential trend was observed for PLR, which when analyzed on a log-scale generated a statistically significant positive linear trend between PLR and TP loading (Figure 22). Without a plateau in PLR observed in Table 9 and Figure 22, it is likely that the full P removal capacity of CW systems was not reached and even greater PLRs could be achieved under greater nutrient loadings. However in such scenarios, the mechanisms of P removal must be considered to maintain the integrity of CW systems and avoid excessive algal growth.

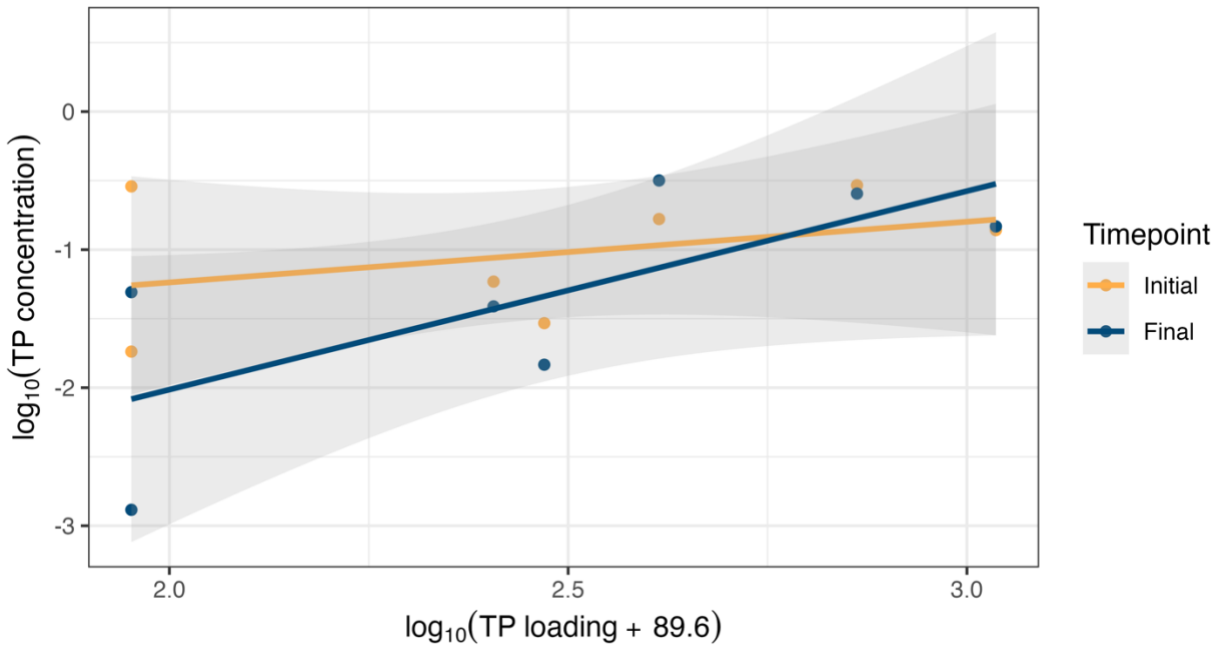

Figure 21. Comparison of total phosphorus (TP) concentrations in EW mesocosm water during initial (day -1) and final (day 69) timepoints of the performance period. General linear models (solid lines) were fit to measured data (points) with 95% confidence intervals (shaded regions). Predictor variables were calculated by adding a constant (89.6) to the TP loading from aquaculture wastewater additions.

Table 9. Calculated and measured parameters relating to the performance of EW systems removing total phosphorus (TP) from aquaculture wastewater (AWW).

Mesocosm type	TP loading for study (mg m^{-2})	TP loading for performance period (mg m^{-2})	C_{max} (mg L^{-1})	C_f (mg L^{-1})	CR (%)	PLR (mg m^{-2} d^{-1})	AWW loading (L d^{-1})	HLR (mm d^{-1})
EW	0 (EW-REF-A)	0.0	0.015	<LOD	90.1*	0.068*	0.000	0.000
	0 (EW-REF-B)	0.0	0.252	0.049	80.5	0.945	0.000	0.000
	165.4	134.4	0.516	0.039	92.5	1.995	0.179	0.047
	205.5	167.3	0.479	0.015	96.9	2.433	0.279	0.059
	321.5	261.6	0.871	0.317	63.6	2.818	0.436	0.092
	638.4	519.5	2.056	0.255	87.6	7.539	0.686	0.182
	997.5	811.7	2.777	0.147	94.7	11.508	1.071	0.284
Unplanted	0 (UP-REF)	0.0	0.139	0.034	75.8	0.322	0.000	0.000

*A value equal to half the LOD was used in calculations

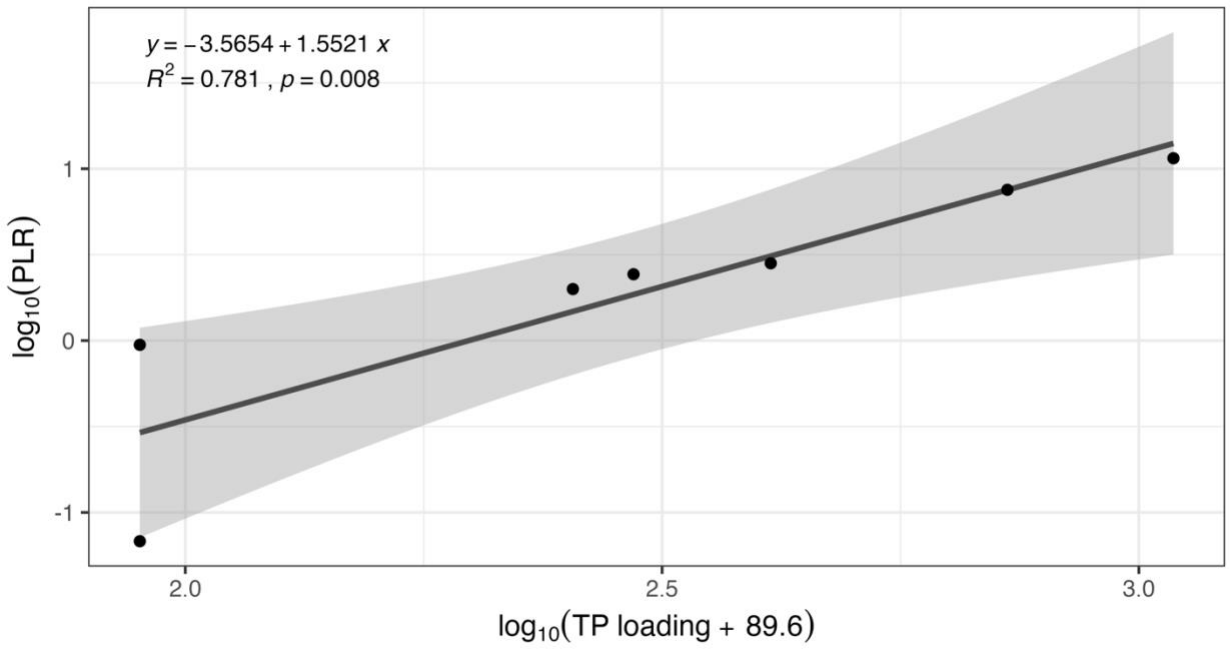

Figure 22. Phosphorus load reduction (PLR) for total phosphorus (TP) in EW mesocosm water during the 70-day performance period. A general linear model (solid line) was fit to calculated data (points) with a 95% confidence interval (shaded region). Predictor variables were calculated by adding a constant (89.6) to the TP loading from aquaculture wastewater additions.

3.3.1.6 Modelling and Interaction Analysis

While the models with statistically significant interaction terms were of primary interest, the results of all fitted LMMs are included in the Appendix (Table A - 4). Statistically significant treatment-time interactions in LMMs were detected for TP ($F = 6.289$, $p = 0.016$), TDP ($F = 5.747$, $p = 0.021$), and PP ($F = 4.931$, $p = 0.031$) among the EW systems. However, no significant contrasts were found when performing a pairwise contrast test between covariate trends on each study day. An accompanying interaction plot visualization for this post hoc analysis is presented in Figure 23. For TP and TDP, two clear groupings of study days were observed; covariate trends on study days -16, -1, and 14 had similar slopes while covariate trends on study days 28, 42, 56, and 69 had similar slopes, with greater slopes observed among the latter group. A similar trend was observed for the y-intercept of covariate trends; study days 42,

56, and 69 had smaller y-intercepts than study days -16, -1, 14, and 28. The post hoc analysis evaluated model response across the gradient of nutrient loadings and compared trends among the different study days. A general decrease in y-intercept with study day was consistent with the elimination of P species from CW water with time among EW reference conditions. Meanwhile, an increasing slope with study day indicated a larger value for response with increasing nutrient loading conditions. Effectively, the analysis conducted here compared the response from each study day to each other study day. Model predictions for P species were impacted by the response of the 997.5 mg m^{-2} mesocosm discussed in Section 3.3.1.2 which did not exhibit the same elevated P species in CW water as was observed for the other high nutrient loading treatments. However, the interaction plots in Figure 23 demonstrate how EW systems responded with time to AWW additions; by study day 28 responses of TP and TDP appear to be impacted by AWW additions and more evident trends across the nutrient loading gradient were observed, while a similar finding for PP was observed on study days 69 and 84. On study day 28, two out of the six total additions had been completed. Therefore the total TP loadings represented were equal to one third of the values presented in Table 7. The beginning of water quality responses on study day 28 suggest that the mean TP loading rates among high-loading treatments (presented in Table 8) were sufficiently high to have an impact on TP and TDP concentrations within the first month of the study. During the start-up phase when biomass production is low and peak growth rates have not been reached, EW systems may be more susceptible to alterations in water quality without forms of biomass to buffer the impacts of nutrient loadings.

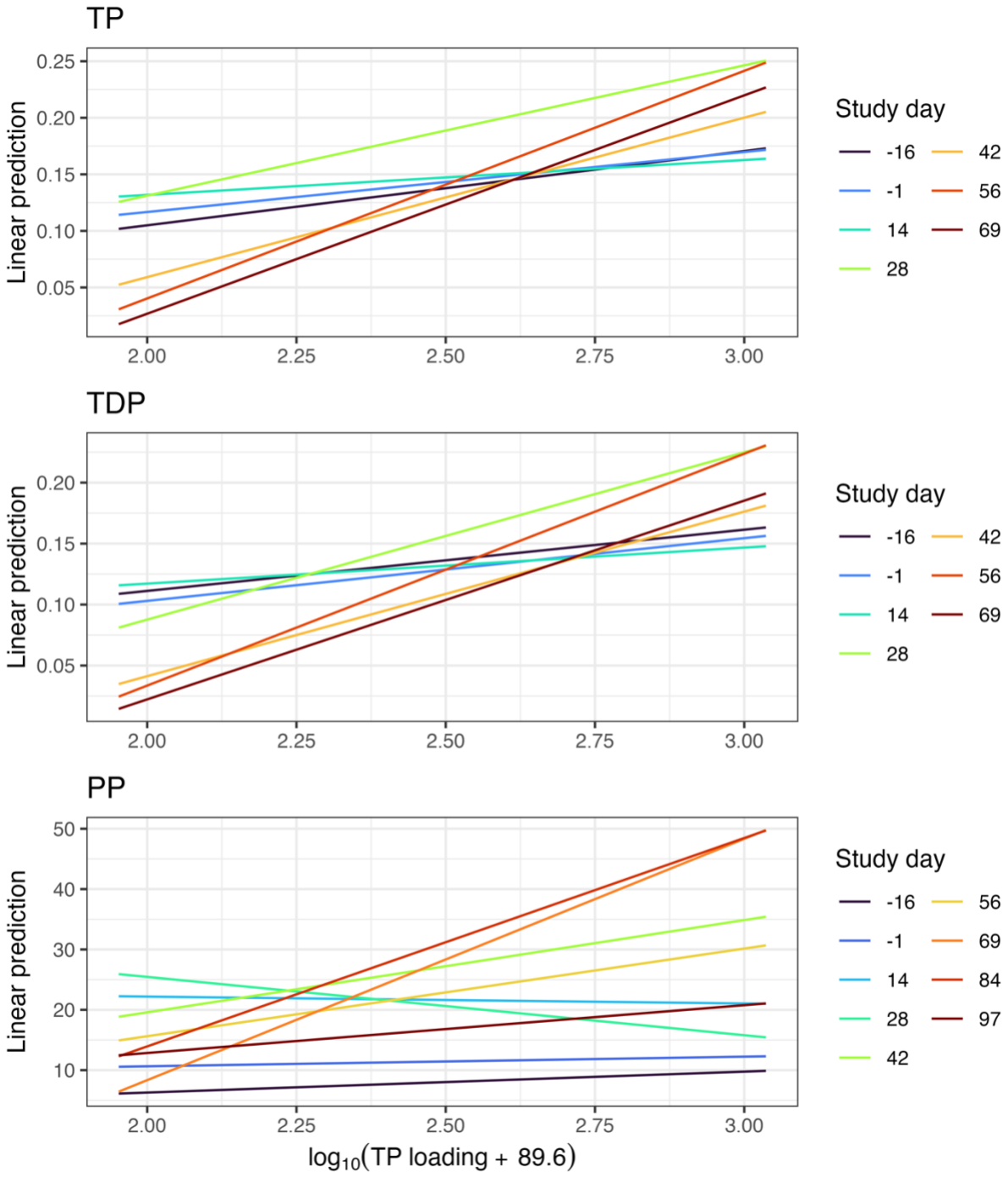

Figure 23. Interaction plots of estimated marginal means based on the fitted linear mixed models for total (TP), total dissolved (TDP), and particulate (PP) phosphorus of the interaction between treatment and time for the EW mesocosms. Predictor variables were calculated by adding a constant (89.6) to the TP loading from aquaculture wastewater additions.

3.3.1.7 Microbial Activity

Microbial activity (measured as tATP) in mesocosm water and wild rice roots is presented in Figure 24. Linear models were not statistically significant for mesocosm water ($p = 0.328$) or for wild rice roots ($p = 0.134$) and high variability was observed for both sample matrices. Microorganisms can be very sensitive to environmental changes and are therefore key biological indicators for use in wetland management (Urakawa & Bernhard, 2017). When AWW is used to irrigate soils, it can dramatically impact microbial communities (Chen et al., 2017). The tATP analysis provided a rapid and low-cost method for monitoring the total active biomass of microbes. Here, tATP in water and roots was not impacted by nutrient loading, however additional temporal resolution could better resolve seasonal trends and offer additional insights into the impacts of AWW on microbial communities. A comprehensive taxonomic assessment of microbial communities in CW systems was beyond the scope of the present study but could be implemented to provide additional insights into microbial community composition.

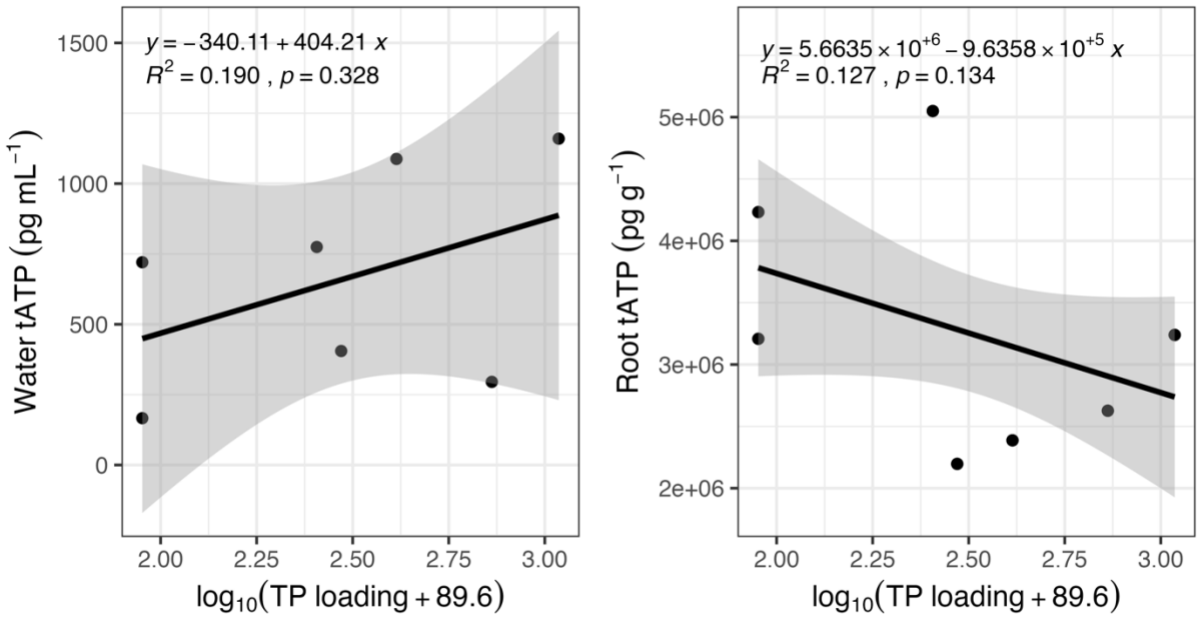

Figure 24. Microbial activity as total ATP (tATP) in EW mesocosm water (left) and wild rice roots (right). General linear models (solid lines) were fit to measured data (points) with 95% confidence intervals (shaded regions). Predictor variables were calculated by adding a constant (89.6) to the total phosphorus (TP) loading from aquaculture wastewater additions.

3.3.1.8 Soil Nutrient Content

Background (day 0) and final (day 100) concentrations of Olsen P (OP) in EW mesocosm soil are presented in Figure 25. No statistically significant linear trends were observed for OP at either timepoint (Figure 25), or when evaluating the change in OP concentration between timepoints (Table A - 5). The results from all general linear models for different soil endpoints are compiled in the Appendix (Table A - 5). A summary of statistically significant relationships for EW soil is presented in Table 10. Background results may be a product of natural variation between mesocosms, however the EW systems were utilized previously (Chapter 2) and cattail plants may have created nutrient discrepancies in the soil because of their high nutrient demand (Dubbe et al., 1988).

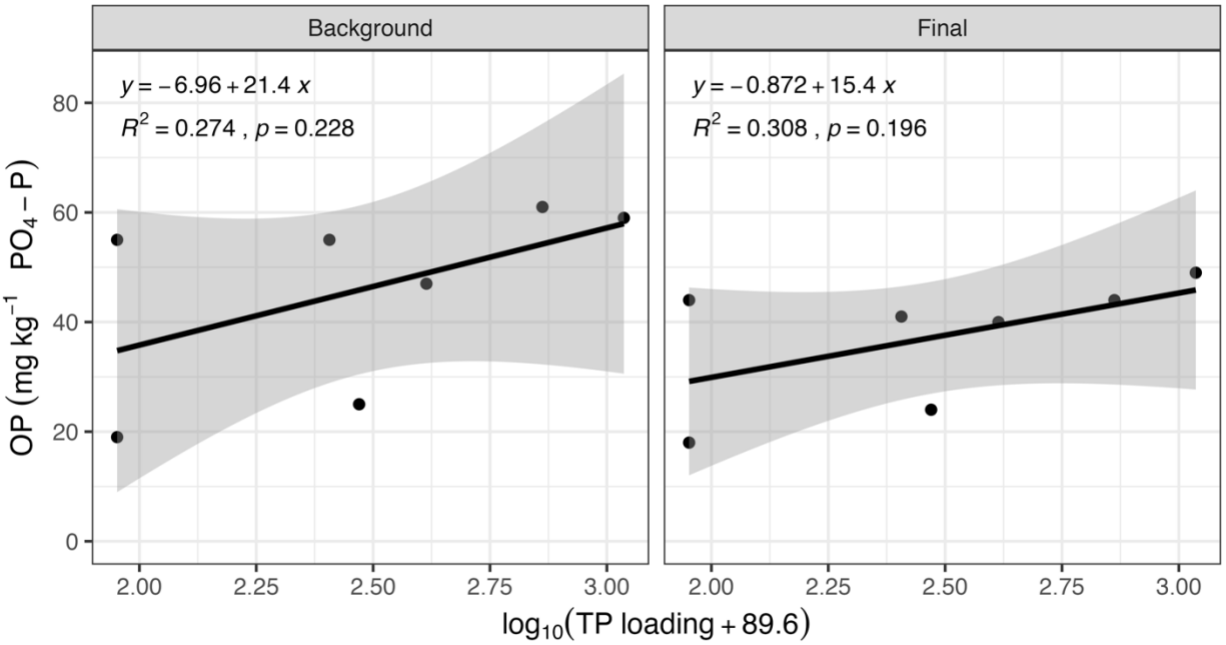

Figure 25. Background (day 0), final (day 100) soil Olsen phosphorus (OP) in EW mesocosms. General linear models (solid lines) were fit to measured data (points) with 95% confidence intervals (shaded regions). Predictor variables were calculated by adding a constant (89.6) to the total phosphorus (TP) loading from aquaculture wastewater additions.

Table 10. Summary of statistically significant results for different endpoints assessed in EW mesocosm soil during day 0 (background) and day 100 (final) samples, and the difference between background and final samples (change). Endpoints were assessed using general linear models and indicated in the table if a statistically significant result was detected. The directionality of the relationship is indicated in parentheses as either positive (+) or negative (-).

Analysis	Endpoint
Background	Cl (-), S (-)
Final	B (+)
Change	Cl (+), S (+), OM (+)

Sun et al. (2020) evaluated the properties of soil which received AWW and found that nutrients (i.e. TP, TN, and total organic C) accumulated in affected soils. Meanwhile, Atkins et al. (1992) added fertilizer to wild rice stands and found that nutrient concentrations in sediment were not correlated to fertilizer application rates, however they did observe elevations in sediment K and

P among the highest treatment evaluated (i.e. 105 and 210 kg ha^{-1} K and P, respectively). In wild rice sediments, pH is known to have a strong impact on the growth of plants and the suitability of sediments and corresponding available P concentrations strongly impact production (Lee & Stewart, 1981, 1984). In EW system soils, changes in nutrient concentrations were significant for Cl, S, and OM (Table 10). Both Cl and S had significant negative relationships in background samples but had positive relationships when evaluating the change in nutrient concentrations, indicating that the initially observed negative relationships were eliminated throughout the study period. Meanwhile, a significant positive relationship was observed for the change in OM. Continued additions of AWW contributed substantial OM to CWs which would be deposited on soils. Similarly, the production of benthic algae could have contributed to the increase in OM observed here. In the long term, OM mineralization can reduce soil pH (McCauley et al., 2009) which can in turn negatively impact wild rice growth (Lee & Stewart, 1981).

3.3.1.9 Plant and Algal Biomass

No statistical differences were observed for the total biomass of wild rice, algal mats, or hornwort collected at the end of the study period (Figure 26). Similarly, no statistical difference in the mean length of wild rice plants at the end of the study period was observed (Figure 27). While Atkins et al. (1992) demonstrated how fertilizer additions can increase tillering among wild rice plants, yield responses in their study were highly variable and no trends were observed. In addition to the wild rice observed among EW systems, notable quantities of hornwort and algal mats were also observed (Figure 28). Competition from other plants can drastically reduce wild rice growth (Atkins et al., 1992; Lee, 1986). Hornwort was a significant contributor to total biomass and therefore a competitor with wild rice in CWs. Other forms of biomass (e.g. cattail,

other flowering aquatic plants) were also observed (Figure 28), however these other forms of biomass comprised a very small proportion of the total biomass (often <15 g of dry biomass and <1% of total biomass) and were therefore grouped together for the purpose of graphical comparison and not analyzed for nutrient content.

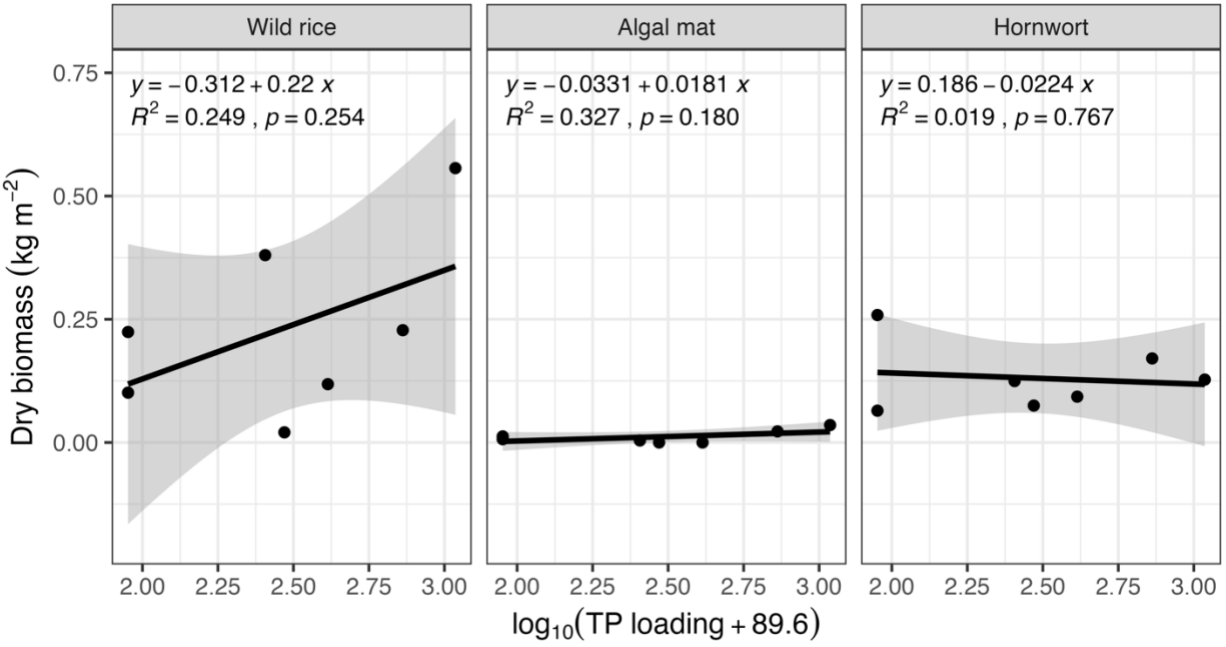

Figure 26. Biomass in EW mesocosms at the end of the study period reported on a dry mass basis. General linear models (solid lines) were fit to measured data (points) with 95% confidence intervals (shaded regions). Predictor variables were calculated by adding a constant (89.6) to the total phosphorus (TP) loading from aquaculture wastewater additions.

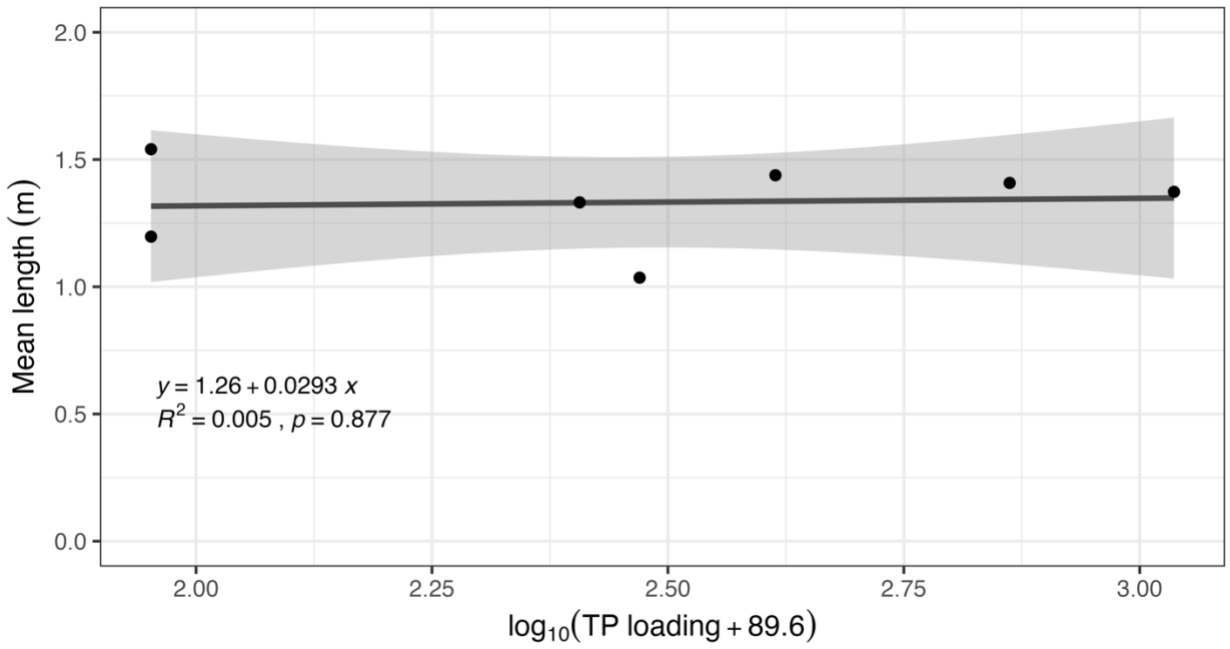

Figure 27. Mean length of wild rice plants in EW mesocosms at the end of the study period. A general linear model (solid line) was fit to measured data (points) with a 95% confidence interval (shaded region). Predictor variables were calculated by adding a constant (89.6) to the total phosphorus (TP) loading from aquaculture wastewater additions.

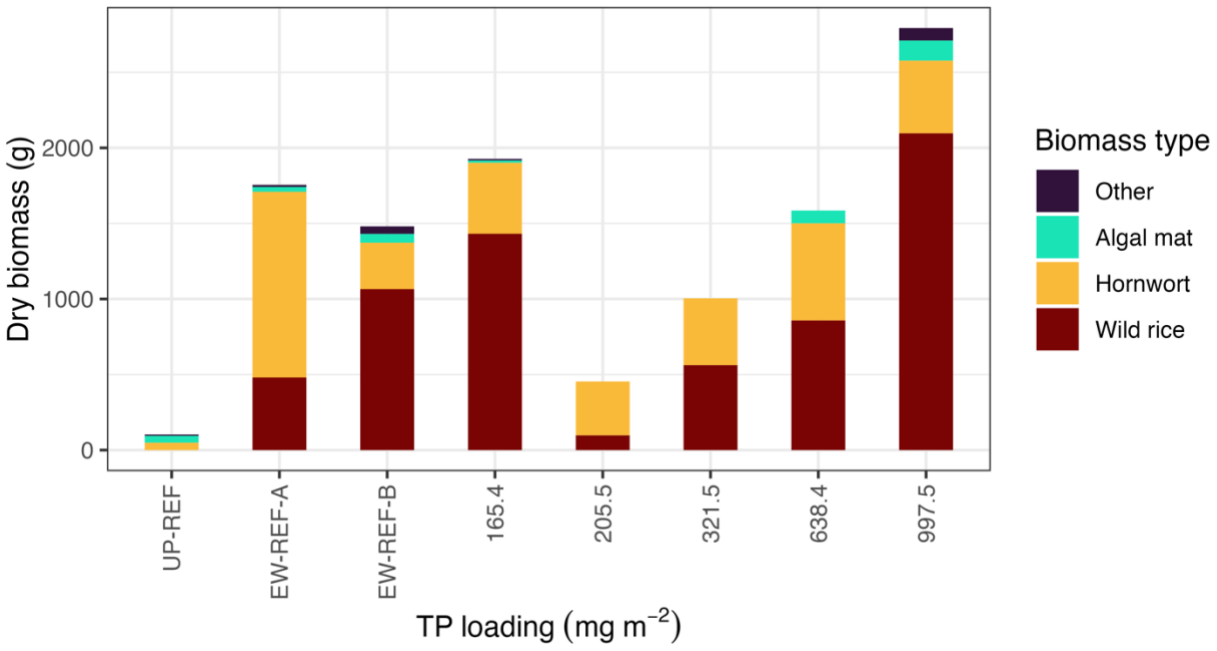

Figure 28. Quantities of different types of biomass in EW mesocosms at the end of the study period reported on a dry mass basis. The total phosphorus (TP) nutrient loadings from aquaculture wastewater are indicated with numerical values or the appropriate reference label.

The greatest production of algal mats was observed in the highest treatment (997.5 mg m^{-2}; Figure 28). In instances where algal mats were found, a positive linear relationship existed between TP content and nutrient loadings ($p = 0.038$; Figure 29), however no significant relationships were observed between TP content and nutrient loading in wild rice roots, wild rice shoots, or hornwort. The results from all fitted models for different biomass tissue endpoints are compiled in the Appendix (Table A - 6). A summary of statistically significant relationships for EW biomass tissues is presented in Table 11.

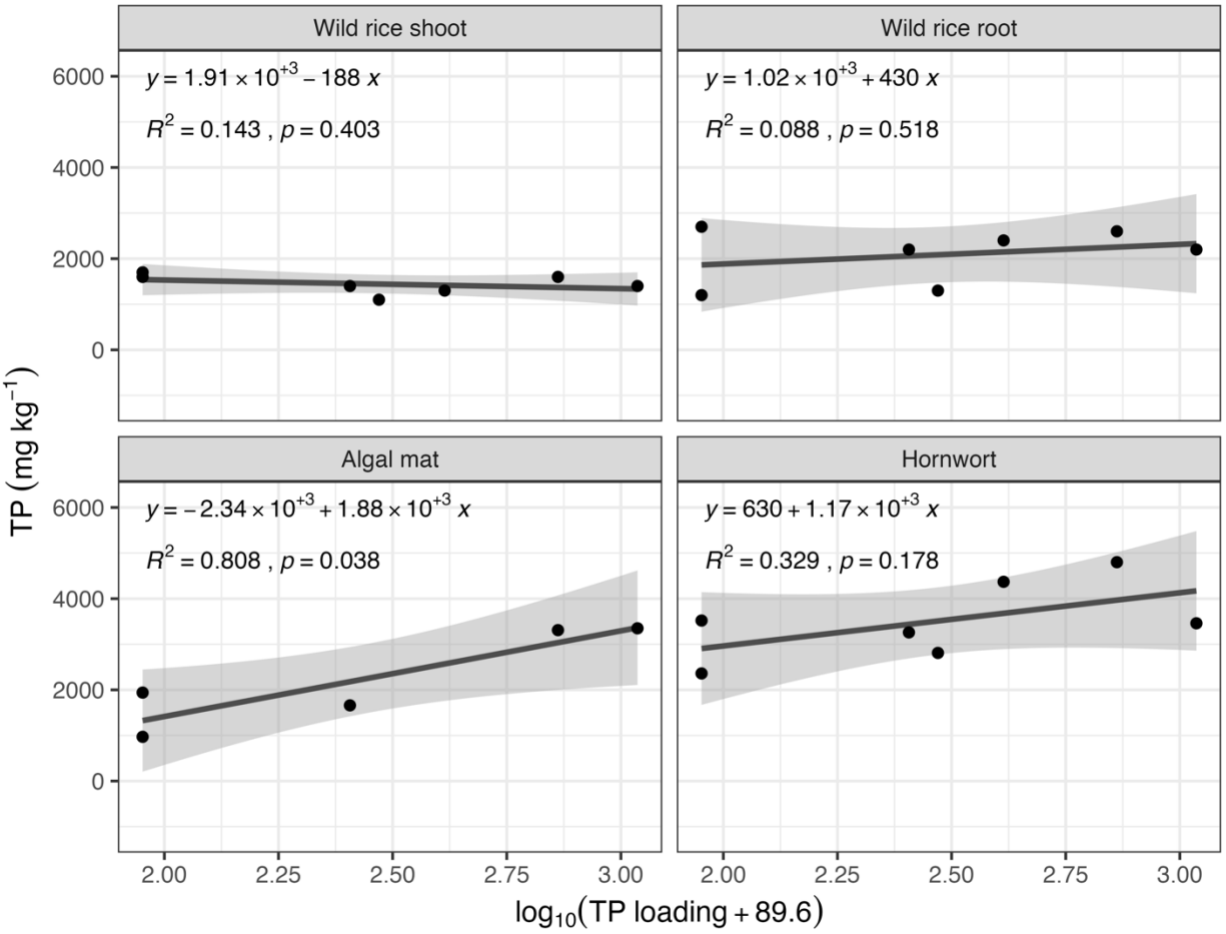

Figure 29. Total phosphorus (TP) content of different forms of biomass in EW mesocosms at the end of the study period. General linear models (solid lines) were fit to measured data (points) with 95% confidence intervals (shaded regions). TP content is reported on a dry mass basis. Predictor variables were calculated by adding a constant (89.6) to the total phosphorus (TP) loading from aquaculture wastewater additions.

Table 11. Summary of results for different endpoints assessed in EW mesocosm biomass tissues at the end of the study. Endpoints were assessed using general linear models and indicated in the table if a statistically significant result was detected. The directionality of the relationship is indicated in parentheses as either positive (+) or negative (-).

Biomass type	Endpoint
Wild rice seed	*NE*
Wild rice shoot	*NSD*
Wild rice root	*NSD*
Algal mat	TP (+)
Hornwort	TS (-), Ca (-)

NE = not evaluated, *NSD* = no statistical differences

3.3.1.10 Phosphorus Mass Balance

In Section 3.3.1.2, P species were characterized and presented as concentrations in Figure 16. An alternative representation of P species for the quantity (mass) of P in mesocosms is presented in Figure 30, and the two methods of presentation generated very similar trends. Possible inputs of P into mesocosms included AWW additions, atmospheric deposition, and additions of water used to maintain the appropriate water depths in mesocosms throughout the study. No clear systematic increase in P quantity was observed in mesocosms water, and therefore the P inputs from other sources can be assumed to be negligible (which was likely the case as only small amounts of water were added relative to the volume of the mesocosm) and/or the P inputs were rapidly taken up and assimilated into other matrices like plant, soil, or algae. However, persistence of P and elevated P concentrations in CW water as a response to AWW additions were observed (previously discussed in Section 3.3.1.2), suggesting that any additional P inputs from other sources would have resulted in further elevations observed within CW water.

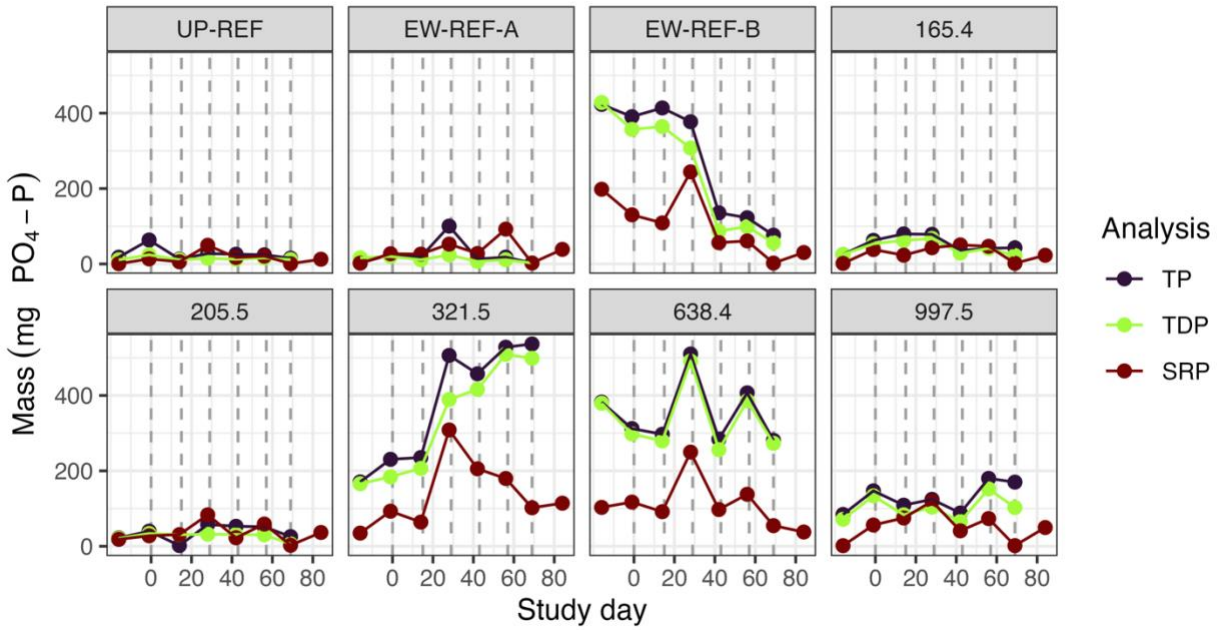

Figure 30. Quantities of total (TP), total dissolved (TDP), and soluble reactive (SRP) phosphorus in EW mesocosm water. Each graphical panel represents a mesocosm with the TP loading from aquaculture wastewater (AWW) additions indicated in units of mg m^{-2}. Vertical dashed lines indicate AWW addition events.

The total quantities and relative proportions of P in each matrix during initial and final timepoints are presented in Figure 31 and Figure 32, respectively. At both timepoints, P from soil was the predominate contributor and P from CW water was relatively very small and a negligible contributor to total P in mesocosms. The change in P quantity for different matrices throughout the study is presented in Figure 33 with no evident treatment-based trends. The overall change in P quantity (calculated as the sum of the differences of individual matrices) between initial and final timepoints is presented alongside P inputs from AWW additions in Figure 34 and demonstrates the large discrepancies and issues tracking P in CW systems. Soil depth surveys were subject to large variation and due to the high quantities of P in soil relative to other matrices, this variation negatively impacted the ability to perform mass balance analyses. Future assessments could involve more direct measures of soil by mass, or may instead implement

hydroponic or aquaponic systems to avoid this significant source of variation. In the literature, hydroponic and aquaponic systems have been successful for mass balance analyses of nutrients such as N and P (Cerozi & Fitzsimmons, 2017; Yang & Kim, 2020). Although hydroponic wild rice systems have been utilized (Fort et al., 2017; Malvick & Percich, 1993; Nayak et al., 2014), studies focused on toxicity, disease, and contaminant accumulation. Large-scale treatment CWs often use some media for plant growth (e.g. soil, gravel) which facilitates the effective treatment of contaminants (Vymazal, 2010). For wild rice systems, hydroponic or small-scale (microcosm) systems containing soil could provide a better understanding of nutrient dynamics. This approach could ultimately improve understandings of the mechanisms by which nutrient removal occurs in the wild rice CWs studied here.

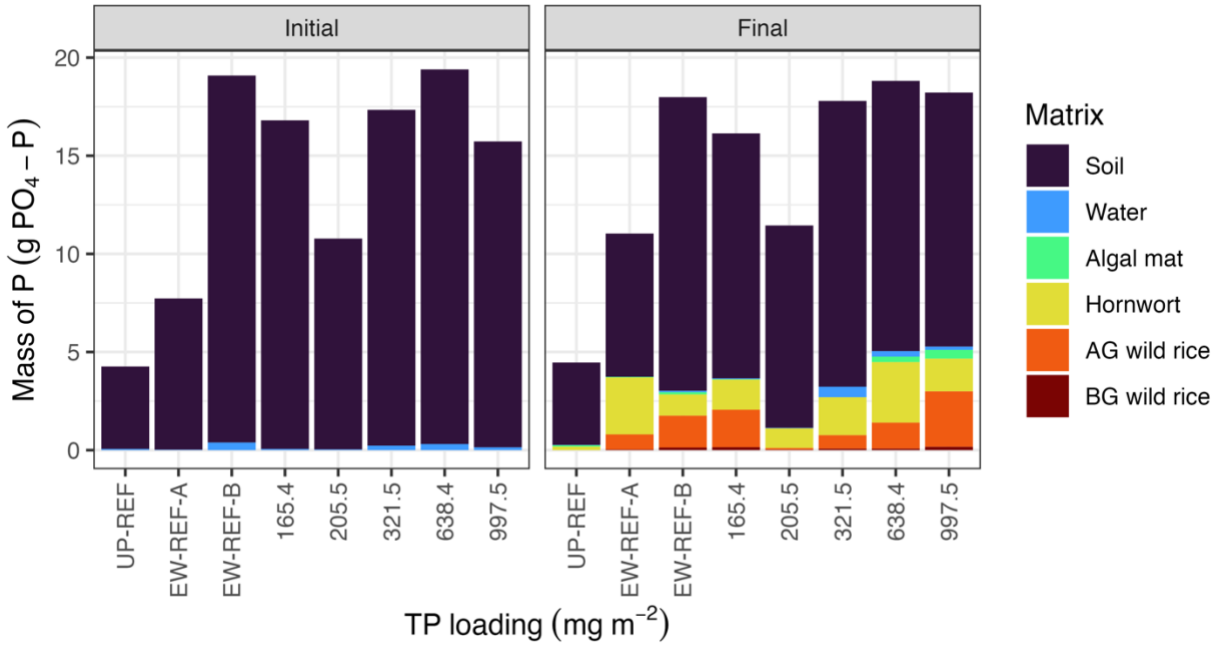

Figure 31. Total quantities of phosphorus (P) in different matrices during initial and final timepoints in EW mesocosms. Wild rice plants are presented as either aboveground (AG; seeds and shoots) or belowground (BG; roots) plant tissues. The total P (TP) nutrient loadings from aquaculture wastewater are indicated with numerical values or the appropriate reference label.

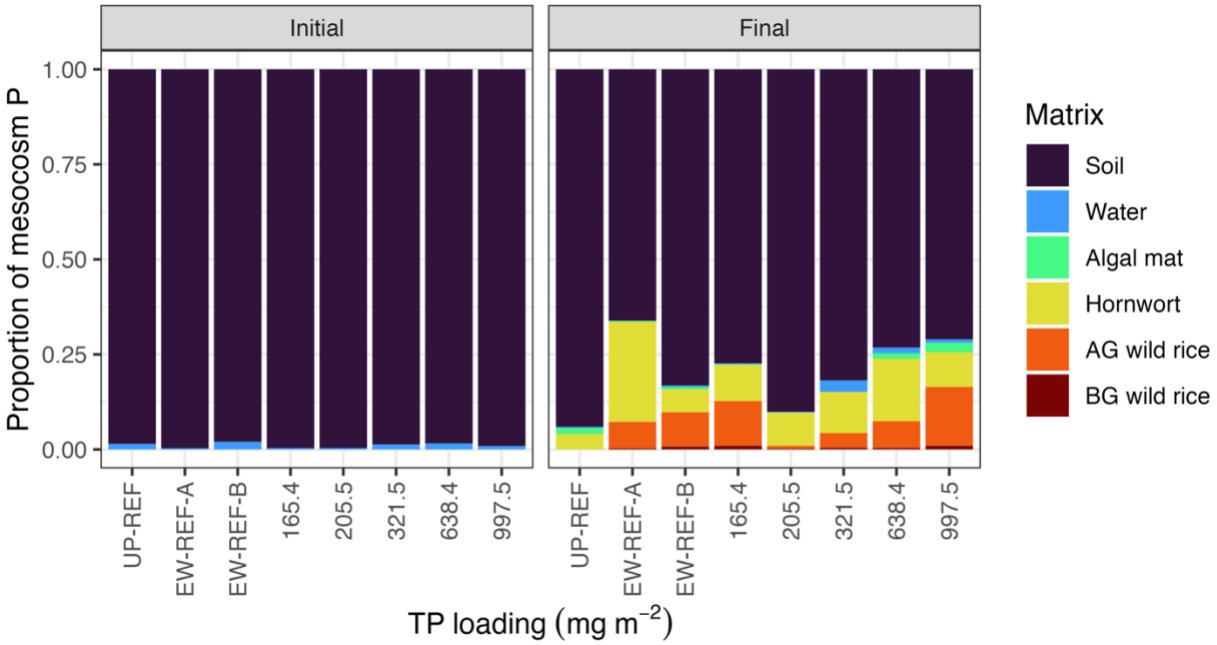

Figure 32. Relative proportions of phosphorus (P) in different matrices during initial and final timepoints in EW mesocosms. Wild rice plants are presented as either aboveground (AG; seeds and shoots) or belowground (BG; roots) plant tissues. The total P (TP) nutrient loadings from aquaculture wastewater are indicated with numerical values or the appropriate reference label.

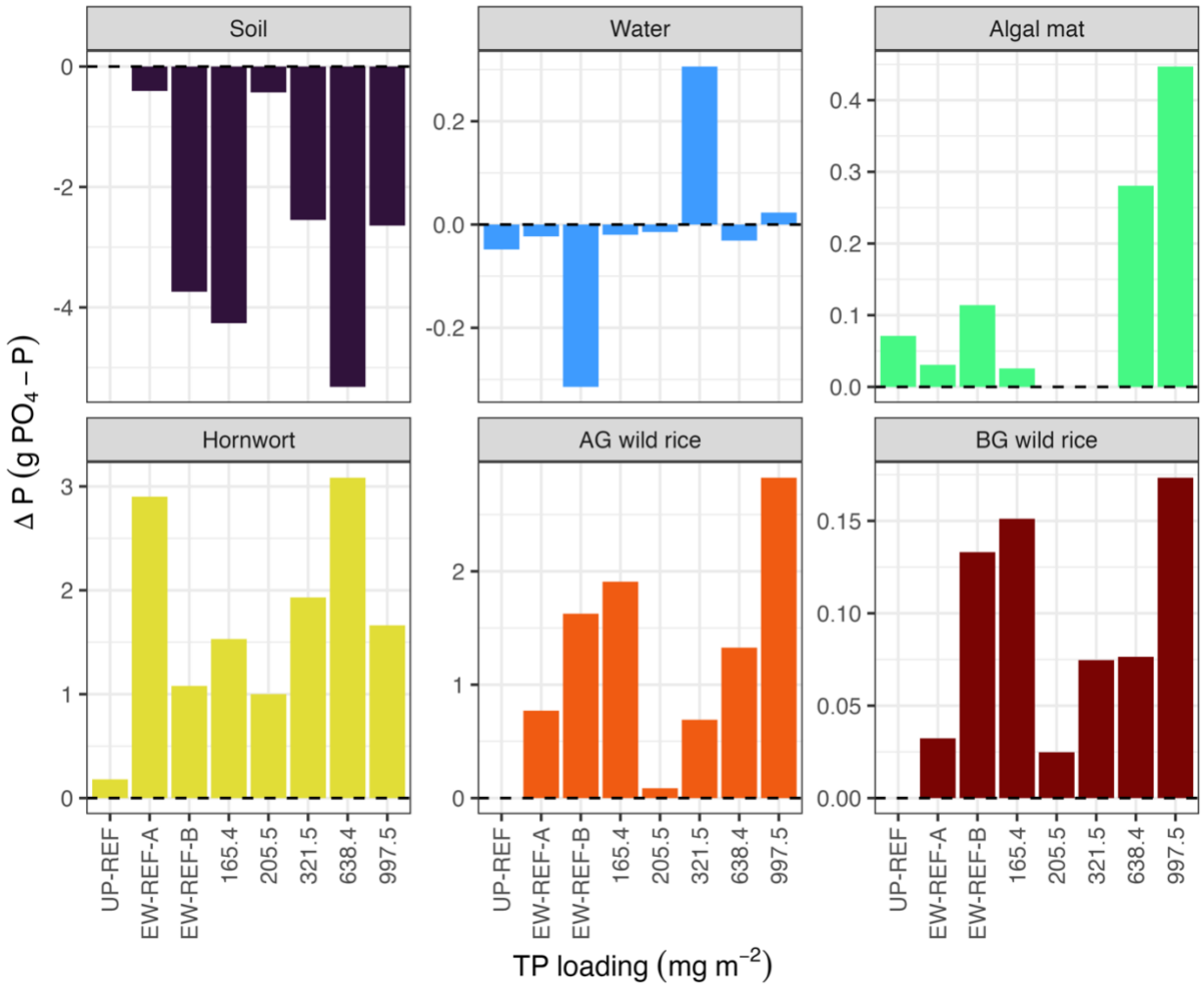

Figure 33. Change in quantity of phosphorus (ΔP) in different matrices between initial and final timepoints in EW mesocosms. Positive values represent increases of P with time while negative values represent decreases of P with time. Wild rice plants are presented as either aboveground (AG; seeds and shoots) or belowground (BG; roots) plant tissues. The total P (TP) nutrient loadings from aquaculture wastewater are indicated with numerical values or the appropriate reference label.

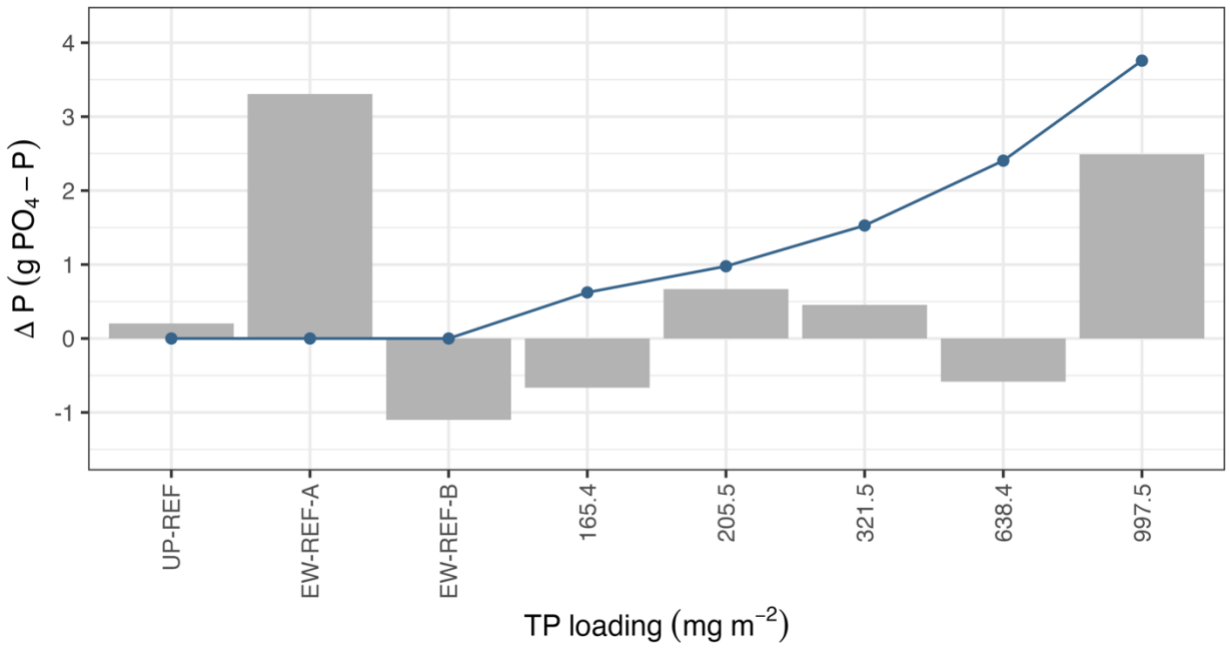

Figure 34. Comparison between the change in total quantity of phosphorus (ΔP) in EW mesocosms between initial and final timepoints (grey bars) and the total quantity of P added through aquaculture wastewater (AWW) additions (blue points). Positive values represent an increase of P with time while negative values represent a decrease of P with time. The total P (TP) nutrient loadings from AWW are indicated with numerical values or the appropriate reference label.

Using the P differences achieved in Figure 33 and assuming initial (day 0) biomass in mesocosms was negligible, P removal rates in plants and algae can be estimated over the 100-day period between the start of the study and decommissioning of mesocosms. For the 997.5 mg m^{-2} treatment, AG wild rice, BG wild rice, hornwort, and algal mats contributed to 7.500, 0.460, 4.414, and 1.186 mg m^{-2} d^{-1} of P removal, respectively. Meanwhile, the mean values for EW-REF-A and EW-REF-B among AG wild rice, BG wild rice, hornwort, and algal mats were 2.522, 0.174, 4.187, 0.152 mg m^{-2} d^{-1} of P removal, respectively. Wild rice was a substantial nutrient sink among high-nutrient loading treatments while hornwort was a more predominate nutrient sink among reference and lower nutrient loading treatments.

3.3.2 New Stand Systems

3.3.2.1 Temperature and Light Data Loggers

Results from data loggers in mesocosms which measured water temperature and light intensity in mesocosms are plotted in Figure 35. Diurnal changes in water temperature were evident, with a mean daily change in temperature of 7.3°C. A decline in water temperature was observed after day 70 for reasons discussed previously (see Section 3.3.1.1).

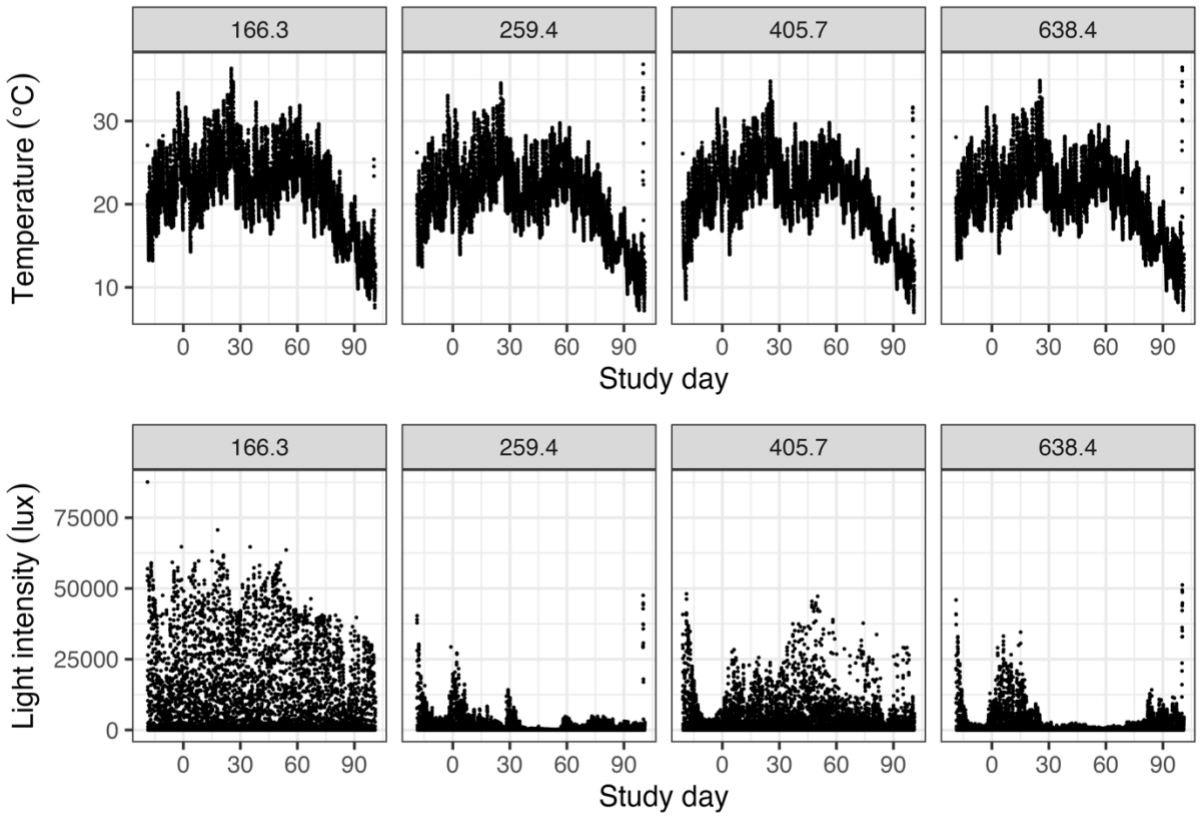

Figure 35. Temperature and light intensity data from loggers in select NS mesocosms. Loggers were set to record data every 20 min. Each graphical panel presents the data from one logger with the total phosphorus loading from aquaculture wastewater indicated in units of mg m^{-2}.

The 166.3 and 405.7 mg m^{-2} treatments did not experience the same reduction in light intensity as was observed in the 259.4 and 638.4 mg m^{-2} treatments (Figure 35). When evaluating the

types and quantities of biomass in NS systems (see Section 3.3.2.9), there were no indicators as to why variations in light intensity occurred amongst these select mesocosms. The UM air remains the more informative measure of incident light conditions because of the unknown influence and potential for soil, plants, and mesocosm walls to obstruct light loggers near the soil-water interface.

3.3.2.2 Phosphorus in Mesocosm Water

Elevations in P species were observed among the 66.5, 259.4, and 638.4 mg m^{-2} treatments but ultimately no treatment-based effects of AWW additions on P species were evident among NS systems (Figure 36). All elevated TP concentrations were below 0.3 mg L^{-1} and notable quantities of algal mats were found in NS-REF-B, NS-REF-C, and 166.3, 405.7, and 997.5 mg m^{-2} treatments (see Section 3.3.2.9; Figure 48). The production of algae, particularly algal mats, can assimilate substantial quantities of P (Krause-Jensen et al., 1999; Pikosz & Messyasz, 2016) and the assimilation of P by algal mats corresponded with elimination of P from CW water. No algal mats and low total biomass was observed in NS-REF-A, and in the 66.5, 106.4, 259.4, and 638.4 mg m^{-2} treatments (see Section 3.3.2.9; Figure 48). Without P assimilation into biomass, elevations in P species in CW water were observed in response to AWW additions. Among higher nutrient loading conditions with low biomass production (i.e. 259.4 and 638.4 mg m^{-2}), elevations of P in CW water occurred, whereas in high loading treatments where there were greater quantities of biomass (i.e. 405.7 and 997.5 mg m^{-2}), elevations of P were smaller.

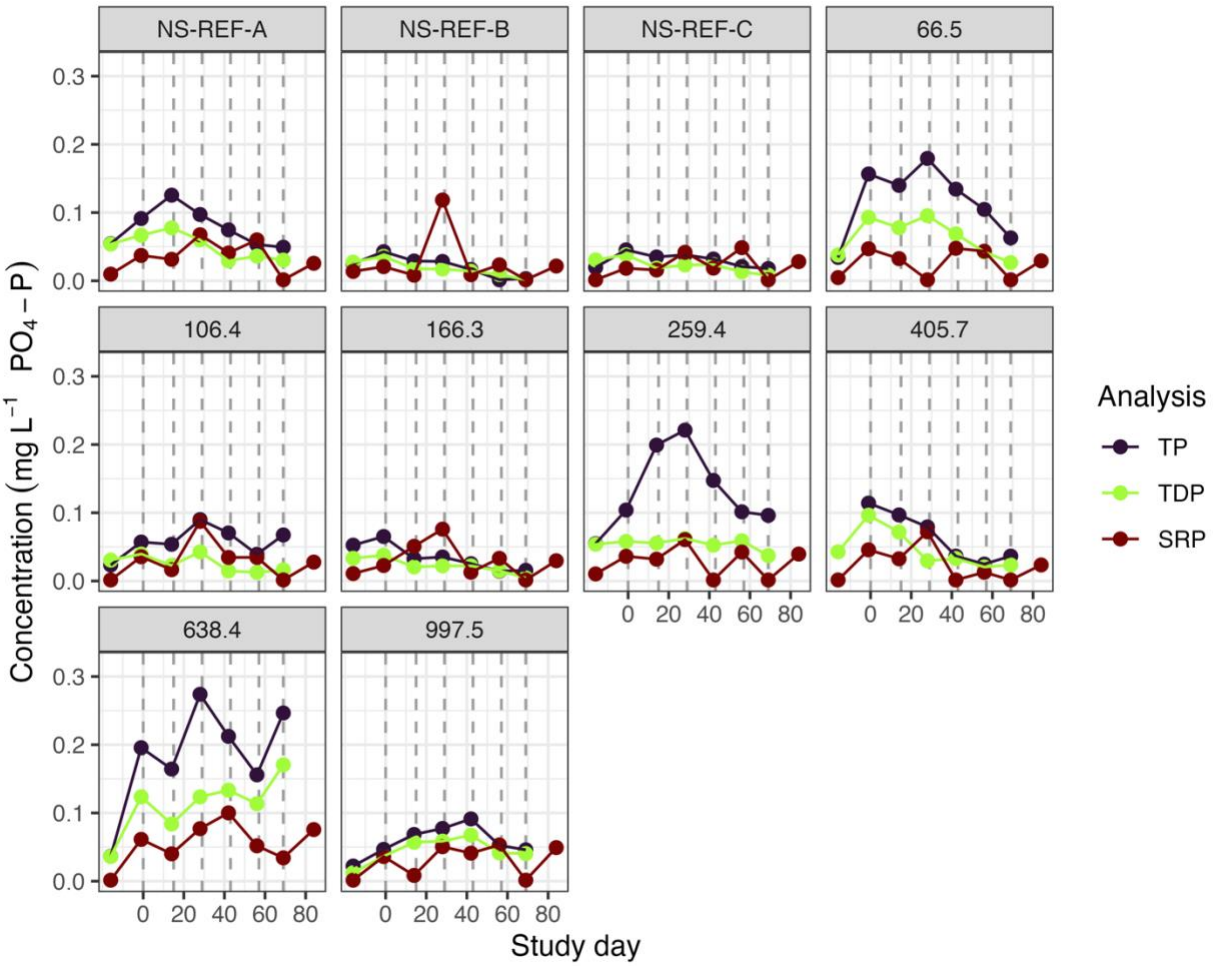

Figure 36. Total (TP), total dissolved (TDP), and soluble reactive (SRP) phosphorus concentrations in NS mesocosm water. Each graphical panel represents a mesocosm with the TP loading from aquaculture wastewater (AWW) additions indicated in units of mg m^{-2}. Vertical dashed lines indicate AWW addition events.

In instances where P elevations were observed, the difference between TP and TDP was substantial (Figure 36). This observation was validated by PP concentrations (Figure A - 24) which corresponded to the difference between TP and TDP. Concentrations of PP were generally below 50 µg L^{-1}, but in instances where elevations occurred, concentrations were in the 50-100 µg L^{-1} range.

With the exception of one value for NS-REF-B on day 28 (which likely resulted from an error during analysis because SRP >> TP and SRP >> TDP), concentrations of SRP were equal to or less than 0.1 mg L^{-1} for the duration of the study and no notable increases observed throughout the study period (Figure 36). The lack of SRP elevations in response to AWW additions could have resulted from P assimilation by phytoplankton. Among mesocosms with elevations of P species in CW water, increases in chl *a* were observed for the 66.5, 259.4, and 638.4 mg m^{-2} treatments which began on day 28 (see Section 3.3.2.4; Figure 40). The uptake of readily available SRP by phytoplankton in the water column reduces the SRP concentration in CW resulting in more pronounced differences between TP and TDP, as phytoplankton would be removed during filtration. Particularly low biomass was observed in NS systems, allowing resident phytoplankton to benefit from the low competition for light and nutrients. Therefore, phytoplankton uptake of SRP occurred rapidly and without the same restrictions that exist in other CW systems with more prolific biomass production. In treatment CWs in the literature, SRP concentrations are often measured near or below detection limits in effluents exiting treatment areas (Juston & DeBusk, 2011; Kadlec, 2016; McCormick et al., 2001). In these scenarios, treatment efforts should address other forms of P being discharged such as PP and DOP which contribute to eutrophication in receiving environments (Correll, 1998; Ji et al., 2017).

The establishment of CWs has an impact on P dynamics and there is often a 1–5 year start-up period during which P can be bound to a variety of sorption sites and greater biomass production occurs (Kadlec et al., 2000). New CWs exhibit greater P removal in the start-up period because soils have not been P-saturated and the establishing vegetation is undergoing rapid growth

(Kadlec, 2016). Therefore, the TP removal of CWs often decreases with age (Rozema, Rozema, & Zheng, 2016). However, classical CWs typically implement dense emergent and perennial forms of vegetation such as cattail (Vymazal, 2010). Northern wild rice is an annual plant which requires seeding each year and therefore nutrient demand from plant growth can be expected to remain similar from year-to-year in CWs, although soil nutrient dynamics would be altered with continued usage of the CW. The NS systems were established with fresh soil and no other forms of vegetation and therefore had a high capacity for P binding to soil (see Section 3.3.2.8). Additionally, SRP in the water column was readily available for phytoplankton growth (as described previously). Ultimately, the net effect was lower SRP and greater chl *a* concentrations in NS mesocosm water when P elevations occurred, and systems had the capacity for P removal from CW water through sorption to soil sites.

Under the nutrient gradient evaluated, NS systems effectively accommodated AWW loadings up to 997.5 mg m^{-2} TP over a period of 69 days (i.e. 14.457 mg m^{-2} d^{-1}). However, the apparent success of P elimination from CW water was directly linked to the production of algal mats. In instances where algal mats were not produced (i.e. among the 259.4 and 638.4 mg m^{-2} treatments), elevations in P species in CW water were observed in response to AWW additions. For continued usage of NS systems, additional CW management strategies might involve the physical removal of algal mats which would prevent the release of P upon algae cell death. In instances where algal mats are not observed in CW systems, caution is warranted when applying AWW loadings as water quality can deteriorate. Very little wild rice production was observed throughout the study period and increasing production in NS through greater seeding rates or

incorporation of AWW fertilizer at the start of the growing season could improve production, prevent water quality deterioration, and provide greater treatment capacity.

3.3.2.3 Nitrogen in Mesocosm Water

The concentrations of the main nitrogen species (TDN, TAN, NO_2-N, NO_3-N) in CW water are presented in Figure 37. Concentrations of TDN increased slightly or were generally constant throughout the study period. The most pronounced increases in TDN were observed among the 405.7 and 997.5 mg m^{-2} treatments, where concentrations exceeded 1.5 mg L^{-1} at the final sampling event. Using the 997.5 mg m^{-2} treatment as an example, TDN concentrations increased from approximately 0.5 mg L^{-1} to 1.0 mg L^{-1} throughout the first three sampling events (i.e. from day -16 to 14), then increased further reaching concentrations of 1.66 and 2.30 mg L^{-1} on days 56 and 84, respectively. While similar increases were observed among reference and low-nutrient loading conditions, the magnitudes of TDN increases were smaller. Meanwhile, no treatment-based differences in TAN or NO_2–N were observed throughout the study period (Figure 37, Figure A - 21, Figure A - 22) and a decrease in NO_3–N concentrations was observed in all CWs on day 42 (Figure 37, Figure A - 23).

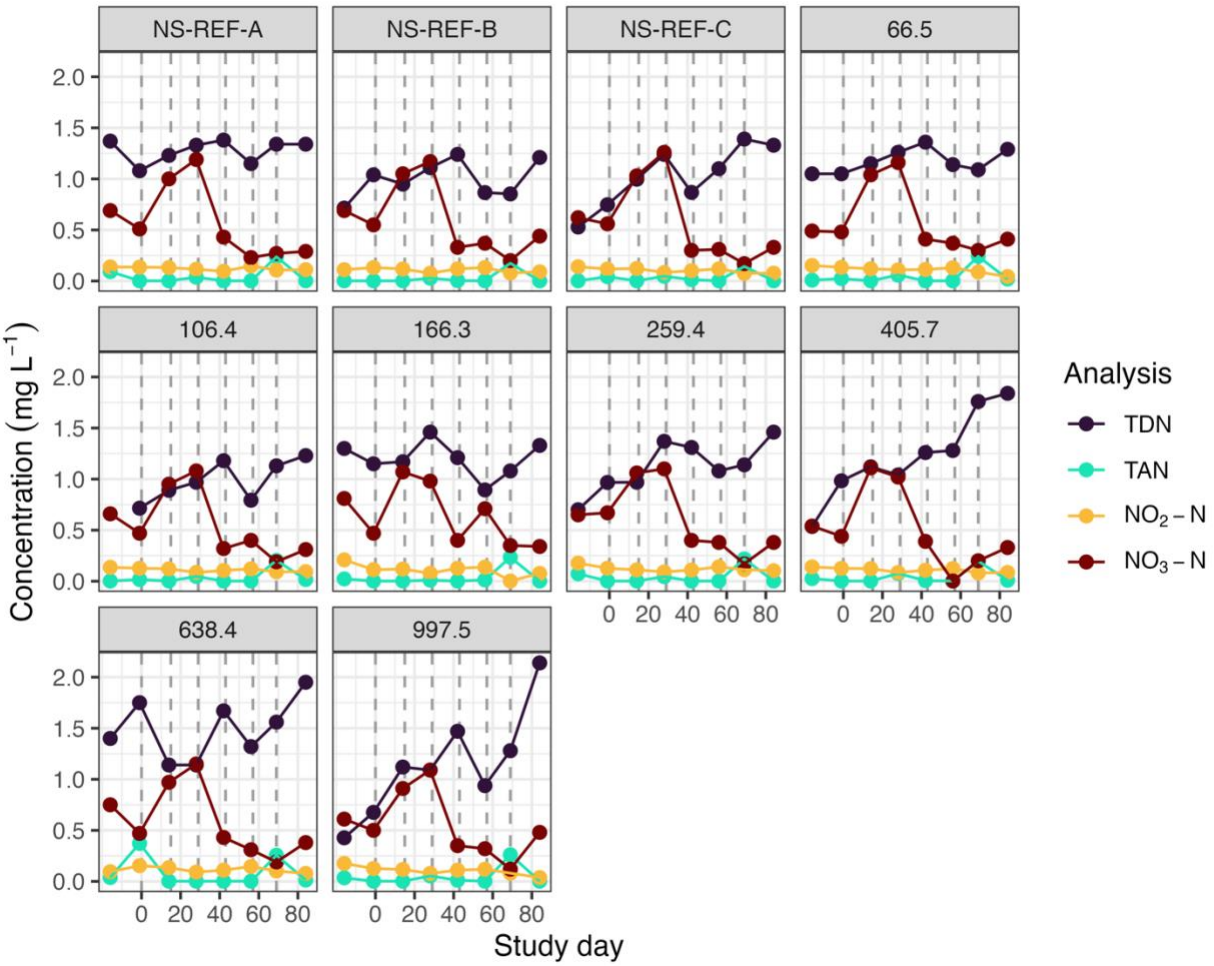

Figure 37. Total dissolved (TDN), total ammonia (TAN), nitrite (NO_2–N), and nitrate (NO_3–N) nitrogen concentrations in NS mesocosm water. Each graphical panel represents a mesocosm with the total phosphorus loading from aquaculture wastewater (AWW) additions indicated in units of mg m^{-2}. Vertical dashed lines indicate AWW addition events.

In a similar manner as was described previously (Section 3.3.1.3), the difference between TDN and NO_3–N was more pronounced during the second half of the study period. However, in NS systems, high biofilm growth rates were observed (see Section 3.3.2.4). Similar logic can be applied here as was discussed for the relationship between P species and chl *a* in mesocosm water; biofilm had low competition for light and nutrients and therefore conditions were more favourable for rapid growth. Declines in DO were not observed in CW water (Figure A - 29),

however the low biomass production in NS system implies that less organic matter (e.g. plant litter or algal mats) is undergoing degradation upon death. The preservation of high DO is promising for treatment as long-term low DO levels in CWs can negatively impact performance (H. Liu et al., 2016). In wetland N cycling, nitrification (i.e. oxidation of NH_4^+ to NO_3^- with NO_2^- as an intermediate) is meditated by chemoautotrophic bacteria which use oxygen as an electron acceptor (Snow et al., 2012). Simultaneously, bacterial-mediated denitrification processes (i.e. conversion of NO_3^- and NO_2^- to N_2 gas) occur in anaerobic conditions, which are created in wetland and paddy soils (Van Cleemput et al., 2007). The CWs receiving AWW were subjected to substantial TAN loadings (Table 7). By supporting the proper microenvironments for nitrification and denitrification, both nitrification and denitrification can be achieved in the CW (Bastviken et al., 2003; Platzer, 1999), facilitating the elimination of TAN from AWW. When considering rearing fish in wild rice ecosystems (Ahmed et al., 2021), the removal of TAN is particularly beneficial as resident biota, especially fish, are susceptible to ammonia toxicity (Randall & Tsui, 2002). The potential for collapse of phytoplankton blooms should be investigated in future studies. Phytoplankton death can lead to DO consumption and further reinforce water quality degradation (Wang & Zhang, 2020), In shallow systems, water level management in can help mitigate this depletion of DO (Miranda et al., 2001).

3.3.2.4 Biofilm and Phytoplankton

Biofilm tile chl *a* concentrations and fitted logistic growth models are plotted in Figure 38. Key model parameters associated with growth curves are found in the Appendix (Table A - 7). Biofilm chl *a* concentrations were generally lower during the first four sampling events, however the inflexion points of growth curves (t_{mid}) were highly variable and no treatment-based trends

were evident. Growth rates were highly variable and high values were observed for NS-REF-B, 166.3 and 259.4 mg m^{-2} treatments. Similarly, no treatment-based differences in AFDM were observed (Figure 39). Aquatic macrophytes can impact nutrient resuspension and modify the flux of N and P from sediments into the water column which can in turn impact algal growth (Nurminen & Horppila, 2009). Submerged aquatic macrophytes (such as hornwort) are able to effectively reduced the amount of nutrients resuspended (Nurminen & Horppila, 2009). With low quantities of hornwort in NS systems, algal growth may have been enhanced as a greater resuspension of nutrients was possible.

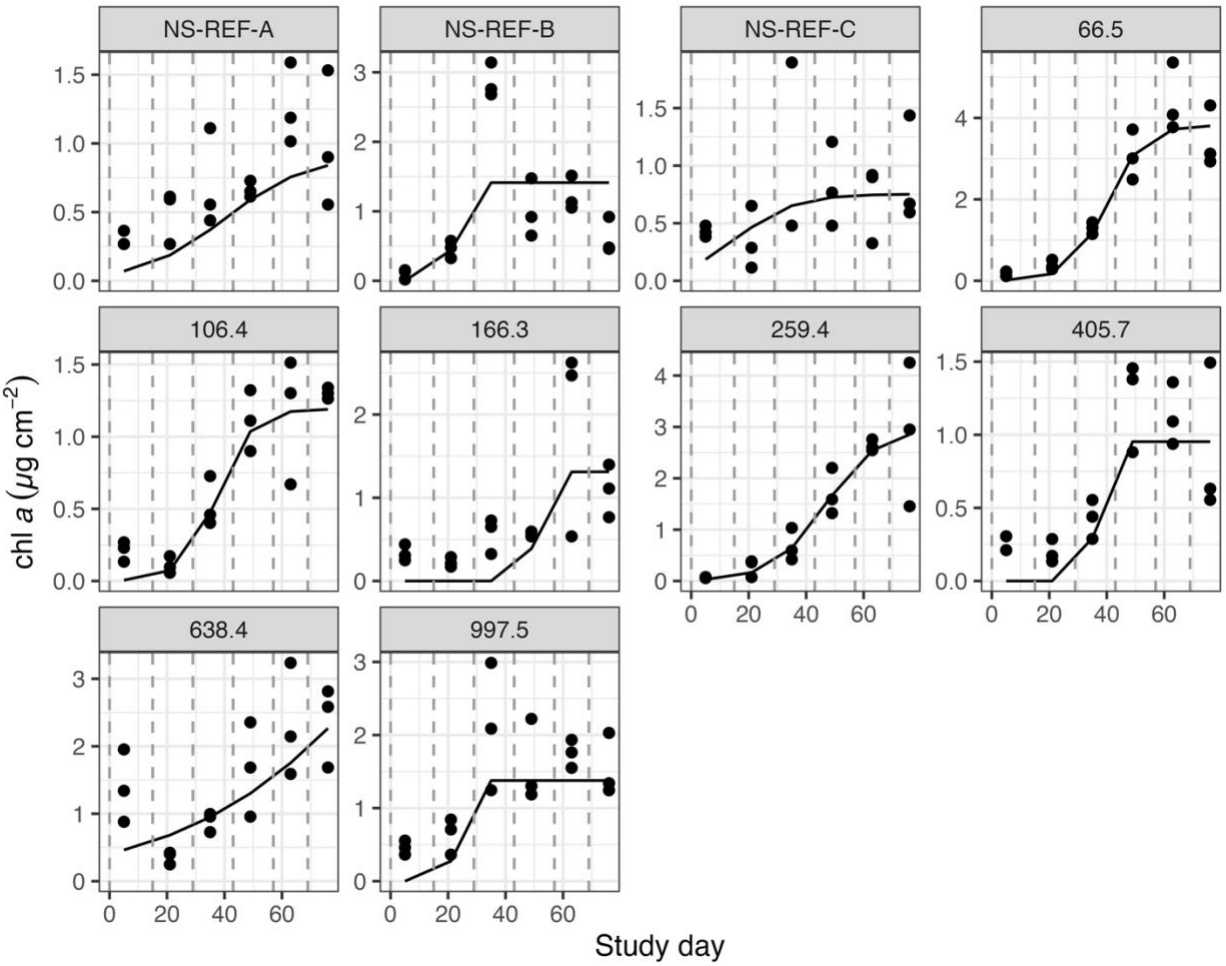

Figure 38. Biofilm tile chlorophyll *a* (chl *a*) concentrations in NS mesocosms. Measured data (points) are included with fitted logistic growth curves (solid lines). Note that different y-axis scales are used across the graphical panels. Each graphical panel represents a mesocosm with the total phosphorus loading from aquaculture wastewater (AWW) additions indicated in units of mg m^{-2}. Vertical dashed lines indicate AWW addition events.

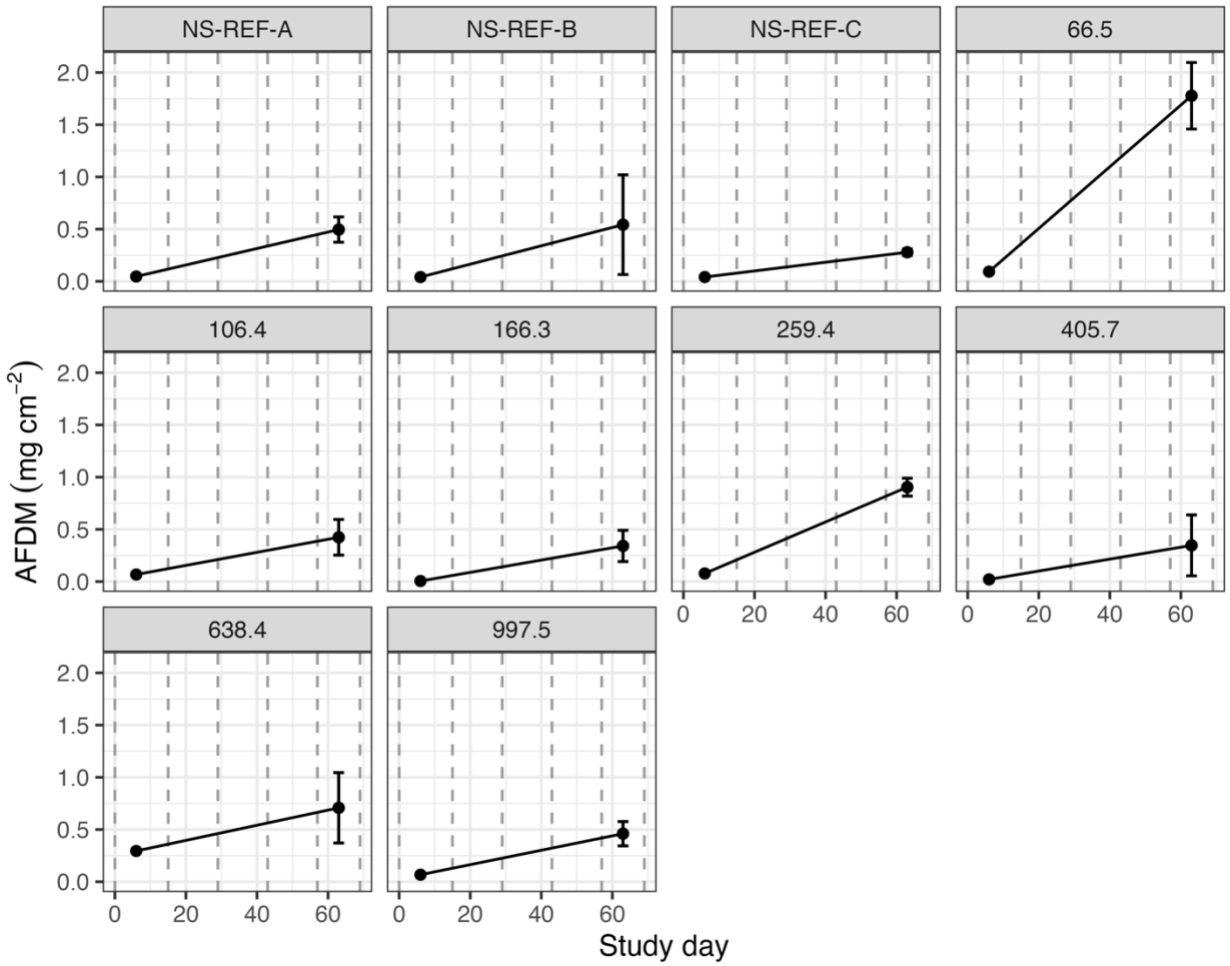

Figure 39. Biofilm tile ash-free dry mass (AFDM) in NS mesocosms. Replicates were pooled on day 6, while the mean (± SD) of three replicates is presented on day 63. Each graphical panel represents a mesocosm with the total phosphorus loading from aquaculture wastewater (AWW) additions indicated in units of mg m^{-2}. Vertical dashed lines indicate AWW addition events.

Water column chl *a* concentrations were generally below 10 µg L^{-1} among NS mesocosms for the duration of the study period (Figure 40). Notable elevations >10 µg L^{-1} were observed among 66.5, 259.4, and 638.4 mg m^{-2} treatments, the same treatments which exhibited elevations in P species in Figure 36. Similarly, elevations in biofilm chl *a* were observed among these treatments (Figure 38). In other treatments, available P contributed to the growth of algal mats (see Section

3.3.2.9). However, in instances where algal mats were not produced, elevations in phytoplankton and biofilm growth were observed.

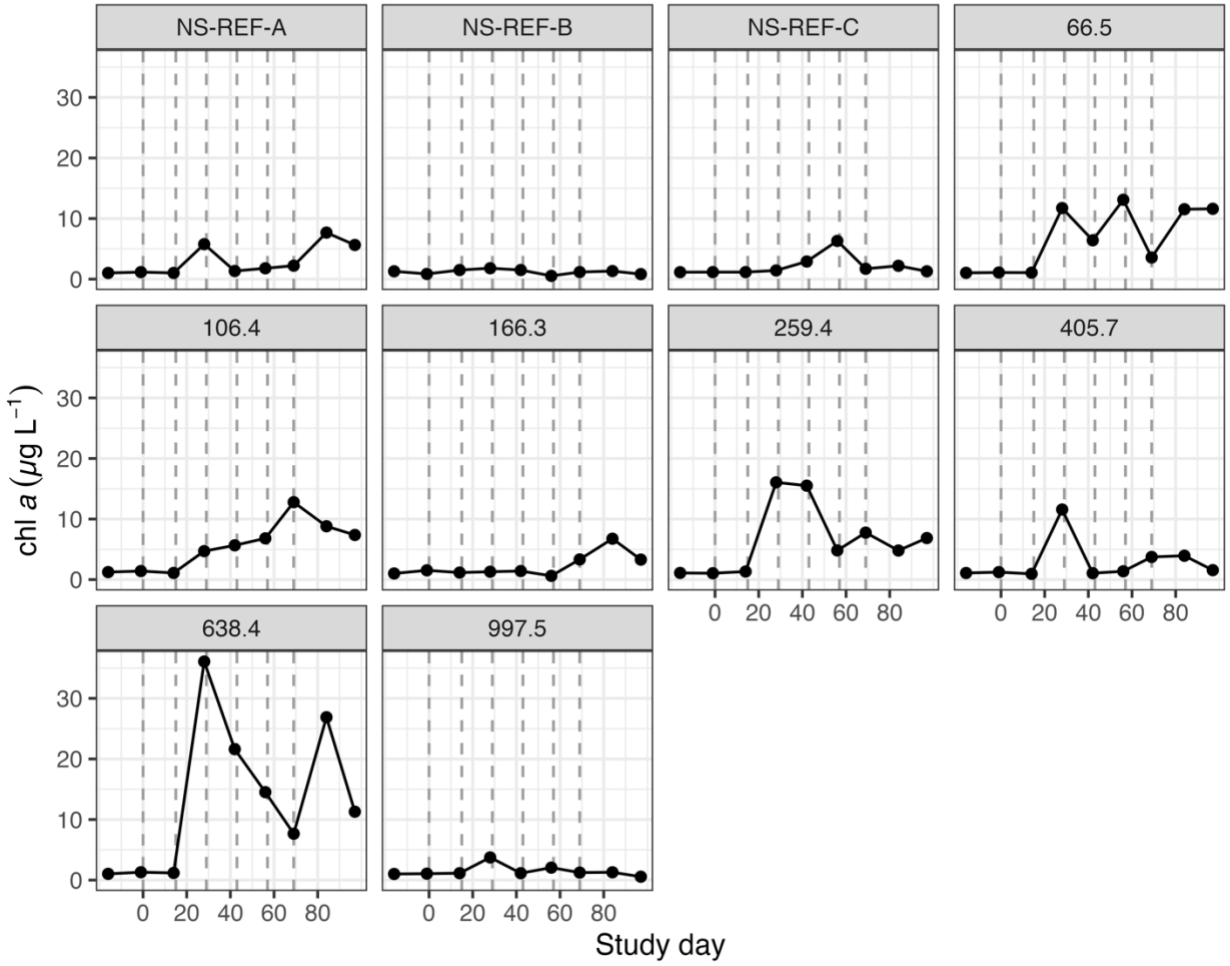

Figure 40. Chlorophyll *a* (chl *a*) concentrations in NS mesocosm water. Each graphical panel represents a mesocosm with the total phosphorus loading from aquaculture wastewater (AWW) additions indicated in units of mg m^{-2}. Vertical dashed lines indicate AWW addition events.

3.3.2.5 Performance of Constructed Wetlands for Phosphorus Treatment

Initial and final TP concentrations in CW water were approximately equal among the high nutrient loading treatments, but diverged slightly among lower nutrient loading treatments where the difference between initial and final TP concentrations became larger (Figure 41). Details and

parameters related to CW performance are presented in Table 12. In all instances the CR of CWs that received AWW was greater than the mean CR of reference treatments (61.2%). Lower CR was observed among the low nutrient loading treatments (i.e. 66.5 and 106.4 mg m^{-2}) than high nutrient loading treatments (i.e. 166.3–997.5 mg m^{-2}). An exponential trend was observed for PLR, which when analyzed on a log-scale generated a statistically significant positive linear trend between PLR and TP loading (Figure 42). As has been discussed previously (see Section 3.3.1.5), the full P removal capacity of CW systems was not reached across the range of applied treatments. However, it is important to note that excessive algae production at higher nutrient loadings would not be an ideal mechanism for P removal when attempting to maintain the long-term functionality of CW systems. Therefore, utilizing higher nutrient loadings, which achieve higher PLR, does not necessarily imply better overall treatment outcomes.

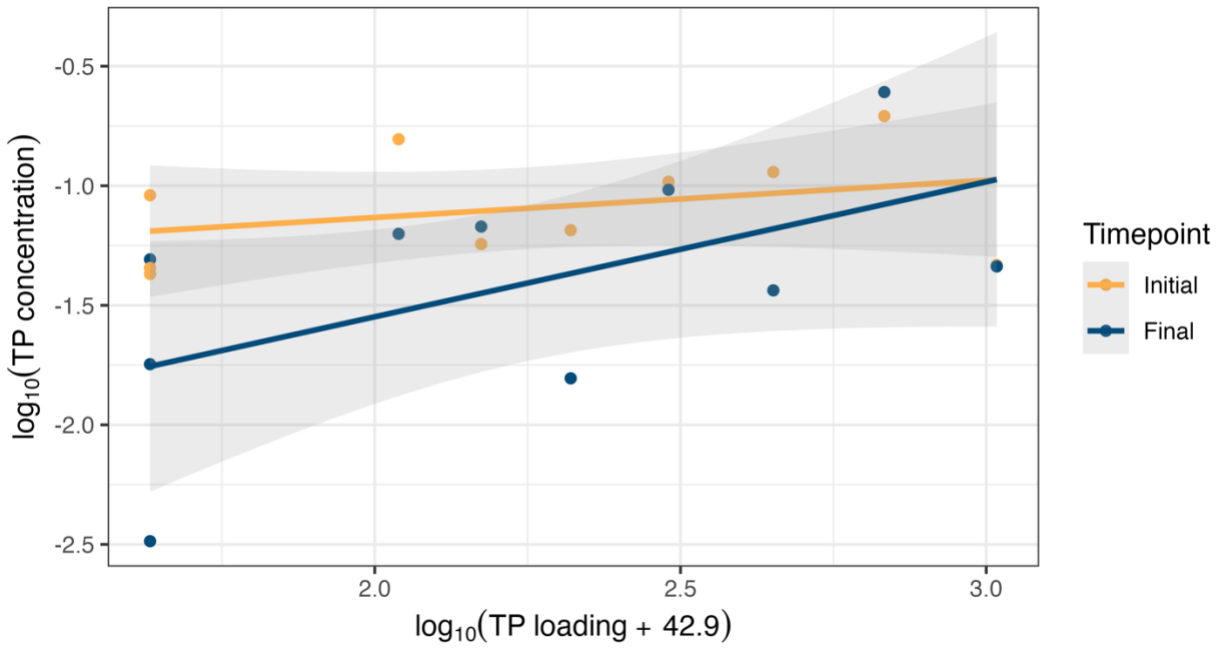

Figure 41. Comparison of total phosphorus (TP) concentrations in NS mesocosm water during initial (day -1) and final (day 69) timepoints of the performance period. General linear models (solid lines) were fit to measured data (points) with 95% confidence intervals (shaded regions). Predictor variables were calculated by adding a constant (42.9) to the TP loading from aquaculture wastewater additions.

Table 12. Calculated and measured parameters relating to the performance of NS systems removing total phosphorus (TP) from aquaculture wastewater (AWW).

TP loading for study (mg m^{-2})	TP loading for performance period (mg m^{-2})	C_{max} (mg L^{-1})	C_f (mg L^{-1})	CR (%)	PLR (mg m^{-2} d^{-1})	AWW loading (L d^{-1})	HLR (mm d^{-1})
0 (NS-REF-A)	0.0	0.084	0.049	41.7	0.168	0.000	0.000
0 (NS-REF-B)	0.0	0.036	0.003	90.9	0.160	0.000	0.000
0 (NS-REF-C)	0.0	0.037	0.018	50.9	0.096	0.000	0.000
66.5	54.1	0.266	0.063	76.3	1.124	0.071	0.019
106.4	86.6	0.269	0.068	74.9	1.114	0.114	0.030
166.3	135.3	0.411	0.016	96.2	2.140	0.179	0.047
259.4	211.1	0.687	0.096	86.0	2.973	0.279	0.074
405.7	330.1	0.915	0.037	96.0	5.030	0.436	0.116
638.4	519.5	1.597	0.247	84.6	7.004	0.686	0.182
997.5	811.7	2.278	0.046	98.0	11.556	1.071	0.284

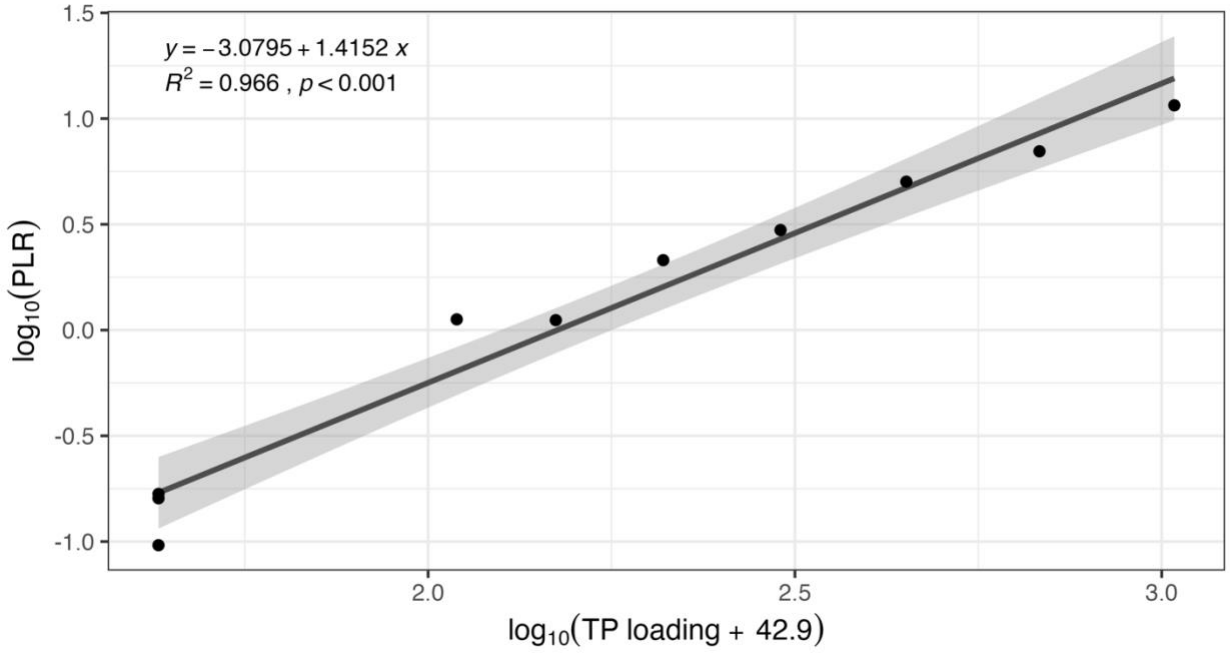

Figure 42. Phosphorus load reduction (PLR) for total phosphorus (TP) in NS mesocosm water during the 70-day performance period. A general linear model (solid line) was fit to calculated data (points) with a 95% confidence interval (shaded region). Predictor variables were calculated by adding a constant (42.9) to the TP loading from aquaculture wastewater additions.

3.3.2.6 Modelling and Interaction Analysis

The results of all fitted LMMs are included in the Appendix (Table A - 4). Statistically significant treatment-time interactions in LMMs were detected for TDP ($F = 10.183$, $p = 0.002$), TDN ($F = 8.363$, $p = 0.005$), and pH ($F = 10.679$, $p = 0.001$) among the NS systems. Statistically significant pairwise contrasts are summarized in Table 13 and an accompanying interaction plot visualization is presented in Figure 43. For TDP, a distinction was observed between study day -16 and all subsequent days. Covariate trends generally exhibited an increasing slope over time, reflecting the development of a TDP trend across the gradient of nutrient loadings. A statistically significant difference was found for the contrast between days -16 and 69 (i.e. the first and last sampling events). A similar pattern was observed for TDN with a significant difference found for the contrast between days -16 and 84. However, minimal changes in TDN were observed

between day 14 and 28 among the highest nutrient loading treatments (Figure 37) which resulted in the negative slope for the covariate trend on day 28. The exact cause of this negative slope for this specific timepoint is difficult to determine but may be attributed to stimulated algal growth preventing further increases of TDN in CW water, or simply may have been the result of natural variation. This trend is observed only on day 28 and not in the timepoints before (day 14) or after (day 42), suggesting that the latter cause may have contributed to the results reported here. Meanwhile, the covariate trends for pH on day -5 and -1 had strong negative slopes which were statistically different from the covariate trends on every study day from day 50-84. Background fluctuations in pH and varying initial values were observed among NS mesocosms (Figure A - 30), which may have resulted in the covariate trends on days -5 and -1. The differences between TDP and TDN at the start and end of the study suggests that the nutrient loadings applied to NS were of sufficient quantity to alter water quality, however these changes required sufficient loadings over several months to exhibit a response.

Table 13. Pairwise contrast test results for water quality parameters with statistically significant interaction terms in fitted linear mixed models for the NS mesocosms. The difference in estimated marginal means (estimate) is reported with standard error (SE).

Response variable	Response units	Contrast	Estimate ± SE	p
TDP	mg L^{-1} PO_4-P	-16 vs. 69	-0.057 ± 0.017	0.024
TDN	mg L^{-1} N	-16 vs. 84	-0.649 ± 0.188	0.022
		28 vs. 84	-0.636 ± 0.188	0.027
pH	Unitless	-5 vs. 50-84	-0.911* ± 0.224*	NA
		-1 vs. 50-84	-0.971* ± 0.224*	NA

*The mean value of several consecutive statistically significant contrasts was calculated for the reported range of study days. NA = not applicable

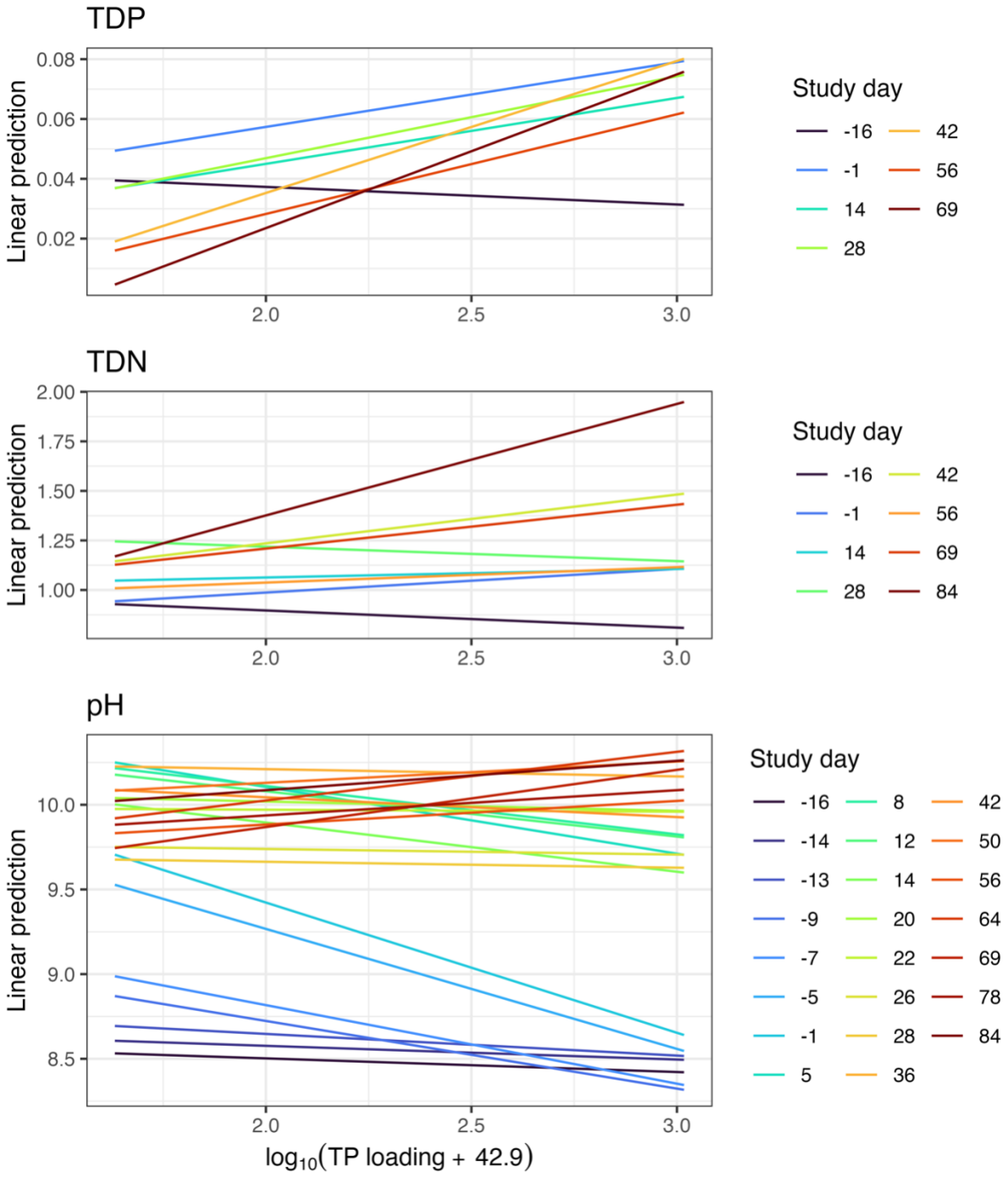

Figure 43. Interaction plots of estimated marginal means based on the fitted linear mixed models for total dissolved phosphorus (TDP), total dissolved nitrogen (TDN), and pH of the interaction between treatment and time for the NS mesocosms. Predictor variables were calculated by adding a constant (42.9) to the total phosphorus loading from aquaculture wastewater additions.

3.3.2.7 Microbial Activity

Microbial activity (measured as tATP) in mesocosm water and wild rice roots is presented in Figure 44. No relationship was observed between tATP in mesocosm water and nutrient loading ($p = 0.682$), however a significant positive linear relationship between tATP in wild rice roots and nutrient loading was observed ($p = 0.010$). The addition of fertilizer can impact the microbiome of plants, altering abundance and community structure of root microbiomes (Ikeda et al., 2014). In aquaponic systems, enrichments of certain taxa are beneficial for the treatment of AWW as they play key roles in nutrient cycling (Oliveira et al., 2020). The results in Figure 44 are highly variable and nutrient loading only accounted for a small portion of the variability in root tATP concentrations ($R^2 = 0.237$). Detailed taxonomic assessments of microbiomes in CW water and on CW plant roots would be beneficial to comprehensively assess the impacts of nutrient loadings on microbial community composition.

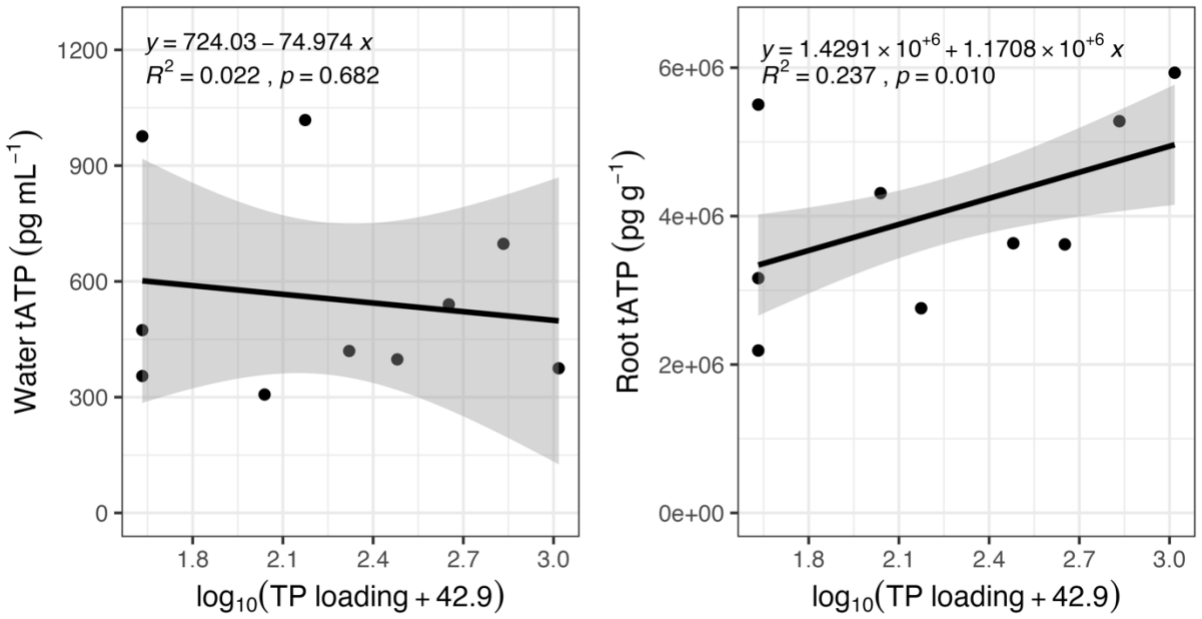

Figure 44. Microbial activity as total ATP (tATP) in NS mesocosm water (left) and wild rice roots (right). General linear models (solid lines) were fit to measured data (points) with 95% confidence intervals (shaded regions). Predictor variables were calculated by adding a constant (42.9) to the total phosphorus (TP) loading from aquaculture wastewater additions.

3.3.2.8 Soil Nutrient Content

Background (day 0) and final (day 100) concentrations of OP in NS mesocosm soil are presented in Figure 45. A statistically significant positive linear relationship between OP concentration and nutrient loading was detected in the final soil samples ($p = 0.045$). However, initial and final OP concentrations and trends were very similar and only minor differences were observed in Figure 45. When assessing the change in OP between these two sampling events, no statistical differences were observed ($p = 0.766$; Table A - 5). The results from all fitted models for various soil endpoints are compiled in the Appendix (Table A - 5) and a summary of statistically significant relationships for NS soil is presented in Table 14. All NS mesocosms were established with fresh soil from the same source and therefore any background differences in soil nutrients are likely a product of random variation or inconsistencies in soil quantities added to

different mesocosms at the start of the study. The elimination of negative relationships for Cu and Fe with time implies that AWW additions alleviated these nutrient gradients, however the effect was small as no statistical differences were detected in the change for either Cu or Fe. As discussed previously (Section 3.3.1.8), both P concentrations and pH of wild rice sediments can have a strong impact on crop success; increasing pH and P concentrations in soil can increase wild rice production (Lee & Stewart, 1981, 1984). Therefore, the impact of AWW additions on soil OP and pH in Table 14 can improve crop success. Long term soil nutrient dynamics in year-to-year CW usage were not assessed here, however continued AWW loadings could provide sufficient quantities of OM which can lower soil pH upon mineralization ultimately leading to reduced nutrient availability (McCauley et al., 2009).

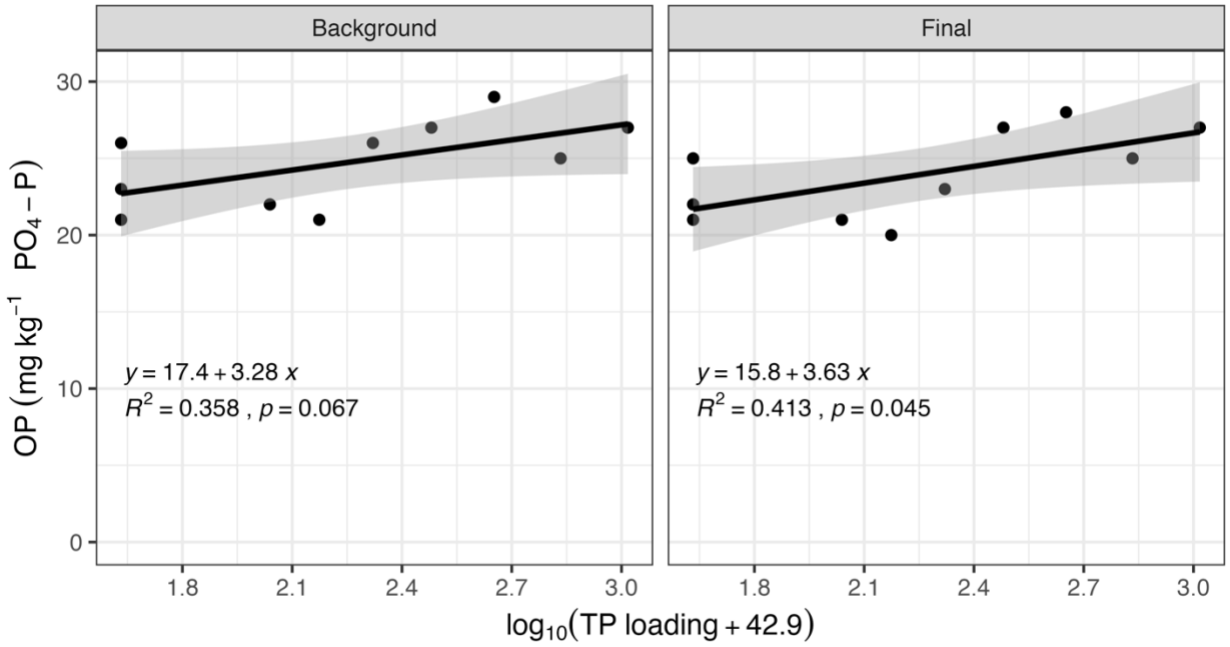

Figure 45. Background (day 0), final (day 100) soil Olsen phosphorus (OP) in NS mesocosms. General linear models (solid lines) were fit to measured data (points) with 95% confidence intervals (shaded regions). Predictor variables were calculated by adding a constant (42.9) to the total phosphorus (TP) loading from aquaculture wastewater additions.

Table 14. Summary of statistically significant results for different endpoints assessed in NS mesocosm soil during day 0 (background) and day 100 (final) samples, and the difference between background and final samples (change). Endpoints were assessed using general linear models and indicated in the table if a statistically significant result was detected. The directionality of the relationship is indicated in parentheses as either positive (+) or negative (-).

Analysis	Endpoint
Background	Cu (-), Fe (-)
Final	OP (+), pH (+)
Change	*NSD*

NSD = no statistical differences

3.3.2.9 Plant and Algal Biomass

No trends were observed for the total dry biomass of wild rice, algal mats, or hornwort collected at the end of the study period (Figure 46). However, a statistically significant positive linear relationship was observed between mean wild rice plant length and nutrient loading ($p = 0.003$; Figure 47). Shoot length of wild rice plants in natural stands has been related to water and sediment depths, however other unknown variables account for variability in shoot length (Peden, 1982). In addition to wild rice, the main forms of biomass in NS systems were algal mats and hornwort (Figure 48). In fact, algal mats often were greater contributors to total biomass than wild rice. Wild rice production was slightly elevated among the four-highest treatments when compared to the low treatments. The production of algal mats was most notable in the NS-REF-B, NS-REF-C, 166.3, 405.7, and 997.5 mg m^{-2} treatments. Note that no wild rice was produced in the 106.4 mg m^{-2} treatment.

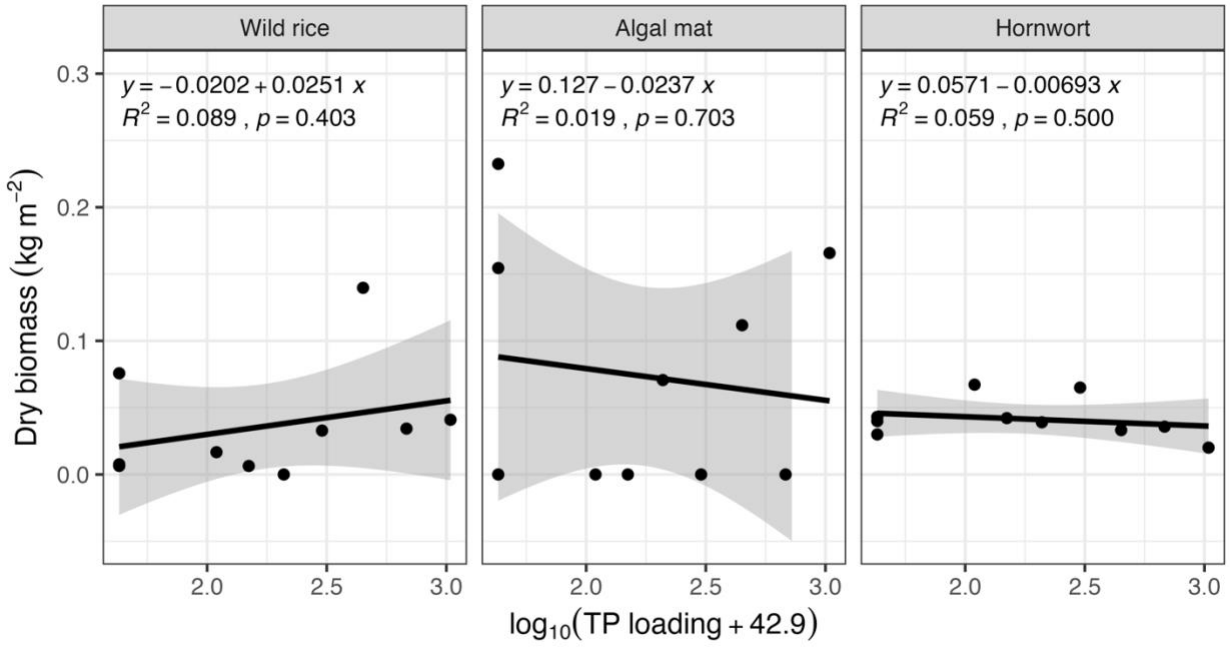

Figure 46. Biomass in NS mesocosms at the end of the study period reported on a dry mass basis. General linear models (solid lines) were fit to measured data (points) with 95% confidence intervals (shaded regions). Predictor variables were calculated by adding a constant (42.9) to the total phosphorus (TP) loading from aquaculture wastewater additions.

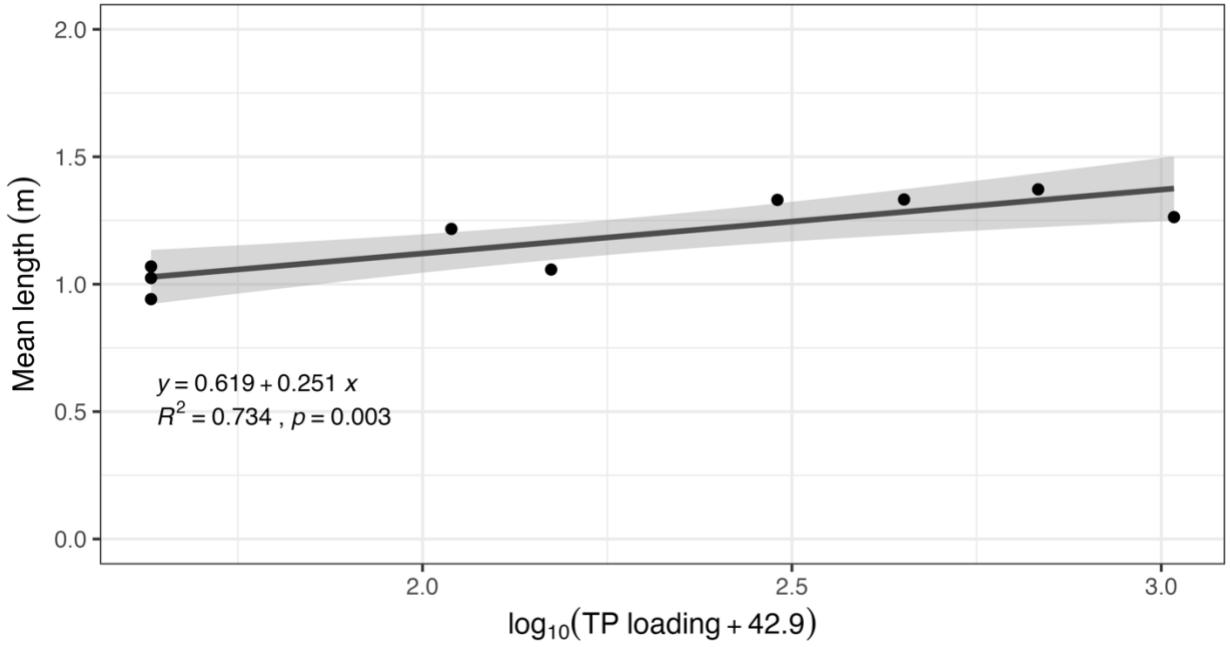

Figure 47. Mean length of wild rice plants in NS mesocosms at the end of the study period. A general linear model (solid line) was fit to measured data (points) with a 95% confidence interval (shaded region). Predictor variables were calculated by adding a constant (42.9) to the total phosphorus (TP) loading from aquaculture wastewater additions.

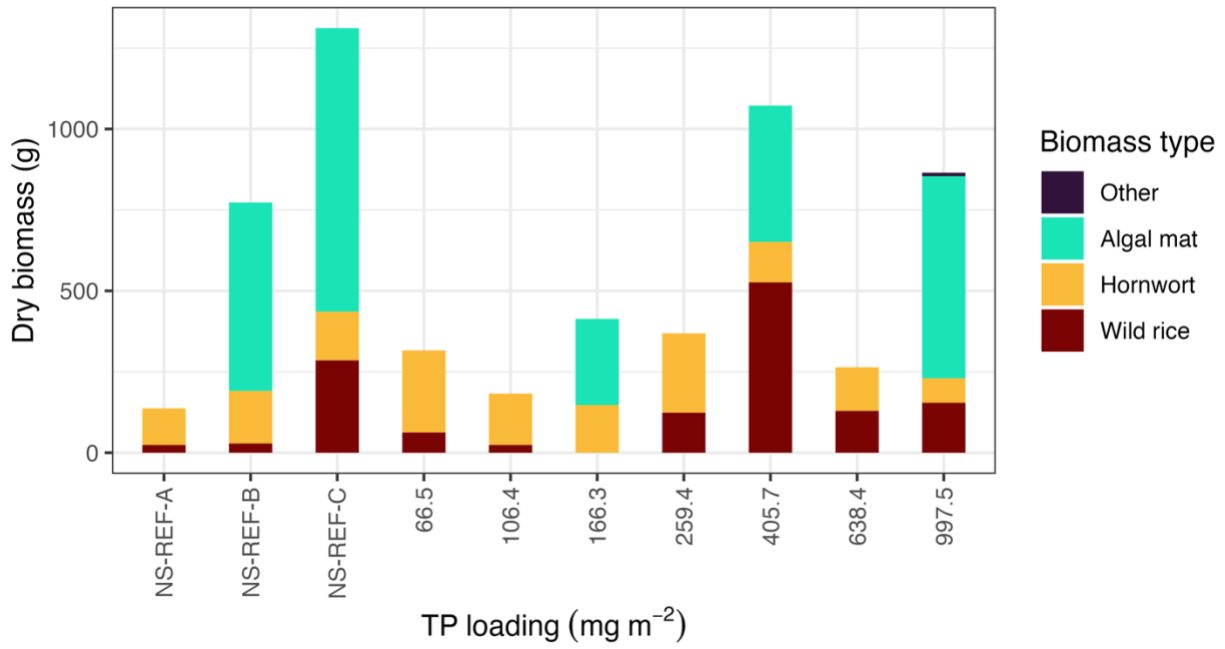

Figure 48. Quantities of different types of biomass in NS mesocosms at the end of the study period reported on a dry mass basis. The total phosphorus (TP) nutrient loadings from aquaculture wastewater are indicated with numerical values or the appropriate reference label.

In instances where algal mats were found, a positive linear relationships was observed between the TP content of algal mats and nutrient loadings ($p = 0.008$; Figure 49), however no significant relationships were observed between TP content and nutrient loading in wild rice roots, wild rice shoots, or hornwort. The results from all fitted models for different biomass tissue endpoints are compiled in the Appendix (Table A - 6). A summary of statistically significant relationships for NS soil is presented in Table 15.

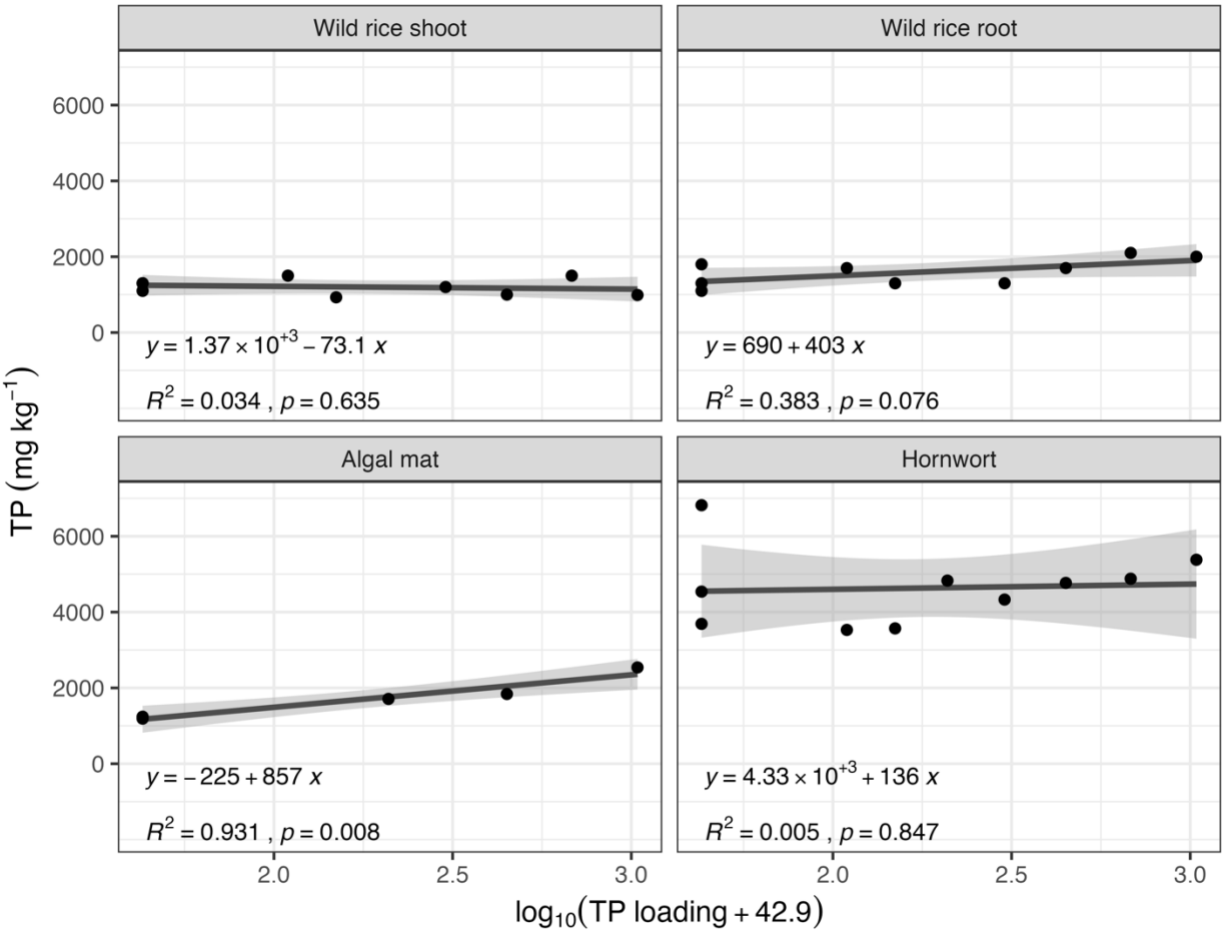

Figure 49. Total phosphorus (TP) content of different forms of biomass in NS mesocosms at the end of the study period. General linear models (solid lines) were fit to measured data (points) with 95% confidence intervals (shaded regions). Predictor variables were calculated by adding a constant (42.9) to the total phosphorus (TP) loading from aquaculture wastewater additions.

Table 15. Summary of results for different endpoints assessed in NS biomass tissues at the end of the study. Endpoints were assessed using general linear models and indicated in the table if a statistically significant result was detected. The directionality of the relationship is indicated in parentheses as either positive (+) or negative (-).

Biomass type	Endpoint
Wild rice seed	*NE*
Wild rice shoot	Length (+)
Wild rice root	*NSD*
Algal mat	TP (+), TN (+), Mg (-)
Hornwort	TN (+), NO_3–N (-), Cu (-), Zn (-)

NE = not evaluated, *NSD* = no statistical differences

3.3.2.10 Phosphorus Mass Balance

In Section 3.3.2.2, P species were characterized and presented as concentrations in Figure 36. An alternative representation of P species for the quantity (mass) of P in mesocosms is presented in Figure 50, and the two methods of presentation generated very similar trends. Similar to the EW systems (discussed in Section 3.3.1.10), no systematic increases in P quantity in mesocosm water were evident, and therefore the P inputs from other sources can be assumed to be negligible and/or P inputs were rapidly taken up and assimilated into other matrices like plant, soil, or algae.

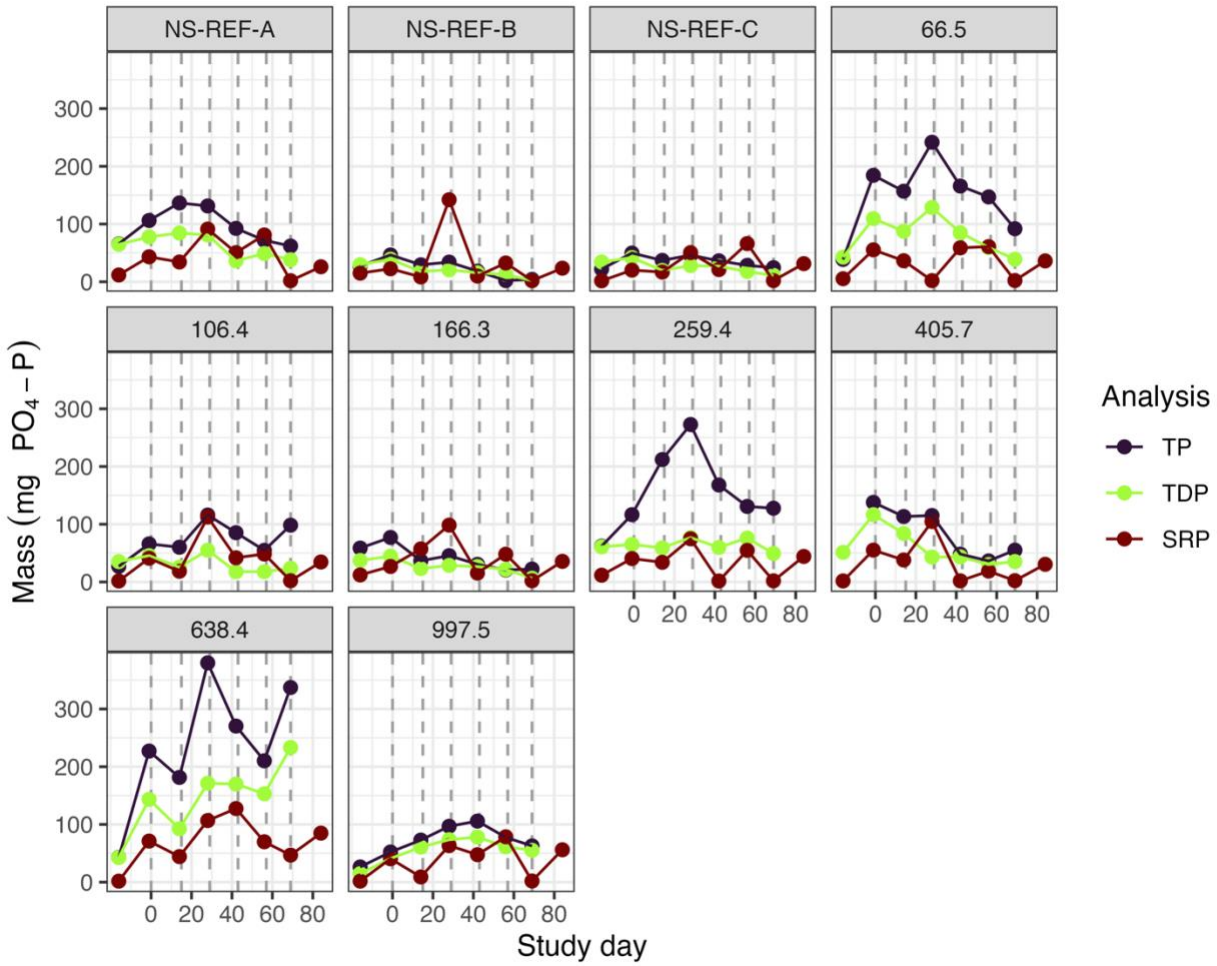

Figure 50. Quantities of total (TP), total dissolved (TDP), and soluble reactive (SRP) phosphorus in NS mesocosm water. Each graphical panel represents a mesocosm with the TP loading from aquaculture wastewater (AWW) additions indicated in units of mg m^{-2}. Vertical dashed lines indicate AWW addition events.

The total quantities and relative proportions of P in each matrix during initial and final timepoints are presented in Figure 51 and Figure 52, respectively. Soil P was the predominate contributor in all cases and because of this, issues occurred with tracking P in CW systems (discussed in Section 3.3.1.10). The change in P quantity for different matrices throughout the study is presented in Figure 53 and the overall change in P quantity (calculated as the sum of the differences of individual matrices) between initial and final timepoints is presented in Figure 54.

Together, these figures demonstrate the discrepancies that exist in the mass balance approach. In Figure 53, the discrepancy between uptake from soil and growth of other matrices was evident while in Figure 54 the discrepancy between the predicted change in P from AWW additions and the observed change was particularly evident among reference and high nutrient loading treatments.

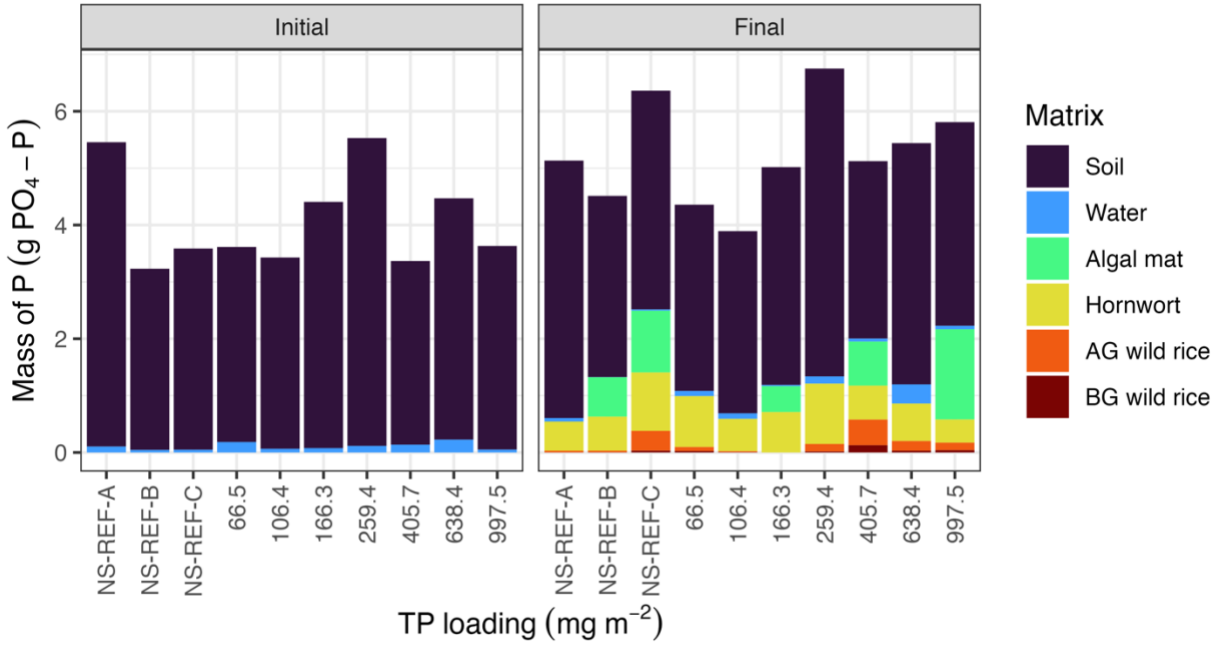

Figure 51. Total quantities of phosphorus (P) in different matrices during initial and final timepoints in NS mesocosms. Wild rice plants are presented as either aboveground (AG; seeds and shoots) or belowground (BG; roots) plant tissues. The total P (TP) nutrient loadings from aquaculture wastewater are indicated with numerical values or the appropriate reference label.

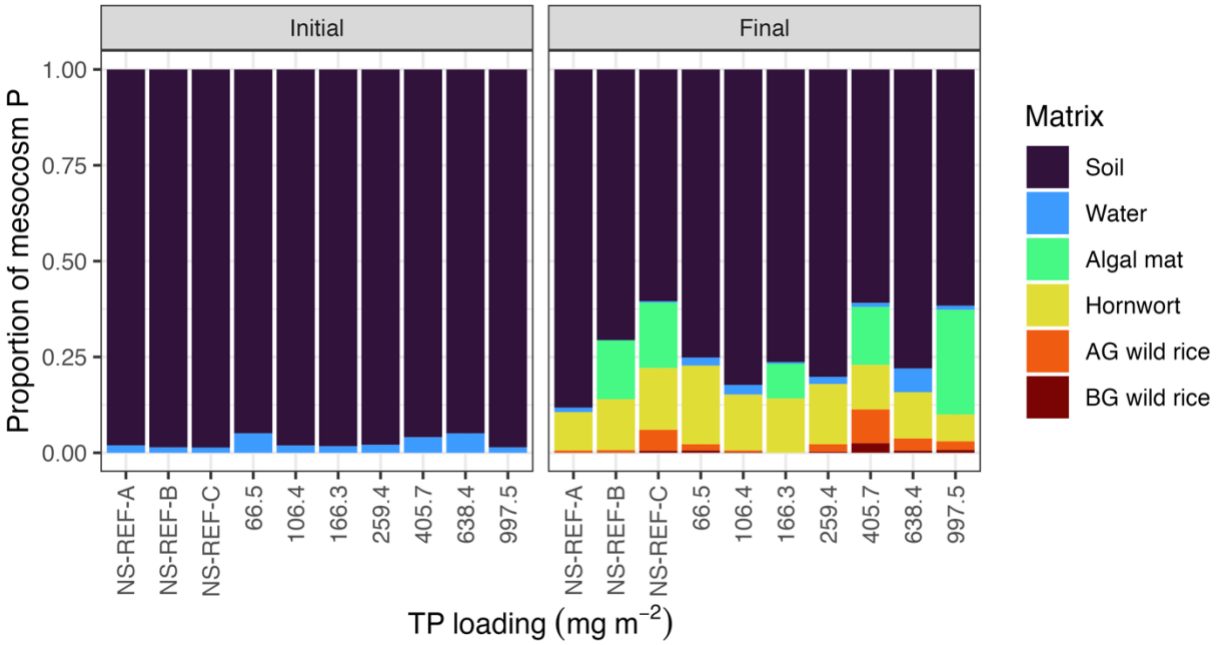

Figure 52. Relative proportions of phosphorus (P) in different matrices during initial and final timepoints in NS mesocosms. Wild rice plants are presented as either aboveground (AG; seeds and shoots) or belowground (BG; roots) plant tissues. The total P (TP) nutrient loadings from aquaculture wastewater are indicated with numerical values or the appropriate reference label.

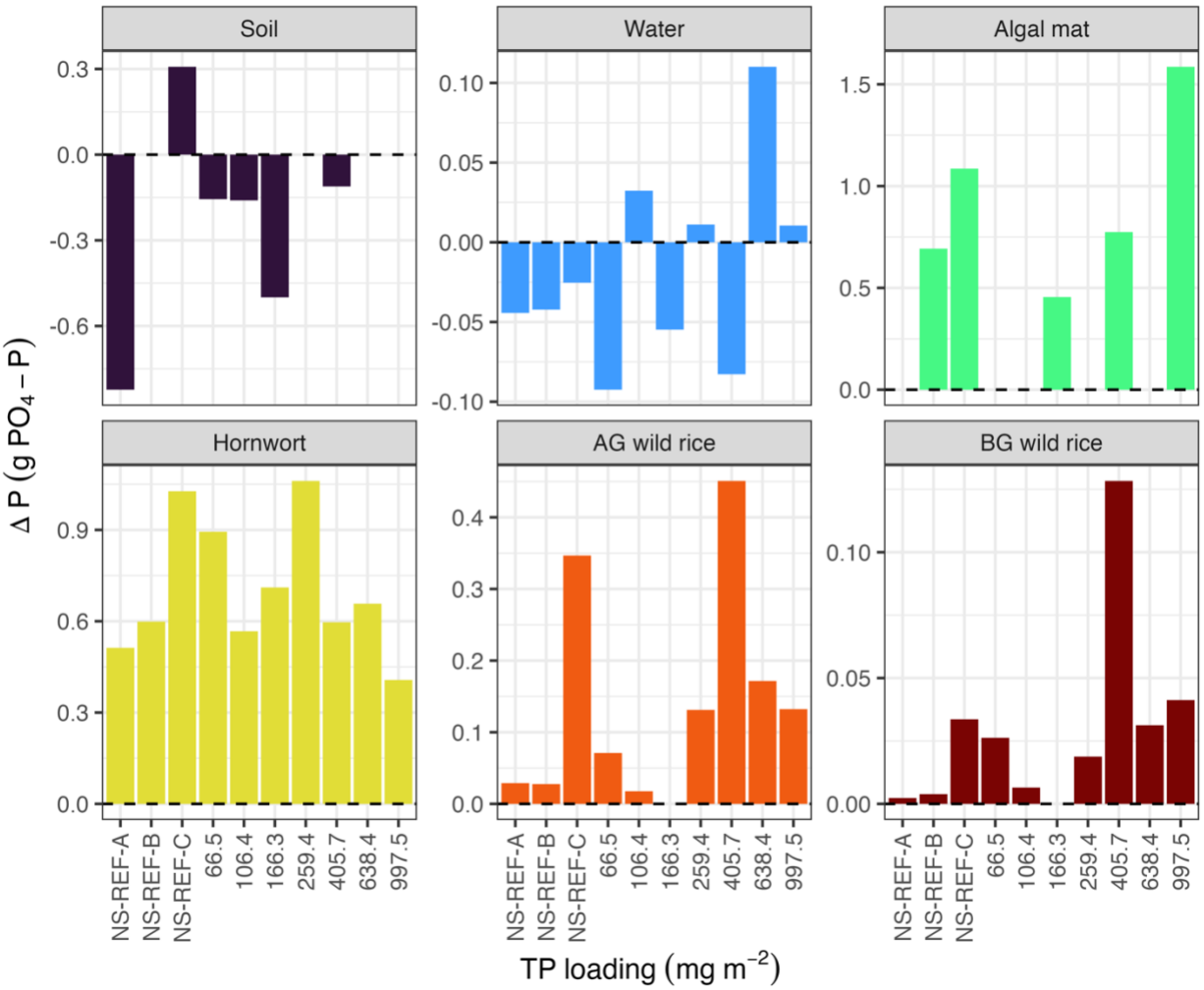

Figure 53. Change in quantity of phosphorus (ΔP) in different matrices between initial and final timepoints in NS mesocosms. Positive values represent increases of P with time while negative values represent decreases of P with time. Wild rice plants are presented as either aboveground (AG; seeds and shoots) or belowground (BG; roots) plant tissues. The total P (TP) nutrient loadings from aquaculture wastewater are indicated with numerical values or the appropriate reference label.

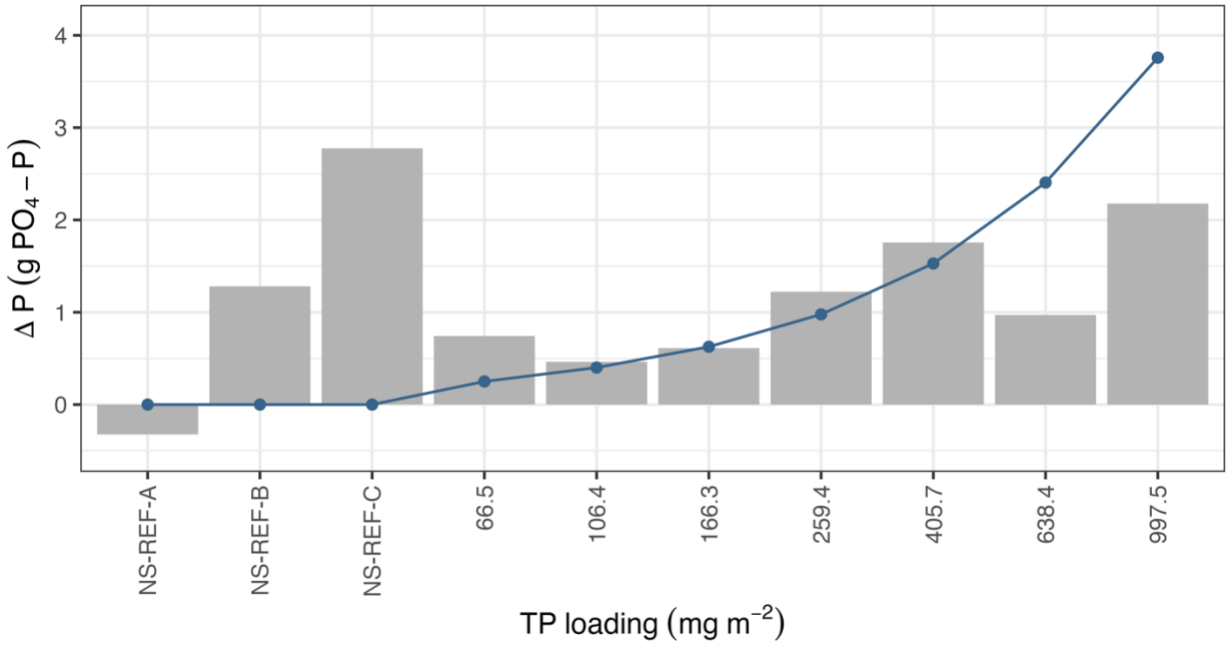

Figure 54. Comparison between the change in total quantity of phosphorus (ΔP) in NS mesocosms between initial and final timepoints (grey bars) and the total quantity of P added through aquaculture wastewater (AWW) additions (blue points). Positive values represent an increase of P with time while negative values represent a decrease of P with time. The total P (TP) nutrient loadings from AWW are indicated with numerical values or the appropriate reference label.

Using the P differences achieved in Figure 53 and assuming initial (day 0) biomass in mesocosms was negligible, P removal rates in plants and algae can be estimated over the 100-day period between the start of the study and decommissioning of mesocosms. For the 997.5 mg m^{-2} treatment, AG wild rice, BG wild rice, hornwort, and algal mats contributed to 0.351, 0.110, 1.081, and 4.210 mg m^{-2} d^{-1} of P removal, respectively. Meanwhile, the mean values for NS-REF-A, NS-REF-B, and NS-REF-C for AG wild rice, BG wild rice, hornwort, and algal mats were 0.357, 0.035, 1.892, 1.574 mg m^{-2} d^{-1} of P removal, respectively. Notably high production of wild rice biomass was observed in the 405.7 mg m^{-2} treatment, with AG and BG wild rice contributing to 1.197 and 0.341 mg m^{-2} d^{-1} of P removal (Figure 53). With the exception of the 405.7 mg m^{-2} treatment, wild rice biomass was not a substantial nutrient sink among NS

mesocosms. Instead, hornwort was a primary nutrient sink among all mesocosms and algal mats were major contributors when present.

3.3.3 Comparison of Constructed Wetland Systems

Interesting comparisons regarding P species can be made between EW and NS systems. All elevated TP concentrations were below 0.5 and 0.3 mg L^{-1} among the EW and NS systems, respectively. Greater quantities of algal mats were produced in the NS systems (Section 3.3.2.9) than the EW systems (Section 3.3.1.9), the production of which can assimilate substantial quantities of P. Ultimately, the response of P in CW water was related to the production of algal mat biomass. When evaluating the difference between TP and TDP among mesocosms in which P elevations occurred, greater differences were observed among NS than EW systems. Additionally, relative to the EW systems, the NS systems did not exhibit elevated SRP to the same extent. The lack of elevated SRP among NS systems can be related to greater production of algae, which utilize SRP as a readily available form of P. Among NS systems, elevated chl *a* was observed in mesocosm water beginning on day 28 in the 66.5, 259.4, and 638.4 mg m^{-2} treatments (Section 3.3.2.9). This can be contrasted with the EW systems where elevations in chl *a* were not observed among mesocosms with elevations of P in CW water (Section 3.3.1.9). In EW systems, elevations in SRP in CW water were observed alongside more substantial biomass production. Conversely, SRP elevations in NS systems were less prominent and lower biomass production was observed. Among mesocosms with elevated P concentrations, increases in chl *a* were greater among the NS mesocosms than the EW mesocosms, relative to their respective reference conditions. Additional biomass in EW mesocosms in the form of wild rice plants and hornwort provided additional shading and competition nutrients, both of which can inhibit

phytoplankton growth. Among the NS mesocosms where particularly low biomass was produced and P elevations were observed, SRP elevations were not as pronounced, especially in the 66.5 and 259.4 mg m^{-2} treatments because of rapid assimilation by phytoplankton. The rapid consumption of SRP is consistent with other wetlands where SRP is often found near or below detection limits in effluents exiting treatment areas (Juston & DeBusk, 2011; Kadlec, 2016; McCormick et al., 2001).

The EW mesocosms, having been previously established and subjected to nutrient loadings from AWW during the 2021 summer (Chapter 2; Blandford et al., 2024), mitigated chl *a* concentrations during the SRP elevations following AWW additions. The usage of EW mesocosms in the previous season contributed to the establishment of other forms of biomass (e.g. hornwort) and P-saturated in soils. Meanwhile, the NS systems had fresh soil with no previously established vegetation. Opportunistic forms of algae in NS systems benefited without the same limitations or competition for resources that were present in EW systems. While in the EW systems, the greater quantities of biomass could uptake greater quantities of P, the NS systems had a high capacity for P binding to soil because of the use of fresh soil and SRP was made available to phytoplankton without high demand/competition from other forms of biomass. The observed effect was lower SRP concentrations in CW water of NS systems than EW systems, in instances where P elevation occurred. The TP removal among CWs can be expected to decrease with age as soils become P-saturated and vegetation is established (Rozema, Rozema, & Zheng, 2016).

The period during which the most rapid biofilm growth was observed occurred earlier for NS than EW mesocosms and corresponded with faster growth rates in NS mesocosms (see Section 3.3.1.4 and Section 3.3.2.4). Again, EW systems were established in the previous growing season and had a variety of other forms of biomass which exhibited a nutrient demand throughout the study period. While EW systems had greater competition for nutrients because of the variety and abundance of biomass in these systems, the biofilm in NS mesocosms had less competition and therefore greater growth rates were observed.

Increases in TDN in mesocosm water were observed among both the EW and NS systems. The temporal trend for TDN concentrations in UP-REF (Figure 17) suggests that sorption to soils was actively occurring throughout the study. However, further investigations into the physical, chemical, and biological properties of soils are required to gain additional insights into nutrient cycling in CW systems.

Declines in DO were observed throughout the study period among the planted EW mesocosms, but were not observed among the planted NS mesocosms (Figure A - 14, Figure A - 29). Oxygen depletion likely resulted from the degradation of organic matter (e.g. plant litter and algae). Long-term low DO levels in CWs can negatively impact performance (H. Liu et al., 2016). The overall lack of organic matter among NS systems likely resulted in DO differences between the different CW systems. Nitrification in wetlands is meditated by chemoautotrophic bacteria under aerobic conditions while denitrification is mediated by facultative bacteria under anaerobic conditions (Snow et al., 2012). Declines in DO, which appear to be related to the presence of

decaying biomass in the present studies, may therefore support the conditions necessary for denitrification.

4.0 Conclusion

This chapter evaluated the performance of EW and NS systems treating AWW. The EW systems contained an abundance of algae and other organisms prior to the start of study, while NS systems did not. When evaluating water quality responses, the impacts of AWW additions on phosphorus were more prevalent than those on nitrogen. The EW systems mitigated the impacts of P loadings. Elevations in water column P were observed at TP loadings of 321.5 mg m^{-2} and greater. Among the 321.5 and 638.4 mg m^{-2} treatments, TP concentrations greater than 0.25 mg L^{-1} were observed in response to AWW additions. However, among the 997.5 mg m^{-2} treatment, TP elevations were generally below 0.2 mg L^{-1}. Elevated chl *a* associated with phytoplankton and biofilm was observed in the 997.5 mg m^{-2} treatment that was not observed among other high nutrient loading treatment to the same extent. In the short term, the production of algae improved CW performance (i.e. removed P from CW water), but long-term CW management should avoid eutrophic conditions to ensure system functionality. Among the NS systems, mesocosms that experienced elevations in P in water were accompanied by increases in chl *a*. Lower biomass was observed in NS systems compared to EW systems, resulting in fewer sinks and enabling phytoplankton to proliferate without competition from other plants and algae. In both EW and NS systems, low wild rice yields allowed for hornwort and algal mats to represent significant nutrient sinks. Management strategies such as increasing seeding application rates, transplanting to increase plant densities, and incorporating AWW fertilizer into the soil prior to seeding can contribute to improved wild rice stand success. These strategies may alter dynamics among

nutrient sinks, however successful wild rice production not only supports nutrient removal but provides the added benefit of crop production, aligning the treatment of AWW with productive agronomy systems.

CHAPTER 4: RESPONSES OF NORTHERN WILD RICE (*Zizania palustris* L.) FLOODED PADDIES FERTILIZED WITH AQUACULTURE WASTEWATER

Preface

A version of this study is currently in preparation for publication. A modified version of the manuscript in preparation for publication is presented here, with additional details regarding methodology and an expanded discussion of results. This chapter shares common methodology with Chapter 3. To avoid repetition, references to Chapter 3 are provided where identical methodology was employed.

Contribution of Authors

The author contributor roles taxonomy (CRediT) statement for the manuscript in preparation is as follows:

Nicholas C. Blandford (University of Manitoba): Conceptualization; formal analysis; funding acquisition; investigation; methodology; project administration; visualization; writing–original draft. **Krista Robertson** (University of Manitoba): Conceptualization; investigation; methodology; writing–review and editing. **Leah Dickenson** (University of Manitoba): Conceptualization; investigation; methodology; writing–review and editing. **Richard Grosshans** (International Institute for Sustainable Development): Conceptualization; methodology; resources; writing–review and editing. **Bruce Hardy** (Myera Group): Conceptualization; funding acquisitions; resources. **Nazim Cicek** (University of Manitoba): Conceptualization; funding acquisition; methodology; resources; supervision; writing–review and editing. **Vince Palace** (International Institute for Sustainable Development – Experimental Lakes Area):

Conceptualization; funding acquisition; methodology; project administration; resources; supervision; writing–review and editing.

1.0 Introduction

Wild rice (*Zizania* spp.) is an aquatic grass that grows in lakes, rivers, streams, and wetlands (Oelke et al., 1982; Terrell et al., 1997). In North America, northern wild rice (*Zizania palustris* L.) is the most commonly cultivated and consumed species of wild rice (Archibold, 2003; Porter, 2019). The grain produced by wild rice plants serves as an important food source for Indigenous peoples across North America, supporting sustenance and livelihood, while also holding cultural and spiritual significance (Matson et al., 2021; Vennum, 1988). Wild rice production methods vary from traditional harvesting in nature to the cultivation of natural stands, and, more recently, to intensified commercial production in flooded paddies (Aiken et al., 1988; Hayes et al., 1989; Oelke et al., 1982).

Anthropogenic activities such as damming and shoreline development have altered ecosystems and led to a decline in natural stands of northern wild rice (Archibold et al., 1989; Hansen, 2008; Strube & Thomas, 2021). The domestication of wild rice within the past 75 years has focused on the development of flooded paddy systems to facilitate commercial production of wild rice (Hayes et al., 1989; Oelke et al., 1982). These systems provide better control over environmental variables, overcoming the inherent variability and sensitivities commonly associated with wild rice production in natural settings (Oelke et al., 1982). Oelke et al. (1982) provide details regarding the construction of wild rice flooded paddies and management practices employed in these systems. This process involves clearing and levelling land, constructing dikes, and flooding

the resulting field using a nearby water source. Water levels are managed throughout the growing season, creating conditions favourable for wild rice growth. In the late summer to early fall, paddies are drained of water to facilitate the harvest and the subsequent tillage of paddy soils. Shatter-resistant and non-shattering varieties of wild rice have been selectively bred to better retain mature grains on the panicle, preventing seed loss, facilitating harvest via combine, and ultimately improve yields (McGilp et al., 2023; Oelke et al., 1982).

Fertilizer regimes implemented in wild rice paddies typically involve applications of nitrogen, phosphorus, and potassium (Kaiser & Piotrowski, 2023; Oelke et al., 1982). Ammonia-based fertilizers are ideal in flooded paddies whereas nitrate fertilizers are less effective because of substantial losses resulting from denitrification in flooded soils (Kaiser & Piotrowski, 2023; Oelke et al., 1982). The top dressing of urea in flooded paddies can effectively achieve high yields (Kaiser & Piotrowski, 2023), although applications of basal nitrogen can be made through the incorporation of fertilizer into soils during paddy preparation (Oelke et al., 1982; Sims et al., 2012). Meanwhile, surface applications of phosphorus fertilizers can lead to eutrophication in the paddy, negatively impacting its functionality (Kaiser & Piotrowski, 2023; Oelke et al., 1982). When wild rice paddies are drained, the discharged effluents can deliver high quantities of nutrients into receiving environments, which can negatively impact water quality and ecosystem health (Aiken et al., 1988; Carpenter et al., 1998). However, wild rice plants have demonstrated the capacity to uptake significant quantities of nutrients and can offer significant improvements in water quality (Atkins et al., 1992; Grava & Raisanen, 1978; Meeker, 1993). The application of fertilizer in flooded wild rice paddies must be managed to achieve optimum crop production while minimizing environmental impacts.

Aquaculture wastewater (AWW) has the potential to be applied as a fertilizer in wild rice paddies because of its nutrient content. Specifically, finfish excrete high quantities of ammonia and urea which are subsequently released in AWW (Dalsgaard et al., 2015; Ip & Chew, 2010). The high proportions of ammonia-based nitrogen in AWW represent a potential organic fertilizer to be applied to wild rice paddies. However, AWW also contains other nutrients such as phosphorus, which require consideration (Lalonde et al., 2015). Aquaculture is a rapidly growing industry and inland aquaculture operations are the primary means of finfish production (FAO, 2022; Garlock et al., 2020). Land-based aquaculture facilities rearing fish create a point source of nutrient-rich AWW effluent which, when discharged, can lead to nutrient enrichment in the receiving environment (Ahmad et al., 2022; Lalonde et al., 2015; Walker et al., 2003).

Various farming models have been implemented in rice paddies across Asia which involve the culture of fish either within or adjacent to the rice paddy (Kangmin, 1988; Phung et al., 2009; Wan et al., 2019). These agronomy systems benefit from reduced costs and concerns associated with fertilizer applications by recycling the nutrients in fish waste for rice production. Properly managed nutrient inputs in rice-fish co-culture systems can reduce pollution while increasing yields and conserving land use, maximizing productivity per unit area while utilizing sustainable agriculture practices (Hu et al., 2013). The intensification of fish farming with land-based systems adopted in Canada requires novel solutions to effectively manage the treatment of nutrient-rich effluents generated by the industry (Bartley, 2022; Noakes, 2018). Ahmed et al. (2021) have proposed an ecosystem approach to wild rice-fish culture in North America which utilizes wild rice habitats to rear fish. Many fish species of commercial significance use wild rice

as habitat in natural ecosystems and are therefore viable for implementation in co-culture systems (Ahmed et al., 2021; Lavergne, 2006).

The present study aimed to investigate the potential for AWW to be used as a fertilizer in wild rice flooded paddies. The AWW generated by aquaculture contains nitrogen primarily in the form of ammonia and urea (Dalsgaard et al., 2015; Ip & Chew, 2010), which are the forms of nitrogen recommended for wild rice fertilization (Kaiser & Piotrowski, 2023; Oelke et al., 1982). The integration of aquaculture and wild rice production represents an opportunity for the creation of a sustainable agriculture system. The treatment of AWW can be achieved in the wild rice paddy, while wild rice plants benefit from the available nutrients. This approach to nutrient recycling avoids a reliance on conventional fertilizers which are costly and known to contribute to environmental degradation (Carpenter et al., 1998; Schindler et al., 2012). However, the capacity for flooded paddies of wild rice to mitigate alterations in water quality in response to AWW is unknown. The optimum rate of AWW application was investigated through the application of a gradient of nutrient loading conditions to wild rice flooded paddies constructed in mesocosms.

2.0 Materials and Methods

2.1 Constructed Paddy Mesocosms and Field Site Details

Wild rice constructed paddies were established in identical mesocosms to those presented in Chapter 3 (see Figure 10). Mesocosms were amended with 20 cm of locally-source topsoil, 30 cm of water (~1,500 L) from a nearby pond, and planted with a shatter-resistant commercial variety of northern wild rice (Franklin; University of Minnesota, St. Paul, MN, USA) at a rate of

80 g m^{-2}. Mesocosms were constructed at the R & L Acres (RL) field site, situated on a commercial farm in Sperling, MB, Canada (49° 31’ 59.2” N, 97° 43’ 8.8 W”). The RL site mesocosms emulated commercial flooded wild rice paddies. These mesocosms were established in the spring of 2022. Prior to seeding in June 2022, wild rice seeds were stored at 4°C for a period of 3 months, as is commonly performed in commercial settings to break dormancy and improve germination success (McGilp et al., 2020). The water and soil used in mesocosms were analyzed for nutrient content (see Appendix; Table A - 8, Table A - 9). Because of the high nutrient content measured in the nearby pond used as the initial water source in mesocosms, all subsequent additions of water to mesocosms were performed using local municipal tap which had lower nutrient concentrations (RM of Carman, MB, Canada; Table A - 10). In an identical manner to the mesocosms in Chapter 3, zooplankton and fathead minnows (*Pimephales promelas*) were added to mesocosms as components of a broader research project not reported on here (Dickenson, *in preparation*; Robertson, *in preparation*).

2.2 Aquaculture Wastewater Collection

Details surrounding AWW collection are identical to those presented in Chapter 3. Approximately halfway through the study at the RL site, a second collection of AWW was required to continue to meet nominal volume addition targets. Identical collection, transportation, and storage methods were used during the second collection of AWW.

2.3 Experimental Design

The RL site consisted of 16 mesocosms; 10 mesocosms received AWW, 5 served as planted references, and 1 served as an unplanted reference (Table 16). The RL site mesocosms are

referred to herein as flooded paddies (FP) because they were designed to emulate commercial wild rice paddy-based systems. The unplanted reference mesocosm at the RL site (UP-REF) was of equivalent dimensions to all other mesocosms at the RL site and contained equivalent quantities of soil and water. Planted references (i.e. mesocosms that contained wild rice but received no AWW) are labelled with the corresponding type of system (i.e. FP), a reference label (i.e. REF), and assigned a letter in alphabetical order, with the three labels separated by dashes (e.g. FP-REF-A).

Table 16. Study design details for the RL site mesocosms. Treatments are expressed as the nominal volumes of aquaculture wastewater (AWW) applied to the mesocosms on a biweekly basis. A total of 5 AWW addition events occurred over a period of 60 days. The fourth and fifth addition events involved the addition of twice the nominal AWW volume applied during the first three addition events.

Mesocosm type	Nominal biweekly addition volume (L)	
	Addition events 1, 2, and 3	Addition events 4 and 5
Unplanted	0 (UP-REF)	0 (UP-REF)
FP	0 (FP-REF-A)	0 (FP-REF-A)
	0 (FP-REF-B)	0 (FP-REF-B)
	0 (FP-REF-C)	0 (FP-REF-C)
	0 (FP-REF-D)	0 (FP-REF-D)
	0 (FP-REF-E)	0 (FP-REF-E)
	1.0	2.0
	1.4	2.8
	1.8	3.6
	2.5	5.0
	3.3	6.6
	4.5	9.0
	6.1	12.2
	8.2	16.4
	11.1	22.2
	15.0	30.0

The FP and unplanted mesocosms were randomly assigned to treatments. A total of five AWW addition events occurred at the RL site which took place on an approximate biweekly basis over

a period of 60 days. In order to capitalize on the nutrient remediation potential of FP systems which contained high densities of plants, the nominal volume of AWW applied to mesocosms during the final two AWW addition events at the RL site was doubled (Table 16). The nominal volume of AWW was selected to target nutrient loadings which followed a logarithmic regression encompassing the nutrient loadings commonly applied to wild rice (Kaiser & Piotrowski, 2023). Additional treatments at the lower and upper ends of the regression were also included to expand the range of investigated nutrient loadings and to further elaborate on the remediation capacity of wild rice FP systems across a gradient of treatments.

2.4 Mesocosm Sampling and Sample Analysis

Important dates pertaining to the sampling of mesocosms are presented in Figure 55, with AWW additions indicated. Initial AWW additions (i.e. day 0) occurred on June 30th, 2022.

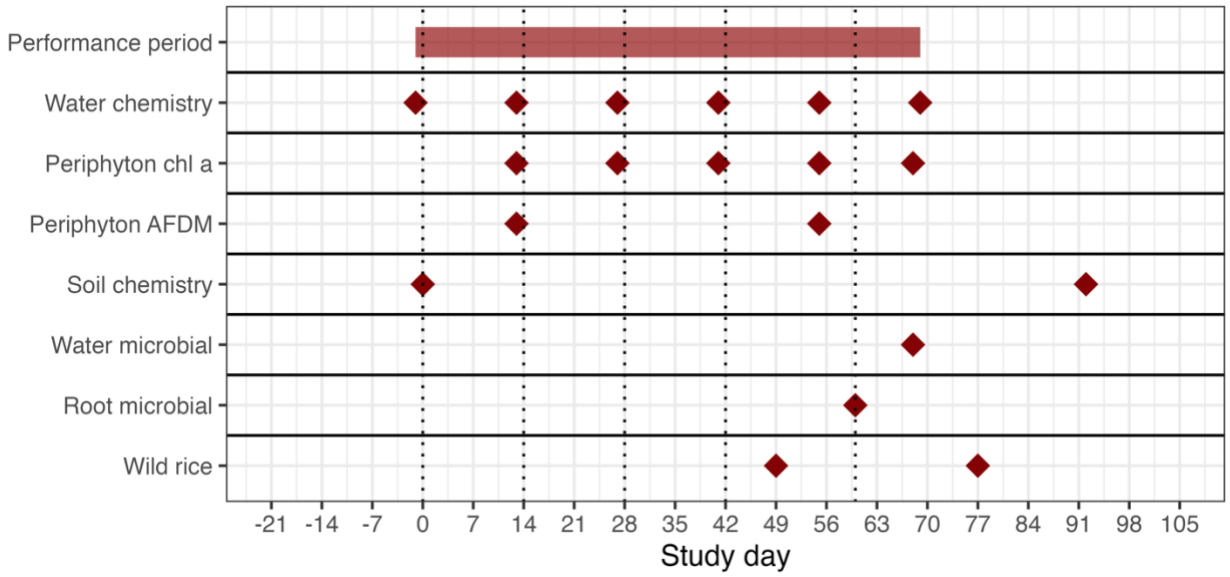

Figure 55. Timeline of sampling events at the RL field site. The first addition of aquaculture wastewater (AWW) to mesocosms is used to indicate the beginning of the study (i.e. study day 0), which is a unique date for each field site. Vertical dashed lines indicate additions of AWW.

2.4.1 Aquaculture Wastewater Additions

Additions of AWW occurred on study days 0, 14, 28, 42, and 60 (Figure 55). Details surrounding AWW additions are identical to those presented in Chapter 3. A grab sample of AWW had to be analyzed for nutrient content for AWW additions on day 0 because commercial laboratory analysis was unavailable. For this sample, nutrient content was analyzed using the same methods applied to mesocosm water samples (see Section 2.4.2).

2.4.2 Water Quality

Water samples were collected on study days -1, 13, 27, 41, 55, and 69 (Figure 55). With the exception of the day 55 water sample, which was collected 5 days prior to an AWW addition event, water samples were collected 0–1 days prior to a subsequent AWW additions. Throughout the study period, frequent in situ measurements of basic water quality parameters (i.e. temperature, pH, dissolved oxygen, conductivity) were taken using a handheld probe (details described in Chapter 3). In general, measurements were collected in the late morning to early afternoon (11:00-15:00). A total of 3 temperature and light data loggers were installed in FP mesocosms, selected at random. An additional logger was placed at the RL field site in an open area to record light intensity without any obstruction or shade resulting from plants, soil, or the sides of mesocosms (further details in Chapter 3).

Details surrounding water sample collection, processing, and analysis are identical to those described in Chapter 3.

2.4.3 Biofilm Tiles

Biofilm tiles were assessed for chl *a* on study days 13, 27, 41, 55, and 68 (Figure 55). Additionally, three tiles were randomly collected from floating containers for ash-free dry mass (AFDM) analysis on days 13 and 55. Details surrounding the installation, collection, processing, and analysis of biofilm tiles are identical to those described in Chapter 3.

2.4.4 Soil

Background soil samples were collected prior to AWW additions on day 0 (Figure 55). Additionally, soil samples were collected several weeks after AWW additions had ended, on day 92. Details surrounding soil sample collection and analysis are identical to those described in Chapter 3.

2.4.5 Microbial

Microbial samples of mesocosm water and wild rice roots were collected on day 68 and 60, respectively (Figure 55). Details surrounding sample collection, processing, and analysis are identical to those described in Chapter 3.

2.4.6 Plant Tissues

Plant tissue samples of wild rice plants were collected on days 49 and 77 (Figure 55). Bundles of 20 plants which were collected at random were submitted as a representative sample for each mesocosm. Details surrounding sample collection, processing, and analysis are identical to those described in Chapter 3.

Decommissioning of mesocosms occurred on day 90. This involved the removal of all plants from the mesocosms. Wild rice plants were removed from soil with roots still attached, rinsed in mesocosm water to remove excess soil, combined, and fresh weight was recorded. A sample of 20 wild rice plants was removed from each mesocosm and individual plant lengths were measured.

2.4.7 Mesocosms Water Volume and Surface Area Estimations

Details surrounding mesocosm water volume and surface area calculations are identical to those described in Chapter 3.

2.5 Nutrient Loading Calculations

Details surrounding nutrient loading calculations are identical to those described in Chapter 3. These was one instance on day 0 where TKN was not measured in AWW samples. For this sample, the mean TKN concentration of the AWW source was used in the determination of nutrient loadings.

2.6 Flooded Paddy Performance Parameters

To assess FP performance, a 70-day period referred to herein as the "performance period" was defined during which TP data was analyzed in mesocosm water (Figure 55). The performance period spanned from study days -1 to 69. This performance period included all AWW addition events (i.e. all five AWW additions). All FP performance parameters were assessed over the 70-day performance period using identical equations to those presented in Chapter 3.

2.7 Mass Balance Analysis

Mass balance calculations were made by multiplying the estimated volume or mass of a given matrix (i.e. soil, water, plant) by the measured concentration of TP. Details surrounding mass balance calculations are identical to those described in Chapter 3.

2.8 Statistical Analysis

All details regarding statistical analyses are identical to those described in Chapter 3. Following the same approach outlined for EW and NS systems, a constant was added prior to $\log_{10}$ transformation of treatment. This constant was derived using the y-intercept of the line-of-best-fit generated from the linear regression of treatment loadings evenly distributed in logarithmic space (Figure 56). The resulting constant applied to the FP system TP loadings prior to log-transformation was 285.2.

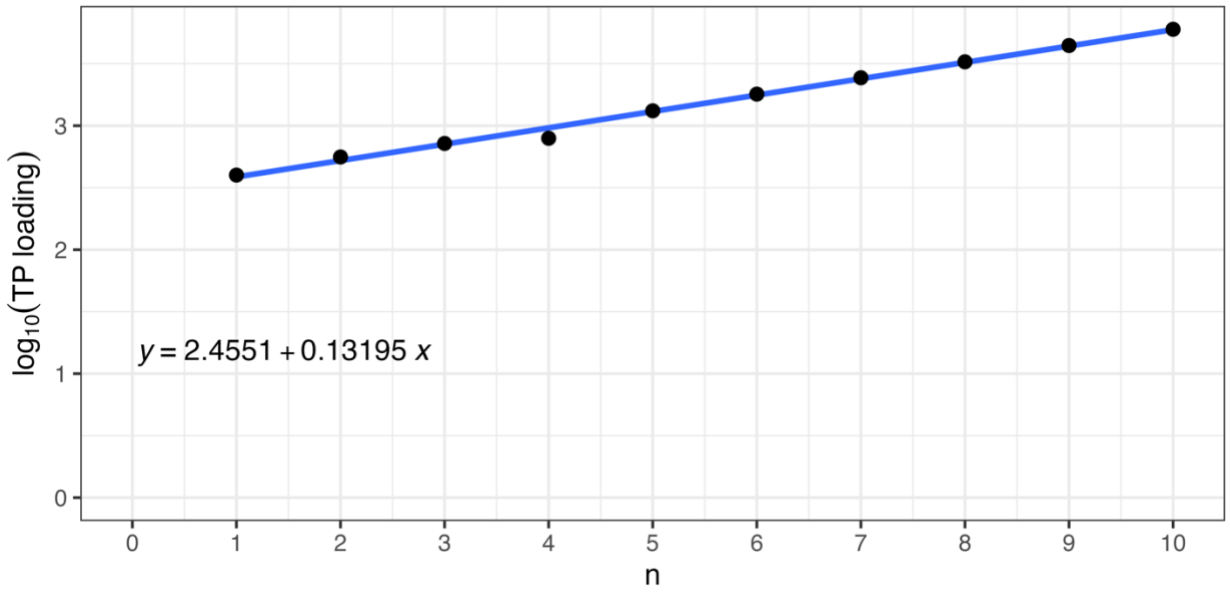

Figure 56. Logarithmic total phosphorus (TP) loadings from aquaculture wastewater additions evenly distributed for flooded paddy (FP) mesocosms. The constant used in data transformations was derived from the y-intercept of the line-of-best fit (solid blue line).

3.0 Results and Discussion

3.1 Aquaculture Wastewater Chemistry

Concentrations of TP, TAN, and total Kjeldahl nitrogen (TKN) as well as density and pH were consistent in the first AWW collected but were variable for the two samples analyzed from the second AWW collection (Figure A - 1). The mean (± SD) values for TP, TAN, TKN, density, and pH are presented for the first AWW collection throughout its usage, whereas ranges (minimum-maximum) are presented for the second AWW collection because only two additions events and therefore only two samples (i.e. initial and final) were assessed (Table 17). Most notably, initial and final TP from the second AWW collection contained 9.7 and 6.4 times more TP than the mean of the first AWW collection, respectively. Note that these differences in nutrient content occurred in response to more solids being targeted during the second AWW collection event. Corresponding TAN concentrations were approximately equal between the different collection events with mean values of 229.2 and 263.6 mg L^{-1} for the first and second AWW collections, respectively. Initial TKN of the second AWW collection was 3.2 times greater than the mean of the first AWW collection, while final TKN was approximately equal to the mean of the first AWW collection. The pH of the second AWW collection was slightly greater than the first. Although TKN analysis does not include nitrite or nitrate, a sample of the first AWW collection was analyzed on three occasions for TAN, NO_2–N, and NO_3–N and was found to contain mean (± SD) concentrations of 267.917 ± 34.011, 2.975 ± 0.254, and 10.383 ± 1.406 mg L^{-1}, respectively. Therefore, similar to Chapter 3, the assumption that TKN ≈ TN can be made here.

Table 17. Mean (± SD) or range (min–max) of total phosphorus (TP), total ammonia nitrogen (TAN), total Kjeldahl nitrogen (TKN), density, and pH of aquaculture wastewater (AWW) sources added to mesocosms. The mean is reported for the first AWW collection event and the range is reported for the second, based on the corresponding sample size. Samples were analyzed at room temperature (20–25°C).

AWW Collection event	Number of samples	TP (mg L^{-1})	TAN (mg L^{-1})	TKN (mg L^{-1})	Density (g mL^{-1})	pH
First	9	43.0 (5.8)	229.2 (44.6)	296.2 (132.6)*	0.998 (0.001)	7.58 (0.09)*
Second	2	275.0–417.0	236.0–291.2	291.2–955.0	0.985–0.996	7.65–7.68

*A reduced sample size (n = 6) was used to calculate mean and standard deviation because of missing data

Nutrient loadings were achieved by applying nominal volumes of AWW, so the second AWW collection event provided substantially more TP to the FP mesocosms, however TAN and TKN were comparable in both AWW collections (Table 17). Higher pH was measured in the second AWW collection favouring a greater proportion of unionized ammonia (see Chapter 3 for a discussion surrounding ammonia toxicity). However, substantial dilution of AWW occurred following its addition into FP mesocosms and the resultant temperature and pH in mesocosm water are the main variables impacting ammonia speciation within the FP system.

With one exception for the initial sample of the second AWW collection, TAN (and not organic nitrogen) was the major fraction comprising TKN. Throughout the use of the first AWW collection, TAN generally comprised upwards of 75% of the corresponding TKN value. Organic nitrogen concentrations (i.e. the difference between TKN and TAN) were 67.0 mg L^{-1} for the first AWW collection (mean value throughout its usage), 719.0 mg L^{-1} for the initial sample of the second AWW collection, and 0.0 mg L^{-1} for the final sample of the second AWW collection. The second AWW collection had very high variability in TKN between the two samples (Table 17). The large decrease in TKN between initial and final timepoints was accompanied by an increase in density (Figure A - 1). The absence of organic nitrogen in the final sample could be the result of solids settling over time in the AWW storage tank, resulting in suspended nitrogen particles being excluding from samples. This could result from improperly mixed samples at the time of sample collection from the AWW stock, or in the laboratory prior to analysis. Meanwhile, the very high (719.0 mg L^{-1}) organic nitrogen content measured in the initial sample of the second AWW collection could have resulted from varying suspended solid content and sample density with a high proportion of organic nitrogen. The use of replicate samples is

advised in future studies involving high concentration AWW to account for the heterogenous nature of samples.

The variation in nutrient content observed across collection events in Table 17 is reflective of the inherent variability of AWW nutrient content. Such variability not only exists between different fish farms, but also within the same, and is influenced by seasonal changes and differences in farming practices (Eikebrokk & Ulgenes, 1993; Hennessy et al., 1996; Lalonde et al., 2015; Walker et al., 2003).

3.2 Resultant Nutrient Loadings in Mesocosms

The study design, including both nominal volumes of AWW and the resulting total nutrient loading rates, are presented in Table 18. A correlation matrix comparing the TP, TAN, and TKN nutrient loadings in Table 18 was computed for the FP mesocosms and nutrient loadings were highly correlated ($R^2 > 0.999$). For simplicity in model fitting, presentation of results, and comparisons between various analyses, the TP nutrient loading was applied as a representative indicator of treatment and used as a predictor variable in fitted models and data visualizations. Unless otherwise stated, nutrient loading treatments are referred to by, and presented as, the total TP nutrient loading (in units of mg m^{-2}) resulting from AWW additions throughout the study period with the exception of reference mesocosms which follow the alphabetical labelling system previously described in Section 2.3.

Table 18. Nominal volumes of aquaculture wastewater (AWW) added to mesocosms with resulting total phosphorus (TP), total ammonia nitrogen (TAN), and total Kjeldahl nitrogen (TKN) loadings. Additions of AWW occurred over a period 60 days at the RL site. Unique labels for reference mesocosms are also included in the TP loading column.

Mesocosm type	Total AWW added (L)	Surface area (m^2)	TP (mg m^{-2})	TAN (mg m^{-2})	TKN (mg m^{-2})
FP	0.0	3.767	0.0 (FP-REF-A)	0.0	0.0
	0.0	3.767	0.0 (FP-REF-B)	0.0	0.0
	0.0	3.767	0.0 (FP-REF-C)	0.0	0.0
	0.0	3.767	0.0 (FP-REF-D)	0.0	0.0
	0.0	4.753	0.0 (FP-REF-E)	0.0	0.0
	7.0	3.767	399.7	461.2	867.8
	9.8	3.767	559.6	645.6	1214.9
	12.6	3.767	719.5	830.1	1562.0
	17.5	4.753	792.0	913.8	1719.4
	23.1	3.767	1319.0	1521.9	2863.7
	31.5	3.767	1798.6	2075.3	3905.0
	42.7	3.767	2438.2	2813.2	5293.4
	57.4	3.767	3277.5	3781.7	7115.8
	77.0	3.767	4436.7	5119.1	9632.3
	105.0	3.767	5995.5	6917.7	13016.7
Unplanted	0.0	4.753	0.0 (UP-REF)	0.0	0.0

The recommended fertilizer application rates for wild rice paddies ranges from 25–40 lb $acre^{-1}$ N (2802–4483 mg m^{-2} N) and from 0–50 lb $acre^{-1}$ P_2O_5 (0–2446 mg m^{-2} P) in commercial settings (Kaiser & Piotrowski, 2023). Grava and Raisanen (1978) applied fertilizer to wild rice paddies at a rate of 40 and 19.7 kg ha^{-1} for N and P, respectively (equivalent to 4000 and 1970 mg m^{-2}, respectively). In a greenhouse study, Walker et al. (2010) subjected individual wild rice plants to various fertilizer applications of 0, 2.39, 4.78, 9.55, and 14.33 g m^{-2} N and 0, 0.87, 1.74, 3.47, 5.21 g m^{-2} P. With the assumption that TKN ≈ TN (Section 3.1), the nutrient gradient loading applied among the FP mesocosms (Table 18) encompasses the N and P fertilizer application rates that are recommended for commercial paddy farms.

A primary objective of the present study was to evaluate the feasibility of pairing wild rice production in paddy-based systems with fish farming. As previously discussed in Chapter 3, surface applications of AWW were used here to simulate application of effluents from land-based fish farming facilities. However, paddy-based systems contained greater densities of plants and were predicted to have substantial nutrient requirements. In anticipation of greater nutrient demand among FP mesocosms, higher nutrient loadings were applied in accordance with the recommendations for commercial paddies of wild rice. The top dressing of P fertilizers in wild rice paddies can cause adverse environmental impacts (Oelke et al., 1982). To mitigate these risks and simulate regular inputs of AWW from a land-based fish farm, the desired total nutrient load was achieved through multiple applications of AWW over several weeks. This gradual nutrient dosing schedule, rather than a single high-dose fertilizer application, aligned with the primary objectives of this study to evaluate the response of FP systems to incremental nutrient inputs.

A comparison between the TP loading rates applied here and the TP produced in the waste from fish farms was made in Table 19. The mean of typical TP waste loading rates (9.55 kg t fish^{-1} yr^{-1}) reported by Hennessy et al. (1996) was applied to the loading rates utilized in the present study. The range of AWW additions applied to FP mesocosms achieved equivalent TP loadings to the waste produced by 959.1–14,386.6 g of fish. As discussed in Chapter 3, large-scale CWs are often over 100,000 times the size of the systems utilized here (Kadlec, 2016). Therefore the study design implemented here, if scaled up to a large scale with the same nutrient loading conditions, would be treating the waste from a fish farm of a commercial scale.

Table 19. Total phosphorus (TP) loadings in RL site mesocosms with an estimate of fish quantities required to produce equivalent TP loadings. Fish waste TP production was assumed to occur at a rate of 9.55 kg t fish^{-1} yr^{-1} (Hennessy et al., 1996).

Mesocosm type	TP (mg m^{-2})	TP loading rate (mg d^{-1})	Mass of fish (g)
RL	0.0 (FP-REF-A)	0.0	0.0
	0.0 (FP-REF-B)	0.0	0.0
	0.0 (FP-REF-C)	0.0	0.0
	0.0 (FP-REF-D)	0.0	0.0
	0.0 (FP-REF-E)	0.0	0.0
	399.7	25.1	959.1
	559.6	35.1	1342.7
	719.5	45.2	1726.4
	792.0	62.7	2397.8
	1319.0	82.8	3165.0
	1798.6	112.9	4316.0
	2438.2	153.1	5850.5
	3277.5	205.8	7864.7
	4436.7	278.5	10646.1
	5995.5	376.4	14386.6
Unplanted	0.0 (UP-REF)	0.0	0.0

3.3 Response of Constructed Wetland Systems to Aquaculture Wastewater

Plots of individual parameters not presented here are included in the Appendix. The response of main phosphorus species (TP, TDP, SRP), nitrogen species (TDN, TAN, NO_2-N, NO_3-N), and algal species (chl *a*) throughout the study were of particular interest for the assessment of water quality responses and for the evaluation of performance and treatment capacity of wild rice FP systems. Visualizations, discussions, and modelling results of water quality parameters are presented in subsections.

3.3.1 Temperature and Light Data Loggers

Results from data loggers which measured water temperature and light intensity in mesocosms are plotted in Figure 57. Diurnal changes in water temperature were evident, with a mean daily change in temperature of 6.2°C. A gradual decline in mesocosm water temperature was observed after day 50. Similar to the UM site air logger described in Chapter 3, unreliable readings were collected for air temperature at the RL site (RL air logger) because of the placement of the logger in contact with the surface of mesocosm material.

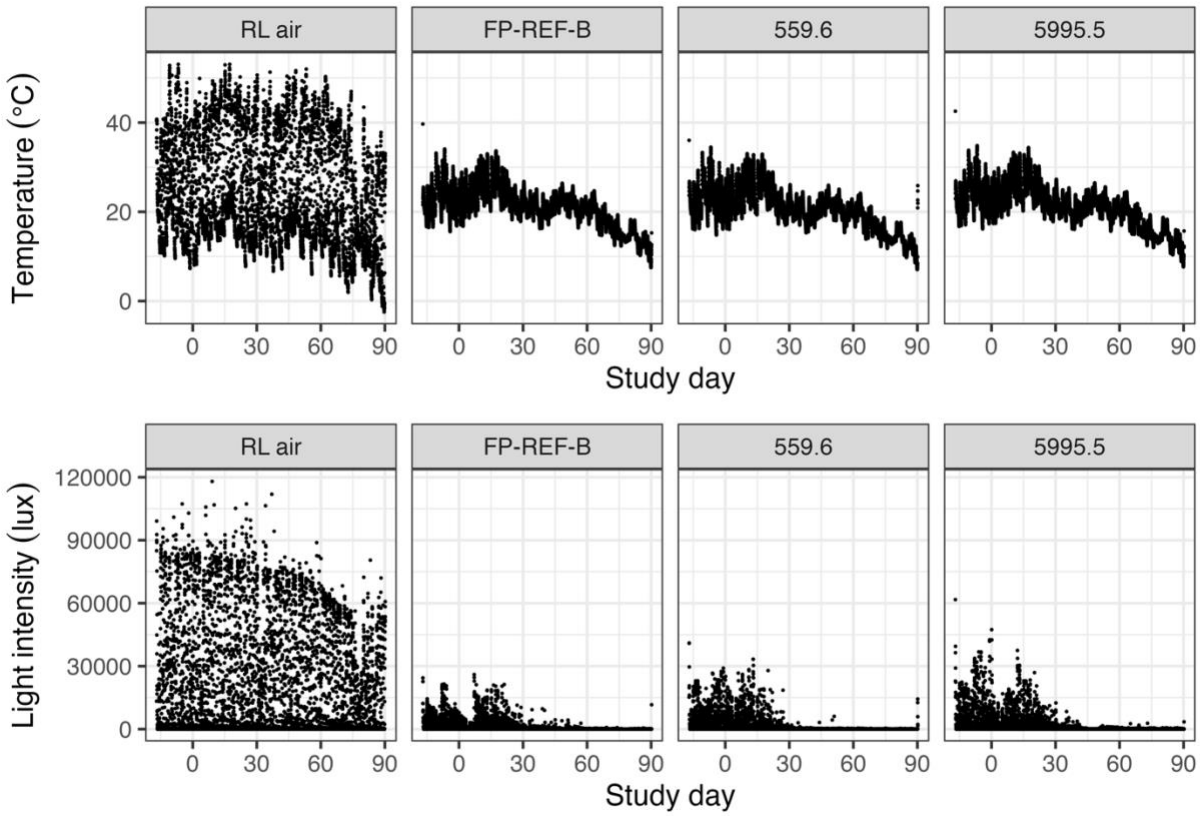

Figure 57. Temperature and light intensity data from loggers placed outside of mesocosms (RL air) and in select FP mesocosms. Loggers were set to record data every 20 min. Each graphical panel presents the data from one logger with the total phosphorus loading from aquaculture wastewater indicated in units of mg m^{-2} where applicable.

The very high densities of wild rice plants in FP systems had an impact on light conditions, resulting in little to no light intensity observed from day 25 onward in any of the three mesocosms containing loggers (Figure 57). As discussed previously (Chapter 3), recorded light was impacted by both shading from biomass and mesocosm walls, as well as turbidity in mesocosm water. Moreover, the light reaching the air-water interface, critical for algal growth, is not necessarily equivalent to the light conditions throughout the water column. However, even in FP systems which had very high plant density providing shade, substantial biofilm growth was observed (see Section 3.3.3.4).

3.3.2 Phosphorus in Mesocosm Water

The source water used at the RL site contained very high concentrations of P (Table A - 8) and resulted in very high levels (>0.75 mg L^{-1}) of background TP in water among all FP systems (Figure 58). By the third sampling event (day 27), major reductions in TP concentrations had occurred and concentrations were approximately one-third of the initial concentration. By the fourth sampling event (day 41), TP and TDP levels continued to decrease, but at a slower rate. After the AWW addition event on day 42 (i.e. the first addition of the second AWW source), substantial increases in both TP and TDP were observed during the next water sampling event (day 55). However, increases in SRP were not observed to the same extent. The magnitude of the increase in TP and TDP on day 55 was proportional to the nutrient loading treatment. Interestingly, following another AWW addition event on day 60, further increases in TP and SRP were not observed in water samples collected on day 69. In fact, the TP concentrations measured on day 69 were approximately equal or slightly lower than the previous values measured on day 55.

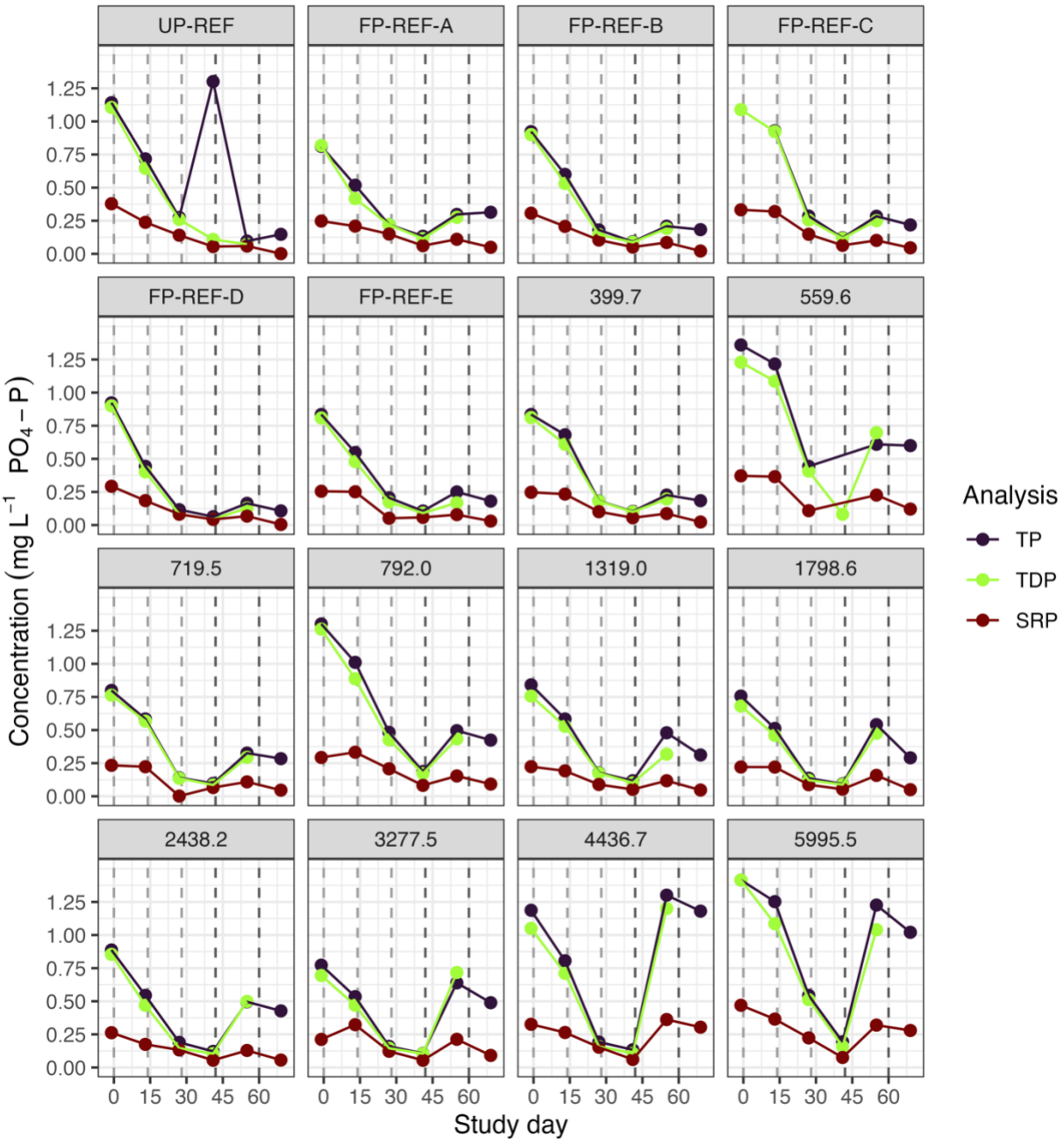

Figure 58. Total (TP), total dissolved (TDP), and soluble reactive (SRP) phosphorus concentrations in FP mesocosm water. Each graphical panel represents a mesocosm with the TP loading from aquaculture wastewater (AWW) additions indicated in units of mg m^{-2}. Vertical dashed lines indicate AWW addition events. The final two AWW addition events (dark dashed lines) were made with a different AWW source and twice the nominal volume of the first three addition events (light dashed lines).

With the exception of one sample for UP-REF, the difference between TP and TDP among FP mesocosms was minor throughout the study period (Figure 58). Corresponding PP concentrations were constant throughout the study period, with the majority of concentrations in the 15–50 µg L^{-1} range, with one major exception observed for the 1798.6 mg m^{-2} treatment on day 55 (Figure A - 39). For this instance, the difference between TP and TDP displayed in Figure 58 was not reflective of the 348.9 µg L^{-1} PP measurement in Figure A - 39. Some variability and error surrounding methodology (described in detail in Chapter 3) may explain the discrepancy between the difference in TP, TDP, and PP.

Similar to TP and TDP, but at a lower concentration, background concentrations of SRP were high (>0.25 mg L^{-1}) and an overall reduction was observed throughout the first four sampling events (i.e. from day -1 to 41; Figure 58). When elevations of TP and TDP occurred on day 55, corresponding SRP elevations did not occur to the same extent. The most notable elevations in SRP were observed among the three-highest treatments (i.e. 3277.5, 4436.7, and 5995.5 mg m^{-2}). With the exception of the two-highest treatments (i.e. 4436.7 and 5995.5 mg m^{-2}), SRP concentrations were below 0.25 mg L^{-1} during the second half of the study period.

While the only form of biomass collected from FP systems during the decommissioning of mesocosms was wild rice plants, substantial production was achieved (see Section 3.3.3.9) The FP systems were able to substantially eliminate P from the water column throughout the first 41 days of the study (Figure 58). The contribution of wild rice plants to nutrient elimination is most evident when comparing planted reference conditions to unplanted reference conditions. During the first 3 sampling events (day -1 to 27), large decreases in TP and TDP were observed among

both planted references. Interestingly, UP-REF also displayed a substantial reduction in TP during this period, although the concentrations of P species remaining in FP water on day 27 were slightly greater in UP-REF than other mesocosms. The fresh soil used in FP systems was expected to have a high capacity for P binding to soil which would explain to reductions of P observed in UP-REF.

In scenarios where TP ≈ TDP and SRP concentrations comprise a small fraction of TP, DOP is likely a primary contributor to TP. The various forms of P, such as DOP, are complex in nature and a dynamic relationship exists between the various forms where P species can be converted to SRP, or deposited to sediments/soils under the proper conditions (Correll, 1998). In natural systems, P retention occurs in bottom sediments and is facilitated by consistently high oxygen levels which prevent the release of P and promote its migration into deeper sediments (Correll, 1998; Wang et al., 2022). Such processes ultimately inhibit the diffusion of P from sediments into the water column, where it could be taken up by algae and contribute to eutrophication. In the present study, mesocosm water was not circulated or aerated, however the large surface area to volume ratio facilitated high DO concentrations during the first half of the study (Figure A - 44). As DO decreased during the second half of the study, biotic communities could have been altered and various forms of P may have been released that would normally be bound to sediments, ultimately reinforcing eutrophic conditions in the affected environment (Correll, 1998). In UP-REF, DO concentrations were constant whereas planted mesocosms experienced a decline in DO throughout the study period (Figure A - 44). This is likely a result of the decomposition of organic matter occurring in the planted mesocosms. Decomposition of wild rice most actively occurs midseason (Lee & Stewart, 1981), and the decline in DOC observed in

FP water corresponded with the degradation of organic matter (Figure A - 42). The release of P from soils in FP systems therefore contributed to the elevated P levels observed in FP water during the second half of the study period. This is most clearly reflected by the increase in P concentrations among planted reference mesocosms on study day 55 (Figure 58). While minor increases in P were observed in planted reference mesocosms between day 41 and 55, the P increases among AWW-dosed mesocosms were larger and generally proportional to the nutrient loading conditions. An initial decline in P was observed in both UP-REF and planted references, suggesting that binding of P to soil or the precipitation and settling of DOP was substantial during the first half of the study. However, conditions within planted mesocosms facilitated the release of P bound to soils, resulting in the release of P into the water column.

Plants and algae were secondary contributors to P elimination from the water column in FP mesocosms. More specifically, the difference between concentrations in UP-REF and planted reference mesocosms suggests an additional source of P elimination other than soil binding. Wild rice plants undergo a rapid 30-day period of growth from late June to late July, during which half of the total plant nutrients are taken up (Grava & Raisanen, 1978). The beginning of this period of rapid growth aligned with the start of the study (i.e. day 0; June 30th, 2022) and therefore high nutrient uptake by wild rice plants was expected during the first month of the study. Biofilm also benefited from excess nutrients; high concentrations of biofilm chl *a* were observed among the high nutrient loading mesocosms (see Section 3.3.3.4; Figure 60).

Under the nutrient gradient evaluated, FP systems effectively accommodated all AWW loadings during the first 41 days of treatment. After 41 days, a deterioration in water quality occurred that

was related to nutrient loading conditions. Elevation in P species in FP mesocosm water were particularly evident at nutrient loading rates of 3277.5 mg m^{-2} and greater over a period of 60 days (i.e. 54.625 mg m^{-2} d^{-1}). The available P species in FP water appear to have resulted in elevated production of biofilm (see Section 3.3.3.4). To maintain continued usage of FP systems, nutrient loadings equal to, or less than 2438.2 mg m^{-2} (i.e. 40.637 mg m^{-2} d^{-1}) could maximize treatment capacity while avoiding substantial elevations in P species in FP water which could negatively impact long-term performance if not properly managed. Additionally, the increase in both AWW nutrient concentrations and nominal addition volumes resulted in increased nutrient loading rates during the second half of the study period. A more consistent application of AWW could help to avoid sudden deteriorations in water quality and improve the overall treatment capacity of FP systems.

3.3.3 Nitrogen in Mesocosm Water

No treatment-based differences were observed for any nitrogen endpoints among the FP systems (Figure 59). Concentrations of TDN were constant and approximately equal to 2 mg L^{-1} throughout the study period, with the exception for day 69 in the UP-REF, FP-REF-C, and 4436.7 mg m^{-2} mesocosms where TDN concentrations exceeded 4 mg L^{-1} during the final timepoint (Figure 59, Figure A - 35). High concentrations of TDN were found in RL site source water which were responsible for the high background concentrations of TDN in mesocosm water (Table A - 8) and no treatment-based impacts of AWW additions on TDN are evident in Figure 59. Stable concentrations of TDN were observed in UP-REF during the first 55 days of the study, suggesting that sorption of TDN with soil did not occur substantially, if at all. Low DO was observed among planted FP systems during the second half of the study period (discussed

previously in Section 3.3.3.2), which may have promoted the necessary conditions for N release to occur from FP soil (Müller et al., 2016). Further, nitrification (i.e. oxidation of NH_4^+ to NO_3^- with NO_2^- as an intermediate) is meditated by chemoautotrophic bacteria which use oxygen as an electron acceptor, while denitrification (i.e. reduction of NO_3^- to N_2 with NO_2^-, NO, and N_2O as intermediates) occurs under anaerobic conditions and is mediated by facultative bacteria (Snow et al., 2012). Declines in DO may therefore have supported the conditions necessary for denitrification. However, further investigations into the properties of wild rice paddy soils are required to elucidate nutrient cycling processes in FP systems.

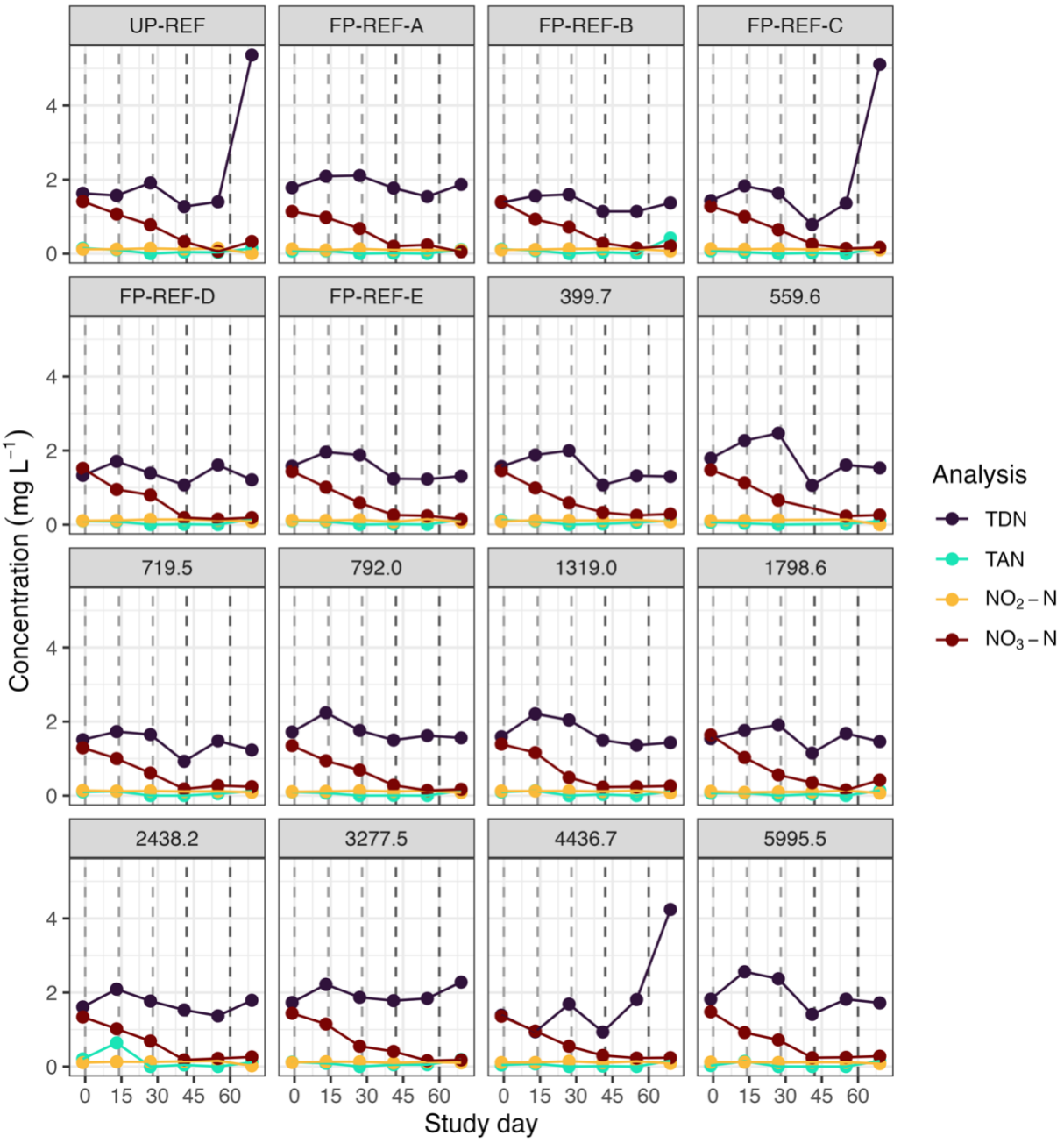

Figure 59. Total dissolved (TDN), total ammonia (TAN), nitrite (NO_2–N), and nitrate (NO_3–N) nitrogen concentrations in FP mesocosm water. Each graphical panel represents a mesocosm with the total phosphorus loading from aquaculture wastewater (AWW) additions indicated in units of mg m^{-2}. Vertical dashed lines indicate AWW addition events. The final two AWW addition events (dark dashed lines) were made with a different AWW source and twice the nominal volume of the first three addition events (light dashed lines).

Concentrations of NO_2-N were in the 0.10–0.15 mg L^{-1} range and remained relatively constant throughout the study period, with a decrease observed in most of the mesocosms on the final sampling day (Figure A - 37). A decrease in NO_3–N from approximately 1.25 to 0.25 mg L^{-1} occurred throughout the first 41 days of the study, after which concentrations remained relatively constant for the remainder of the study period (Figure A - 38). Primary nutrient sinks in FP systems included phytoplankton, biofilm, and wild rice plants. The impacts of plants on NO_3–N elimination did not appear to be substantial; similar decreases in NO_3–N were observed in the unplanted mesocosm UP-REF as in planted FP mesocosms (Figure 59). Microbial growth is expected to occur on the soil surface and on plant roots which contribute to nutrient cycling processes (Snow et al., 2012), and wetland plants growing in flooded soils can capture NO_3^- formed by the rhizosphere (Kirk & Kronzucker, 2005). While uptake by plants may have resulted in slightly greater rates of elimination of NO_3–N (Figure A - 38), the elimination of NO_3–N from FP water appears to have been driven by processes other than plant uptake. Wild rice plants receiving fertilizer additions injected into sediments will undergo a plastic shift in nutrient allocation toward shoots and have greater growth rates (Sims et al., 2012) and foliar concentrations of N and P are known to increase with the addition of fertilizers incorporated into sediments (Atkins et al., 1992). However, the AWW applied here was not incorporated into mesocosm soil. Furthermore, with multiple nutrient sinks present, the direct uptake of N and P by plants does not always play a substantial role in the overall treatment of nutrients in wastewater in constructed wetlands (Snow et al., 2012). An expanded discussion surrounding wild rice responses in mesocosms is included in Section 3.3.3.9. Meanwhile, declines of DO in FP mesocosm water may have supported denitrification, however the period of maximum biofilm growth which occurred immediately following NO_3–N depletion suggests that biofilm

was a primary nutrient sink and the growth of this algae was a major contributor to NO_3–N elimination (see Section 3.3.3.4; Figure 60).

TAN concentrations were consistently low in FP mesocosms throughout the study, and typically in the 0.05–0.15 mg L^{-1} range during the first two sampling events (i.e. day -1 and 13; Figure 59, Figure A - 36). TAN concentrations then decreased to levels near or below limits of detection before undergoing an increase during the final sampling event (i.e. day 69); the final concentrations of TAN observed in FP mesocosm water were comparable to those measured initially. Despite high concentrations of TAN in RL site source water (Table A - 8), TAN was able to undergo biological uptake, nitrification, denitrification, volatilization, or binding to soils or other organic matter in wetlands, facilitating its removal from the water column (White & Reddy, 2009). Alkaline pH conditions were observed in FP mesocosm water, particularly during the beginning of the study period (Figure A - 45). Such conditions were favourable for the conversion of ammonium (NH_4^+) to ammonia (NH_3), which can subsequently undergo volatilisation, where ammonia gas exits the water column and enters the atmosphere (White & Reddy, 2009). Ammonia fertilizers that are broadcast into high pH waters of flooded rice soils are particularly vulnerable to losses through ammonia volatilization (Mikkelsen et al., 1978). Loses can be as high as 20% with the majority of losses occurring in the 3 days following fertilizer application (Mikkelsen et al., 1978). Alternatively, ammonia fertilizers can be incorporated into soils to reduce losses by volatilization and economize on fertilizer use (Mikkelsen et al., 1978; Oelke et al., 1982), in instances where wastewater treatment is a primary objective, the same considerations are not required. Moreover, in wild rice FP systems, the incorporation of fertilizer (as AWW or otherwise) is only feasible at the start of the season prior

to germination. Losses from ammonia volatilization can contribute to the removal of nitrogen and are beneficial for overall wastewater treatment (Poach et al., 2002; Vendramelli et al., 2017). When considering pairing wild rice production with fish farming, the use of wild rice paddies could capitalize on both of these elements; AWW could be incorporated as a fertilizer at the start of the season to promote wild rice growth and obtain high yields while continued AWW loadings throughout the growing season can be applied to benefit from the nitrogen removal through ammonia volatilization.

3.3.4 Biofilm and Phytoplankton

Biofilm tile chl *a* concentrations and fitted logistic growth models are plotted in Figure 60. Key model parameters associated with growth curves are found in the Appendix (

Table A - 11). Among all FP systems, a rapid increase in biofilm growth was observed between the third (day 41) and fourth (day 55) sampling events. Lower mean (± SD) K was observed among the three-highest treatments (i.e. 3277.5, 4436.7, 5995.5 mg m^{-2}; 3.84 ± 1.45 µg cm^{-2}) than the planted reference treatments (7.32 ± 3.67 µg cm^{-2}). The mean (± SD) t_{mid} for the three-highest treatments (43.60 ± 0.53 d) was lower than the planted reference treatments (48.25 ± 3.07 d). A higher mean (± SD) r value was observed for the three-highest treatments (0.64 ± 0.09) than for the planted reference treatments (0.26 ± 0.12). In response to AWW additions, total biofilm growth was augmented (greater K) and growth occurred more rapidly (greater r and lower t_{mid}). In natural settings, AWW effluents increase periphytic algal growth (Carr & Goulder, 1990). Biofilm substrates could be implemented in FP systems to promote the remediation of nutrient-rich wastewaters such as AWW. For example, Wu et al. (2014) have proposed in situ

periphyton devices which contain periphyton biofilms that can be implemented for the remediation of surface waters. Here, biofilm responses (as chl *a*) to AWW additions were evident. An increase in mean AFDM was observed in all FP mesocosms between days 13 and 55, however no treatment-based trends were evident (Figure 61).

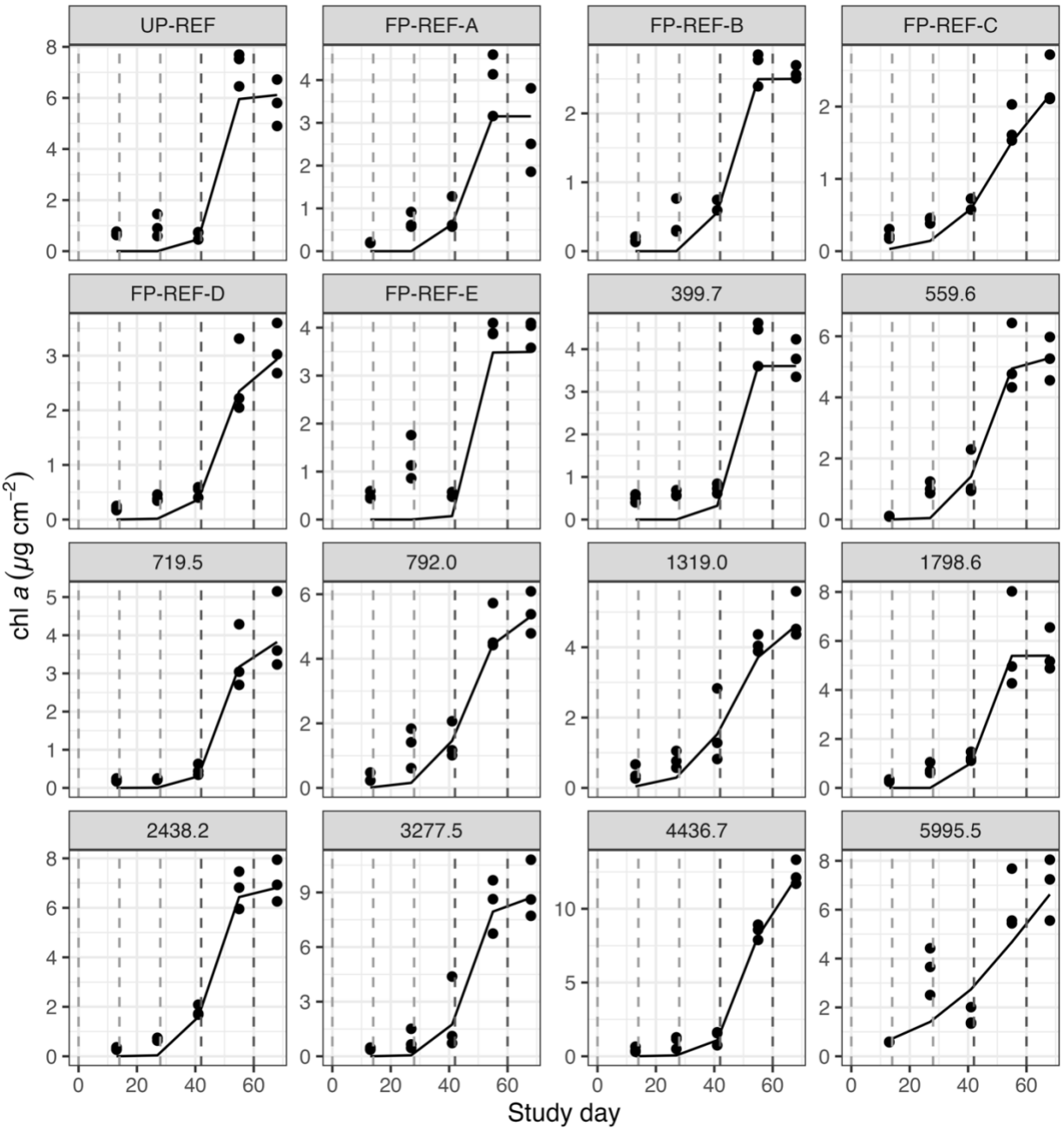

Figure 60. Biofilm tile chlorophyll *a* (chl *a*) concentrations in FP mesocosms. Measured data (points) are included with fitted logistic growth curves (solid lines). Note that different y-axis scales are used across the graphical panels. Each graphical panel represents a mesocosm with the total phosphorus loading from aquaculture wastewater (AWW) additions indicated in units of mg m^{-2}. Vertical dashed lines indicate AWW addition events. The final two AWW addition events (dark dashed lines) were made with a different AWW source and twice the nominal volume of the first three addition events (light dashed lines).

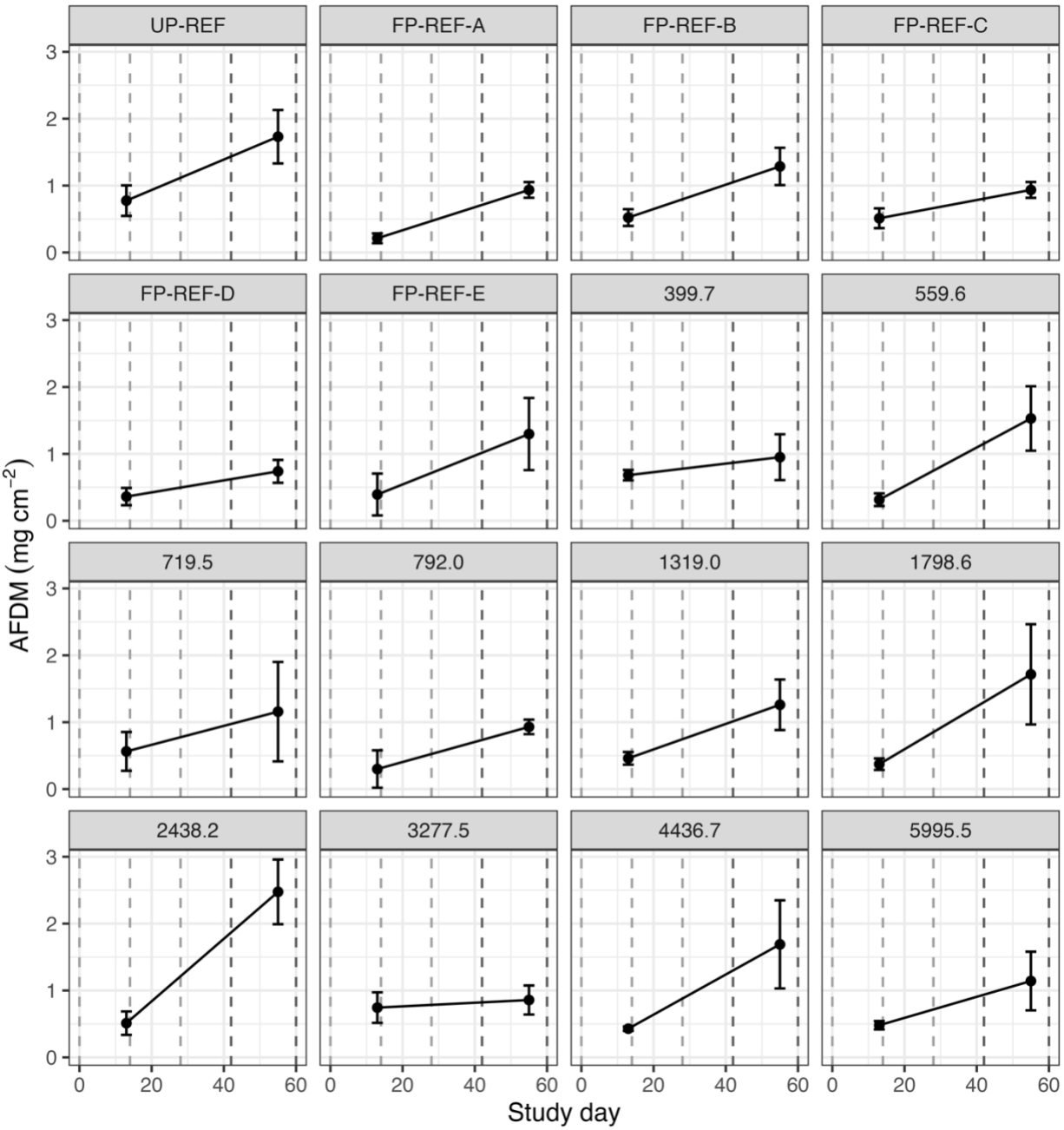

Figure 61. Biofilm tile ash-free dry mass (AFDM) in FP mesocosms. The mean (± SD) of three replicates is presented for each sampling event. Each graphical panel represents a mesocosm with the total phosphorus loading from aquaculture wastewater (AWW) additions indicated in units of mg m^{-2}. Vertical dashed lines indicate AWW addition events. The final two AWW addition events (dark dashed lines) were made with a different AWW source and twice the nominal volume of the first three addition events (light dashed lines).

Water column chl *a* was generally below 5 µg L^{-1}, especially during the first 41 days of the study period (Figure 62). Notable increases were observed in UP-REF, 559.6, 1798.6, 2438.2, 4436.7, 5995.5 mg m^{-2} treatments. Elevations in chl *a* among high nutrient loading treatments occurred in response to the elevated available P concentration in mesocosm water (Figure 58). The production of certain algae could be particularly valuable in a circular economy approach to wild rice and fish farming. Microalgae can be recycled in the circular economy system as fish feed (Ansari et al., 2021; Chen et al., 2021), or harvested as a high-value product with application in human nutrition, cosmetics, and pharmaceuticals (Pulz & Gross, 2004; Richmond, 2004). When pairing the production of wild rice with the treatment of AWW while simultaneously supporting the growth of algae, avoiding eutrophic conditions is important for long-term system functionality. Here, nutrient loadings equal and greater than 1798.6 mg m^{-2} over 60 days (i.e. 29.977 mg m^{-2} d^{-1}) resulted in water quality deterioration which led to excessive phytoplankton and biofilm growth when compared to reference conditions. However, the long-term impacts of such alterations were not evaluated in the present study. Future studies should address how elevated algal growth and increased water column nutrients can impact FP functionality and the feasibility of the proposed circular economy under continued multi-year, long-term usage.

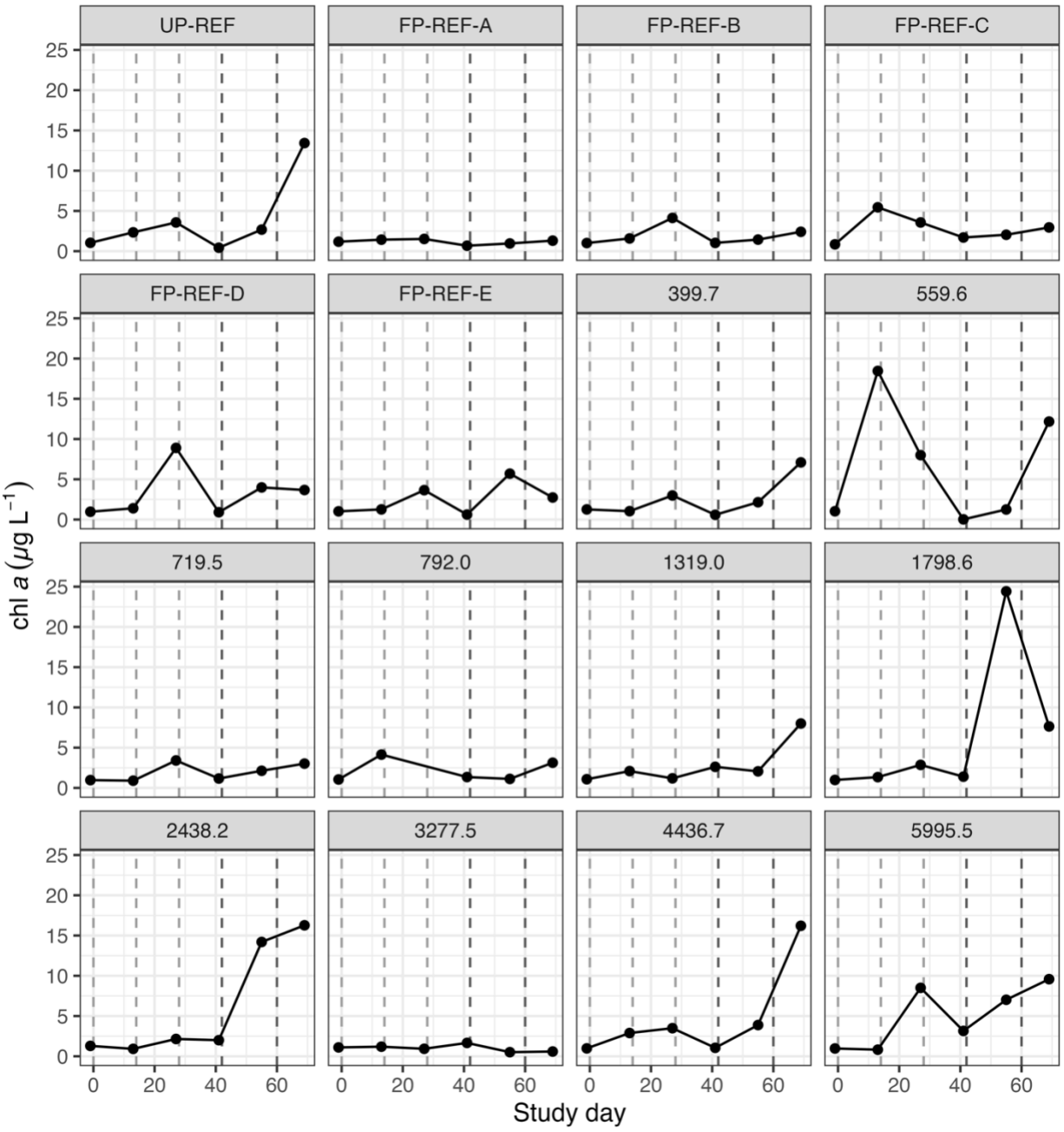

Figure 62. Chlorophyll *a* (chl *a*) concentrations in FP mesocosm water. Each graphical panel represents a mesocosm with the total phosphorus loading from aquaculture wastewater (AWW) additions indicated in units of mg m^{-2}. Vertical dashed lines indicate AWW addition events. The final two AWW addition events (dark dashed lines) were made with a different AWW source and twice the nominal volume of the first three addition events (light dashed lines).

3.3.5 Performance of Constructed Wetland for Phosphorus Treatment

Initial and final TP concentrations in FP water were approximately equal among the highest nutrient loading treatments, but concentrations diverged along the nutrient loading gradient with greater differences in TP concentration observed at lower nutrient loading treatment (Figure 63). Details and parameters related to FP performance are presented in Table 20. In all instances the CR of FPs that received AWW was greater than the mean CR of reference treatments (84.4%). An exponential trend was observed for PLR, which when analyzed on a log-scale generated a statistically significant positive linear trend between PLR and TP loading (Figure 64). As discussed previously (Section 3.3.1.5 and Section 3.3.2.5), the lack of plateau in PLR does not necessarily imply greater capacity for AWW remediation among FP systems. However, the FPs were able to substantially reduce the final TP concentration in FP water (C_f) from what would be expected if no P elimination occurred (C_{max}). Therefore, FP water could be discharged without contributing substantial nutrients to the receiving environment. Continued monitoring of FP performance throughout long-term use of FP systems would be beneficial to properly characterize P dynamics that occur in response to extended usage and operational practices. With long-term usage, FP soils would become P-saturated and therefore reduced P removal would be expected (Kadlec, 2016). Further, the reflooding of wild rice paddies after drainage has the potential to release additional P from soil, potentially resulting in a deterioration of water quality and negatively impacting FP system performance (Olila et al., 1997).

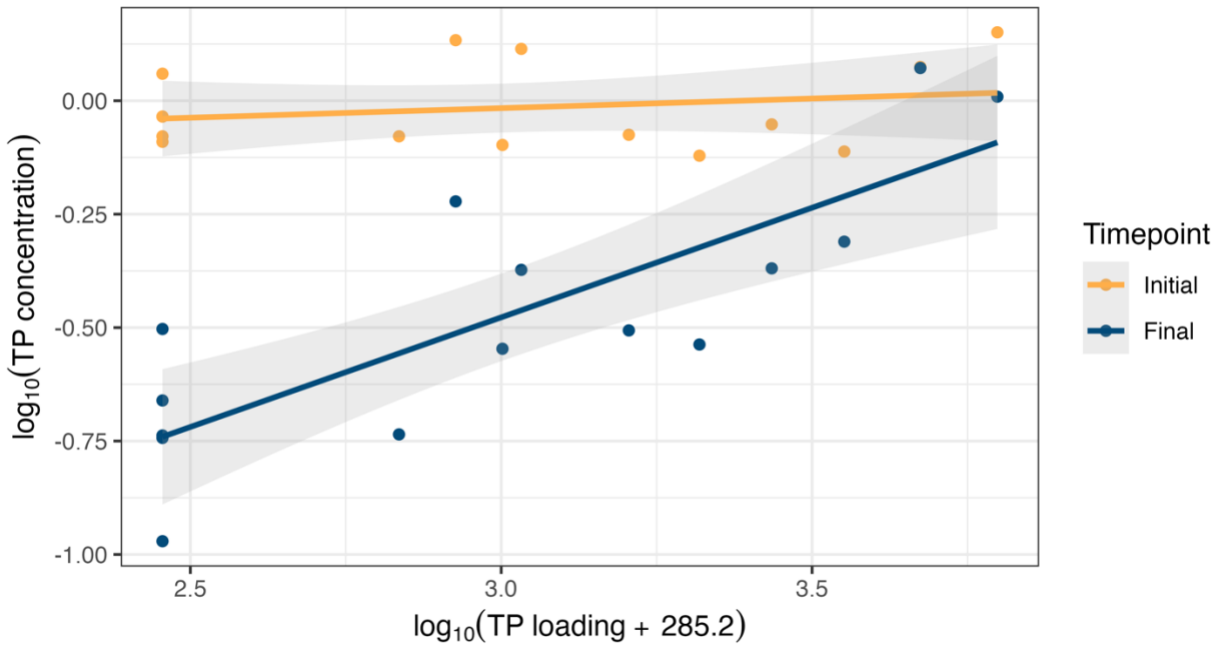

Figure 63. Comparison of total phosphorus (TP) concentrations in FP mesocosm water during initial (day -1) and final (day 69) timepoints of the performance period. General linear models (solid lines) were fit to measured data (points) with 95% confidence intervals (shaded regions). Predictor variables were calculated by adding a constant (285.2) to the TP loading from aquaculture wastewater additions.

Table 20. Calculated and measured parameters relating to the performance of FP systems removing total phosphorus (TP) from aquaculture wastewater (AWW).

Mesocosm type	TP loading for study (mg m^{-2})	TP loading for performance period (mg m^{-2})	C_{max} (mg L^{-1})	C_f (mg L^{-1})	CR (%)	PLR (mg m^{-2} d^{-1})	AWW loading (L d^{-1})	HLR (mm d^{-1})
FP	0 (FP-REF-A)	0.0	1.029	0.314	69.5	2.289	0.000	0.000
	0 (FP-REF-B)	0.0	1.186	0.183	84.6	3.016	0.000	0.000
	0 (FP-REF-C)	0.0	4.652	0.218	95.3	11.780	0.000	0.000
	0 (FP-REF-D)	0.0	1.185	0.107	91.0	3.526	0.000	0.000
	0 (FP-REF-E)	0.0	0.989	0.181	81.7	2.808	0.000	0.000
	399.7	399.7	2.884	0.184	93.6	8.545	0.100	0.027
	559.6	559.6	5.554	0.600	89.2	10.934	0.140	0.037
	719.5	719.5	4.054	0.284	93.0	12.631	0.180	0.048
	792.0	792.0	4.636	0.424	90.9	15.346	0.250	0.053
	1319.0	1319.0	7.152	0.312	95.6	21.206	0.330	0.088
	1798.6	1798.6	14.731	0.290	98.0	27.334	0.450	0.119
	2438.2	2438.2	10.032	0.427	95.7	37.115	0.610	0.162
	3277.5	3277.5	14.222	0.489	96.6	48.260	0.820	0.218
	4436.7	4436.7	22.484	1.180	94.7	64.672	1.110	0.295
	5995.5	5995.5	32.316	1.021	96.8	88.074	1.500	0.398
Unplanted	0 (UP-REF)	0.0	1.161	0.147	87.3	4.249	0.000	0.000

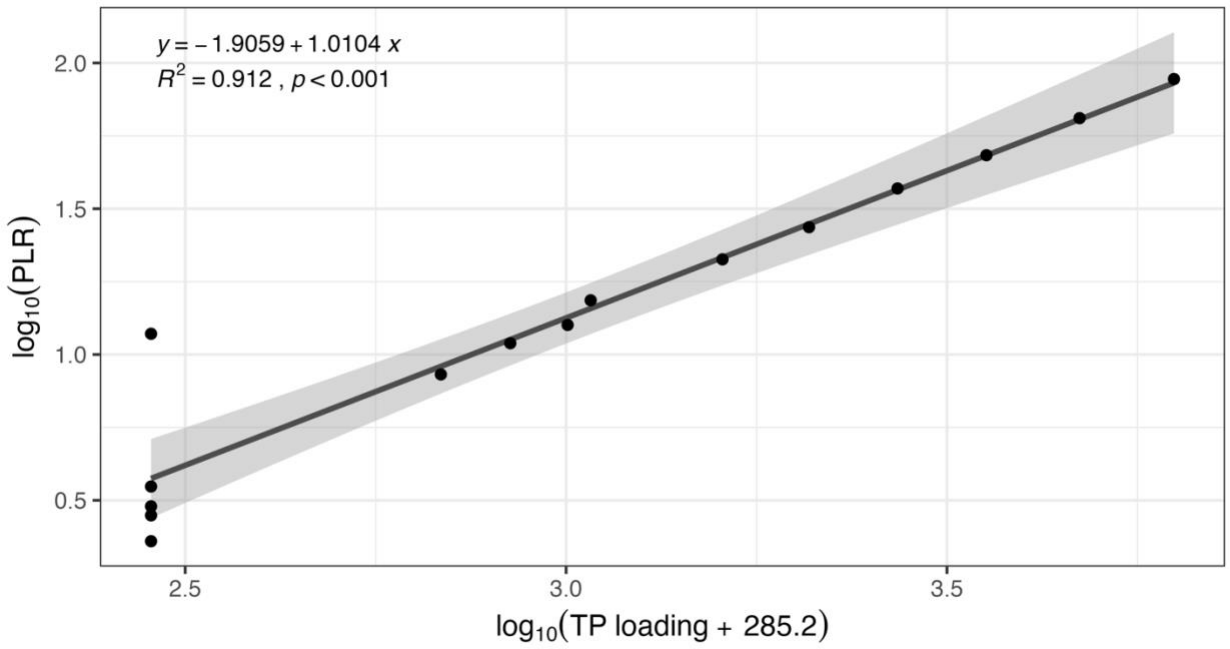

Figure 64. Phosphorus load reduction (PLR) for total phosphorus (TP) in FP mesocosm water during the 70-day performance period. A general linear model (solid line) was fit to calculated data (points) with a 95% confidence interval (shaded region). Predictor variables were calculated by adding a constant (285.2) to the TP loading from aquaculture wastewater additions.

3.3.6 Modelling and Interaction Analysis

The results of all fitted LMMs are included in the Appendix (Table A - 4). Statistically significant treatment-time interactions in LMMs were detected for TP ($F = 4.456$, $p = 0.038$), SRP ($F = 6.213$, $p = 0.015$), PP ($F = 7.329$, $p = 0.008$), chl *a* ($F = 7.782$, $p = 0.007$), SRSi ($F = 4.677$, $p = 0.034$), and SPC ($F = 8.143$, $p = 0.005$) among the FP systems. Statistically significant pairwise contrasts are summarized in Table 21 and an accompanying interaction plot visualization is presented in Figure 65. Several statistically significant contrasts were found for TP, SRP, and SPC while a single significant contrast was found for SRSi and none were found for PP. Most notably, study days 55 and 69 were statistically different than other sampling days for TP and SRP, however these two sampling days were not different from each other (i.e. the 55 vs. 69 contrast was not statistically significant for TP or SRP). This finding is depicted in Figure

65 which demonstrated how the large positive slopes of covariate trends on days 55 and 69 differed from all other study days, implying that trends across the nutrient gradient occurred on day 55 and were then present for the remainder of the study period. Similar trends were observed for PP, however the contrasts were not statistically significant.

Table 21. Pairwise contrast test results for water quality parameters with statistically significant interaction terms in fitted linear mixed models for the FP mesocosms. The difference in estimated marginal means (estimate) is reported with standard error (SE).

Response variable	Response units	Contrast	Estimate ± SE	p
TP	mg L^{-1} PO_4-P	-1 vs. 55	-0.457 ± 0.097	<0.001
		-1 vs. 69	-0.348 ± 0.097	0.008
		13 vs. 55	-0.447 ± 0.094	<0.001
		13 vs. 69	-0.339 ± 0.094	0.008
		27 vs. 55	-0.536 ± 0.094	<0.001
		27 vs. 69	-0.428 ± 0.094	<0.001
		41 vs. 55	-0.574 ± 0.094	<0.001
		41 vs. 69	-0.465 ± 0.094	<0.001
SRP	mg L^{-1} PO_4-P	-1 vs. 55	-0.119 ± 0.031	0.004
		-1 vs. 69	-0.106 ± 0.031	0.014
		13 vs. 55	-0.106 ± 0.031	0.014
		13 vs. 69	-0.094 ± 0.031	0.042
		27 vs. 55	-0.103 ± 0.031	0.019
		41 vs. 55	-0.141 ± 0.031	<0.001
		41 vs. 69	-0.129 ± 0.031	0.002
SRSi	mg L^{-1}	-1 vs. 69	3.061 ± 0.932	0.020
SPC	µS cm^{-1}	12 vs. 69	151.463 ± 40.2	0.025
		13 vs. 69	146.122 ± 40.2	0.039
		21 vs. 69	158.269 ± 40.2	0.014
		35 vs. 69	143.638 ± 40.2	0.047

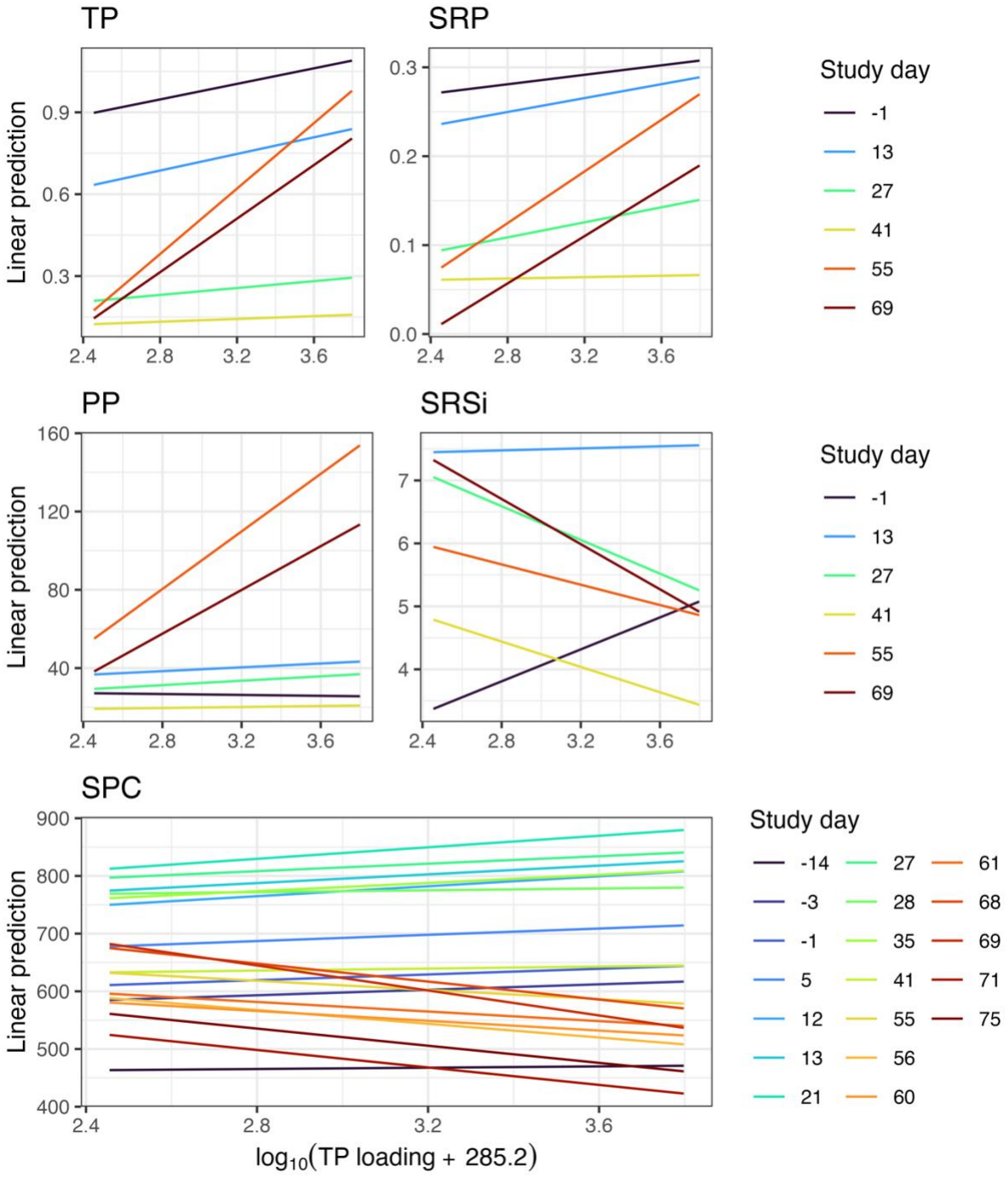

Figure 65. Interaction plots of estimated marginal means based on the fitted linear mixed models for total phosphorus (TP), soluble reactive phosphorus (SRP), particulate phosphorus (PP), soluble reactive silica (SRSi), and specific conductance (SPC) of the interaction between treatment and time for the FP mesocosms. Predictor variables were calculated by adding a constant (285.2) to the TP loading from aquaculture wastewater additions.

3.3.7 Microbial Activity

Microbial activity (measured as tATP) in mesocosm water and wild rice roots is presented in Figure 66. No statistically significant relationships between tATP and nutrient loading were observed for either endpoint. For both water and roots, results were highly variable. Microbial communities on wild rice roots are known to play crucial roles in nutrient cycling and distinct community differences exist between those in water and those in the roots and sediments of wild rice stands (McMillian, 2021). Detailed taxonomic assessment of microbial communities would provide further insight into the composition, functional roles, and impacts of AWW additions within FP systems. By characterizing microbial dynamics, the efficiency and capacity of wild rice FPs fertilized with AWW can be better understood.

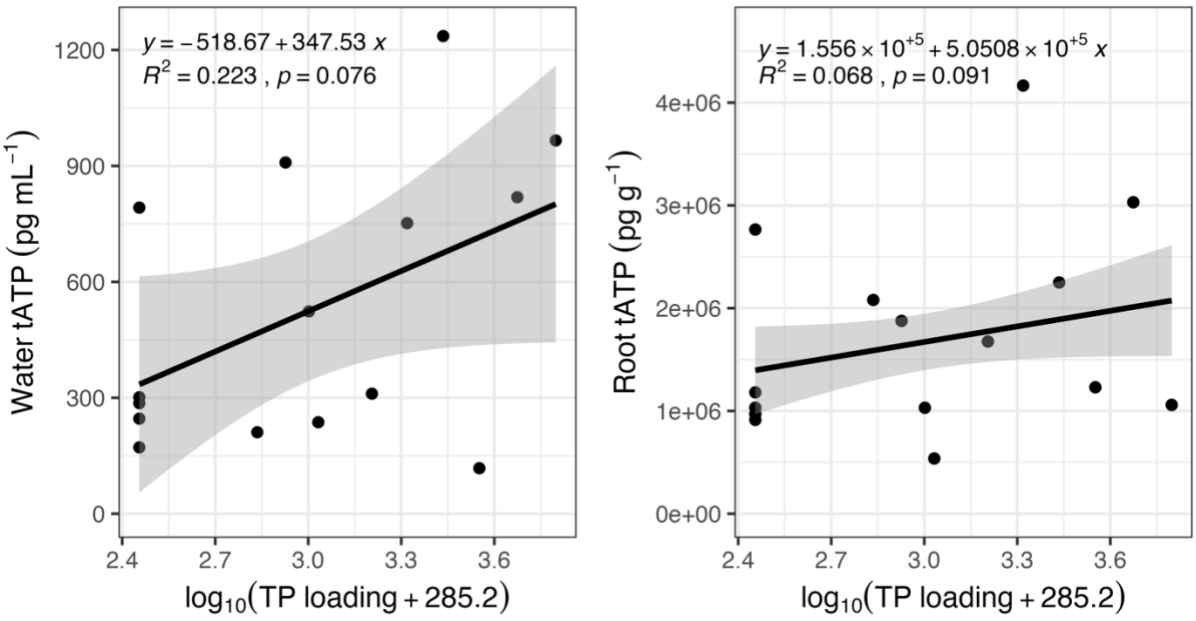

Figure 66. Microbial activity as total ATP (tATP) in FP mesocosm water (left) and wild rice roots (right). General linear models (solid lines) were fit to measured data (points) with 95% confidence intervals (shaded regions). Predictor variables were calculated by adding a constant (285.2) to the total phosphorus (TP) loading from aquaculture wastewater additions.

3.3.8 Soil Nutrient Content

Background (day 0) and final (day 92) concentrations of OP in FP mesocosm soil are presented in Figure 67. No statistically significant linear relationships between soil OP concentration and nutrient loadings were found for either timepoint (Figure 67), or when evaluating the change in OP between timepoints (Table A - 5). The results from all fitted models for different soil endpoints are compiled in the Appendix (Table A - 5) and a summary of statistically significant relationships for FP soil is presented in Table 22.

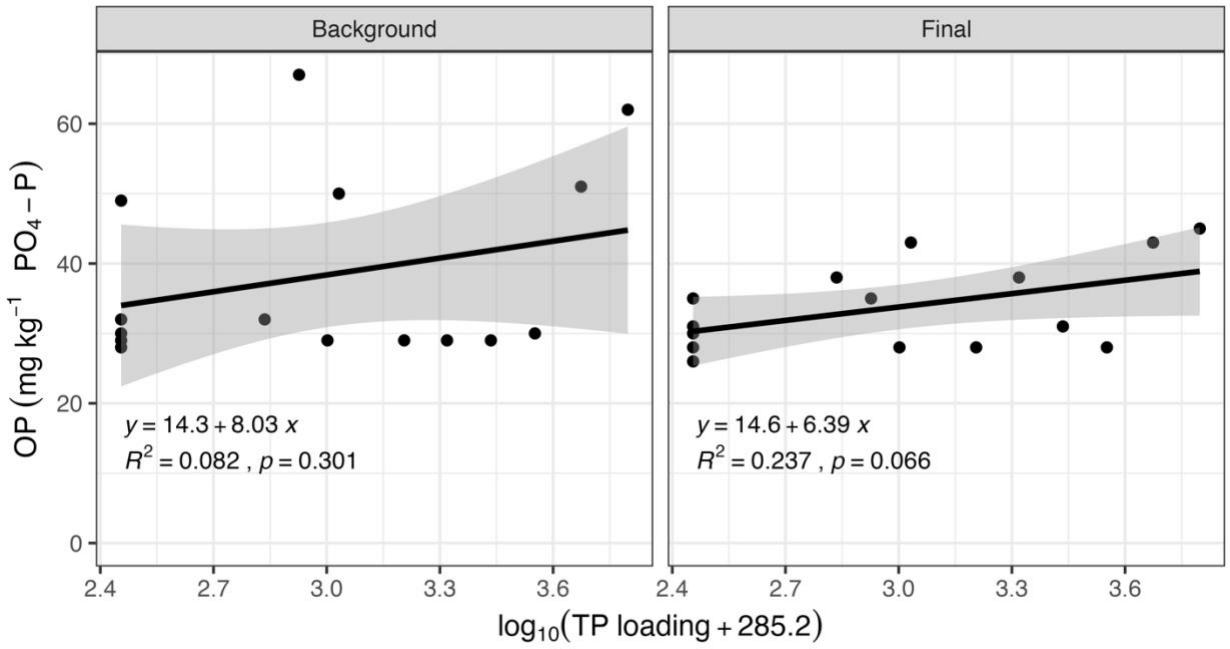

Figure 67. Background (day 0), final (day 98) soil Olsen phosphorus (OP) in FP mesocosms. General linear models (solid lines) were fit to measured data (points) with 95% confidence intervals (shaded regions). Predictor variables were calculated by adding a constant (285.2) to the total phosphorus (TP) loading from aquaculture wastewater additions.

Table 22. Summary of statistically significant results for different endpoints assessed in FP mesocosm soil during day 0 (background) and day 98 (final) samples, and the difference between background and final samples (change). Endpoints were assessed using general linear models and indicated in the table if a statistically significant result was detected. The directionality of the relationship is indicated in parentheses as either positive (+) or negative (-).

Analysis	Endpoint
Background	Ca (+), CEC (+)
Final	Na (+)
Change	S (+), Ca (-), CEC (-)

Background trends in both Ca and CEC were a product of natural variation in FP systems and both of these trends were eliminated throughout the study period (Table 22). In scenarios where AWW is discharged into the environment, elevated sulphate can occur downstream from the discharge location (Lalonde et al., 2015). Here, sulphate could be deposited on FP soils resulting in the positive relationship observed between S concentration and nutrient loading. While sulphate concentrations of 5000 mg L^{-1} can cause phytotoxic effects and decrease root length, shoot length, and leaf number (Fort et al., 2014), concentrations as high as 1350 mg L^{-1} have been shown to have no adverse impacts on wild rice paddies, suggesting that sulphate may not impact wild rice phenology and productivity as strongly as previously believed (Tedrow & Lee, 2022). Meanwhile, conductivity, particularly Na, is quite high in AWW and can result in elevated concentrations downstream from AWW discharge (Lalonde et al., 2015). In general, wild rice does not grow well in saline water (Archibold, 2003) and saline soils reduce plant growth significantly (Pitman & Läuchli, 2002). Salinity negatively impacts plant growth through osmotic stress, ion toxicities, and nutrient imbalances (Kopittke, 2012). The low pH of saline sediments can also result in the release of metals (DeLaune & Smith, 1985) which can accumulate in, and be harmful to wild rice plants (Bennett et al., 2000; Fort et al., 2014).

3.3.9 Plant and Algal Biomass

No trends were observed between total dry biomass of wild rice and nutrient loading at the end of the study period (Figure 68). A statistically significant positive relationship was observed between mean wild rice plant length and nutrient loading at the end of the study period (p = 0.021; Figure 69). Shoot length is affected by many unknown variables (Peden, 1982), however the allocation of resources among wild rice plants is impacted by additions of nutrients and light conditions (Sims et al., 2012). Further, while nutrient additions can increase wild rice tillering (Atkins et al., 1992), in instances of high plant density, resources may be directed away from tillering and instead directed toward vertical growth. In such a case, plants would benefit from additions of nutrients and a relationship between shoot length and nutrient loading as was observed in Figure 69 could develop.

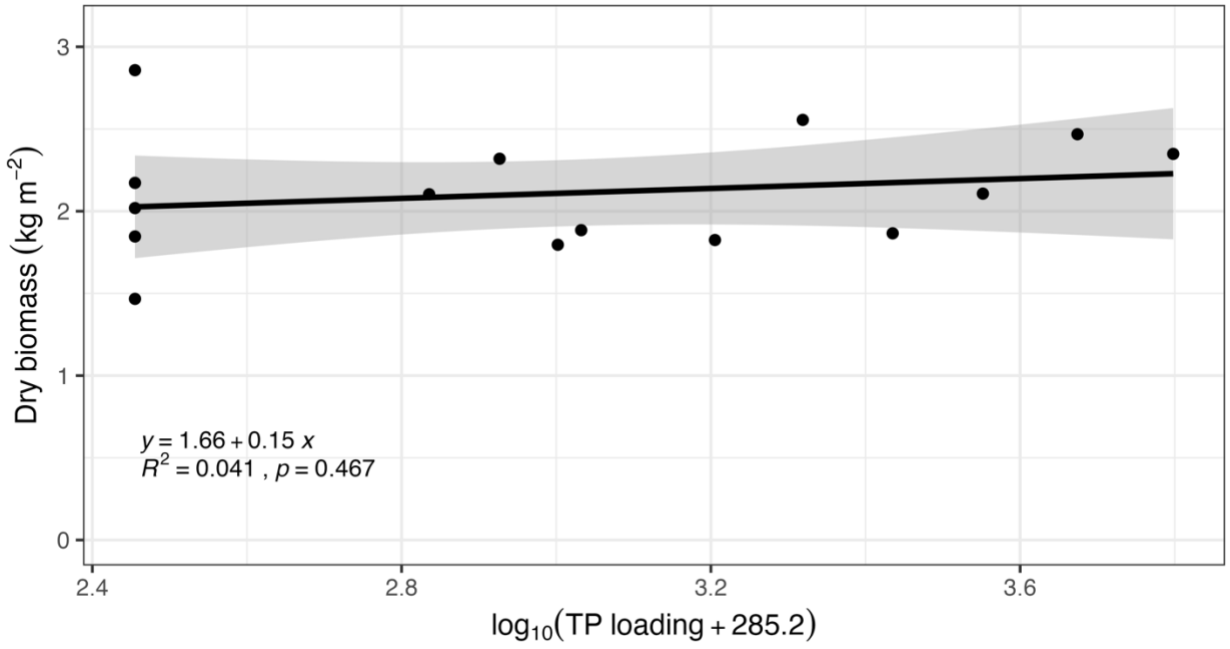

Figure 68. Wild rice biomass in FP mesocosms at the end of the study period reported on a dry mass basis. A general linear model (solid line) was fit to measured data (points) with a 95% confidence interval (shaded region). Predictor variables were calculated by adding a constant (285.2) to the total phosphorus (TP) loading from aquaculture wastewater additions.

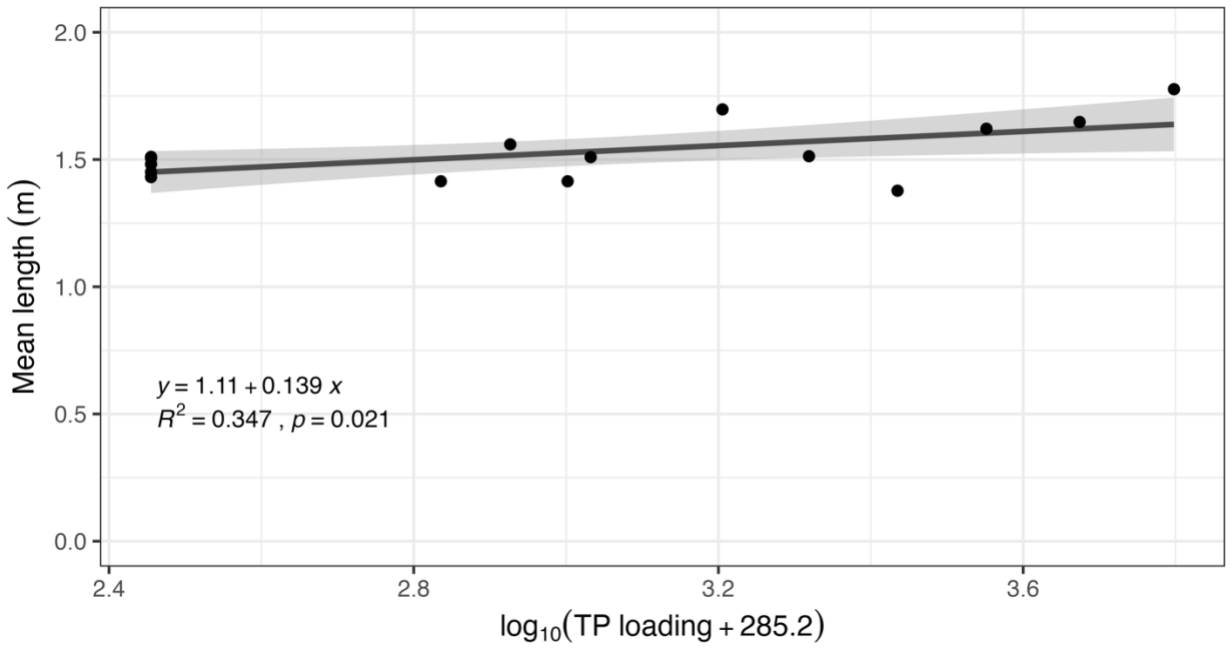

Figure 69. Mean length of wild rice plants in FP mesocosms at the end of the study period. A general linear model (solid line) was fit to measured data (points) with a 95% confidence interval (shaded region). Predictor variables were calculated by adding a constant (285.2) to the total phosphorus (TP) loading from aquaculture wastewater additions.

Positive linear relationships were observed between the TP content of wild rice roots and nutrient loading on day 77 ($p = 0.012$; Figure 70), however no significant relationships were observed for seeds on day 77, in shoots on day 49 or 77, or in roots on day 49. The results from all fitted models for different biomass tissue endpoints are compiled in the Appendix (Table A - 12). A summary of statistically significant relationships for FP plant tissues is presented in Table 23. As discussed above (Section 3.3.2.8), metals can accumulate in wild rice tissues and have the potential to pose concerns for human health (Bennett et al., 2000). In a survey of wild rice grain in Wisconsin, Bennett et al. (2000) found baseline concentrations of Cu, Zn, and Mg in wild rice seeds and identified elevations of As and Pb as potentially problematic for human health. However, the impact of ambient nutrient concentrations were not considered by Bennett et al. (2000). The addition of phosphate fertilizers can substantially impact the uptake of heavy metals

from soil (Gupta et al., 2014). A detailed discussion of the mechanism for Cu and Zn in response to fertilizer additions is found in Gupta et al. (2014). The result of increased concentration and overall yield results in greater quantities of metals in plant tissues. While metals like Cu and Zn are essential nutrients for plant growth, elevated levels can result in toxic effects for the plant (Hall, 2002). Although As and Pb were not assessed in plant tissues in the present study, the mobility of As increases as the oxidation state is reduced, as pH is increased, or when phosphate fertilizers are applied (Gupta et al., 2014; Kabata-Pendias, 2000). While Pb forms stable complexes with organic matter, it can be mobilized in response to P fertilizer additions alongside other metals such as As and Sb (Davenport & Peryea, 1991; Gupta et al., 2014). Heavy metals have proven to be a threat to aquaculture sustainability (Emenike et al., 2022) and continued monitoring should be implemented among aquaculture systems and food products produced as a result of agronomy systems paired with fish production.

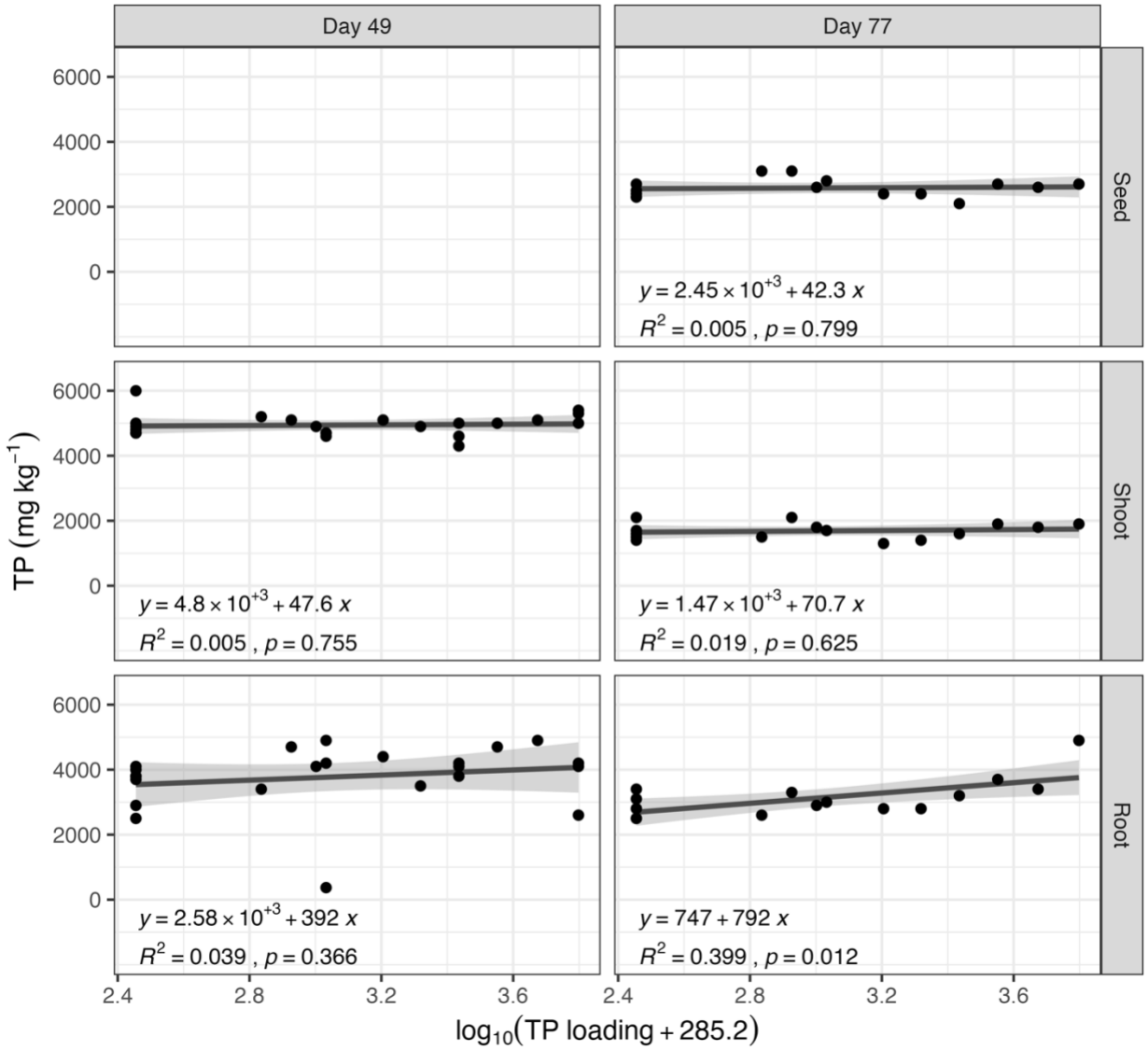

Figure 70. Total phosphorus (TP) content of different portions of wild rice biomass in FP mesocosms study days 49 and 77. Nutrient content is reported on a dry mass basis. General linear models (solid lines) were fit to measured data (points) with 95% confidence intervals (shaded regions). Predictor variables were calculated by adding a constant (285.2) to the TP loading from aquaculture wastewater additions. Note that wild rice seeds were not evaluated for TP content on study day 49.

Table 23. Summary of results for different endpoints assessed in RL biomass tissues on day 49 and 77. Endpoints were assessed using general linear models and indicated in the table if a statistically significant result was detected. The directionality of the relationship is indicated in parentheses as either positive (+) or negative (-).

Biomass type	Endpoint	
	Day 49	Day 77
Wild rice seed	*NE*	Cu (+), Zn (+)
Wild rice shoot	Ca (+)	Length (+)
Wild rice root	*NSD*	TP (+), TN (+), TS (+), Mn (-)

NE = not evaluated, *NSD* = no statistical differences

3.3.10 Phosphorus Mass Balance

In Section 3.3.3.2, P species were characterized and presented as concentrations in Figure 58. An alternative representation of P species for the quantity (mass) of P in mesocosms is presented in Figure 71, and the two methods of presentation generated very similar trends. No systematic increases in P quantity were observed in mesocosms water, and therefore the P inputs from other sources (e.g. atmospheric deposition) can be assumed to be negligible and/or the P inputs were rapidly taken up and assimilated into other matrices like plant, soil, or algae.

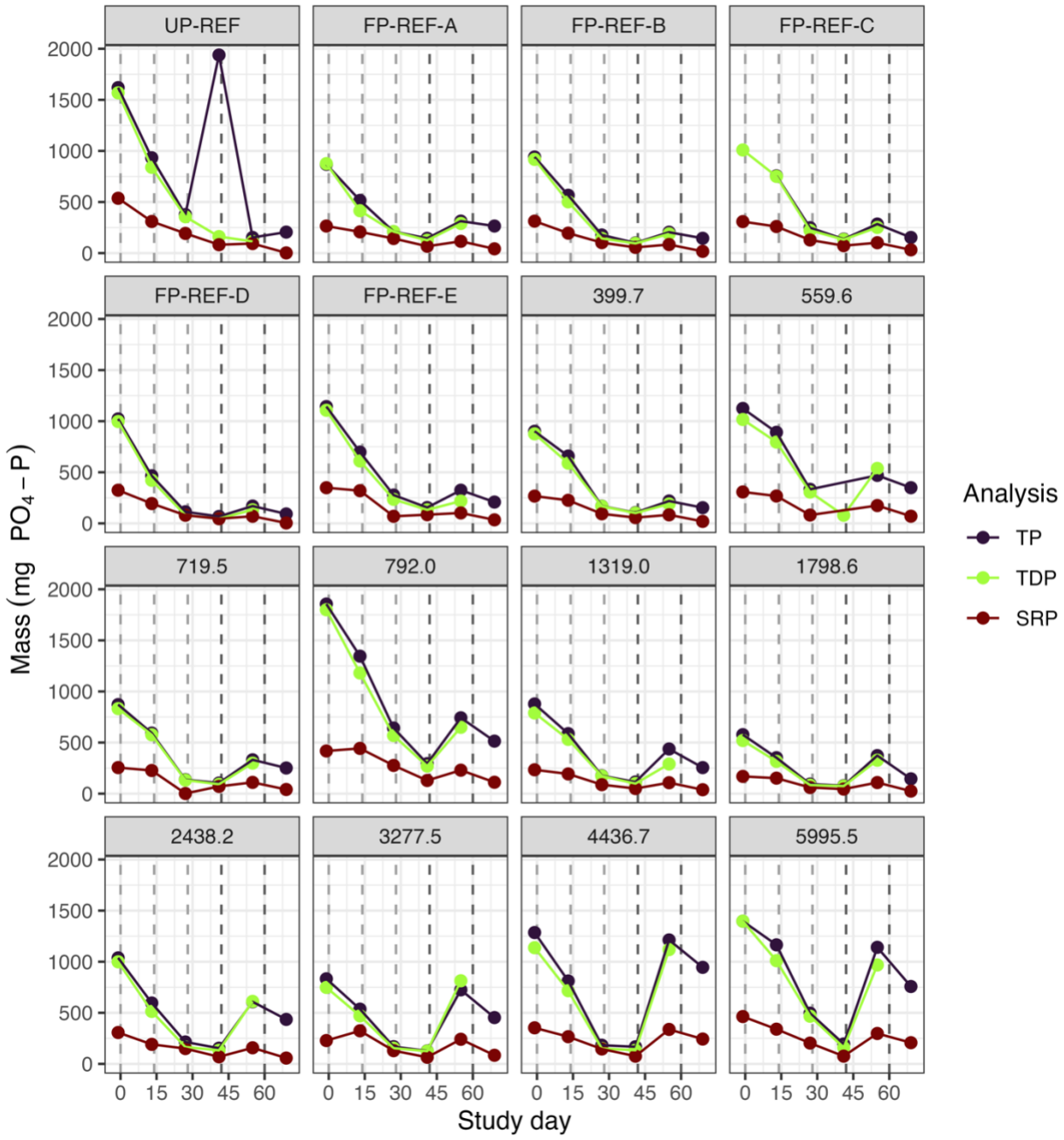

Figure 71. Quantities of total (TP), total dissolved (TDP), and soluble reactive (SRP) phosphorus in FP mesocosm water. Each graphical panel represents a mesocosm with the TP loading from aquaculture wastewater (AWW) additions indicated in units of mg m^{-2}. Vertical dashed lines indicate AWW addition events. The final two AWW addition events (dark dashed lines) were made with a different AWW source and twice the nominal volume of the first three addition events (light dashed lines).

The total quantities and relative proportions of P in each matrix during initial and final timepoints are presented in Figure 72 and Figure 73, respectively. At both timepoints, P from soil was the major contributor of P in FP systems. No treatment-based trends were evident for AG or BG wild rice. The total difference in P quantity between initial and final timepoints for each mesocosms is presented in Figure 74 and demonstrates the large discrepancies that existed between P reductions and P increases. Among planted FPs, wild rice biomass often contributed >10 g of P. However, the decreases in P among soil and water were often much less than 10 g. This issue is believed to results from issues tracking P in FP systems, or more broadly, treatment systems with soil. When evaluating the difference between expected P increase (i.e. from AWW additions) and the overall change in P quantity (calculated as the sum of the differences of individual matrices) between initial and final timepoints (Figure 75), this discrepancy becomes evident, especially among the reference treatments which received no AWW and had P increases >5 g. The FP systems contained high density of wild rice plants and therefore had substantial masses of wild rice roots. The volume of belowground biomass could result in greater soil volume estimates being recorded at the final timepoint than the initial timepoint (when no wild rice was present). However, similar quantities of plants were observed in all planted FPs and therefore this effect would be systematic across the nutrient loading gradient.

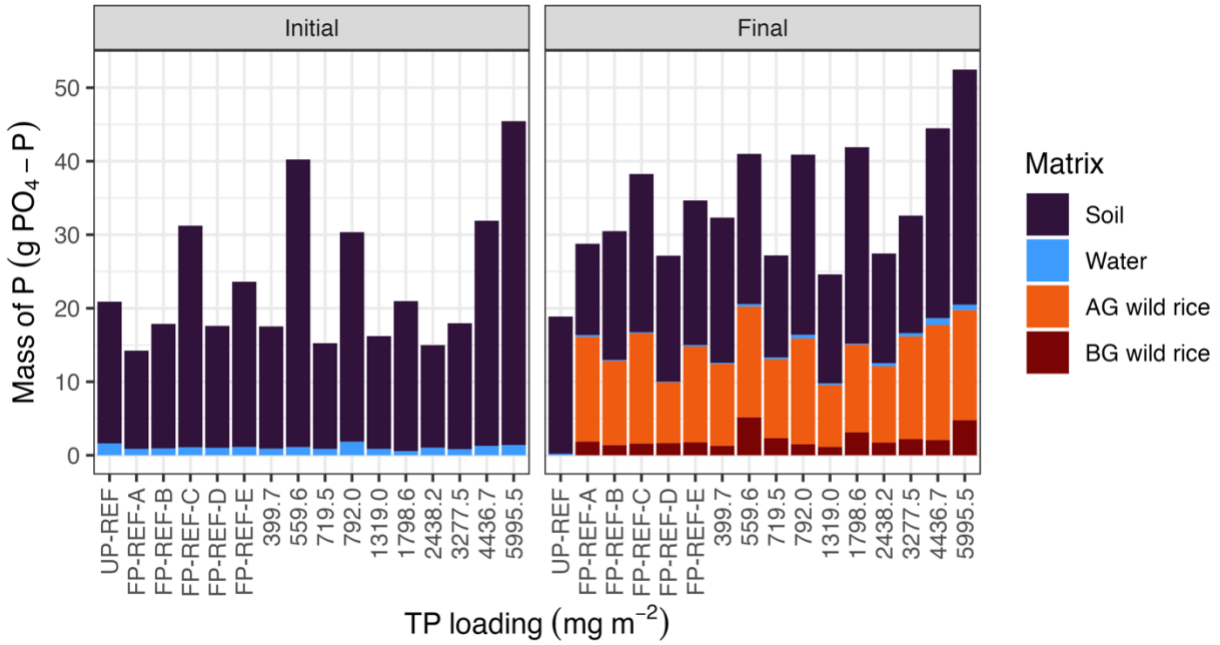

Figure 72. Total quantities of phosphorus (P) in different matrices during initial and final timepoints in FP mesocosms. Wild rice plants are presented as either aboveground (AG; seeds and shoots) or belowground (BG; roots) plant tissues. The total P (TP) nutrient loadings from aquaculture wastewater are indicated with numerical values or the appropriate reference label.

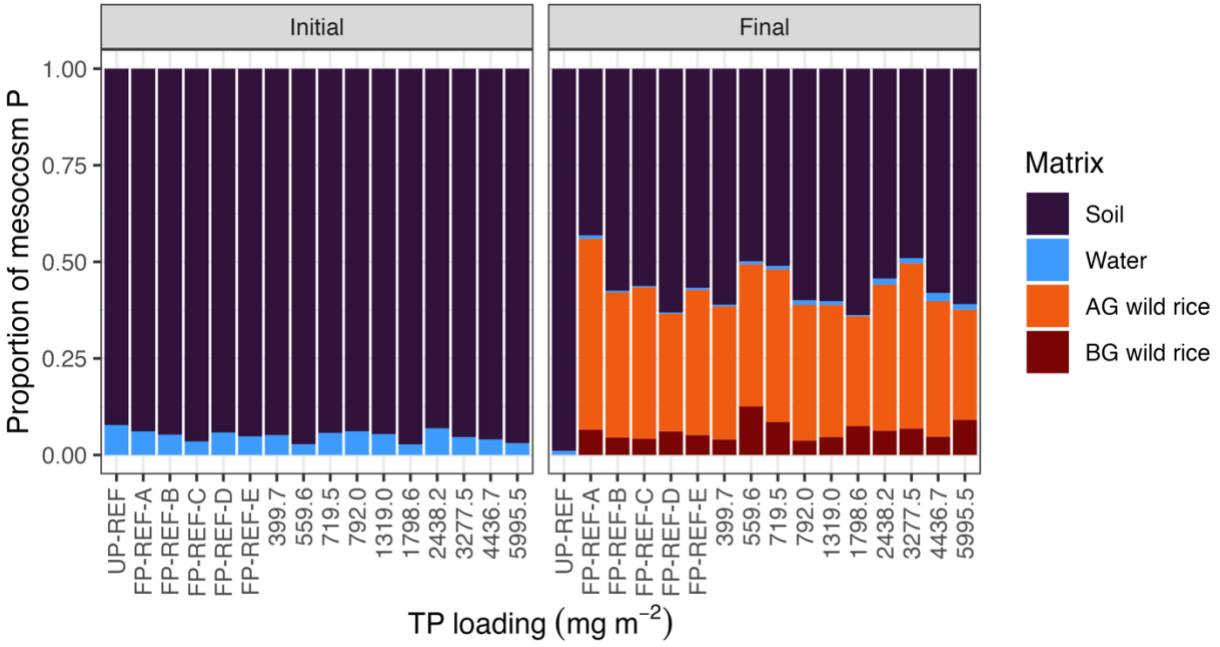

Figure 73. Relative proportions of phosphorus (P) in different matrices between initial and final timepoints in FP mesocosms. Wild rice plants are presented as either aboveground (AG; seeds and shoots) or belowground (BG; roots) plant tissues. The total P (TP) nutrient loadings from aquaculture wastewater are indicated with numerical values or the appropriate reference label.

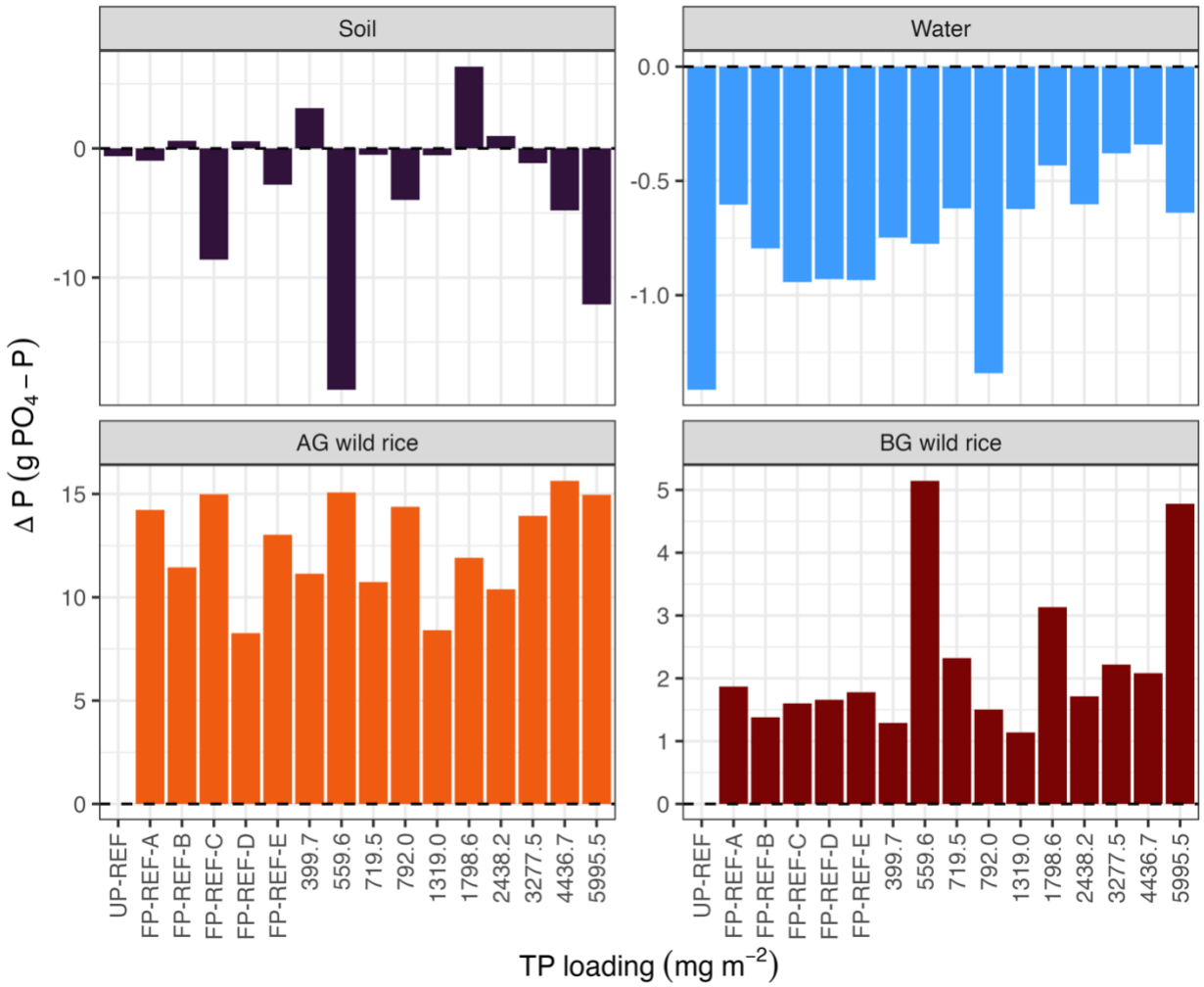

Figure 74. Change in quantity of phosphorus (ΔP) in different matrices between initial and final timepoints in FP mesocosms. Positive values represent increases of P with time while negative values represent decreases of P with time. Wild rice plants are presented as either aboveground (AG; seeds and shoots) or belowground (BG; roots) plant tissues. The total P (TP) nutrient loadings from aquaculture wastewater are indicated with numerical values or the appropriate reference label.

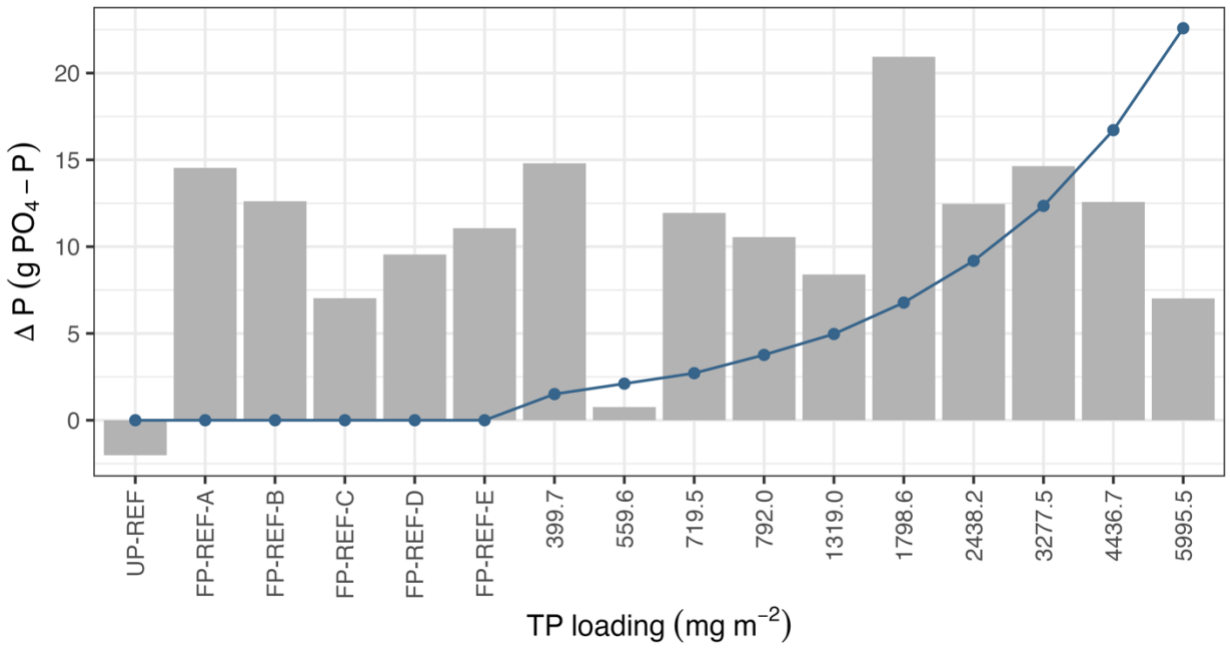

Figure 75. Comparison between the change in total quantity of phosphorus (ΔP) in FP mesocosms between initial and final timepoints (grey bars) and the total quantity of P added through aquaculture wastewater (AWW) additions (blue points). Positive values represent an increase of P with time while negative values represent a decrease of P with time. The total P (TP) nutrient loadings from AWW are indicated with numerical values or the appropriate reference label.

Using the P differences achieved in Figure 74 and assuming initial (day 0) biomass in mesocosms was negligible, P removal rates in plants and algae can be estimated over the 90-day period between the start of the study and decommissioning of mesocosms. The greatest wild rice uptake was observed in the 559.6 and 5995.5 mg m^{-2} treatments and was mainly driven by greater BG biomass relative to other mesocosms. However, P uptake by wild rice was similar among all planted FP mesocosms. The mean rate of P uptake among all planted FP mesocosms was 35.951 and 6.476 mg m^{-2} d^{-1} for AG and BG wild rice tissues, respectively. Wild rice represents a major nutrient sink among FP systems and biomass harvesting can effectively remove substantial quantities of nutrients.

4.0 Conclusion

This chapter evaluated the performance of FP systems fertilized with AWW. The phosphorus removal capabilities of FP systems were evident within the first four weeks of the study when high background P concentrations in the water column were eliminated, achieving ~70% TP reductions over 27 days. To maximize nutrient removal, greater nutrient loadings should be applied during this period of rapid plant growth. Water quality responses to AWW additions were observed for phosphorus endpoints, but not to the same extent among nitrogen endpoints. Following high-nutrient AWW applications during the second half of the study, TP concentrations in FP water increased proportionally to loading conditions. In the following two weeks, TP levels decreased, but concentrations generally exceeded 0.25 mg L^{-1}. The application of TP loadings of 3277.5 mg m^{-2} or greater had adverse effects on water quality, including increases in biofilm and phytoplankton growth toward the end of the study. Excess nutrients in FP systems can promote the proliferation of algae, which can impair the long-term performance and functionality of FP systems. Significant wild rice production was achieved in all FP systems, despite water quality alterations. Wild rice was a primary nutrient sink and contributed to approximately 10 g of P uptake in each planted mesocosm. Management strategies should coordinate the release of FP effluents with periods of low P concentration. Detailed temporal analysis of nutrient content in FP soils and biomass are beneficial to understanding nutrient dynamics in FP systems and should be incorporated in future studies. Long-term evaluation of FP performance will provide additional insights into nutrient management practices, including the effectiveness of different fertilization schedules, the resilience of FP systems to water quality deteriorations, the optimization of crop production, and the potential for scaling wild rice production to a commercial scale.

CHAPTER 5: GENERAL CONCLUSIONS

1.0 Summary and Overview

Aquaculture has been widely adopted as a sustainable alternative for the production of aquatic animal products because of its ability to reduce environmental impacts while addressing global food security (FAO, 2024). In particular, land-based aquaculture systems have undergone substantial growth in the past 50 years (FAO, 2024; Garlock et al., 2020). However, the discharge of wastewater from these systems contains high quantities of nutrients, creating a risk of eutrophication in receiving environments (Ahmad et al., 2022). Meanwhile, wetland plants such as cattail and wild rice provide improvements in water quality because of their high nutrient demand (Ahmed et al., 2021; Drewes & Silbernagel, 2012; Dubbe et al., 1988). The implementation of wetland plants in constructed wetland (CW) treatment systems treating aquaculture wastewater (AWW) was assessed here, with consideration of the potential for AWW to be utilized as a fertilizer in wild rice production. Model CWs were constructed in mesocosms and subjected to AWW loadings. Nutrient content in plants, soil, and water was considered alongside biomass production. In Chapter 2, the performance of cattail CWs treating AWW was assessed. Particular emphasis was placed on water quality responses to AWW additions during end-of-season usage. In Chapter 3, the performance of two different wild rice CWs treating AWW was assessed. These two systems, established wetlands (EW) and new stands (NS), utilized a natural variety of wild rice and were designed to emulate natural wetlands and managed stands of wild rice, respectively. In Chapter 4, the performance of a commercial flooded paddy (FP) of wild rice treating AWW was assessed.

2.0 Chapter 2 Summary

The objective of Chapter 2 was to evaluate the performance of cattail CWs treating AWW. Mesocosms were constructed with soil, water, and cattail plants. A gradient of weekly applications of AWW was applied to mesocosms for a total of five weeks. The resulting TN and TP loadings ranged from 13.7–209.2 mg m^{-2} and 3.01–45.97 mg m^{-2} over 28 days, respectively. Cattail growth was monitored throughout the study and cattail shoots were collected for nutrient content during the middle and end of the study period. Water quality in mesocosms was monitored on a weekly basis for N and P species. No relationships were observed between nutrient loadings and cattail growth metrics (i.e. shoot density, height, and biomass) or the TP content of cattail shoots. Additions of AWW to CW systems began around the time that peak cattail biomass production had begun to decline. Therefore, the observed elimination of nutrients from CW water is indicative of the potential for cattail CW usage to extend into the fall months. Elevations of TP in CW water persisted among high nutrient loading treatments (i.e. 28.67 and 45.97 mg m^{-2}) for 3–4 weeks, but were reduced by >95% after 33 days of treatment to concentrations <0.05 mg L^{-1}. This study demonstrated the ability for cattail CWs to remove nutrients during AWW treatment and provided new information regarding the operational timeline of cattail CW systems. This work served as a pilot study and provided information on the design of the wild rice studies presented in Chapters 3 and 4.

3.0 Chapter 3 Summary

The objective of Chapter 3 was to evaluate the performance of two types of wild rice CWs treating AWW. This chapter focused on the responses of water quality, soil, and biomass to nutrient loadings. Two types of CW mesocosms were constructed; EW systems emulated wild

rice wetlands and NS systems emulated newly established managed stands of wild rice. A gradient of AWW was added to mesocosms on a biweekly basis, for a period of 69 days. The resulting TKN and TP loadings among EW systems ranged from 1383.5–7381.8 mg m^{-2} and 165.4–997.5 mg m^{-2}, respectively. The resulting TKN and TP loadings among NS systems ranged from 492.1–7381.8 mg m^{-2} and 66.5–997.5 mg m^{-2}, respectively. Biweekly water quality and biofilm samples were collected throughout the study period, soil samples were collected at the beginning and end of the study, and all biomass was collected from the mesocosms at the end of the study. Among the EW systems, water column TP concentrations exceeded 0.25 mg L^{-1} under TP loading conditions of 321.5 mg m^{-2} or higher. However, at 997.5 mg m^{-2}, TP concentrations in the water column were generally below 0.2 mg L^{-1}, with nutrient additions instead driving increases in algal growth. Among the NS systems, elevated TP concentrations in CW water were accompanied by an increase of chl *a* in the water column. In both CW systems, nutrient sinks such as hornwort and algal mats benefited due to the low density of wild rice plants. While the growth of hornwort and algal mats contributes to P removal from CW water, it also represents a missed opportunity, as these nutrients could have supported wild rice production if greater seeding rates were used in EW and NS systems. Prioritizing wild rice production is crucial to realize the circular economy between wild rice cultivation and fish farming proposed in Chapter 1.

4.0 Chapter 4 Summary

The objective of Chapter 4 was to evaluate the performance of wild rice flooded paddies fertilized with AWW. This study was conducted concurrently with the Chapter 3 studies, sharing similar experimental designs, methodologies, and endpoints. Similar to Chapter 3, this chapter

focused on the responses of water quality, soil, and biomass to nutrient loadings. However, the FP mesocosms were constructed with greater plant densities and using a commercial variety of wild rice, emulating commercial wild rice paddies. Additionally, these systems received greater nutrient loadings than the EW and NS systems presented in Chapter 3. A gradient of AWW was added to mesocosms on a biweekly basis for a period of 60 days. The resulting TKN and TP loadings among FP systems ranged from 867.8–13016.7 mg m^{-2} and 399.7–5995.5 mg m^{-2}, respectively. Biweekly water quality and biofilm samples were collected throughout the study period, while soil samples were taken at the beginning and end. Wild rice tissue samples were collected in the middle and at the end of the study. The FP systems demonstrated excellent potential for P removal, achieving ~70% TP reduction over the first 27 days of the study. Responses of TP in FP water was directly related to treatment, with increases in TP and TDP proportional to nutrient loading conditions. Adverse effects on water quality were observed at TP loadings of 3277.5 mg m^{-2} or greater. Water quality responses included elevated P species in the water column as well as increased biofilm and phytoplankton growth. Excellent wild rice production was achieved in FP mesocosms and wild rice represented a significant nutrient sink, capable of TP uptake rates of ~42.4 mg m^{-2} d^{-1}. The temporal assessment of water quality presented in this chapter provides insights into the operational timeline of FP systems and how effluent release from these systems can be coordinated with periods of low nutrient concentration. While AWW can be utilized as an effective fertilizer for wild rice production, nutrient additions should be managed to avoid long-term degradation of water quality, which can in turn negatively impact production and increase environmental concerns associated with the drainage of flooded paddies.

5.0 Comparison of Treatment Systems

This section will focus on broad comparisons between cattail CWs and wild rice EW, NS, and FP systems. It is important to note that substantial differences (e.g. soil source, water source, plant species) existed across the different treatment systems analyzed. The similarities among Chapter 3 studies allowed for more detailed comparisons between EW and NS (Section 3.3.3). The comparisons presented here are intended to be broad and highlight overarching ideas rather than specific outcomes.

Increases in TDN following AWW additions were not observed among cattail CWs and FP systems in the same manner as those observed among EW and NS systems. Consistent TDN concentrations were observed in UP-REF among the cattail CWs and FP systems, suggesting that sorption of TDN was not actively occurring to the same extent as it was among the EW systems. Lower DO was observed in the UP-REF among FP systems than in EW systems (Figure A - 44, Figure A - 14), which may have promoted the necessary conditions for N release to occur from CW soil (Müller et al., 2016). However, further investigations into soil properties are required to further understanding of nutrient cycling in these types of treatment systems.

Declines in DO were observed throughout the study period among EW and FP systems, but not among NS systems (Figure A - 14, Figure A - 29, Figure A - 44). Oxygen depletion likely resulted from the degradation of organic matter (e.g. plant litter and algae), and long-term low DO levels in CWs can negatively impact performance (H. Liu et al., 2016). The lack of organic matter in NS systems appears to have resulted in this discrepancy in DO among the different

wild rice treatment systems. Declines in DO, which appear to be related to the presence of decaying biomass, can support the conditions necessary for denitrification (Snow et al., 2012).

Among FP systems, a gradual decrease in NO_3–N from approximately 1.25 to 0.25 mg L^{-1} occurred throughout the first 41 days of the study, after which concentrations remained consistent (Figure A - 38). Interestingly, this decline in NO_3–N was more gradual among FP mesocosms than EW and NS mesocosms. The growth of algal mats and hornwort in EW and NS systems may have contributed to a sharper decline in NO_3–N (neither algal mats nor hornwort were present in FP systems). Declines of DO in FP mesocosm water may have supported denitrification, however the period of maximum biofilm growth occurred immediately following NO_3–N depletion, which suggests that biofilm was a nutrient sink and the growth of this algae was a major contributor to NO_3–N elimination from FP water (see Section 3.3.4).

Meanwhile, the presence of wild rice plants did not appear to have a substantial effect on NO_3–N elimination for EW, NS, or FP systems. Similar decreases in NO_3–N were observed in UP-REF as the corresponding planted references. This finding is particularly interesting for the FP systems as the high density of wild rice plants relative to EW and NS systems would suggest additional contributions to N elimination would occur through direct uptake, or indirectly through the support of microbial communities capable of N cycling. In fact, FP systems had approximately 10 and 30 times the final wild rice biomass of EW and NS systems, respectively. Interestingly, while water microbial samples had similar tATP concentrations for all wild rice treatment systems, root tATP concentrations were lower among the FP mesocosms than the EW and NS mesocosms. While other site variables, including the variety of wild rice, may be

influential, Ibekwe et al. (2007) demonstrated how reduced plant cover in CWs can promote the growth of diverse microbial communities. Microbial communities associated with plant roots and rhizomes are crucial drivers of remediation success (Cheng et al., 2021; Kamaludeen & Ramasamy, 2008; Stanley et al., 2022). In CWs and in AWW treatment systems, microbial community dynamics and their interactions with plants must be considered when evaluating both the overall effectiveness and mechanisms of remediation.

Concentrations of TP in wild rice biomass were slightly greater among FP systems than EW and NS systems at the end of their respective study periods. While this difference could be attributed to differences in physiology associated with different wild rice varieties, sampling an additional timepoint among FP systems revealed notably greater TP content in wild rice tissues on day 49 than on day 77 (Figure 70). This finding suggests that TP concentrations in wild rice tissues reached a peak sometime before the end of the study period. Understanding the seasonal variability of TP content in wild rice biomass in each type of CW can improve nutrient management in these treatment systems. This information could be used to better coordinate nutrient loadings, achieving the desired fertilization for optimum plant growth during periods of high uptake while reducing excess nutrient inputs during periods of low uptake. The timing of harvest and subsequent removal of plant biomass could be coordinated with elevated nutrient content in plant tissues, achieving a greater overall reduction of nutrients in the CW system.

6.0 Conclusion

While rice-fish agronomy concepts have been utilized for decades, this thesis presents a novel approach by integrating cattail and wild rice production with land-based aquaculture. The results

presented here indicate that nutrient treatment, particularly phosphorus removal, can be effectively achieved in cattail constructed wetlands, wild rice wetlands, wild rice stands, and wild rice flooded paddies. However, the management of nutrient loadings is crucial to avoid water quality deteriorations that can negatively impact the performance of treatment systems. High-nutrient effluents from aquaculture operations can also serve as an organic, ammonia-based fertilizers for wild rice production, enhancing agricultural productivity while reducing environmental impacts associated with conventional fertilizer usage. Furthermore, treatment systems demonstrated the potential to support algal growth, which can be harvested for use as fish feed, thereby completing a circular economy involving wild rice production and fish farming.

REFERENCES

Abbasi, H. N., Xie, J., Hussain, S. I., & Lu, X. (2019). Nutrient removal in hybrid constructed wetlands: Spatial-seasonal variation and the effect of vegetation. *Water Science and Technology*, *79*(10), 1985-1994. https://doi.org/10.2166/wst.2019.196

Ahmad, A. L., Chin, J. Y., Harun, M. H. Z. M., & Low, S. C. (2022). Environmental impacts and imperative technologies towards sustainable treatment of aquaculture wastewater: A review. *Journal of Water Process Engineering*, *46*, 102553. https://doi.org/10.1016/j.jwpe.2021.102553

Ahmed, N., Thompson, S., Hardy, B., & Turchini, G. M. (2021). An ecosystem approach to wild rice-fish cultivation. *Reviews in Fisheries Science & Aquaculture*, *29*(4), 549-565. https://doi.org/10.1080/23308249.2020.1833833

Ahmed, N., & Turchini, G. M. (2021). Recirculating aquaculture systems (RAS): Environmental solution and climate change adaptation. *Journal of Cleaner Production*, *297*, 126604. https://doi.org/10.1016/j.jclepro.2021.126604

Aiken, S., Lee, P., Punter, D., & Stewart, J. (1988). *Wild rice in Canada*. New Canada Publications.

Allison, E. H. (2011). *Aquaculture, fisheries, poverty and food security* [Working Paper 2011-65]. The WorldFish Center. https://hdl.handle.net/20.500.12348/1163

Ansari, F. A., Guldhe, A., Gupta, S. K., Rawat, I., & Bux, F. (2021). Improving the feasibility of aquaculture feed by using microalgae. *Environmental Science and Pollution Research*, *28*(32), 43234-43257. https://doi.org/10.1007/s11356-021-14989-x

Ansari, F. A., Singh, P., Guldhe, A., & Bux, F. (2017). Microalgal cultivation using aquaculture wastewater: Integrated biomass generation and nutrient remediation. *Algal Research*, *21*, 169-177. https://doi.org/10.1016/j.algal.2016.11.015

Archibold, O. (2003). Wild rice. In B. Caballero, L. Trugo, & P. M. Finglas (Eds.), *Encyclopedia of food sciences and nutrition* (pp. 6183-6189). Elsevier Academic Press. https://doi.org/10.1016/B0-12-227055-X/01294-3

Archibold, O., Sutherland, J., & Good, A. (1989). Annual variation in wild rice (*Zizania palustris* L.) growth and potential yield in Saskatchewan. *Canadian Journal of Plant Science*, *69*(3), 653-665. https://doi.org/10.4141/cjps89-081

Archibold, O. W. (1995). *Wild rice in Saskatchewan: Agriculture development in harmony with nature - a reference manual*. Saskatchewan Education, Training and Employment.

Atkins, T., Lee, P., & Stewart, J. (1992). Growth of wild rice (*Z. palustris* L.) in fertilized flocculent sediments. *Journal of Environmental Management*, *35*(3), 217-228. https://doi.org/10.1016/S0301-4797(05)80121-5

Avnimelech, Y., Verdegem, M., Kurup, M., & Keshavanath, P. (2008). Sustainable land-based aquaculture: Rational utilization of water, land and feed resources. *Mediterranean Aquaculture Journal*, *1*(1), 45-54.

Badhe, N., Saha, S., Biswas, R., & Nandy, T. (2014). Role of algal biofilm in improving the performance of free surface, up-flow constructed wetland. *Bioresource Technology*, *169*, 596-604. https://doi.org/10.1016/j.biortech.2014.07.050

Baker, M. T., Lu, P., Parrella, J. A., & Leggette, H. R. (2022). Consumer acceptance toward functional foods: A scoping review. *International Journal of Environmental Research and Public Health*, *19*(3), 1217. https://doi.org/10.3390/ijerph19031217

Barbier, E. B. (2011). Wetlands as natural assets. *Hydrological Sciences Journal*, *56*(8), 1360-1373. https://doi.org/10.1080/02626667.2011.629787

Bartley, D. M. (2022). *World Aquaculture 2020 - A brief overview* [FAO Fisheries and Aquaculture Circular No. 1233]. Food and Agriculture Organization of the United Nations. https://doi.org/10.4060/cb7669en

Bastviken, S. K., Eriksson, P. G., Martins, I., Neto, J. M., Leonardson, L., & Tonderski, K. (2003). Potential nitrification and denitrification on different surfaces in a constructed treatment wetland. *Journal of Environmental Quality*, *32*(6), 2414-2420. https://doi.org/10.2134/jeq2003.2414

Bean, R. C. (1950). Review: The eighth edition of Gray's manual of botany. *Rhodora*, *52*(621), 226-228.

Béné, C. (2006). *Small-scale fisheries: assessing their contribution to rural livelihoods in developing countries* [FAO Fisheries Circular No. 1008]. Food and Agriculture Organization of the United Nations.

Béné, C., Barange, M., Subasinghe, R., Pinstrup-Andersen, P., Merino, G., Hemre, G.-I., & Williams, M. (2015). Feeding 9 billion by 2050 – Putting fish back on the menu. *Food Security*, *7*(2), 261-274. https://doi.org/10.1007/s12571-015-0427-z

Bennett, J. P., Chiriboga, E., Coleman, J., & Waller, D. M. (2000). Heavy metals in wild rice from northern Wisconsin. *Science of the Total Environment*, *246*(2-3), 261-269. https://doi.org/10.1016/S0048-9697(99)00464-7

Bennich, T. (2015). *The economic sustainability of land-based aquaculture systems: An integrated analysis* [Master's Thesis, The University of Bergen]. Bergen Open Research Archive. https://hdl.handle.net/1956/11616

Benoy, G. A., Jenkinson, R. W., Robertson, D. M., & Saad, D. A. (2016). Nutrient delivery to Lake Winnipeg from the Red-Assiniboine River Basin – A binational application of the SPARROW model. *Canadian Water Resources Journal/Revue Canadienne des Ressources Hydriques*, *41*(3), 429-447. https://doi.org/10.1080/07011784.2016.1178601

Berman, T., & Bronk, D. A. (2003). Dissolved organic nitrogen: a dynamic participant in aquatic ecosystems. *Aquatic Microbial Ecology*, *31*, 279-305. https://doi.org/10.3354/ame031279

Bhari, B. (2018). Sustainable aquaculture: Socio-economic and environmental assessment. In F. Hai, C. Visvanathan, & R. Boopathy (Eds.), *Sustainable aquaculture* (pp. 63-93). Springer, Cham. https://doi.org/10.1007/978-3-319-73257-2_2

Blandford, N. C., McCorquodale-Bauer, K., Grosshans, R., Hardy, B., Cicek, N., & Palace, V. (2024). Removal of nutrients from aquaculture wastewater using cattail (*Typha* spp.) constructed wetlands. *Journal of Environmental Quality*, *53*(5), 767-775. https://doi.org/10.1002/jeq2.20608

Boaventura, R., Pedro, A. M., Coimbra, J., & Lencastre, E. (1997). Trout farm effluents: Characterization and impact on the receiving streams. *Environmental Pollution*, *95*(3), 379-387. https://doi.org/10.1016/S0269-7491(96)00117-0

Boström, B. (1984). Potential mobility of phosphorus in different types of lake sediment. *Internationale Revue der gesamten Hydrobiologie und Hydrographie*, *69*(4), 457-474. https://doi.org/10.1002/iroh.19840690402

Boyd, C. E., & Schmittou, H. (1999). Achievement of sustainable aquaculture through environmental management. *Aquaculture Economics & Management*, *3*(1), 59-69. https://doi.org/10.1080/13657309909380233

Bricker, S. B., Clement, C., Pirhalla, D., Orlando, S., & Farrow, D. (1999). *National estuarine eutrophication assessment: Effects of nutrient enrichment in the nation's estuaries*. NOAA National Ocean Service Projects Office and the National Centers for Coastal Ocean Science.

Brix, H. (2003). Plants used in constructed wetlands and their functions. In: V. Dias, & J. Vymazal (Eds.), *1st International Seminar on the use of Aquatic Macrophytes for Wastewater Treatment in Constructed Wetlands* (pp. 81-109).

Brouwer, I. D., van Liere, M. J., de Brauw, A., Dominguez-Salas, P., Herforth, A., Kennedy, G., Lachat, C., Omosa, E. B., Talsma, E. F., & Vandevijvere, S. (2021). Reverse thinking: taking a healthy diet perspective towards food systems transformations. *Food Security, 13*, 1497-1523. https://doi.org/10.1007/s12571-021-01204-5

Burdige, D. J., & Zheng, S. (1998). The biogeochemical cycling of dissolved organic nitrogen in estuarine sediments. *Limnology and Oceanography*, *43*(8), 1796-1813. https://doi.org/10.4319/lo.1998.43.8.1796

Bureau, D. P. (2004). Factors affecting metabolic waste outputs in fish. In: L. E. Cruz Suárez, D. Ricque Marie, M. G. Nieto López, D. Villarreal, U. Scholz, & M. González (Eds.), *Avances en Nutrición Acuicola VII*.

Camargo, J. A., Alonso, A., & Salamanca, A. (2005). Nitrate toxicity to aquatic animals: A review with new data for freshwater invertebrates. *Chemosphere*, *58*(9), 1255-1267. https://doi.org/10.1016/j.chemosphere.2004.10.044

Cape, J., Cornell, S., Jickells, T., & Nemitz, E. (2011). Organic nitrogen in the atmosphere—Where does it come from? A review of sources and methods. *Atmospheric Research*, *102*(1-2), 30-48. https://doi.org/10.1016/j.atmosres.2011.07.009

Carpenter, S. R., Caraco, N. F., Correll, D. L., Howarth, R. W., Sharpley, A. N., & Smith, V. H. (1998). Nonpoint pollution of surface waters with phosphorus and nitrogen. *Ecological Applications*, *8*(3), 559-568. https://doi.org/10.1890/1051-0761(1998)008[0559:NPOSWW]2.0.CO;2

Carpenter, S. R., & Lodge, D. M. (1986). Effects of submersed macrophytes on ecosystem processes. *Aquatic Botany*, *26*, 341-370. https://doi.org/10.1016/0304-3770(86)90031-8

Carr, O., & Goulder, R. (1990). Fish-farm effluents in rivers—II. Effects on inorganic nutrients, algae and the macrophyte *Ranunculus penicillatus*. *Water research*, *24*(5), 639-647. https://doi.org/10.1016/0043-1354(90)90197-E

Castine, S. A., Paul, N. A., Magnusson, M., Bird, M. I., & de Nys, R. (2013). Algal bioproducts derived from suspended solids in intensive land-based aquaculture. *Bioresource Technology*, *131*, 113-120. https://doi.org/10.1016/j.biortech.2012.12.094

Catling, P., & Small, E. (2001). Blossoming treasures of biodiversity: 2. North American wild rice (*Zizania* species)—A wild epicurean crop. *Biodiversity*, *2*(3), 24-25. https://doi.org/10.1080/14888386.2001.9712553

Cerozi, B.S., & Fitzsimmons, K. (2017). Phosphorus dynamics modeling and mass balance in an aquaponics system. *Agricultural Systems*, *153*, 94-100. https://doi.org/10.1016/j.agsy.2017.01.020

Chen, F., Leng, Y., Lu, Q., & Zhou, W. (2021). The application of microalgae biomass and bio-products as aquafeed for aquaculture. *Algal Research*, *60*, 102541. https://doi.org/10.1016/j.algal.2021.102541

Chen, L., Feng, Q., Li, C., Wei, Y., Zhao, Y., Feng, Y., Zheng, H., Li, F., & Li, H. (2017). Impacts of aquaculture wastewater irrigation on soil microbial functional diversity and

community structure in arid regions. *Scientific Reports*, *7*(1), 11193. https://doi.org/10.1038/s41598-017-11678-z

Chen, M., Ding, S., Chen, X., Sun, Q., Fan, X., Lin, J., Ren, M., Yang, L., & Zhang, C. (2018). Mechanisms driving phosphorus release during algal blooms based on hourly changes in iron and phosphorus concentrations in sediments. *Water Research*, *133*, 153-164. https://doi.org/10.1016/j.watres.2018.01.040

Cheng, R., Zhu, H., Shutes, B., & Yan, B. (2021). Treatment of microcystin (MC-LR) and nutrients in eutrophic water by constructed wetlands: Performance and microbial community. *Chemosphere*, *263*, 128139. https://doi.org/10.1016/j.chemosphere.2020.128139

Cicek, N., Lambert, S., Venema, H., Snelgrove, K., Bibeau, E., & Grosshans, R. (2006). Nutrient removal and bio-energy production from Netley-Libau Marsh at Lake Winnipeg through annual biomass harvesting. *Biomass and Bioenergy*, *30*(6), 529-536. https://doi.org/10.1016/j.biombioe.2005.12.009

Ciria, M., Solano, M., & Soriano, P. (2005). Role of macrophyte *Typha latifolia* in a constructed wetland for wastewater treatment and assessment of its potential as a biomass fuel. *Biosystems Engineering*, *92*(4), 535-544. https://doi.org/10.1016/j.biosystemseng.2005.08.007

Constable, M., Charlton, M., Jensen, F., McDonald, K., Craig, G., & Taylor, K. W. (2003). An ecological risk assessment of ammonia in the aquatic environment. *Human and Ecological Risk Assessment*, *9*(2), 527-548. https://doi.org/10.1080/713609921

Correll, D. L. (1998). The role of phosphorus in the eutrophication of receiving waters: A review. *Journal of Environmental Quality*, *27*(2), 261-266. https://doi.org/10.2134/jeq1998.00472425002700020004x

Craft, C. B., Vymazal, J., & Richardson, C. J. (1995). Response of Everglades plant communities to nitrogen and phosphorus additions. *Wetlands*, *15*, 258-271. https://doi.org/10.1007/BF03160706

Cripps, S. J., & Bergheim, A. (2000). Solids management and removal for intensive land-based aquaculture production systems. *Aquacultural Engineering*, *22*(1-2), 33-56. https://doi.org/10.1016/S0144-8609(00)00031-5

Cronk, J. K., & Mitsch, W. J. (1994). Periphyton productivity on artificial and natural surfaces in constructed freshwater wetlands under different hydrologic regimes. *Aquatic Botany*, *48*(3-4), 325-341. https://doi.org/10.1016/0304-3770(94)90024-8

Cross, S. F., Flaherty, M., & Byrne, A. (2017). Diversification of aquaculture in North America. In B. Harvey, D. Soto, J. Carolsfeld, M. Beveridge, & D. M. Bartley (Eds.), *Planning for aquaculture diversification: The importance of climate change and other drivers* [FAO Fisheries and Aquaculture Proceedings 47]. Food and Agriculture Organization of the United Nations.

Crouse, C., Davidson, J., May, T., Summerfelt, S., & Good, C. (2021). Production of market-size European strain Atlantic salmon (*Salmo salar*) in land-based freshwater closed containment aquaculture systems. *Aquacultural Engineering*, *92*, 102138. https://doi.org/10.1016/j.aquaeng.2020.102138

Dalsgaard, J., Larsen, B. K., & Pedersen, P. B. (2015). Nitrogen waste from rainbow trout (*Oncorhynchus mykiss*) with particular focus on urea. *Aquacultural Engineering*, *65*, 2-9. https://doi.org/10.1016/j.aquaeng.2014.10.004

Daniel, T., Sharpley, A., & Lemunyon, J. (1998). Agricultural phosphorus and eutrophication: A symposium overview. *Journal of Environmental Quality*, *27*(2), 251-257. https://doi.org/10.2134/jeq1998.00472425002700020002x

Daugherty, W. E. (1986). *Treaty Research Report - Treaty Three (1873)*. Treaties and Historical Research Centre. Indian and Northern Affairs Canada.

Davenport, J., & Peryea, F. J. (1991). Phosphate fertilizers influence leaching of lead and arsenic in a soil contaminated with lead arsenate. *Water, Air, and Soil Pollution*, *57*, 101-110. https://doi.org/10.1007/BF00282873

Davidson, J., May, T., Good, C., Waldrop, T., Kenney, B., Terjesen, B. F., & Summerfelt, S. (2016). Production of market-size North American strain Atlantic salmon *Salmo salar* in a land-based recirculation aquaculture system using freshwater. *Aquacultural Engineering*, *74*, 1-16. https://doi.org/10.1016/j.aquaeng.2016.04.007

Day, W., & Lee, P. (1990). Mineral deficiencies of wild rice grown in flocculent sediments. *Journal of Aquatic Plant Management*, *28*, 84-88.

Day, W. R. (1988). *Growth of wild rice, Zizania aquatica L., in flocculent sediments* [Master's Thesis, Lakehead University]. Lakehead Knowledge Commons. http://knowledgecommons.lakeheadu.ca/handle/2453/1689

DeBusk, W. F. (1999). *Wastewater treatment wetlands: Contaminant removal processes*. University of Florida Institute of Food and Agricultural Sciences Cooperative Extension Service. https://ufdc.ufl.edu/IR00005414/00001/pdf

DeLaune, R., & Smith, C. (1985). Release of nutrients and metals following oxidation of freshwater and saline sediment. *Journal of Environmental Quality*, *14*(2), 164-168. https://doi.org/10.2134/jeq1985.00472425001400020002x

Dickenson, L. (in preparation). *Evaluating the effect of aquaculture wastewater to zooplankton communities in wild rice planted mesocosms* [Unpublished Master's Thesis, University of Manitoba].

Dodds, W. K. (2003). The role of periphyton in phosphorus retention in shallow freshwater aquatic systems. *Journal of Phycology*, *39*(5), 840-849. https://doi.org/10.1046/j.1529-8817.2003.02081.x

Dodds, W. K., & Smith, V. H. (2016). Nitrogen, phosphorus, and eutrophication in streams. *Inland Waters*, *6*(2), 155-164. https://doi.org/10.5268/IW-6.2.909

Drengstig, A., & Bergheim, A. (2013). Commercial land-based farming of European lobster (*Homarus gammarus* L.) in recirculating aquaculture system (RAS) using a single cage approach. *Aquacultural Engineering*, *53*, 14-18. https://doi.org/10.1016/j.aquaeng.2012.11.007

Drewes, A. D., & Silbernagel, J. (2012). Uncovering the spatial dynamics of wild rice lakes, harvesters and management across Great Lakes landscapes for shared regional conservation. *Ecological Modelling*, *229*, 97-107. https://doi.org/10.1016/j.ecolmodel.2011.09.015

Dubbe, D., Garver, E., & Pratt, D. (1988). Production of cattail (*Typha* spp.) biomass in Minnesota, USA. *Biomass*, *17*(2), 79-104. https://doi.org/10.1016/0144-4565(88)90073-X

Durborow, R. M., Crosby, D. M., & Brunson, M. W. (1997). *Ammonia in fish ponds* [Publication No. 463]. Southern Regional Aquaculture Center.

Eddy, F. (2005). Ammonia in estuaries and effects on fish. *Journal of Fish Biology*, *67*(6), 1495-1513. https://doi.org/10.1111/j.1095-8649.2005.00930.x

Eikebrokk, B., & Ulgenes, Y. (1993). Characterization of treated and untreated effluents from landbased fish farms. In H. Keinertsen, L. Dahle, L. Jorgenson, & K. Tvinnereim (Eds.), *Fish Farming Technology* (1 ed., pp. 361-366). CRC Press.

Emenike, E. C., Iwuozor, K. O., & Anidiobi, S. U. (2022). Heavy metal pollution in aquaculture: Sources, impacts and mitigation techniques. *Biological Trace Element Research*, *200*, 4476-4492. https://doi.org/10.1007/s12011-021-03037-x

Emerson, K., Russo, R. C., Lund, R. E., & Thurston, R. V. (1975). Aqueous ammonia equilibrium calculations: effect of pH and temperature. *Journal of the Fisheries Board of Canada*, *32*(12), 2379-2383. https://doi.org/10.1139/f75-274

Enduta, A., Jusoh, A., Ali, N. a., & Wan Nik, W. (2011). Nutrient removal from aquaculture wastewater by vegetable production in aquaponics recirculation system. *Desalination and water treatment*, *32*(1-3), 422-430. https://doi.org/10.5004/dwt.2011.2761

FAO. (2020). *The state of world fisheries and aquaculture 2020: Sustainability in* action. Food and Agriculture Organization of the United Nations. https://doi.org/10.4060/ca9229en

FAO. (2022). *The state of world fisheries and aquaculture 2022: Towards blue transformation*. Food and Agriculture Organization of the United Nations. https://doi.org/10.4060/cc0461en

FAO. (2024). *The state of world fisheries and aquaculture 2024: Blue transformation in action*. Food and Agriculture Organization of the United Nations. https://doi.org/10.4060/cd0683en

Fassett, N. C. (1924). A study of the genus *Zizania*. *Rhodora*, *26*(308), 153-160.

Fassett, N. C. (1927). Notes from the herbarium of the University of Wisconsin–I. *Rhodora*, *29*(347), 227-234. http://www.jstor.org.uml.idm.oclc.org/stable/23298095

Fernandes, T., Eleftheriou, A., Ackefors, H., Eleftheriou, M., Ervik, A., Sanchez-Mata, A., Scanlon, T., White, P., Cochrane, S., Pearson, T., & Read, P. (2001). The scientific principles underlying the monitoring of the environmental impacts of aquaculture. *Journal of Applied Ichthyology*, *17*(4), 145-206. https://doi.org/10.1046/j.1439-0426.2001.00315.x

Fort, D. J., Mathis, M. B., Walker, R., Tuominen, L. K., Hansel, M., Hall, S., Richards, R., Grattan, S., & Anderson, K. (2014). Toxicity of sulfate and chloride to early life stages of wild rice (Zizania palustris). *Environmental Toxicology and Chemistry*, *33*(12), 2802-2809. https://doi.org/10.1002/etc.2744

Fort, D. J., Todhunter, K., Fort, T. D., Mathis, M. B., Walker, R., Hansel, M., Hall, S., Richards, R., & Anderson, K. (2017). Toxicity of sulfide to early life stages of wild rice (*Zizania palustris*). *Environmental Toxicology and Chemistry*, *36*(8), 2217-2226. https://doi.org/10.1002/etc.3759

Gao, X., Wang, Y., Sun, B., & Li, N. (2019). Nitrogen and phosphorus removal comparison between periphyton on artificial substrates and plant-periphyton complex in floating treatment wetlands. *Environmental Science and Pollution Research*, *26*, 21161-21171. https://doi.org/10.1007/s11356-019-05455-w

Garlock, T., Asche, F., Anderson, J., Bjørndal, T., Kumar, G., Lorenzen, K., Ropicki, A., Smith, M. D., & Tveterås, R. (2020). A global blue revolution: Aquaculture growth across regions, species, and countries. *Reviews in Fisheries Science & Aquaculture*, *28*(1), 107-116. https://doi.org/10.1080/23308249.2019.1678111

Gorgoglione, A., & Torretta, V. (2018). Sustainable management and successful application of constructed wetlands: A critical review. *Sustainability*, *10*(11), 3910. https://doi.org/10.3390/su10113910

Graber, A., & Junge, R. (2009). Aquaponic Systems: Nutrient recycling from fish wastewater by vegetable production. *Desalination*, *246*(1-3), 147-156. https://doi.org/10.1016/j.desal.2008.03.048

Grava, J., & Raisanen, K. (1978). Growth and nutrient accumulation and distribution in wild rice[1]. *Agronomy Journal*, *70*(6), 1077-1081. https://doi.org/10.2134/agronj1978.00021962007000060044x

Grey, S., & Patel, R. (2015). Food sovereignty as decolonization: Some contributions from Indigenous movements to food system and development politics. *Agriculture and Human Values*, *32*, 431-444. https://doi.org/10.1007/s10460-014-9548-9

Grosshans, R., & Grieger, L. (2013). *Cattail Biomass to Energy: Commercial-scale harvesting of cattail biomass for biocarbon and solid fuel*. International Institute for Sustainable Development. https://www.iisd.org/publications/report/cattail-biomass-energy-commercial-scale-harvesting-cattail-biomass-biocarbon

Grosshans, R. E., Venema, H., Cicek, N., & Goldsborough, G. (2011). Cattail farming for water quality: Harvesting cattails for nutrient removal and phosphorous recovery in the

watershed. *Proceedings of WEF-IWA Nutrient Recovery and Management 2011*. Water Environment Federation.

Guo, Z., Liu, Y., Guo, H., Yan, S., & Mu, J. (2013). Microalgae cultivation using an aquaculture wastewater as growth medium for biomass and biofuel production. *Journal of Environmental Sciences*, *25*(1, Suppl.), S85-S88. https://doi.org/10.1016/S1001-0742(14)60632-X

Gupta, D., Chatterjee, S., Datta, S., Veer, V., & Walther, C. (2014). Role of phosphate fertilizers in heavy metal uptake and detoxification of toxic metals. *Chemosphere*, *108*, 134-144. https://doi.org/10.1016/j.chemosphere.2014.01.030

Hall, J. (2002). Cellular mechanisms for heavy metal detoxification and tolerance. *Journal of Experimental Botany*, *53*(366), 1-11. https://doi.org/10.1093/jexbot/53.366.1

Hall, S. J., Delaporte, A., Phillips, M. J., Beveridge, M., & O'Keefe, M. (2011). *Blue frontiers: managing the environmental costs of aquaculture*. The WorldFish Center. https://hdl.handle.net/20.500.12348/1148

Hambrey, J., Edwards, P., & Belton, B. (2008). An ecosystem approach to freshwater aquaculture: a global review. In D. Soto, J. Aguilar-Manjarrez, & N. Hishamunda (Eds.), *Building an Ecosystem Approach to Aquaculture* [FAO Fisheries and Aquaculture Proceedings 14]. Food and Agriculture Organization of the United Nations.

Hammer, D. A. (1989). *Constructed wetlands for wastewater treatment: municipal, industrial and agricultural*. CRC Press.

Han, P., Lu, Q., Fan, L., & Zhou, W. (2019). A review on the use of microalgae for sustainable aquaculture. *Applied Sciences*, *9*(11), 2377. https://doi.org/10.3390/app9112377

Han, W., Mao, Y., Wei, Y., Shang, P., & Zhou, X. (2020). Bioremediation of aquaculture wastewater with algal-bacterial biofilm combined with the production of selenium rich biofertilizer. *Water*, *12*(7), 2071. https://doi.org/10.3390/w12072071

Hansen, D. (2008). *Natural wild rice in Minnesota*. Minnesota Department of Natural Resources.

Hauser, S. C. (2014). *Wild rice: An essential guide to cooking, history, and harvesting*. Simon and Schuster.

Hawrot-Paw, M., Koniuszy, A., Gałczyńska, M., Zając, G., & Szyszlak-Bargłowicz, J. (2019). Production of microalgal biomass using aquaculture wastewater as growth medium. *Water*, *12*(1), 106. https://doi.org/10.3390/w12010106

Hayes, P., Stucker, R., & Wandrey, G. (1989). The domestication of American wildrice. *Economic Botany*, *43*, 203-214. https://doi.org/10.1007/BF02859862

Healy, M. G., Rodgers, M., & Mulqueen, J. (2007). Treatment of dairy wastewater using constructed wetlands and intermittent sand filters. *Bioresource Technology*, *98*(12), 2268-2281. https://doi.org/10.1016/j.biortech.2006.07.036

Heller, M. (2017). *Food product environmental footprint literature summary: Land-based aquaculture*. Center for Sustainable Systems, University of Michigan.

Hennessy, M., Wilson, L., Struthers, W., & Kelly, L. A. (1996). Waste loadings from two freshwater Atlantic salmon juvenile farms in Scotland. *Water, Air, and Soil Pollution*, *86*, 235-249. https://doi.org/10.1007/BF00279159

Hill, I. R., Heimbach, F., Leeuwangh, P., & Matthiessen, P. (1994). *Freshwater field tests for hazard assessment of chemicals*. CRC Press.

Hozumi, A., Hong, P.-Y., Kaartvedt, S., Røstad, A., & Jones, B. H. (2018). Water quality, seasonality, and trajectory of an aquaculture-wastewater plume in the Red Sea. *Aquaculture Environment Interactions*, *10*, 61-77. https://doi.org/10.3354/aei00254

Hu, L., Ren, W., Tang, J., Li, N., Zhang, J., & Chen, X. (2013). The productivity of traditional rice–fish co-culture can be increased without increasing nitrogen loss to the environment. *Agriculture, Ecosystems & Environment*, *177*, 28-34. https://doi.org/10.1016/j.agee.2013.05.023

Ibekwe, A. M., Lyon, S., Leddy, M., & Jacobson-Meyers, M. (2007). Impact of plant density and microbial composition on water quality from a free water surface constructed wetland. *Journal of Applied Microbiology*, *102*(4), 921-936. https://doi.org/10.1111/j.1365-2672.2006.03181.x

Ikeda, S., Sasaki, K., Okubo, T., Yamashita, A., Terasawa, K., Bao, Z., Liu, D., Watanabe, T., Murase, J., & Asakawa, S. (2014). Low nitrogen fertilization adapts rice root microbiome to low nutrient environment by changing biogeochemical functions. *Microbes and Environments*, *29*(1), 50-59. https://doi.org/10.1264/jsme2.ME13110

Ip, Y. K., & Chew, S. F. (2010). Ammonia production, excretion, toxicity, and defense in fish: a review. *Frontiers in Physiology*, *1*, 134. https://doi.org/10.3389/fphys.2010.00134

Jeffrey, S., & Humphrey, G. (1975). New spectrophotometric equations for determining chlorophylls a, b, c1 and c2 in higher plants, algae and natural phytoplankton. *Biochemie und Physiologie der Pflanzen*, *167*(2), 191-194. https://doi.org/10.1016/S0015-3796(17)30778-3

Jenks, A. E. (1899). *The wild rice gatherers of the Upper Lakes: A study in American primitive economics* [19th Annual Report of the Bureau of American Ethnology to the Secretary of

the Smithsonian Institution]. Wisconsin Historical Society. http://www.wisconsinhistory.org/turningpoints/search.asp?id=1065

Ji, N., Wang, S., & Zhang, L. (2017). Characteristics of dissolved organic phosphorus inputs to freshwater lakes: a case study of Lake Erhai, southwest China. *Science of the Total Environment, 601-602*, 1544-1555. https://doi.org/10.1016/j.scitotenv.2017.05.265

Jing, M., Lin, D., Lin, J., Li, Q., Yan, H., & Feng, X. (2021). Mercury, microcystins and Omega-3 polyunsaturated fatty acids in farmed fish in eutrophic reservoir: Risk and benefit assessment. *Environmental Pollution*, *270*, 116047. https://doi.org/10.1016/j.envpol.2020.116047

John, E. M., Krishnapriya, K., & Sankar, T. V. (2020). Treatment of ammonia and nitrite in aquaculture wastewater by an assembled bacterial consortium. *Aquaculture*, *526*, 735390. https://doi.org/10.1016/j.aquaculture.2020.735390

Johnson, D. R., & Percich, J. A. (1992). Wild rice domestication, fungal brown spot disease, and the future of commercial production in Minnesota. *Plant Disease*, *76*(12), 1193-1198.

Johnston, C. A. (1991). Sediment and nutrient retention by freshwater wetlands: effects on surface water quality. *Critical Reviews in Environmental Science and Technology*, *21*(5-6), 491-565. https://doi.org/10.1080/10643389109388425

Jorgenson, K. (2013). *Northern wild rice (Zizania palustris L.) as a phytoremediation species in eutrophic wetlands-investigation of root-sediment interactions* [Master's Thesis, Lakehead University]. Lakehead Knowledge Commons. http://knowledgecommons.lakeheadu.ca/handle/2453/552

Juston, J. M., & DeBusk, T. A. (2011). Evidence and implications of the background phosphorus concentration of submerged aquatic vegetation wetlands in stormwater treatment areas

for Everglades restoration. *Water Resources Research*, *47*(1). https://doi.org/10.1029/2010WR009294

Kabata-Pendias, A. (2000). *Trace elements in soils and plants* (3 ed.). CRC press. https://doi.org/10.1201/9781420039900

Kadlec, R., Knight, R., Vymazal, J., Brix, H., Cooper, P., & Haberl, R. (2000). *Constructed wetlands for pollution control: processes, performance, design and operation*. IWA publishing.

Kadlec, R. H. (2016). Large constructed wetlands for phosphorus control: A review. *Water*, *8*(6), 243. https://doi.org/10.3390/w8060243

Kadlec, R. H., & Wallace, S. (2008). *Treatment wetlands* (2 ed.). CRC press. https://doi.org/10.1201/9781420012514

Kaiser, D., & Piotrowski, K. (2023). *Fertilizing wild rice in Minnesota*. Retrieved November 1, 2023 from https://extension.umn.edu/crop-specific-needs/wild-rice-fertilizer-guidelines

Kajimura, M., Croke, S. J., Glover, C. N., & Wood, C. M. (2004). Dogmas and controversies in the handling of nitrogenous wastes: the effect of feeding and fasting on the excretion of ammonia, urea and other nitrogenous waste products in rainbow trout. *Journal of Experimental Biology*, *207*(12), 1993-2002. https://doi.org/10.1242/jeb.00901

Kamal, A. G., Linklater, R., Thompson, S., Dipple, J., & I.M.C. (2015). A recipe for change: Reclamation of Indigenous food sovereignty in O-Pipon-Na-Piwin Cree Nation for decolonization, resource sharing, and cultural restoration. *Globalizations*, *12*(4), 559-575. https://doi.org/10.1080/14747731.2015.1039761

Kamaludeen, S., & Ramasamy, K. (2008). Rhizoremediation of metals: harnessing microbial communities. *Indian Journal of Microbiology*, *48*, 80-88. https://doi.org/10.1007/s12088-008-0008-3

Kamilya, T., Majumder, A., Yadav, M. K., Ayoob, S., Tripathy, S., & Gupta, A. K. (2022). Nutrient pollution and its remediation using constructed wetlands: Insights into removal and recovery mechanisms, modifications and sustainable aspects. *Journal of Environmental Chemical Engineering*, *10*(3), 107444. https://doi.org/10.1016/j.jece.2022.107444

Kangmin, L. (1988). Rice-fish culture in China: A review. *Aquaculture*, *71*(3), 173-186. https://doi.org/10.1016/0044-8486(88)90257-8

Kinew, K. A. (1995). *Manito Gitigaan: governing in the Great Spirit's garden: wild rice in Treaty #3* [Doctoral Dissertation, University of Manitoba]. MSpace. http://hdl.handle.net/1993/3684

Kirk, G., & Kronzucker, H. (2005). The potential for nitrification and nitrate uptake in the rhizosphere of wetland plants: A modelling study. *Annals of Botany*, *96*(4), 639-646. https://doi.org/10.1093/aob/mci216

Koerselman, W., & Meuleman, A. F. (1996). The vegetation N:P ratio: A new tool to detect the nature of nutrient limitation. *Journal of Applied Ecology*, *33*(6), 1441-1450. https://doi.org/10.2307/2404783

Kopittke, P. M. (2012). Interactions between Ca, Mg, Na and K: alleviation of toxicity in saline solutions. *Plant and Soil*, *352*, 353-362. https://doi.org/10.1007/s11104-011-1001-x

Kouki, S., Saidi, N., M'hiri, F., Hafiane, A., & Hassen, A. (2016). Co-composting of macrophyte biomass and sludge as an alternative for sustainable management of constructed wetland by-products. *Clean*, *44*(6), 694-702. https://doi.org/10.1002/clen.201500346

Kovach, D. A., & Bradford, K. J. (1992). Temperature dependence of viability and dormancy of *Zizania palustris* var. *interior* seeds stored at high moisture contents. *Annals of Botany*, *69*(4), 297-301. https://doi.org/10.1093/oxfordjournals.aob.a088345

Krause-Jensen, D., Christensen, P. B., & Rysgaard, S. (1999). Oxygen and nutrient dynamics within mats of the filamentous macroalga *Chaetomorpha linum*. *Estuaries*, *22*, 31-38. https://doi.org/10.2307/1352924

Kurniawan, S. B., Abdullah, S. R. S., Imron, M. F., Ahmad, A., Mohd Said, N. S., Mohd Rahim, N. F., Mohammad Alnawajha, M., Abu Hasan, H., Othman, A. R., & Purwanti, I. F. (2021). Potential of valuable materials recovery from aquaculture wastewater: an introduction to resource reclamation. *Aquaculture Research*, *52*(7), 2954-2962. https://doi.org/10.1111/are.15180

Kyambadde, J., Kansiime, F., & Dalhammar, G. (2005). Nitrogen and phosphorus removal in substrate-free pilot constructed wetlands with horizontal surface flow in Uganda. *Water, Air, and Soil Pollution*, *165*, 37-59. https://doi.org/10.1007/s11270-005-4643-6

Lalonde, B. A., Ernst, W., & Garron, C. (2015). Chemical and physical characterisation of effluents from land-based fish farms in Atlantic Canada. *Aquaculture International*, *23*, 535-546. https://doi.org/10.1007/s10499-014-9834-y

Lang, D. A., King, R. S., & Scott, J. T. (2012). Divergent responses of biomass and enzyme activities suggest differential nutrient limitation in stream periphyton. *Freshwater Science*, *31*(4), 1096-1104. https://doi.org/10.1899/12-031.1

Lavergne, C. S. (2006). *Introduced wild rice: Impacts to littoral fishes and fish habitat in Northwestern Manitoba boreal lakes* [Master's Thesis, University of Manitoba]. MSpace. http://hdl.handle.net/1993/7949

Lawson, T. B. (1995). *Fundamentals of aquacultural engineering*. Chapman & Hall.

Lawton, R. J., Mata, L., de Nys, R., & Paul, N. A. (2013). Algal bioremediation of waste waters from land-based aquaculture using *Ulva*: Selecting target species and strains. *PLOS ONE*, *8*(10), e77344. https://doi.org/10.1371/journal.pone.0077344

Lee, P. (1986). Ecological relationships of wild rice, *Zizania aquatica*. 4. Environmental regions within a wild rice lake. *Canadian Journal of Botany*, *64*(9), 2037-2044. https://doi.org/10.1139/b86-266

Lee, P., & Stewart, J. (1981). Ecological relationships of wild rice, *Zizania aquatica*. 1. A model for among-site growth. *Canadian Journal of Botany*, *59*(11), 2140-2151. https://doi.org/10.1139/b81-279

Lee, P., & Stewart, J. (1984). Ecological relationships of wild rice, *Zizania aquatica*. 3. Factors affecting seeding success. *Canadian Journal of Botany*, *62*(8), 1608-1615. https://doi.org/10.1139/b84-215

Lekang, O.-I., Bergheim, A., & Dalen, H. (2000). An integrated wastewater treatment system for land-based fish-farming. *Aquacultural Engineering*, *22*(3), 199-211. https://doi.org/10.1016/S0144-8609(00)00039-X

Lenth, R. V. (2022). *emmeans: Estimated marginal means, aka least-squares means*. *R package version 1.7.5*. https://CRAN.R-project.org/package=emmeans

Li, L., Li, Y., Biswas, D. K., Nian, Y., & Jiang, G. (2008). Potential of constructed wetlands in treating the eutrophic water: evidence from Taihu Lake of China. *Bioresource Technology*, *99*(6), 1656-1663. https://doi.org/10.1016/j.biortech.2007.04.001

Li, W., Guo, Y., & Fu, K. (2011). Enclosure experiment for influence on algae growth by shading light. *Procedia Environmental Sciences*, *10*, 1823-1828. https://doi.org/10.1016/j.proenv.2011.09.285

Li, Z., Liu, J., Wang, Q., & Silva, S. S. D. (2018). Inland aquaculture: Trends and prospects. *Aquaculture in China: Success Stories and Modern Trends*, 25-37. https://doi.org/10.1002/9781119120759.ch1_2

Lichtenthaler, H. K., & Buschmann, C. (2001). Chlorophylls and carotenoids: Measurement and characterization by UV-VIS spectroscopy. *Current Protocols in Food Analytical Chemistry*, *1*, F4. 3.1-F4. 3.8. https://doi.org/10.1002/0471142913.faf0403s01

Lin, Y.-F., Jing, S.-R., Lee, D.-Y., & Wang, T.-W. (2002). Nutrient removal from aquaculture wastewater using a constructed wetlands system. *Aquaculture*, *209*(1-4), 169-184. https://doi.org/10.1016/S0044-8486(01)00801-8

Linde, A. F., Janish, T., & Smith, D. (1976). *Cattail: The significance of its growth, phenology and carbohydrate storage to its control and management*. Wisconsin Department of Natural Resources. https://digital.library.wisc.edu/1711.dl/7Z7HKPI4YNUSL86

Little, D. C., Newton, R., & Beveridge, M. (2016). Aquaculture: a rapidly growing and significant source of sustainable food? Status, transitions and potential. *Proceedings of the Nutrition Society*, *75*(3), 274-286. https://doi.org/10.1017/S0029665116000665

Liu, H., Hu, Z., Zhang, J., Ngo, H. H., Guo, W., Liang, S., Fan, J., Lu, S., & Wu, H. (2016). Optimizations on supply and distribution of dissolved oxygen in constructed wetlands: a

review. *Bioresource Technology*, *214*, 797-805. https://doi.org/10.1016/j.biortech.2016.05.003

Liu, Y., Rosten, T. W., Henriksen, K., Hognes, E. S., Summerfelt, S., & Vinci, B. (2016). Comparative economic performance and carbon footprint of two farming models for producing Atlantic salmon (*Salmo salar*): Land-based closed containment system in freshwater and open net pen in seawater. *Aquacultural Engineering*, *71*, 1-12. https://doi.org/10.1016/j.aquaeng.2016.01.001

Lu, R., Chen, M., Feng, Y., Yuan, N., Zhang, Y., Cao, M., Liu, J., Wang, Y., Hang, Y., & Sun, X. (2022). Comparative plastome analyses and genomic resource development in wild rice (*Zizania* spp., Poaceae) using genome skimming data. *Industrial Crops and Products*, *186*, 115244. https://doi.org/10.1016/j.indcrop.2022.115244

Luby, B. (2023). Treaty through a planting lens: A study of Manoomin harvesting rights in Anishinaabe-Aki, 1873–Present. *The American Indian Quarterly*, *47*(4), 352-387. https://doi.org/10.1353/aiq.2023.a921874

LuminUltra. (2017). *Product instructions. PhotonMaster™ Luminometer & Bluetooth® Module*.

LuminUltra. (2023). *2nd Generation ATP® Testing*. Retrieved August 30, 2023 from https://www.luminultra.com/tech/2nd-generation-atp/

Malvick, D., & Percich, J. (1993). Hydroponic culture of wild rice (*Zizania palustris* L.) and its application to studies of silicon nutrition and fungal brown spot disease. *Canadian Journal of Plant Science*, *73*(4), 969-975. https://doi.org/10.4141/cjps93-127

Manitoba Water Stewardship. (2011). *Manitoba water quality standards, objectives, and guidelines* [Report 2011-01].

Marcum, D. B. (2007). *Cultivated wild rice production in California* [Publication 21622]. University of California, Agriculture and Natural Resources.

Matson, L., Ng, G.-H. C., Dockry, M., Nyblade, M., King, H. J., Bellcourt, M., Bloomquist, J., Bunting, P., Chapman, E., & Dalbotten, D. (2021). Transforming research and relationships through collaborative tribal-university partnerships on Manoomin (wild rice). *Environmental Science & Policy*, *115*, 108-115. https://doi.org/10.1016/j.envsci.2020.10.010

Matties, Z. (2016). Unsettling settler food movements: Food sovereignty and decolonization in Canada. *Cuizine*, *7*(2). https://doi.org/10.7202/1038478ar

McCall, S. J., Hale, M. S., Smith, J. T., Read, D. S., & Bowes, M. J. (2017). Impacts of phosphorus concentration and light intensity on river periphyton biomass and community structure. *Hydrobiologia*, *792*, 315-330. https://doi.org/10.1007/s10750-016-3067-1

McCauley, A., Jones, C., & Jacobsen, J. (2009). *Soil pH and organic matter* [Nutrient Management Module 8, #4449-8]. Montana State University Extension Service.

McCormick, P. V., O'Dell, M. B., Shuford III, R. B., Backus, J. G., & Kennedy, W. C. (2001). Periphyton responses to experimental phosphorus enrichment in a subtropical wetland. *Aquatic Botany*, *71*(2), 119-139. https://doi.org/10.1016/S0304-3770(01)00175-9

McGilp, L., Castell-Miller, C., Haas, M., Millas, R., & Kimball, J. (2023). Northern Wild Rice (*Zizania palustris* L.) breeding, genetics, and conservation. *Crop Science*, *63*(4), 1904-1933. https://doi.org/10.1002/csc2.20973

McGilp, L., Duquette, J., Braaten, D., Kimball, J., & Porter, R. (2020). Investigation of variable storage conditions for cultivated northern wild rice and their effects on seed viability and

dormancy. *Seed Science Research*, *30*(1), 21-28. https://doi.org/10.1017/S0960258520000033

McMillian, S. (2021). *Water chemistry and microbial nitrogen cycling in wild rice wetlands* [Master's Thesis, University of Minnesota]. University Digital Conservancy. https://hdl.handle.net/11299/226337

Meeker, J. E. (1993). *The ecology of "wild" wild-rice (Zizania palustris var. palustris) in the Kakagon Sloughs, a riverine wetland on Lake Superior* [Doctoral Dissertation, The University of Wisconsin-Madison]. ProQuest. https://www.proquest.com/openview/50641c008a97ac88e9b49151c73fcd95/1

Melanson, R., & Payne, F. (1988). *Wetlands habitat management through nutrient enrichment* [Occasional Paper No. 1]. Nova Scotia Department of Lands and Forests, Wildlife Division.

Miao, S., Newman, S., & Sklar, F. H. (2000). Effects of habitat nutrients and seed sources on growth and expansion of Typha domingensis. *Aquatic Botany*, *68*(4), 297-311. https://doi.org/10.1016/S0304-3770(00)00127-3

Mikkelsen, D., De Datta, S., & Obcemea, W. (1978). Ammonia volatilization losses from flooded rice soils. *Soil Science Society of America Journal*, *42*(5), 725-730. https://doi.org/10.2136/sssaj1978.03615995004200050014x

Miranda, L., Hargreaves, J., & Raborn, S. (2001). Predicting and managing risk of unsuitable dissolved oxygen in a eutrophic lake. *Hydrobiologia*, *457*, 177-185. https://doi.org/10.1023/A:1012283603339

Moodie, D. W. (1991). Manomin: Historical-geographical perspectives on the Ojibwa production of wild Rice. In K. Abel & J. Friesen (Eds.), *Aboriginal Resource Use in Canada:*

Historical and Legal Aspects (pp. 71-79). University of Manitoba Press. https://doi.org/10.1515/9780887553097-006

Müller, S., Mitrovic, S. M., & Baldwin, D. S. (2016). Oxygen and dissolved organic carbon control release of N, P and Fe from the sediments of a shallow, polymictic lake. *Journal of Soils and Sediments*, *16*, 1109-1120. https://doi.org/10.1007/s11368-015-1298-9

Mummert, A. K., Neves, R. J., Newcomb, T. J., & Cherry, D. S. (2003). Sensitivity of juvenile freshwater mussels (*Lampsilis fasciola*, *Villosa iris*) to total and un-ionized ammonia. *Environmental Toxicology and Chemistry*, *22*(11), 2545-2553. https://doi.org/10.1897/02-341

Nagarajan, D., Varjani, S., Lee, D.-J., & Chang, J.-S. (2021). Sustainable aquaculture and animal feed from microalgae – Nutritive value and techno-functional components. *Renewable and Sustainable Energy Reviews*, *150*, 111549. https://doi.org/10.1016/j.rser.2021.111549

Näsholm, T., Kielland, K., & Ganeteg, U. (2009). Uptake of organic nitrogen by plants. *New Phytologist*, *182*(1), 31-48. https://doi.org/10.1111/j.1469-8137.2008.02751.x

Nayak, J., Mathan, J., Mohanty, M., & Pradhan, C. (2014). An in vitro hydroponic study on physiological and biochemical responses of indian wild rice to varying doses of hexavalent chromium. *International Research Journal of Environment Sciences*, *3*(11), 20-28.

Naylor, R. L., Hardy, R. W., Buschmann, A. H., Bush, S. R., Cao, L., Klinger, D. H., Little, D. C., Lubchenco, J., Shumway, S. E., & Troell, M. (2021). A 20-year retrospective review of global aquaculture. *Nature, 591*(7851), 551-563. https://doi.org/10.1038/s41586-021-03308-6

Naylor, S. J., Moccia, R. D., & Durant, G. M. (1999). The chemical composition of settleable solid fish waste (manure) from commercial rainbow trout farms in Ontario, Canada. *North American Journal of Aquaculture*, *61*(1), 21-26. https://doi.org/10.1577/1548-8454(1999)061%3C0021:TCCOSS%3E2.0.CO;2

Neil, L. L., Fotedar, R., & Shelley, C. C. (2005). Effects of acute and chronic toxicity of unionized ammonia on mud crab, *Scylla serrata* (Forsskål, 1755) larvae. *Aquaculture Research*, *36*(9), 927-932. https://doi.org/10.1111/j.1365-2109.2005.01304.x

Neilson, A. H., & Larsson, T. (1980). The utilization of organic nitrogen for growth of algae: physiological aspects. *Physiologia Plantarum*, *48*(4), 542-553. https://doi.org/10.1111/j.1399-3054.1980.tb03302.x

Nelson, R. N., & Dahl, R. P. (1986). *The wild rice industry: Economic analysis of rapid growth and implications for Minnesota* [Staff Paper P86-25]. University of Minnesota. https://doi.org/10.22004/ag.econ.13406

Nimptsch, J., & Pflugmacher, S. (2007). Ammonia triggers the promotion of oxidative stress in the aquatic macrophyte *Myriophyllum mattogrossense*. *Chemosphere*, *66*(4), 708-714. https://doi.org/10.1016/j.chemosphere.2006.07.064

Noakes, D. J. (2018). Oceans of opportunity: A review of Canadian aquaculture. *Marine Economics and Management*, *1*(1), 43-54. https://doi.org/10.1108/MAEM-06-2018-002

Nõges, P., Adrian, R., Anneville, O., Arvola, L., Blenckner, T., George, G., Jankowski, T., Järvinen, M., Maberly, S., Padisák, J., Straile, D., Teubner, K., & Weyhenmeyer, G. (2010). The impact of variations in the climate on seasonal dynamics of phytoplankton. In G. George (Ed.), *The Impact of Climate Change on European Lakes*. Springer. https://doi.org/10.1007/978-90-481-2945-4_14

Nora'aini, A., Mohammad, A. W., Jusoh, A., Hasan, M., Ghazali, N., & Kamaruzaman, K. (2005). Treatment of aquaculture wastewater using ultra-low pressure asymmetric polyethersulfone (PES) membrane. *Desalination*, *185*(1-3), 317-326. https://doi.org/10.1016/j.desal.2005.03.084

Norton, S. (2007). *Removal mechanisms in constructed wastewater wetlands*. https://api.semanticscholar.org/CorpusID:13345147

Nurminen, L., & Horppila, J. (2009). Life form dependent impacts of macrophyte vegetation on the ratio of resuspended nutrients. *Water Research*, *43*(13), 3217-3226. https://doi.org/10.1016/j.watres.2009.04.041

Oelke, E., Teynor, T., Carter, P., Percich, J., Noetzel, D., Bloom, P., Porter, R., Schertz, C., Boedicker, J., & Fuller, E. (1997). Wild rice. In *Alternative Field Crops Manual* (pp. 315-334). University of Minnesota.

Oelke, E. A., & Boedicker, J. J. (2000). Wild rice: Processing and utilization. In *Handbook of Cereal Science and Technology, Revised and Expanded* (2 ed., pp. 275-295). CRC Press.

Oelke, E. A., Grava, J., Noetzel, D., Barron, D., Percich, J., Schertz, C., Strait, J., & Stucker, R. (1982). *Wild rice production in Minnesota* [Extension Bulletin No. 464]. University of Minnesota. https://hdl.handle.net/11299/169068

Oelke, E. A., & Schreiner, R. (2007). *Saga of the Grain: A Tribute to Minnesota Cultivated Wild Rice Growers*. Hobar Publications.

Olila, O., Reddy, K., & Stites, D. (1997). Influence of draining on soil phosphorus forms and distribution in a constructed wetland. *Ecological Engineering*, *9*(3-4), 157-169. https://doi.org/10.1016/S0925-8574(97)10006-4

Olin, P. G., Smith, J., & Nabi, R. (2012). *Regional review on status and trends in aquaculture development in North America: Canada and the United States of America – 2010* [FAO Fisheries and Aquaculture Circular No. 1061/2]. Food and Agriculture Organization of the United Nations. https://escholarship.org/uc/item/1946b7nm

Oliveira, V., Martins, P., Marques, B., Cleary, D. F., Lillebø, A. I., & Calado, R. (2020). Aquaponics using a fish farm effluent shifts bacterial communities profile in halophytes rhizosphere and endosphere. *Scientific Reports*, *10*, 10023. https://doi.org/10.1038/s41598-020-66093-8

Ottinger, M., Clauss, K., & Kuenzer, C. (2016). Aquaculture: Relevance, distribution, impacts and spatial assessments – A review. *Ocean & Coastal Management*, *119*, 244-266. https://doi.org/10.1016/j.ocecoaman.2015.10.015

Paine, M. D. (1996). Repeated measures designs. *Environmental Toxicology and Chemistry*, *15*(9), 1439-1441. https://doi.org/10.1002/etc.5620150901

Paolacci, S., Stejskal, V., Toner, D., & Jansen, M. A. (2022). Wastewater valorisation in an integrated multitrophic aquaculture system; assessing nutrient removal and biomass production by duckweed species. *Environmental Pollution*, *302*, 119059. https://doi.org/10.1016/j.envpol.2022.119059

Peden, D. G. (1982). Factors associated with growth of wild rice in Northern Saskatchewan. *Arctic*, *35*(2), 307-311.

Phung, V., Nguyen, B., Kim Hoang, T., & Bell, R. (2009). Recycling of fishpond waste from rice cultivation in Cuu Long Delta, Vietnam. In J. Nair, C. Furedy, C. Hoysala, & J. Doelle (Eds.), *Technologies and Management for Sustainable Biosystems* (pp. 85-97). Nova Science Publishers.

Pikosz, M., & Messyasz, B. (2016). Characteristics of and coexisting filamentous algae in relation to environmental factors in freshwater ecosystems in Poland. *Oceanological and Hydrobiological Studies*, *45*(2), 202-215. https://doi.org/10.1515/ohs-2016-0019

Pinheiro, J., & Bates, D. (2000). *Mixed-effects Models in S and S-PLUS*. Springer. https://doi.org/10.1007/b98882

Pinheiro, J., Bates, D., & R Core Team. (2022). *nlme: Linear and Nonlinear Mixed Effects Models. R package version 3.1-158.* https://CRAN.R-project.org/package=nlme

Pitman, M. G., & Läuchli, A. (2002). Global impact of salinity and agricultural ecosystems. In A. Läuchli & U. Lüttge (Eds.), *Salinity: Environment-plants-molecules*. Springer. https://doi.org/10.1007/0-306-48155-3_1

Platzer, C. (1999). Design recommendations for subsurface flow constructed wetlands for nitrification and denitrification. *Water Science and Technology*, *40*(3), 257-263. https://doi.org/10.1016/S0273-1223(99)00420-5

Poach, M., Hunt, P., Sadler, E., Matheny, T., Johnson, M., Stone, K., Humenik, F., & Rice, J. (2002). Ammonia volatilization from constructed wetlands that treat swine wastewater. *Transactions of the ASAE*, *45*(3), 619-927. https://doi.org/10.13031/2013.8825

Poe, A. C., Piehler, M. F., Thompson, S. P., & Paerl, H. W. (2003). Denitrification in a constructed wetland receiving agricultural runoff. *Wetlands*, *23*, 817-826. https://doi.org/10.1672/0277-5212(2003)023[0817:DIACWR]2.0.CO;2

Porter, R. (2019). Wildrice (*Zizania* L.) in North America: Genetic resources, conservation, and use. In S. Greene, K. Williams, C. Khoury, M. Kantar, & L. Marek (Eds.), *North American Crop Wild Relatives, Volume 2* (pp. 83-97). Springer, Cham. https://doi.org/10.1007/978-3-319-97121-6_3

Ptacnik, R., Lepistö, L., Willén, E., Brettum, P., Andersen, T., Rekolainen, S., Lyche Solheim, A., & Carvalho, L. (2008). Quantitative responses of lake phytoplankton to eutrophication in Northern Europe. *Aquatic Ecology, 42*, 227-236. https://doi.org/10.1007/s10452-008-9181-z

Pulz, O., & Gross, W. (2004). Valuable products from biotechnology of microalgae. *Applied Microbiology and Biotechnology*, *65*, 635-648. https://doi.org/10.1007/s00253-004-1647-x

Qiu, Y., Liu, Q., & Beta, T. (2009). Antioxidant activity of commercial wild rice and identification of flavonoid compounds in active fractions. *Journal of Agricultural and Food Chemistry*, *57*(16), 7543-7551. https://doi.org/10.1021/jf901074b

R Core Team. (2021). *R: A language and environment for statistical computing*. R Foundation for Statistical Computing.

Randall, D. J., & Tsui, T. (2002). Ammonia toxicity in fish. *Marine Pollution Bulletin*, *45*(1-12), 17-23. https://doi.org/10.1016/S0025-326X(02)00227-8

Raster, A., & Hill, C. G. (2017). The dispute over wild rice: an investigation of treaty agreements and Ojibwe food sovereignty. *Agriculture and Human Values*, *34*, 267-281. https://doi.org/10.1007/s10460-016-9703-6

Reinhardt, M., Müller, B., Gächter, R., & Wehrli, B. (2006). Nitrogen removal in a small constructed wetland: an isotope mass balance approach. *Environmental Science & Technology*, *40*(10), 3313-3319. https://doi.org/10.1021/es052393d

Rice, E., Bridgewater, L., & American Public Health Association. (2012). *Standard methods for the examination of water and wastewater*. American Public Health Association.

Richmond, A. (2004). *Handbook of microalgal culture: biotechnology and applied phycology*. Blackwell Publishing Ltd. https://doi.org/10.1002/9780470995280

Robertson, K. J. (in preparation). *Assessing nutrient toxicity in fathead minnows using a multi-omics approach* [Unpublished Master's Thesis, University of Manitoba].

Robinson, B. L., & Fernald, M. L. (1908). *Gray's new manual of botany: A handbook of the flowering plants and ferns of the Central and Northeastern United States and adjacent Canada* (7 ed.). American Book Company.

Rogers, G. L., & Klemetson, S. L. (1985). Ammonia removal in selected aquaculture water reuse biofilters. *Aquacultural Engineering*, *4*(2), 135-154. https://doi.org/10.1016/0144-8609(85)90010-X

Rousseau, D. P., Lesage, E., Story, A., Vanrolleghem, P. A., & De Pauw, N. (2008). Constructed wetlands for water reclamation. *Desalination*, *218*(1-3), 181-189. https://doi.org/10.1016/j.desal.2006.09.034

Rozema, E. R., Rozema, L. R., & Zheng, Y. (2016). A vertical flow constructed wetland for the treatment of winery process water and domestic sewage in Ontario, Canada: Six years of performance data. *Ecological Engineering*, *86*, 262-268. https://doi.org/10.1016/j.ecoleng.2015.11.006

Rozema, E. R., VanderZaag, A. C., Wood, J. D., Drizo, A., Zheng, Y., Madani, A., & Gordon, R. J. (2016). Constructed wetlands for agricultural wastewater treatment in Northeastern North America: A review. *Water*, *8*(5), 173. https://doi.org/10.3390/w8050173

Ruxton, C. (2011). The benefits of fish consumption. *Nutrition Bulletin*, *36*(1), 6-19. https://doi.org/10.1111/j.1467-3010.2010.01869.x

Sain, P. (1984). Decomposition of wild rice (*Zizania aquatica*) straw in two natural lakes of northwestern Ontario. *Canadian Journal of Botany*, *62*(7), 1352-1356. https://doi.org/10.1139/b84-183

Sánchez-Carrillo, S., Angeler, D. G., Álvarez-Cobelas, M., & Sánchez-Andrés, R. (2011). Freshwater Wetland Eutrophication. In A. A. Ansari, S. Singh Gill, G. R. Lanza, & W. Rast (Eds.), *Eutrophication: Causes, Consequences and Control* (pp. 195-210). Springer. https://doi.org/10.1007/978-90-481-9625-8_9

Sarma, S., Mangas-Ramírez, E., & Nandini, S. (2003). Effect of ammonia toxicity on the competition among three species of cladocerans (Crustacea: Cladocera). *Ecotoxicology and Environmental Safety*, *55*(2), 227-235. https://doi.org/10.1016/S0147-6513(02)00120-3

Schindler, D. W., Hecky, R. E., & McCullough, G. K. (2012). The rapid eutrophication of Lake Winnipeg: Greening under global change. *Journal of Great Lakes Research*, *38*, 6-13. https://doi.org/10.1016/j.jglr.2012.04.003

Shadhin, M., Rahman, M., Jayaraman, R., & Mann, D. (2021). Novel cattail fiber composites: converting waste biomass into reinforcement for composites. *Bioresources and Bioprocessing*, *8*, 101. https://doi.org/10.1186/s40643-021-00453-8

Sharma, S., Asolekar, S. R., Thakur, V. K., & Asokan, P. (2023). Valorization of cellulosic fiber derived from waste biomass of constructed wetland as a potential reinforcement in polymeric composites: A technological approach to achieve circular economy. *Journal of Environmental Management*, *340*, 117850. https://doi.org/10.1016/j.jenvman.2023.117850

Sherwood, J. (2020). The significance of biomass in a circular economy. *Bioresource Technology*, *300*, 122755. https://doi.org/10.1016/j.biortech.2020.122755

Sims, L., Pastor, J., Lee, T., & Dewey, B. (2012). Nitrogen, phosphorus and light effects on growth and allocation of biomass and nutrients in wild rice. *Oecologia*, *170*, 65-76. https://doi.org/10.1007/s00442-012-2296-x

Snow, A., Anderson, B., & Wootton, B. (2012). Flow-through land-based aquaculture wastewater and its treatment in subsurface flow constructed wetlands. *Environmental Reviews*, *20*(1), 54-69. https://doi.org/10.1139/a11-023

Snow, A. M. (2007). *Purification of aquaculture wastewater and production of fish feed using agricultural and aquatic plants* [Master's Thesis, Dalhousie University]. Theses Canada. https://library-archives.canada.ca/eng/services/services-libraries/theses/Pages/item.aspx?idNumber=633130068

Sojda, R. S., & Solberg, K. L. (1993). 13.4.13. Management and control of cattails. In D. H. Cross, & P. Vohs (Eds.), *Waterfowl Management Handbook*. US Fish & Wildlife Service. https://digitalcommons.unl.edu/icwdmwfm/33

Sprouffske, K. (2020). *growthcurver: Simple Metrics to Summarize Growth Curves. R package version 0.3.1*. https://CRAN.R-project.org/package=growthcurver

Stainton, M., Capel, M., & Armstrong, F. (1977). *The chemical analysis of freshwater* (2nd ed.).

Stanley, M., Palace, V., Grosshans, R., & Levin, D. B. (2022). Floating treatment wetlands for the bioremediation of oil spills: A review. *Journal of Environmental Management*, *317*, 115416. https://doi.org/10.1016/j.jenvman.2022.115416

Staudenmann, J., & Junge-Berberovic, R. (2003). The Otelfingen Aquaculture Project: Recycling nutrients from industrial waste water in a temperate climate. *Journal of Applied Aquaculture*, *13*(1-2), 67-101. https://doi.org/10.1300/J028v13n01_04

Stein, O. R., & Hook, P. B. (2005). Temperature, plants, and oxygen: How does season affect constructed wetland performance? *Journal of Environmental Science and Health, Part A*, *40*(6-7), 1331-1342. https://doi.org/10.1081/ESE-200055840

Strube, J., & Thomas, K. A. (2021). Damming Rainy Lake and the ongoing production of hydrocolonialism in the US-Canada boundary waters. *Water Alternatives*, *14*(1), 135-157.

Subasinghe, R., Soto, D., & Jia, J. (2009). Global aquaculture and its role in sustainable development. *Reviews in Aquaculture*, *1*(1), 2-9. https://doi.org/10.1111/j.1753-5131.2008.01002.x

Sun, H., He, Z., Zhang, M., Yen, L., Cao, Y., Hu, Z., Peng, Y., & Lee, S. Y. (2020). Spatial variation of soil properties impacted by aquaculture effluent in a small-scale mangrove. *Marine Pollution Bulletin*, *160*, 111511. https://doi.org/10.1016/j.marpolbul.2020.111511

Sundaravadivel, M., & Vigneswaran, S. (2001). Constructed wetlands for wastewater treatment. *Critical Reviews in Environmental Science and Technology*, *31*(4), 351-409. https://doi.org/10.1080/20016491089253

Surendiran, G., Alsaif, M., Kapourchali, F. R., & Moghadasian, M. H. (2014). Nutritional constituents and health benefits of wild rice (*Zizania* spp.). *Nutrition Reviews*, *72*(4), 227-236. https://doi.org/10.1111/nure.12101

Surendiran, G., Goh, C., Le, K., Zhao, Z., Askarian, F., Othman, R., Nicholson, T., Moghadasian, P., Wang, Y.-J., & Aliani, M. (2013). Wild rice (*Zizania palustris* L.)

prevents atherogenesis in LDL receptor knockout mice. *Atherosclerosis*, *230*(2), 284-292. https://doi.org/10.1016/j.atherosclerosis.2013.07.042

Taube, E. (1951). Wild rice. *The Scientific Monthly*, *73*(6), 369-375. https://www.jstor.org/stable/i202242

Taziki, M., Ahmadzadeh, H., Murry, M. A., & Lyon, S. R. (2015). Nitrate and nitrite removal from wastewater using algae. *Current Biotechnology*, *4*(4), 426-440. https://doi.org/http://dx.doi.org/10.2174/2211550104666150828193607

Tedrow, O. N. R., & Lee, P. F. (2022). Use of wild rice (*Zizania palustris* L.) in paddy-scale bioassays for assessing potential use of mining-influenced water for irrigation. *Mine Water and the Environment*, *41*(4), 938-953. https://doi.org/10.1007/s10230-022-00908-0

Terrell, E. E., Peterson, P. M., Reveal, J. L., & Duvall, M. R. (1997). Taxonomy of North American species of *Zizania* (Poaceae). *SIDA, Contributions to Botany*, *17*(3), 533-549. https://biostor.org/reference/158973

Thurston, R. V., Russo, R. C., & Vinogradov, G. (1981). Ammonia toxicity to fishes. Effect of pH on the toxicity of the unionized ammonia species. *Environmental Science & Technology*, *15*(7), 837-840. https://doi.org/10.1021/es00089a012

Tian, X.-L., & Dong, S.-L. (2023). Land-based intensive aquaculture systems. In S.-L. Dong, X.-L. Tian, Q. Gao, & Y. Dong (Eds.), *Aquaculture Ecology* (pp. 369-402). Springer. https://doi.org/10.1007/978-981-19-5486-3_10

Tom, A. P., Jayakumar, J. S., Biju, M., Somarajan, J., & Ibrahim, M. A. (2021). Aquaculture wastewater treatment technologies and their sustainability: A review. *Energy Nexus*, *4*, 100022. https://doi.org/10.1016/j.nexus.2021.100022

Tomasso, J. (1994). Toxicity of nitrogenous wastes to aquaculture animals. *Reviews in Fisheries Science*, *2*(4), 291-314. https://doi.org/10.1080/10641269409388560

Tossavainen, M., Lahti, K., Edelmann, M., Eskola, R., Lampi, A.-M., Piironen, V., Korvonen, P., Ojala, A., & Romantschuk, M. (2019). Integrated utilization of microalgae cultured in aquaculture wastewater: wastewater treatment and production of valuable fatty acids and tocopherols. *Journal of Applied Phycology*, *31*, 1753-1763. https://doi.org/10.1007/s10811-018-1689-6

Troell, M., Kautsky, N., Beveridge, M., Henriksson, P., Primavera, J., Rönnbäck, P., & Folke, C. (2013). Aquaculture. In S. M. Scheiner (Ed.), *Encyclopedia of Biodiversity* (3rd ed). Academic Press. https://doi.org/10.1016/B978-0-12-822562-2.00403-5

Troell, M., Naylor, R. L., Metian, M., Beveridge, M., Tyedmers, P. H., Folke, C., Arrow, K. J., Barrett, S., Crépin, A.-S., & Ehrlich, P. R. (2014). Does aquaculture add resilience to the global food system? *Proceedings of the National Academy of Sciences*, *111*(37), 13257-13263. https://doi.org/10.1073/pnas.1404067111

Twilley, R. R., Blanton, L. R., Brinson, M. M., & Davis, G. J. (1985). Biomass production and nutrient cycling in aquatic macrophyte communities of the Chowan River, North Carolina. *Aquatic Botany*, *22*(3-4), 231-252. https://doi.org/10.1016/0304-3770(85)90002-6

Urakawa, H., & Bernhard, A. E. (2017). Wetland management using microbial indicators. *Ecological Engineering*, *108*, 456-476. https://doi.org/10.1016/j.ecoleng.2017.07.022

Van Cleemput, O., Boeckx, P., Lindgren, P.-E., & Tonderski, K. (2007). Chapter 23 – Denitrification in wetlands. In H. Bothe, S. Ferguson, & W. Newton (Eds.), *Biology of*

the Nitrogen Cycle (pp. 359-367). Elsevier. https://doi.org/10.1016/B978-044452857-5.50024-2

Vendramelli, R. A., Vijay, S., & Yuan, Q. (2017). Mechanism of nitrogen removal in wastewater lagoon: A case study. *Environmental Technology*, *38*(12), 1514-1523. https://doi.org/10.1080/09593330.2016.1235232

Vennum, T. (1988). *Wild rice and the Ojibway people*. Minnesota Historical Society Press.

Viegas, C., Gouveia, L., & Gonçalves, M. (2021). Aquaculture wastewater treatment through microalgal. Biomass potential applications on animal feed, agriculture, and energy. *Journal of Environmental Management*, *286*, 112187. https://doi.org/10.1016/j.jenvman.2021.112187

Vymazal, J. (2007). Removal of nutrients in various types of constructed wetlands. *Science of the Total Environment*, *380*(1-3), 48-65. https://doi.org/10.1016/j.scitotenv.2006.09.014

Vymazal, J. (2010). Constructed wetlands for wastewater treatment. *Water*, *2*(3), 530-549. https://doi.org/10.3390/w2030530

Vymazal, J. (2011a). Constructed wetlands for wastewater treatment: Five decades of experience. *Environmental Science & Technology*, *45*(1), 61-69. https://doi.org/10.1021/es101403q

Vymazal, J. (2011b). Plants used in constructed wetlands with horizontal subsurface flow: A review. *Hydrobiologia*, *674*(1), 133-156. https://doi.org/10.1007/s10750-011-0738-9

Vymazal, J. (2013). Emergent plants used in free water surface constructed wetlands: A review. *Ecological Engineering*, *61*, 582-592. https://doi.org/10.1016/j.ecoleng.2013.06.023

Vymazal, J. (2020). Removal of nutrients in constructed wetlands for wastewater treatment through plant harvesting – Biomass and load matter the most. *Ecological Engineering*, *155*, 105962. https://doi.org/10.1016/j.ecoleng.2020.105962

Waki, M., Yasuda, T., Suzuki, K., Komada, M., & Abe, K. (2015). Distribution of anammox bacteria in a free-water-surface constructed wetland with wild rice (*Zizania latifolia*). *Ecological Engineering*, *81*, 165-172. https://doi.org/10.1016/j.ecoleng.2015.04.005

Walker, R. D., & Doerfler, J. (2009). *Wild rice: The Minnesota legislature, a distinctive crop, GMOs, and Ojibwe perspectives*. University of Minnesota. https://hdl.handle.net/11299/189319

Walker, R. E. D., Pastor, J., & Dewey, B. W. (2010). Litter quantity and nitrogen immobilization cause oscillations in productivity of wild rice (*Zizania palustris* L.) in Northern Minnesota. *Ecosystems*, *13*, 485-498. https://doi.org/10.1007/s10021-010-9333-6

Walker, S. L., Dixit, S. S., Andersen, D., Caux, P. Y., Chambers, P. A., Charlton, M. C., Howes, L. A., & Kingsley, L. (2003). *Scoping science assessment of the impacts of freshwater aquaculture on the Canadian environment* [NWRI contribution 03-522]. National Water Research Institute, Environment Canada. https://publications.gc.ca/pub?id=9.868692&sl=0

Wan, N.-F., Li, S.-X., Li, T., Cavalieri, A., Weiner, J., Zheng, X.-Q., Ji, X.-Y., Zhang, J.-Q., Zhang, H.-L., & Zhang, H. (2019). Ecological intensification of rice production through rice-fish co-culture. *Journal of Cleaner Production*, *234*, 1002-1012. https://doi.org/10.1016/j.jclepro.2019.06.238

Wang, J., & Zhang, Z. (2020). Phytoplankton, dissolved oxygen and nutrient patterns along a eutrophic river-estuary continuum: Observation and modeling. *Journal of Environmental Management*, *261*, 110233. https://doi.org/10.1016/j.jenvman.2020.110233

Wang, X., Li, J., Chen, J., Cui, L., Li, W., Gao, X., & Liu, Z. (2020). Water quality criteria of total ammonia nitrogen (TAN) and un-ionized ammonia (NH_3-N) and their ecological risk in the Liao River, China. *Chemosphere*, *243*, 125328. https://doi.org/10.1016/j.chemosphere.2019.125328

Wang, Z., Wang, C., Jiang, H., & Liu, H. (2022). Higher dissolved oxygen levels promote downward migration of phosphorus in the sediment profile: Implications for lake restoration. *Chemosphere*, *301*, 134705. https://doi.org/10.1016/j.chemosphere.2022.134705

Wellburn, A. R. (1994). The spectral determination of chlorophylls *a* and *b*, as well as total carotenoids, using various solvents with spectrophotometers of different resolution. *Journal of Plant Physiology*, *144*(3), 307-313. https://doi.org/10.1016/S0176-1617(11)81192-2

Werker, A. G., Dougherty, J. M., McHenry, J. L., & Van Loon, W. A. (2002). Treatment variability for wetland wastewater treatment design in cold climates. *Ecological Engineering*, *19*(1), 1-11. https://doi.org/10.1016/S0925-8574(02)00016-2

White, J. R., & Reddy, K. (2009). Biogeochemical dynamics I: Nitrogen cycling in wetlands. In E. Maltby, & T. Barker (Eds.), *The Wetlands Handbook* (1 ed., pp. 213-227). Wiley-Blackwell.

Wickham, H. (2016). *ggplot2: Elegant Graphics for Data Analysis*. Springer. https://doi.org/10.1007/978-3-319-24277-4

Wickham, H., Averick, M., Bryan, J., Chang, W., McGowan, L. D. A., François, R., Grolemund, G., Hayes, A., Henry, L., & Hester, J. (2019). Welcome to the Tidyverse. *Journal of Open Source Software*, *4*(43), 1686. https://doi.org/10.21105/joss.01686

Winchell, E. H., & Dahl, R. P. (1984). *Wild rice production, prices, and marketing* [Miscellaneous Publication 29]. Minnesota Agricultural Experiment Station. https://hdl.handle.net/11299/112696

Wu, H., Zhang, J., Ngo, H. H., Guo, W., Hu, Z., Liang, S., Fan, J., & Liu, H. (2015). A review on the sustainability of constructed wetlands for wastewater treatment: Design and operation. *Bioresource Technology*, *175*, 594-601. https://doi.org/10.1016/j.biortech.2014.10.068

Wu, Y., Xia, L., Yu, Z., Shabbir, S., & Kerr, P. G. (2014). In situ bioremediation of surface waters by periphytons. *Bioresource Technology*, *151*, 367-372. https://doi.org/10.1016/j.biortech.2013.10.088

Wurts, W. A. (2003). Daily pH cycle and ammonia toxicity. *World Aquaculture*, *34*(2), 20-21.

Xu, X. W., Wu, J. W., Qi, M. X., Lu, Q. X., Lee, P. F., Lutz, S., Ge, S., & Wen, J. (2015). Comparative phylogeography of the wild-rice genus *Zizania* (Poaceae) in Eastern Asia and North America. *American Journal of Botany*, *102*(2), 239-247. https://doi.org/10.3732/ajb.1400323

Yang, J., Zhang, X., Xie, Y., Song, C., Sun, J., Zhang, Y., Giesy, J. P., & Yu, H. (2017). Ecogenomics of zooplankton community reveals ecological threshold of ammonia nitrogen. *Environmental Science & Technology*, *51*(5), 3057-3064. https://doi.org/10.1021/acs.est.6b05606

Yang, T., & Kim, H.-J. (2020). Comparisons of nitrogen and phosphorus mass balance for tomato-, basil-, and lettuce-based aquaponic and hydroponic systems. *Journal of Cleaner Production*, *274*, 122619. https://doi.org/10.1016/j.jclepro.2020.122619

Yarkina, N. N., & Logunova, N. N. (2022). Fisheries and aquaculture: Implementing sustainable development goals. In: A. G. Arkhipov (Ed.), *Sustainable Fisheries and Aquaculture: Challenges and Prospects for the Blue Bioeconomy* (pp. 149-160). Springer, Cham. https://doi.org/10.1007/978-3-031-08284-9_15

Ye, F., & Li, Y. (2009). Enhancement of nitrogen removal in towery hybrid constructed wetland to treat domestic wastewater for small rural communities. *Ecological Engineering*, *35*(7), 1043-1050. https://doi.org/10.1016/j.ecoleng.2009.03.009

Zhang, H., & Zhai, C. k. (2016). Effects of Chinese and North American wild rice on blood lipids, oxidative stress, and inflammation factors in hyperlipidemic rats. *Cereal Chemistry*, *93*(4), 357-363. https://doi.org/10.1094/CCHEM-06-15-0119-R

Zhu, M., Zhu, G., Zhao, L., Yao, X., Zhang, Y., Gao, G., & Qin, B. (2013). Influence of algal bloom degradation on nutrient release at the sediment–water interface in Lake Taihu, China. *Environmental Science and Pollution Research*, *20*, 1803-1811. https://doi.org/10.1007/s11356-012-1084-9

APPENDIX

Appendix Tables

Table A - 1. Water quality parameters of source water used in UM site mesocosms.

Parameter	Result	Units
Cl	4.4*	mg L^{-1}
Ca	20.776*	mg L^{-1}
Fe	0.05230*	mg L^{-1}
Mg	6.321*	mg L^{-1}
Na	30.019*	mg L^{-1}
K	1.237*	mg L^{-1}
SO_4	72.1*	mg L^{-1}
Conductivity	303*	µS cm^{-1}
pH	7.66*	Unitless
Alkalinity	69.7*	mg L^{-1} as $CaCO_3$
Total P	0.440+	mg L^{-1} as PO_4–P
Total dissolved P	0.356+	mg L^{-1} as PO_4–P
Soluble reactive P	0.172+	mg L^{-1} as PO_4–P
Total dissolved N	0.42+	mg L^{-1}
Total ammonia N	0.024+	mg L^{-1}
Nitrite N	0.104+	mg L^{-1}
Nitrate N	0.557+	mg L^{-1}
Dissolved organic C	12.528+	mg L^{-1}

* Data is compiled from the City of Winnipeg's 2021 water treatment plant treated water quality test results

+Samples were collected and analyzed following the method described in the text; the mean of three samples collected at the start, middle, and end of the 2022 summer is reported

Table A - 2. Soil quality parameters of source soil used in UM site mesocosms. Results are reported on a dry mass basis, where applicable.

Parameter	Result	Units
N	93	mg kg^{-1}
Olsen P	46.0	mg kg^{-1} as PO_4–P
K	690	mg kg^{-1}
S	110	mg kg^{-1}
Ca	6200	mg kg^{-1}
Mg	1800	mg kg^{-1}
Na	180	mg L^{-1}
pH	7.6	Unitless
Conductivity	2.02	dS m^{-1}
Organic matter	6.5	%
Cation exchange capacity	48.3	meq per 100 g
Wet density	1.46	g cm^{-3}
Dry density	0.89	g cm^{-3}

Table A - 3. Parameters of logistic growth models fit to biofilm tile chlorophyll *a* data. P_0 = initial chl *a* concentration, K = carrying capacity, r = growth rate, df = degrees of freedom, σ = goodness of fit, t_{mid} = time where half K is reached.

Mesocosm type	Total P loading (mg m^{-2})	P_0 (µg cm^{-2})	K (µg cm^{-2})	r (d^{-1})	df	σ	t_{mid} (d)
EW	0 (EW-REF-A)	1.66×10^{-3}	1.60	0.13	15	0.32	54.55
	0 (EW-REF-B)	1.34×10^{-12}	3.87	0.56	15	0.93	50.84
	165.4	6.67×10^{-13}	1.07	0.54	15	0.27	52.43
	205.5	4.04×10^{-2}	4.13	0.08	15	0.67	61.28
	321.5	7.37×10^{-1}	4.02×10^{6}	0.01	15	0.51	1047.26
	638.4	1.10×10^{-1}	2.85	0.07	15	0.58	45.95
	997.5	1.33×10^{-2}	3.00	0.12	15	0.68	43.36
Unplanted	0 (UP-REF)	5.94×10^{-4}	1.26	1.13	15	0.45	6.79

Table A - 4. Results from fitted linear mixed models (LMMs) for water quality parameters. Instances where response variables were log_{10}-transformed to meet model assumptions are indicated.

Mesocosm type	Response variable	Treatment		Time		Treatment x Time	
		F	p	F	p	F	p
EW	TP	0.243	0.642	**6.695**	**0.013**	**6.289**	**0.016**
	TDP	0.249	0.637	**6.531**	**0.015**	**5.747**	**0.021**
	SRP	0.225	0.649	0.914	0.344	0.619	0.435
	TDN	3.199	0.118	0.690	0.410	0.113	0.739
	TAN	<0.001	0.990	0.075	0.785	0.050	0.824
	NO_2–N	0.300	0.586	0.716	0.401	0.004	0.951
	$log_{10}(NO_3–N)$	0.226	0.637	0.233	0.631	0.035	0.852
	PP	0.013	0.913	3.144	0.082	**4.931**	**0.031**
	log_{10}(chl *a*)	0.060	0.811	<0.001	0.990	0.364	0.549
	log_{10}(SRSi)	0.222	0.653	0.147	0.703	0.417	0.522
	Alk	<0.001	0.986	0.308	0.586	0.975	0.336
	DOC	0.133	0.717	0.640	0.427	0.045	0.832
	Temp	0.046	0.831	0.001	0.975	0.078	0.781
	DO	0.327	0.587	1.041	0.309	0.700	0.404
	pH	0.139	0.724	0.156	0.693	<0.001	0.990
	SPC	0.959	0.329	1.110	0.294	0.959	0.329
NS	TP	2.488	0.141	0.132	0.717	0.017	0.895
	TDP	0.526	0.486	**12.052**	**0.001**	**10.183**	**0.002**
	SRP	0.116	0.735	0.299	0.586	0.476	0.492
	TDN	0.033	0.858	2.283	0.135	**8.363**	**0.005**
	log_{10}(TAN)	0.797	0.375	0.549	0.461	0.117	0.734
	NO_2–N	0.532	0.468	0.072	0.790	1.281	0.261
	$log_{10}(NO_3–N)$	0.109	0.743	1.594	0.211	0.022	0.883
	PP	0.794	0.393	0.001	0.981	0.041	0.840
	chl *a*	0.625	0.444	0.028	0.868	0.268	0.606
	SRSi	0.175	0.685	0.120	0.730	0.002	0.967
	Alk	1.651	0.207	0.648	0.426	0.002	0.965
	DOC	0.214	0.645	2.887	0.093	0.254	0.616
	Temp	0.131	0.718	0.245	0.621	0.034	0.854
	DO	1.151	0.307	1.039	0.309	2.088	0.150
	pH	2.658	0.136	0.042	0.838	**10.679**	**0.001**
	SPC	0.133	0.724	0.056	0.812	1.005	0.317
FP	TP	0.172	0.681	**8.531**	**0.005**	**4.456**	**0.038**
	TDP	0.001	0.981	**7.572**	**0.008**	3.128	0.082
	SRP	0.063	0.804	**14.841**	**<0.001**	**6.213**	**0.015**
	TDN	0.199	0.657	0.173	0.679	0.178	0.674
	TAN	1.096	0.298	0.831	0.365	0.866	0.355
	NO_2–N	0.002	0.965	0.093	0.761	0.044	0.835
	NO_3–N	0.056	0.814	**13.763**	**<0.001**	0.055	0.815
	PP	0.484	0.488	**3.997**	**0.049**	**7.329**	**0.008**
	log_{10}(chl *a*)	1.122	0.294	**4.825**	**0.031**	**7.782**	**0.007**
	SRSi	0.402	0.531	**5.170**	**0.026**	**4.677**	**0.034**
	Alk	NA	NA	NA	NA	NA	NA
	DOC	0.007	0.933	0.900	0.345	0.090	0.764
	Temp	0.072	0.788	2.907	0.089	0.144	0.704
	DO	0.269	0.604	**12.468**	**<0.001**	0.366	0.545
	pH	0.560	0.455	1.005	0.317	2.315	0.129
	SPC	2.676	0.106	3.347	0.068	**8.143**	**0.005**

Bold values indicate statistical significance at a significance level (alpha) of 0.05. NA = not applicable.

Table A - 5. Results from general linear models for soil quality parameters. Response variables were analyzed in units of mg kg^{-1} (on a dry mass basis) with the exception of pH (unitless), EC (mS cm^{-1}), OM (%), and CEC (mg per 100 g). Predictor variables were calculated by adding a unique constant for each mesocosm type (C) to the total phosphorus (TP) loading from aquaculture wastewater additions. Values for C were as follows: EW = 89.6, NS = 42.9, FP = 285.2.

Mesocosm type	Response variable	Background			Final			Change		
		Equation	p	R^2	Equation	p	R^2	Equation	p	R^2
EW	OP	-6.96 + 21.4X	0.228	0.274	-0.872 + 15.4X	0.196	0.308	6.09 – 5.99X	0.366	0.165
	K	445 + 28.2X	0.355	0.172	557 – 36.9X	0.218	0.284	112 + 65.1X	0.243	0.260
	S	169 – 50.2X	**0.017**	0.714	31 + 8.02X	0.499	0.096	-138 + 58.2X	**0.005**	0.816
	Ca	5.4E3 + 83X	0.794	0.015	4.8E3 + 2.1X	0.988	<0.001	-643 – 80.7X	0.843	0.009
	Mg	2.04E3 – 176X	0.372	0.161	1.74E3 – 95.6X	0.542	0.079	-299 + 80.7X	0.360	0.169
	Na	279 – 56.9X	0.244	0.258	183 – 19.4X	0.640	0.047	-95.3 + 37.5X	0.143	0.376
	B	0.583 + 0.0184X	0.884	0.005	0.819 + 0.293X	**0.029**	0.647	0.236 + 0.274X	0.066	0.525
	Cu	7.64 + 0.434X	0.381	0.156	6.37 + 0.676X	0.470	0.109	-1.27 + 1.11X	0.081	0.488
	Fe	132 + 12X	0.635	0048	94.8 + 42X	0.267	0.238	-36.9 + 30X	0.150	0.366
	Mn	46.1 + 29.1X	0.196	0.308	29.9 + 38.7X	0.312	0.202	-16.2 + 9.61X	0.618	0.053
	Zn	4.15 – 0.956X	0.265	0.240	6.13 – 1.54X	0.190	0.315	1.98 – 0.588X	0.303	0.209
	Cl	111 – 30X	**0.028**	0.655	-17.2 + 27.7X	0.148	0.368	-128 + 57.7X	**0.014**	0.735
	pH	8.09 – 0.0229X	0.855	0.007	7.72 + 0.0107X	0.966	<0.001	-0.369 + 0.0336X	0.888	0.004
	EC	1.13 – 0.16X	0.146	0.372	0.519 + 0.012X	0.734	0.025	-0.606 + 0.172X	0.075	0.501
	OM	6.11 + 0.162X	0.821	0.011	4.07 + 0.687X	0.339	0.183	-2.04 + 0.524X	**0.022**	0.682
	CEC	46 – 1.1X	0.609	0.056	39.9 – 0.81X	0.649	0.045	-6.15 + 0.291X	0.917	0.002
NS	OP	17.4 + 3.28X	0.067	0.358	15.8 + 3.63X	**0.045**	0.413	-1.6 + 0.359X	0.766	0.012
	K	500 + 10.4X	0.722	0.017	501 – 3.16X	0.860	0.004	1.41 – 13.6X	0.695	0.020
	S	33.4 – 2.21X	0.841	0.005	17.9 + 5.11X	0.186	0.208	-15.5 + 7.31X	0.416	0.084
	Ca	5E3 + 110X	0.541	0.049	4.2E3 + 160X	0.379	0.098	-826 + 51.9X	0.849	0.005
	Mg	1.6E3 + 64.8X	0.467	0.068	1.55E3 + 26.3X	0.799	0.009	-53.7 – 38.5X	0.705	0.019
	Na	133 + 7.6X	0.768	0.011	144 – 3.73X	0.728	0.016	11.4 – 11.3X	0.549	0.047
	B	0.533 – 0.0591X	0.466	0.068	0.851 + 0.164X	0.052	0.393	0.318 + 0.223X	0.095	0.309
	Cu	5.57 – 0.514X	**0.006**	0.635	4.33 + 1.79X	0.186	0.208	-1.24 + 2.3X	0.108	0.290
	Fe	93.5 – 9.51X	**0.033**	0.453	101 + 18.2X	0.316	0.125	7.79 + 27.7X	0.118	0.278
	Mn	72.3 – 0.56X	0.868	0.004	21.7 + 29.1X	0.185	0.208	-50.6 + 29.6X	0.163	0.228
	Zn	4.1 + 0.105X	0.952	<0.001	-5.46 + 4.81X	0.123	0.271	-9.56 + 4.7X	0.198	0.198
	Cl	14.4 – 0.92X	0.685	0.022	31.8 – 2.66X	0.459	0.070	17.3 – 1.74X	0.469	0.067
	pH	7.88 + 0.137X	0.388	0.094	7.48 + 0.174X	**0.036**	0.442	-0.403 + 0.0368X	0.855	0.004
	EC	0.407 + 0.0634X	0.463	0.069	0.401 + 0.0432X	0.097	0.306	-0.00606 – 0.0202X	0.798	0.009
	OM	6.16 – 0.141X	0.523	0.053	5.46 – 0.168X	0.117	0.279	-0.701 – 0.0264X	0.901	0.002
	CEC	40.3 + 1.01X	0.503	0.058	35 + 1.2X	0.497	0.059	-5.32 + 0.184X	0.931	<0.001
FP	OP	14.3 + 8.03X	0.301	0.082	14.6 + 6.39X	0.066	0.237	0.336 – 1.64X	0.783	0.006
	K	312 + 20.6X	0.580	0.024	290 – 10.4X	0.580	0.024	-22.2 – 31X	0.281	0.089
	S	20.3 – 1.77X	0.292	0.085	0.316 + 8.11X	0.067	0.235	-20 + 9.88X	**0.047**	0.270
	Ca	2.6E3 + 620X	**0.028**	0.319	4.E3 + 14X	0.936	<0.001	1.45E3 – 610X	**0.037**	0.294
	Mg	486 + 29.8X	0.502	0.035	589 + 5.75X	0.843	0.003	103 – 24.1X	0.479	0.039
	Na	17.4 + 1.92X	0.095	0.200	19.3 + 4.82X	**0.021**	0.347	1.88 + 2.9X	0.055	0.254
	B	0.188 + 0.0549X	0.468	0.041	0.892 + 0.191X	0.137	0.162	0.703 + 0.137X	0.139	0.160
	Cu	1.18 + 1.01X	0.257	0.098	5.07 – 0.0282X	0.938	<0.001	3.89 – 1.04X	0.150	0.152
	Fe	30.6 + 24.4X	0.129	0.168	181 – 2.35X	0.841	0.003	150 – 26.8X	0.207	0.120
	Mn	168 + 4.88X	0.850	0.003	232 – 5.59X	0.327	0.074	64.1 – 10.5X	0.690	0.013
	Zn	1.02 + 0.399X	0.340	0.070	1.57 + 0.0402X	0.881	0.002	0.556 – 0.358X	0.270	0.093
	Cl	6.76 + 0.838X	0.515	0.033	7.52 + 4.73	0.208	0.119	0.765 + 3.89X	0.250	0.101
	pH	8.3 – 0.00427X	0.937	<0.001	7.3 + 0.0302X	0.625	0.019	-1 + 0.0345X	0.697	0.012
	EC	0.502 + 0.0236X	0.509	0.034	0.252 + 0.0427X	0.100	0.194	-0.25 + 0.019X	0.533	0.031
	OM	3.66 + 0.761X	0.245	0.102	4.34 + 0.314X	0.222	0.112	0.682 – 0.447X	0.443	0.046
	CEC	17.7 + 3.43X	**0.036**	0.295	26 + 0.0501X	0.960	<0.001	8.23 – 3.38X	**0.042**	0.282

Bold values indicate statistical significance at a significance level (alpha) of 0.05

Table A - 6. Results from general linear models for plant tissue nutrient parameters at the UM field site. Response variables were analyzed in units of mg kg^{-1} (on a dry mass basis).

Mesocosm type	Response variable	Wild rice shoots			Wild rice roots			Algal mats			Hornwort		
		Equation	p	R^2	Equation	p	R^2	Equation	p	R^2	Equation	p	R^2
EW	TN	5.79E3 + 169X	0.845	0.008	7.33E3 – 443X	0.536	0.081	-1.91E3 + 9.29E3X	0.061	0.741	3.25E4 – 5.42E3X	0.295	0.215
	NO_3–N	19.5 – 4.89X	0.394	0.148	14.3 – 3.18X	0.409	0.140	-9.53 + 8.97X	0.469	0.186	6.75 + 0.746X	0.936	0.001
	K	2.6E4 + 110X	0.991	<0.001	2.1E4 + 640X	0.899	0.004	2E4 – 4.2E3X	0.331	0.309	1.4E4 – 600X	0.844	0.008
	TS	986 – 144X	0.299	0.212	1.87E3 + 98.8X	0.847	0.008	2.15E3 + 1.36E3X	0.763	0.035	6.5E3 – 1.12E3X	**0.023**	0.675
	Ca	4.19E3 – 336X	0.642	0.047	9.82E3 + 198X	0.932	0.002	2.26E4 + 2.54E4X	0.471	0.184	7.16E4 – 1.43E4X	**0.020**	0.695
	Mg	1.28E3 + 66.3X	0.792	0.015	8.47E3 – 938X	0.369	0.163	1.33E4 – 2.78E3X	0.116	0.616	7.11E3 – 126X	0.873	0.006
	B	4.75 – 0.89X	0.374	0.160	15 + 0.292X	0.863	0.007	44.2 + 2.99X	0.926	0.003	265 – 53X	0.612	0.055
	Cu	3.56 – 0.585X	0.129	0.398	20.3 – 3.71X	0.314	0.200	5.13 + 2.81X	0.215	0.450	4.9 + 2.51X	0.317	0.198
	Fe	217 – 19.7X	0.567	0.070	1.22E4 + 276X	0.862	0.007	6.56E3 – 1.75E3X	0.118	0.612	-3.31E3 + 2.46E3X	0.295	0.215
	Mn	-4.62 + 55.2X	0.337	0.184	451 – 33.1X	0.769	0.019	-1.08E3 + 769X	0.153	0.547	-730 + 853X	0.569	0.069
	Zn	-28.6 + 51.3X	0.653	0.044	163 – 28.2X	0.537	0.081	864 – 238X	0.280	0.365	206 + 3.24X	0.962	<0.001
NS	TN	5.64E3 + 184X	0.779	0.012	5.55E3 + 169X	0.729	0.018	7.01E3 + 3.13E3X	**0.017**	0.887	3.89E3 + 4.59E3X	**0.033**	0.452
	NO_3–N	20.2 – 4.24X	0.407	0.100	11.4 – 1.36X	0.699	0.023	-10 + 8.92X	0.268	0.380	19.6 – 5.55X	**0.031**	0.460
	K	9.9E3 + 3.4E3X	0.105	0.331	6.8E3 + 4.4E3X	0.248	0.185	9.4E3 + 1.7E3X	0.439	0.209	1.6E4 – 580X	0.683	0.022
	TS	1.04E3 – 131X	0.235	0.194	2.19E3 + 15.5X	0.965	<0.001	9.02E3 + 1.46E3X	0.487	0.172	6.16E3 – 760X	0.257	0.157
	Ca	4.09E3 + 121X	0.906	0.002	1.56E4 – 1.7E3X	0.378	0.112	1.42E5 – 3.44E4X	0.238	0.418	4.16E4 – 1.86E3X	0.928	0.001
	Mg	1.33E3 + 172X	0.359	0.121	9.07E3 – 1.07E3X	0.228	0.199	1.28E4 – 2.13E3X	**0.036**	0.815	8.55E3 – 599X	0.299	0.134
	B	4.05 – 0.158X	0.793	0.010	16.5 + 2.22X	0.602	0.041	66.7 + 39.2X	0.088	0.675	-16.9 + 68.5X	0.478	0.065
	Cu	3.73 – 0.214X	0.806	0.009	20.1 – 2.03X	0.370	0.116	20.8 – 4.13X	0.227	0.433	24.7 – 3.99X	**0.047**	0.407
	Fe	731 – 76.1X	0.797	0.010	1.65E4 – 1.38E3X	0.461	0.080	8.17E3 – 2.25E3X	0.121	0.605	1.82E3 – 185X	0.741	0.014
	Mn	136 + 19.6X	0.470	0.077	300 – 7.85X	0.755	0.015	200 – 23.1X	0.484	0.175	248 – 17.7X	0.580	0.040
	Zn	157 – 19.4X	0.700	0.022	229 – 30.8X	0.796	0.010	133 – 12.1X	0.583	0.111	325 – 72.1X	**0.019**	0.516

Bold values indicate statistical significance at a significance level (alpha) of 0.05.

Table A - 7. Parameters of logistic growth models fit to biofilm tile chlorophyll *a* data for NS mesocosms. P_0 = initial chl *a* concentration, K = carrying capacity, r = growth rate, df = degrees of freedom, σ = goodness of fit, t_{mid} = time where half K is reached.

Total phosphorus loading (mg m^{-2})	P_0 (µg cm^{-2})	K (µg cm^{-2})	r (d^{-1})	df	*σ*	t_{mid} (d)
0 (NS-REF-A)	5.05×10^{-2}	0.91	0.07	15	0.30	40.23
0 (NS-REF-B)	3.83×10^{-10}	1.41	1.01	15	0.80	21.78
0 (NS-REF-C)	1.25×10^{-1}	0.75	0.10	14	0.44	16.23
66.5	6.25×10^{-3}	3.82	0.16	15	0.58	40.10
106.4	1.71×10^{-2}	2.97	0.11	15	0.56	46.76
166.3	3.83×10^{-10}	1.41	1.01	15	0.80	21.78
259.4	1.12×10^{-9}	1.38	0.93	15	0.47	22.50
405.7	8.54×10^{-13}	1.31	0.56	15	0.55	50.56
638.4	2.41×10^{-3}	1.19	0.17	15	0.21	37.50
997.5	1.25×10^{-1}	0.75	0.10	14	0.44	16.23

Table A - 8. Water quality parameters of source water used in RL site mesocosms (i.e. pond water). Concentrations of nutrients are reported as mg L^{-1} with phosphorus parameters reported as PO_4–P.

TP	TDP	SRP	TDN	TAN	NO_2–N	NO_3–N
2.319	1.950	0.770	2.550	0.657	0.182	1.48

Table A - 9. Soil quality parameters of source soil used in RL site mesocosms. Results are reported on a dry mass basis, where applicable.

Parameter	Result	Units
N	7	mg kg^{-1}
Olsen P	46.0	mg kg^{-1} as PO_4–P
K	620	mg kg^{-1}
S	22	mg kg^{-1}
Ca	4700	mg kg^{-1}
Mg	820	mg kg^{-1}
Na	28	mg L^{-1}
pH	8.1	Unitless
Conductivity	0.79	dS m^{-1}
Organic matter	6.2	%
Cation exchange capacity	31.7	meq per 100 g
Wet density	1.60	g cm^{-3}
Dry density	0.63	g cm^{-3}

Table A - 10. Water quality parameters of water used to maintain water levels in RL site mesocosms (i.e. RM of Carman water). Concentrations of nutrients are reported as mg L^{-1} with phosphorus parameters reported as PO_4–P. Results are reported as the mean (± SD) of two samples collected at the middle and end of the 2022 summer.

TP	TDP	SRP	TDN	TAN	NO_2–N	NO_3–N	SRSi	DOC
0.058 (0.012)	0.048 (0.019)	0.076 (0.032)	0.295 (0.005)	<LOD	0.120 (0.025)	0.575 (0.318)	0.911*	15.706 (5.584)

*Sample size of n = 1

Table A - 11. Parameters of logistic growth models fit to biofilm tile chlorophyll *a* data for FP mesocosms. P_0 = initial chl *a* concentration, K = carrying capacity, r = growth rate, df = degrees of freedom, σ = goodness of fit, t_{mid} = time where half K is reached.

Mesocosm type	Total phosphorus loading (mg m^{-2})	P_0 (µg cm^{-2})	K (µg cm^{-2})	r (d^{-1})	df	σ	t_{mid} (d)
FP	0 (FP-REF-A)	8.42×10^{-9}	6.12	0.44	12	0.81	46.73
	0 (FP-REF-B)	1.93×10^{-4}	12.49	0.21	12	0.58	52.05
	0 (FP-REF-C)	6.55×10^{-3}	2.46	0.12	12	0.20	51.02
	0 (FP-REF-D)	1.67×10^{-5}	6.82	0.29	12	0.52	45.18
	0 (FP-REF-E)	4.28×10^{-5}	8.73	0.26	12	1.25	46.26
	399.7	6.99×10^{-3}	4.84	0.14	12	0.56	46.51
	559.6	2.70×10^{-5}	2.97	0.24	12	0.36	49.35
	719.5	1.27×10^{-3}	5.43	0.18	12	0.72	46.58
	792.0	6.12×10^{-14}	3.49	0.68	12	0.47	46.70
	1319.0	3.21×10^{-1}	10.37	0.06	11	1.62	58.36
	1798.6	2.10×10^{-13}	3.15	0.71	12	0.74	42.97
	2438.2	2.58×10^{-6}	3.84	0.29	12	0.54	49.58
	3277.5	2.54×10^{-14}	3.60	0.74	12	0.35	44.14
	4436.7	1.11×10^{-11}	2.53	0.61	13	0.22	43.07
	5995.5	1.11×10^{-10}	5.40	0.56	12	0.95	43.60
Unplanted	0 (UP-REF)	4.42×10^{-5}	5.30	0.26	12	0.77	44.91

Table A - 12. Results from general linear models for plant tissue nutrient parameters at the RL field site. Response variables were analyzed in units of mg kg^{-1} (on a dry mass basis).

Study day	Response variable	Seed			Shoot			Root		
		Equation	p	R^2	Equation	p	R^2	Equation	p	R^2
49	TN				4.8E3 + 47.6X	0.755	0.005	2.58E3 + 392X	0.366	0.039
	NO_3–N				7.4 + 2.41X	0.536	0.019	-9.06 + 7.05X	0.083	0.213
	K				4.34E4 – 355X	0.712	0.007	2.27E4 + 1.51E3X	0.676	0.008
	TS				1.66E3 + 81.3X	0.261	0.060	2.28E3 + 351X	0.409	0.033
	Ca				-823 + 1.95E3X	**0.008**	0.294	1.92E3 + 1.7E3X	0.090	0.130
	Mg				1.2E3 + 64.5X	0.243	0.064	2.81E3 + 46.3X	0.891	<0.001
	B				4.73 + 0.542X	0.536	0.018	-2.32 + 6.51X	0.062	0.156
	Cu				3.99 – 0.023X	0.963	<0.001	4.94 + 2.24X	0.365	0.039
	Fe				456 – 11.5X	0.825	0.002	5.19E3 + 525X	0.616	0.012
	Mn				1.02E3 + 350X	0.186	0.082	2.68E3 + 172X	0.752	0.005
	Zn				16.6 + 23.8X	0.608	0.013	-117 + 113X	0.526	0.019
77	TN	2.45E3 + 42.3X	0.799	0.005	1.47E3 + 70.7X	0.625	0.019	747 + 792X	**0.012**	0.399
	NO_3–N	8.04 – 1.66X	0.208	0.119	7.54 – 1.38X	0.409	0.053	9.73 – 1.75X	0.582	0.024
	K	9.02E3 – 881X	0.224	0.112	3.45E4 – 649X	0.785	0.006	3.08E4 + 1.51E3X	0.474	0.040
	TS	877 + 56.2X	0.423	0.050	379 + 68X	0.095	0.200	-284 + 789X	**<0.001**	0.613
	Ca	2.4E3 + 94X	0.769	0.007	6.09E3 – 256X	0.639	0.017	8.36E3 – 489X	0.552	0.028
	Mg	1.89E3 + 46.4	0.819	0.004	1.57E3 – 88.7X	0.465	0.042	4.26E3 – 252X	0.291	0.092
	B	5.36 – 0.198X	0.866	0.002	10.1 – 1X	0.369	0.062	9.46 + 2.16X	0.551	0.028
	Cu	2.3 + 0.969X	**0.032**	0.307	3.02 – 0.275X	0.090	0.205	2.17 + 1.68X	0.330	0.073
	Fe	21 + 19.2X	0.089	0.207	0.627 + 77.5X	0.081	0.216	1.35E4 – 1.05E3X	0.381	0.059
	Mn	28.7 + 12.9X	0.300	0.082	615 + 45.1X	0.757	0.008	7.07E3 – 1.38E3X	**0.048**	0.267
	Zn	-4.9 + 21.7X	**0.027**	0.323	79.6 – 8.08X	0.216	0.115	275 – 30.9X	0.355	0.066

Bold values indicate statistical significance at a significance level (alpha) of 0.05.

Appendix Figures

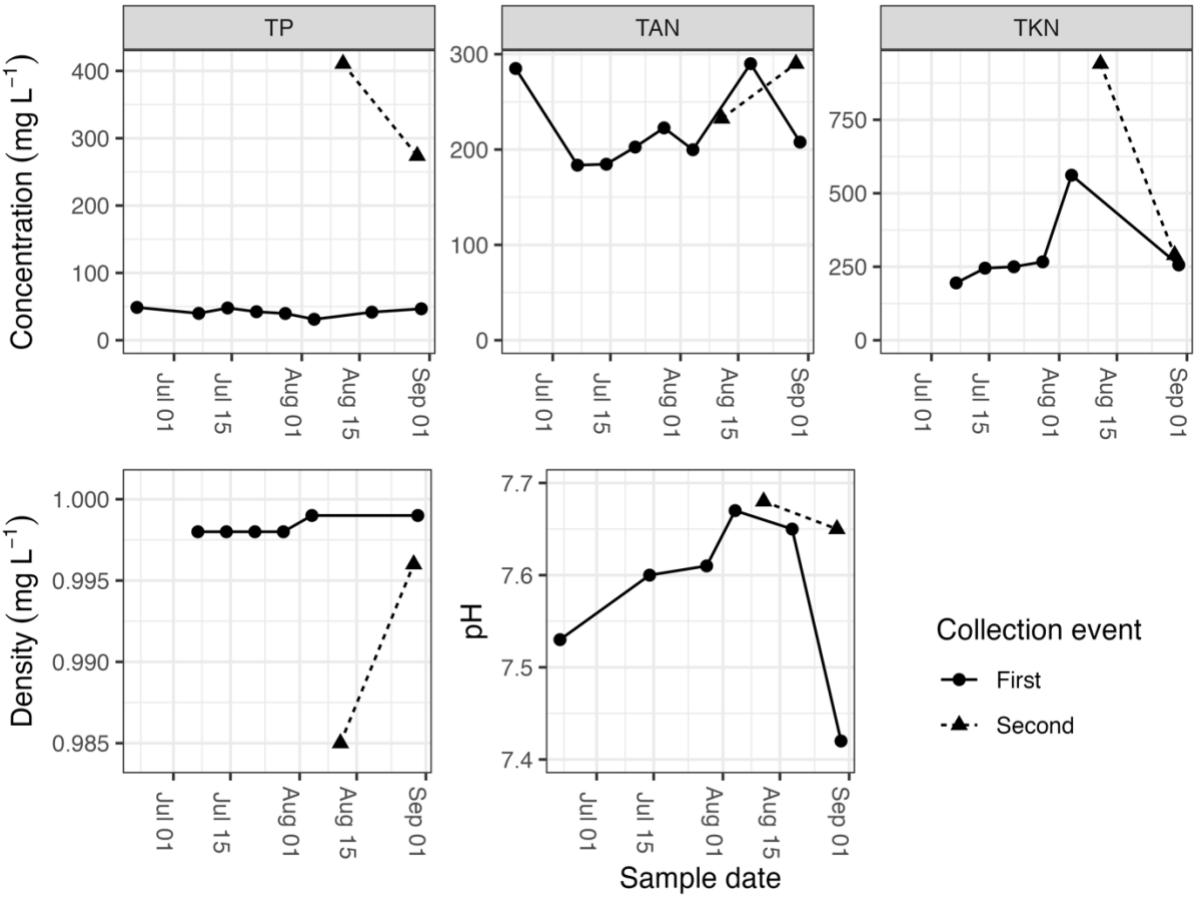

Figure A - 1. Nutrient content, density, and pH of aquaculture wastewater (AWW) applied to mesocosms throughout the 2022 field studies. The second AWW collection was used only at the RL field site. Nutrient content analysis of AWW included total phosphorus (TP), total ammonia nitrogen (TAN), total Kjeldahl nitrogen (TKN).

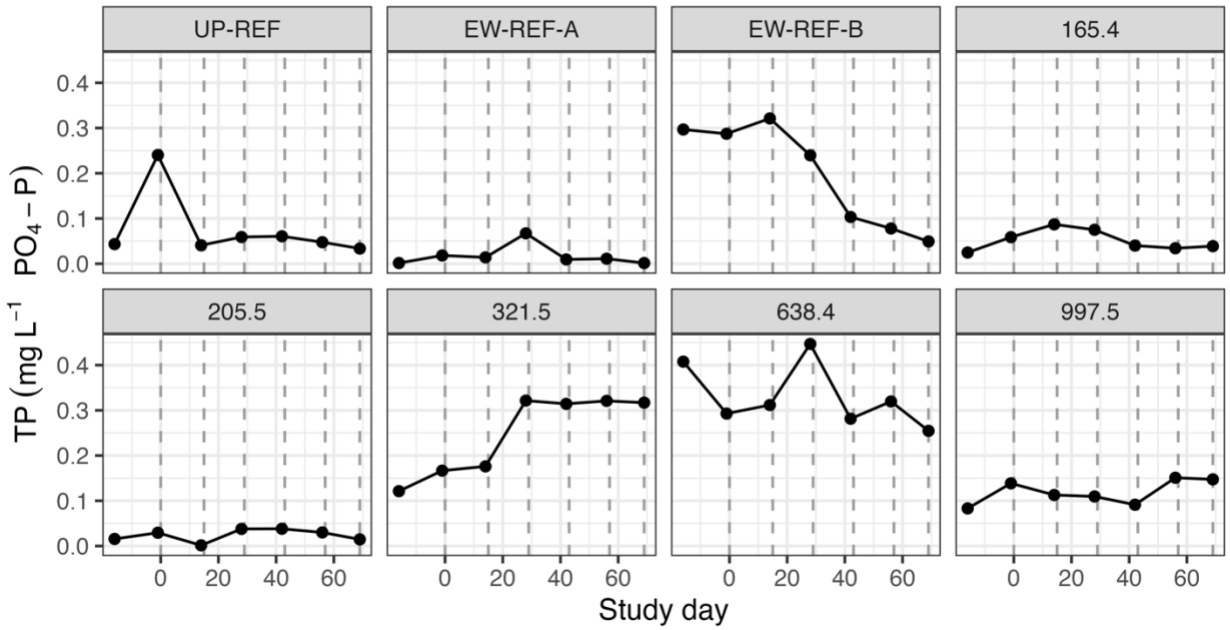

Figure A - 2. Total phosphorus (TP) in EW mesocosm water. Graphical panels indicate total phosphorus loadings (as mg m^{-2}). Vertical dashed lines indicate aquaculture wastewater additions.

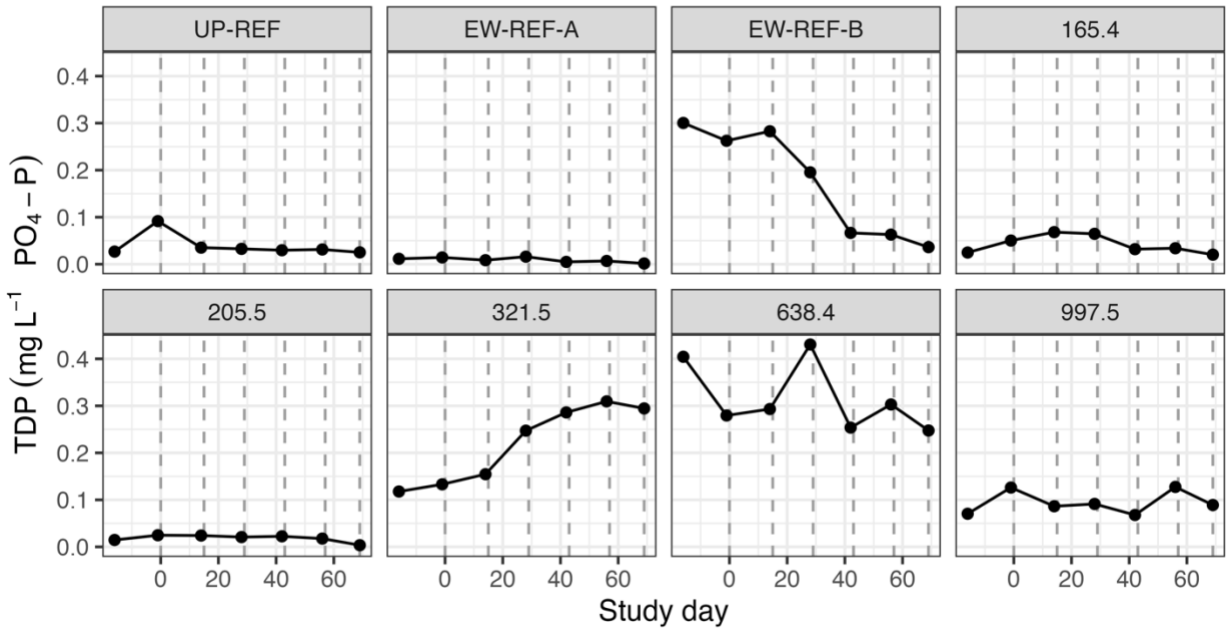

Figure A - 3. Total dissolved phosphorus (TDP) in EW mesocosm water. Graphical panels indicate total phosphorus loadings (as mg m^{-2}). Vertical dashed lines indicate aquaculture wastewater additions.

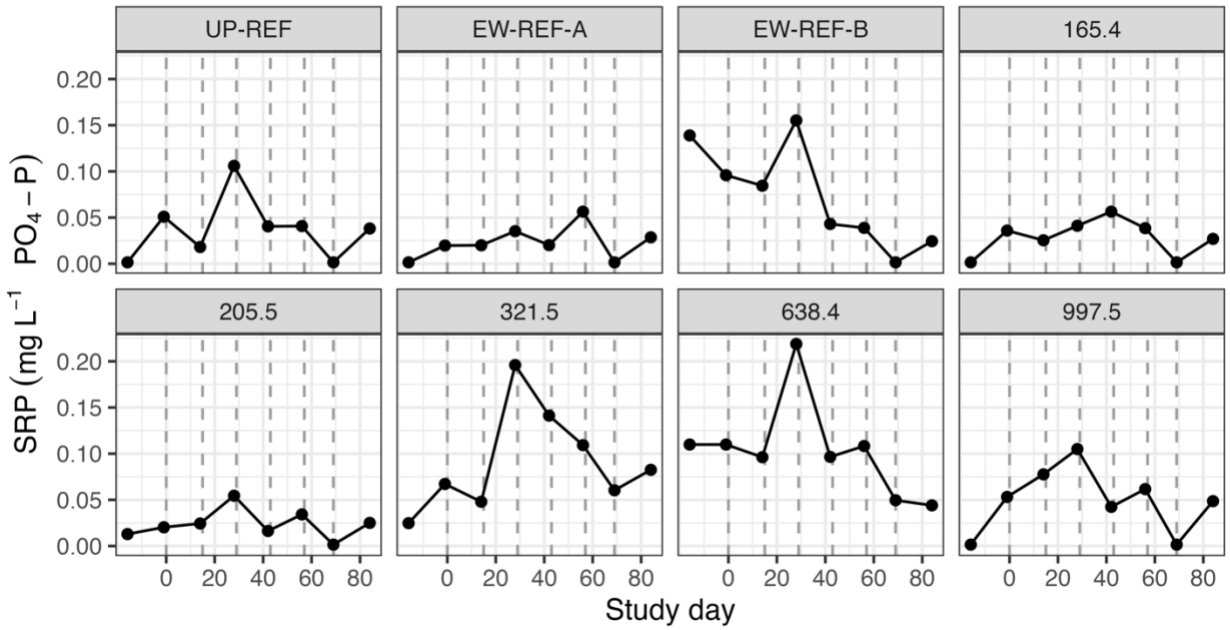

Figure A - 4. Soluble reactive phosphorus (SRP) in EW mesocosm water. Graphical panels indicate total phosphorus loadings (as mg m^{-2}). Vertical dashed lines indicate aquaculture wastewater additions.

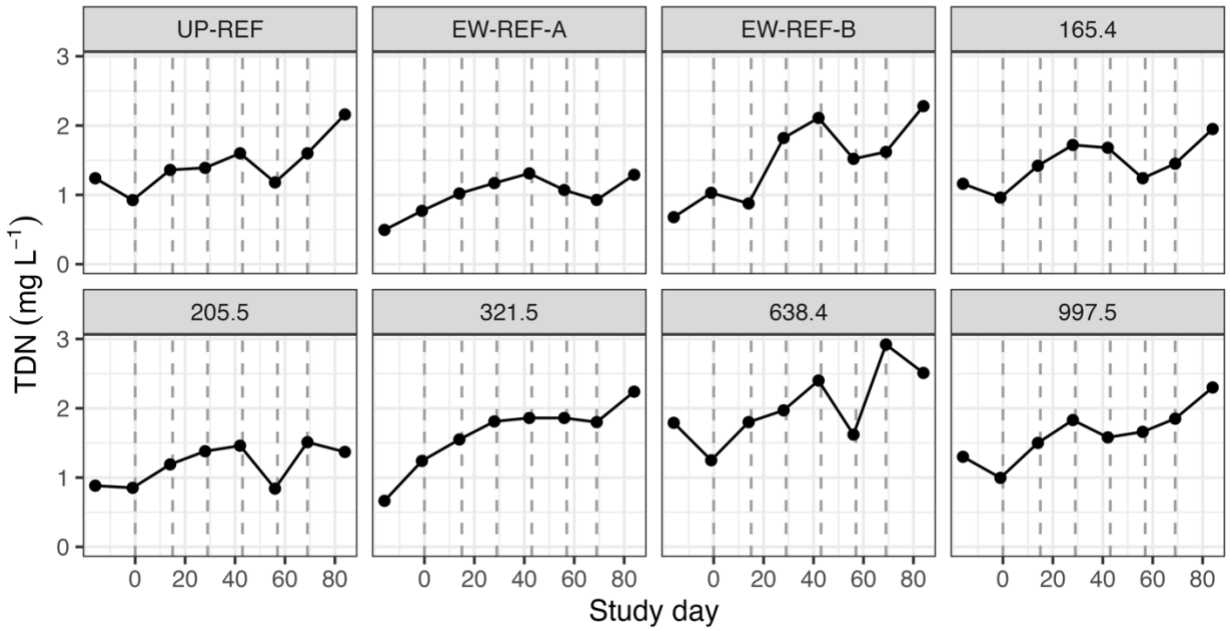

Figure A - 5. Total dissolved nitrogen (TDN) in EW mesocosm water. Graphical panels indicate total phosphorus loadings (as mg m^{-2}). Vertical dashed lines indicate aquaculture wastewater additions.

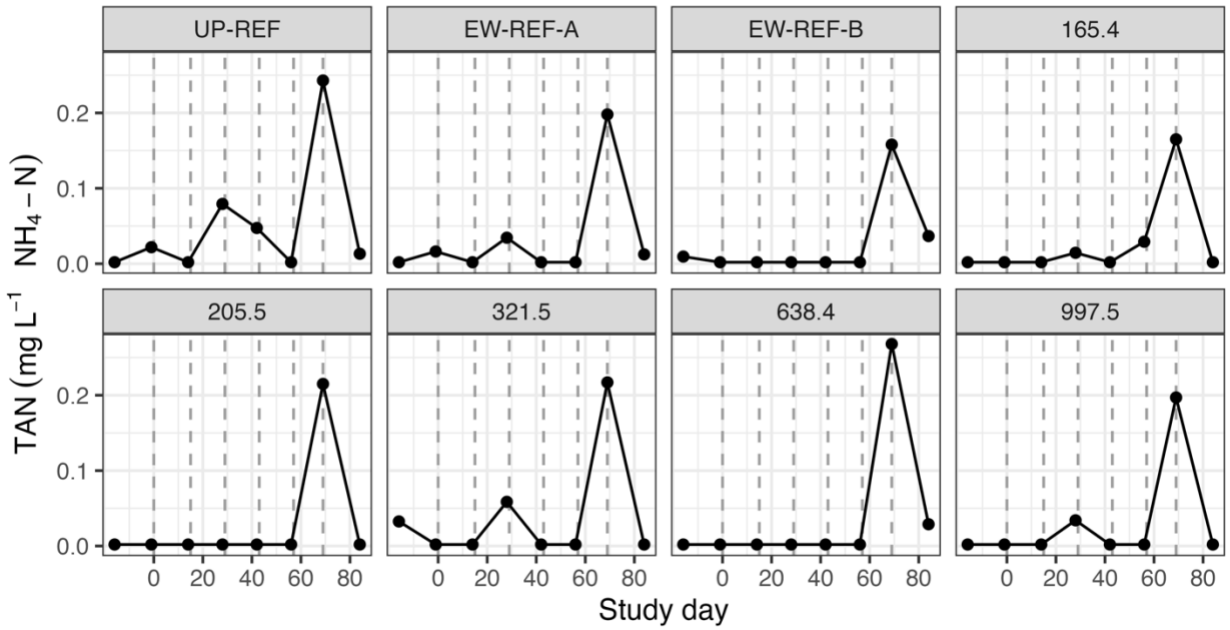

Figure A - 6. Total ammonia nitrogen (TAN) in EW mesocosm water. Graphical panels indicate total phosphorus loadings (as mg m^{-2}). Vertical dashed lines indicate aquaculture wastewater additions.

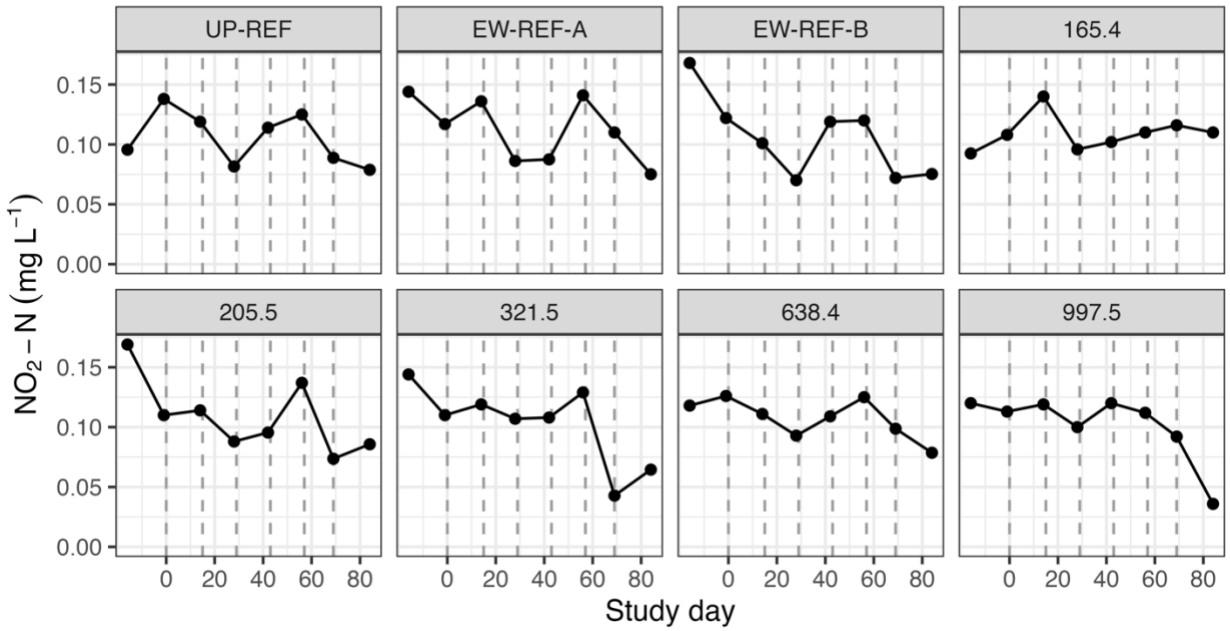

Figure A - 7. Nitrite nitrogen (NO_2–N) in EW mesocosm water. Graphical panels indicate total phosphorus loadings (as mg m^{-2}). Vertical dashed lines indicate aquaculture wastewater additions.

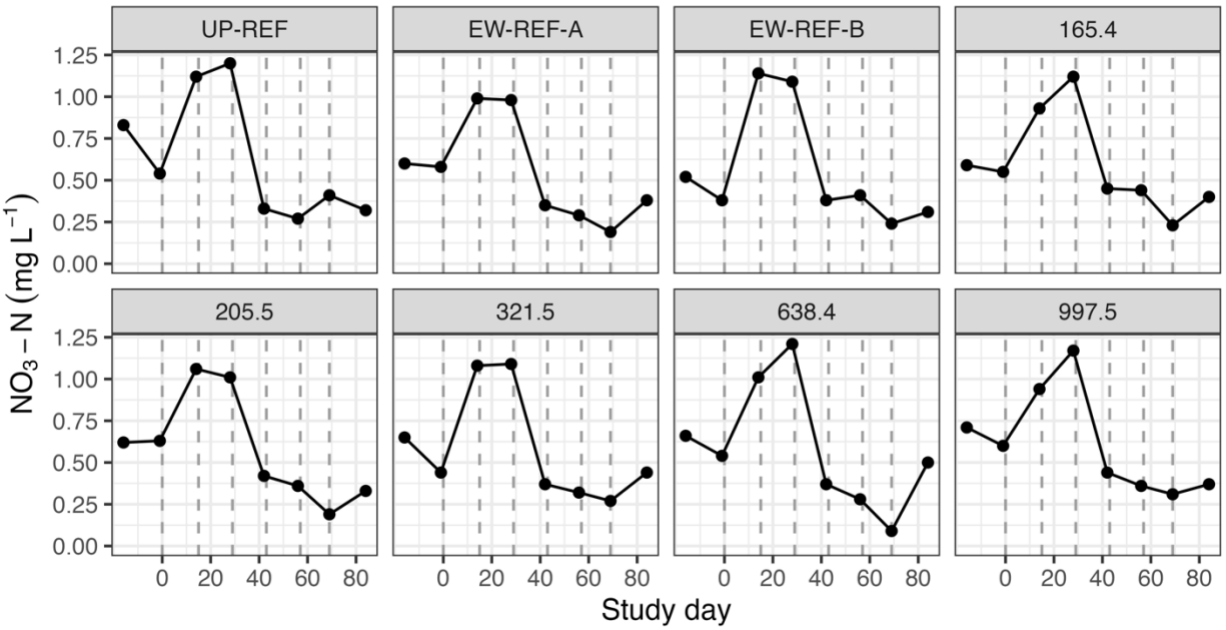

Figure A - 8. Nitrate nitrogen (NO_3–N) in EW mesocosm water. Graphical panels indicate total phosphorus loadings (as mg m^{-2}). Vertical dashed lines indicate aquaculture wastewater additions.

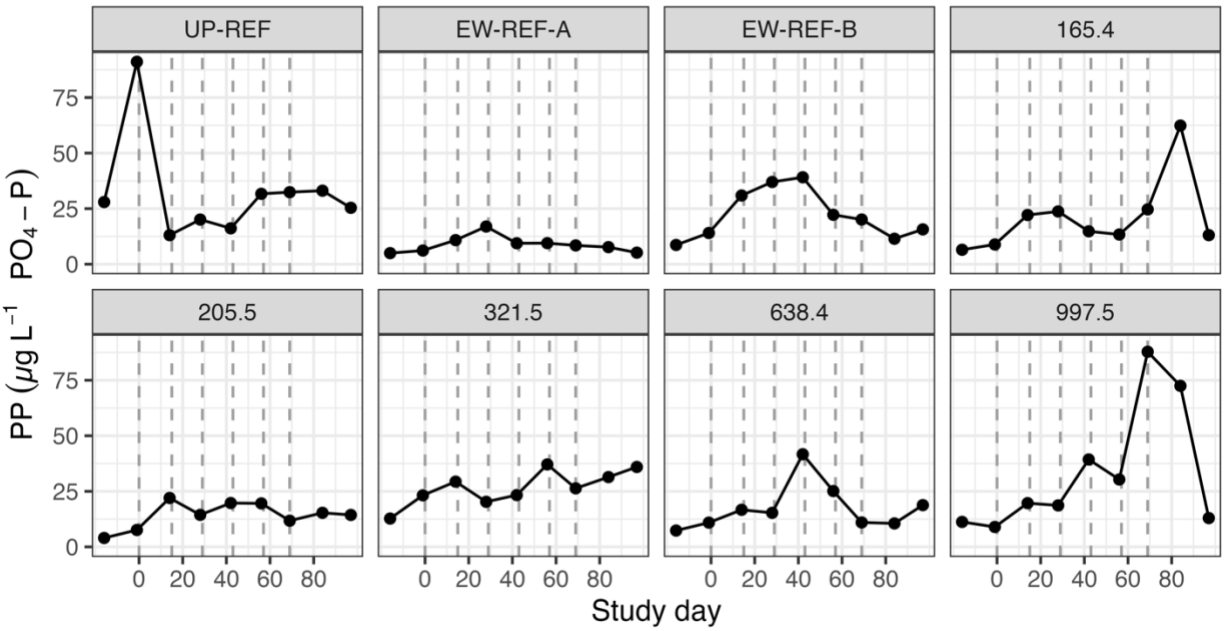

Figure A - 9. Particulate phosphorus (PP) in EW mesocosm water. Graphical panels indicate total phosphorus loadings (as mg m^{-2}). Vertical dashed lines indicate aquaculture wastewater additions.

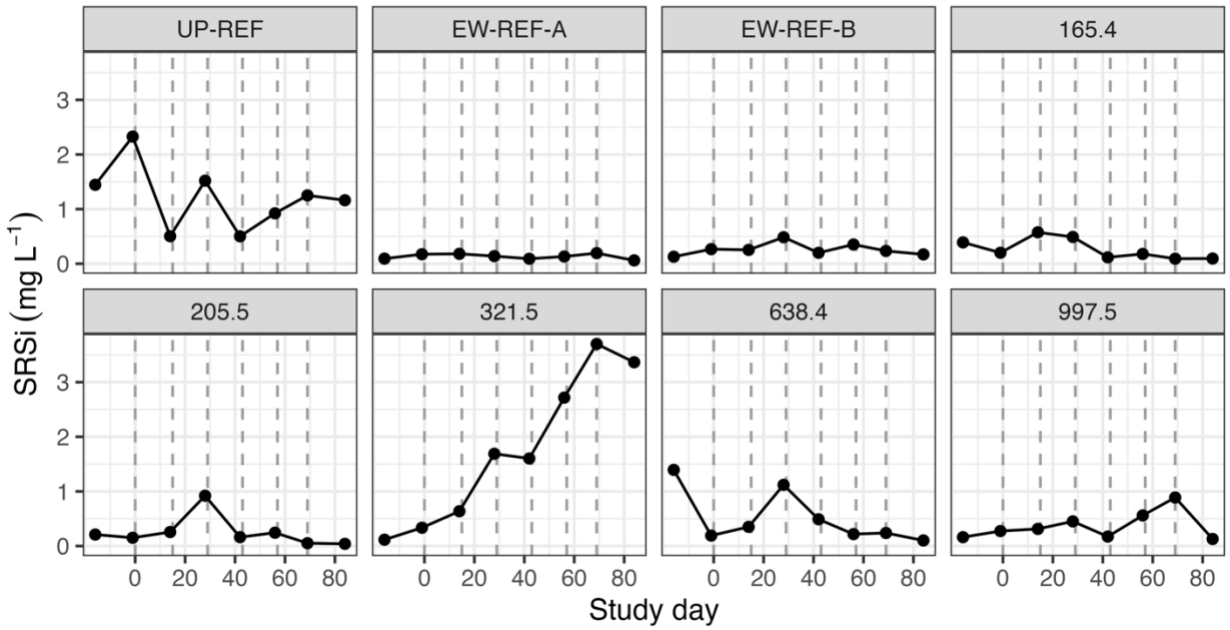

Figure A - 10. Soluble reactive silica (SRSi) in EW mesocosm water. Graphical panels indicate total phosphorus loadings (as mg m^{-2}). Vertical dashed lines indicate aquaculture wastewater additions.

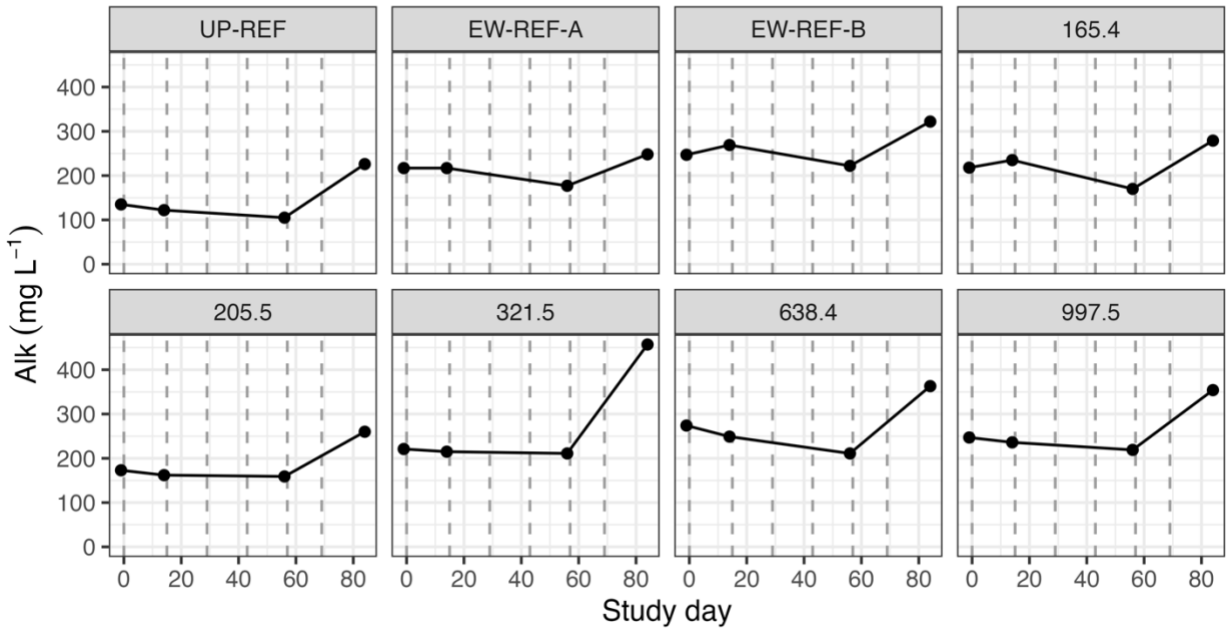

Figure A - 11. Total alkalinity (Alk) in EW mesocosm water. Graphical panels indicate total phosphorus loadings (as mg m^{-2}). Vertical dashed lines indicate aquaculture wastewater additions.

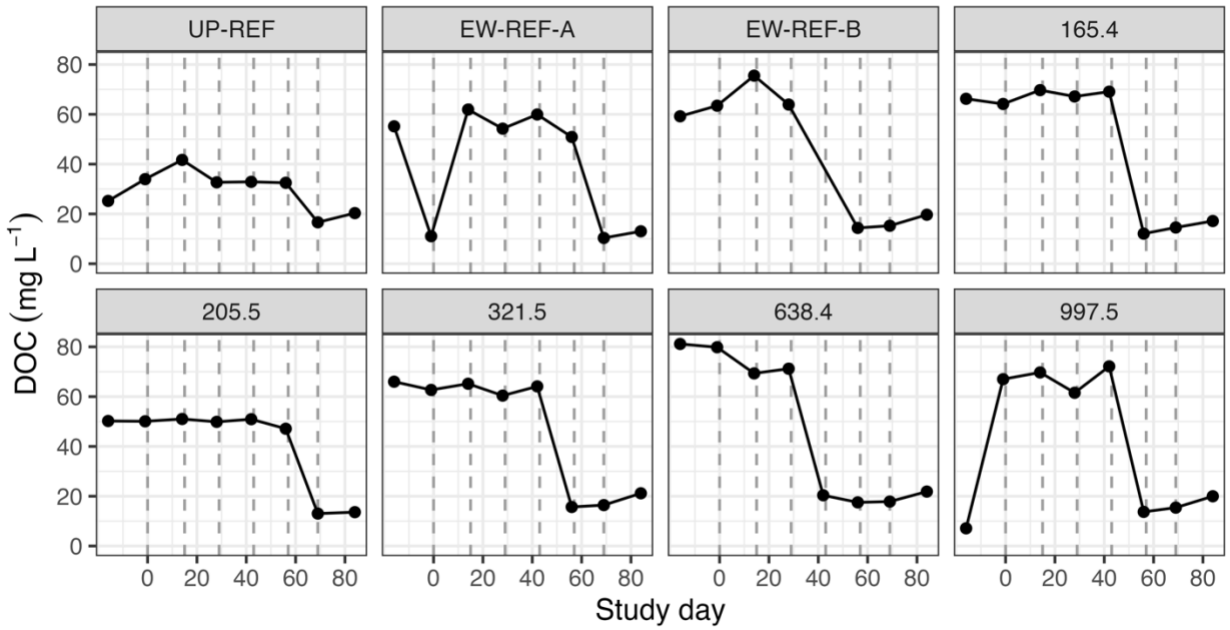

Figure A - 12. Dissolved organic carbon (DOC) in EW mesocosm water. Graphical panels indicate total phosphorus loadings (as mg m^{-2}). Vertical dashed lines indicate aquaculture wastewater additions.

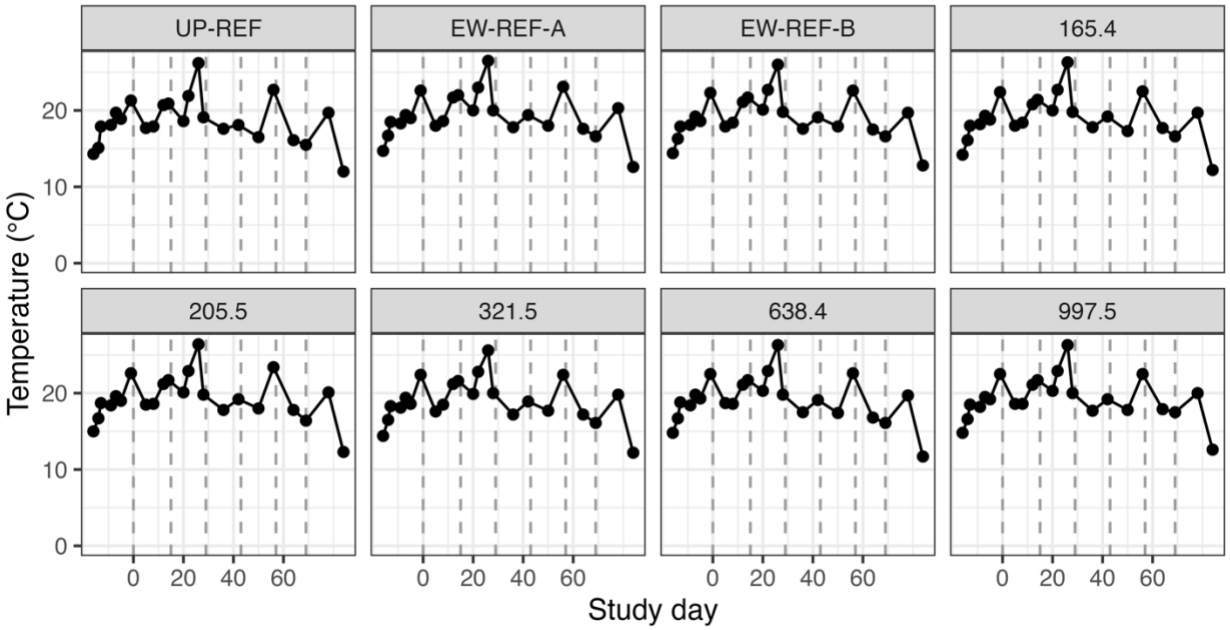

Figure A - 13. Temperature in EW mesocosm water. Graphical panels indicate total phosphorus loadings (as mg m^{-2}). Vertical dashed lines indicate aquaculture wastewater additions.

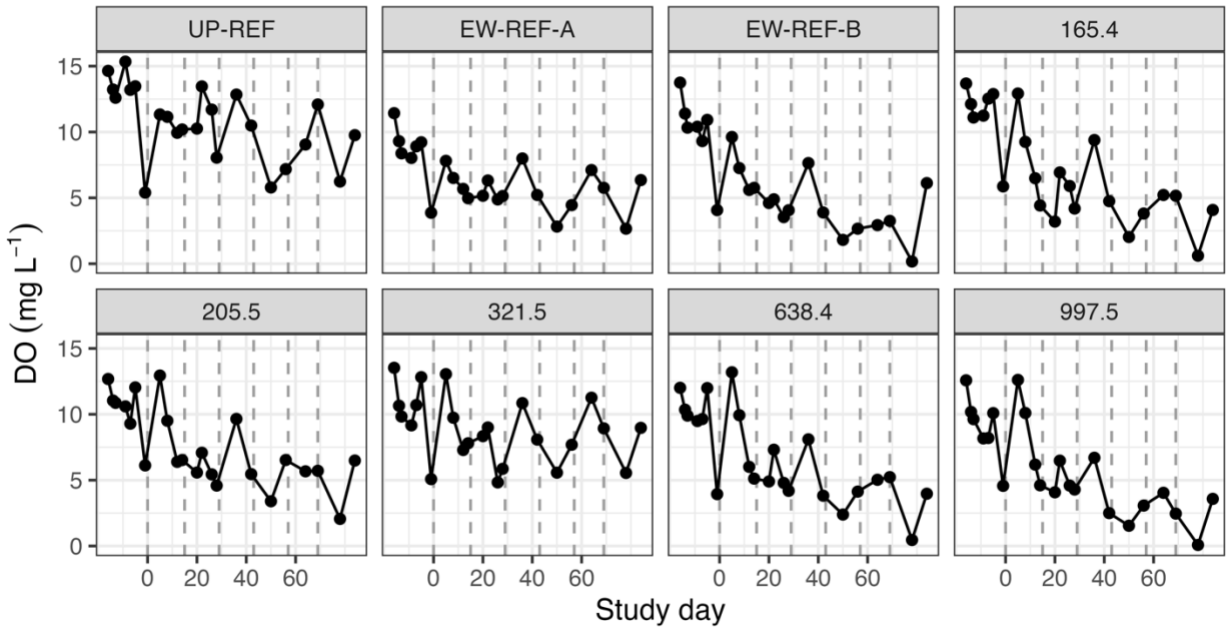

Figure A - 14. Dissolved oxygen (DO) in EW mesocosm water. Graphical panels indicate total phosphorus loadings (as mg m^{-2}). Vertical dashed lines indicate aquaculture wastewater additions.

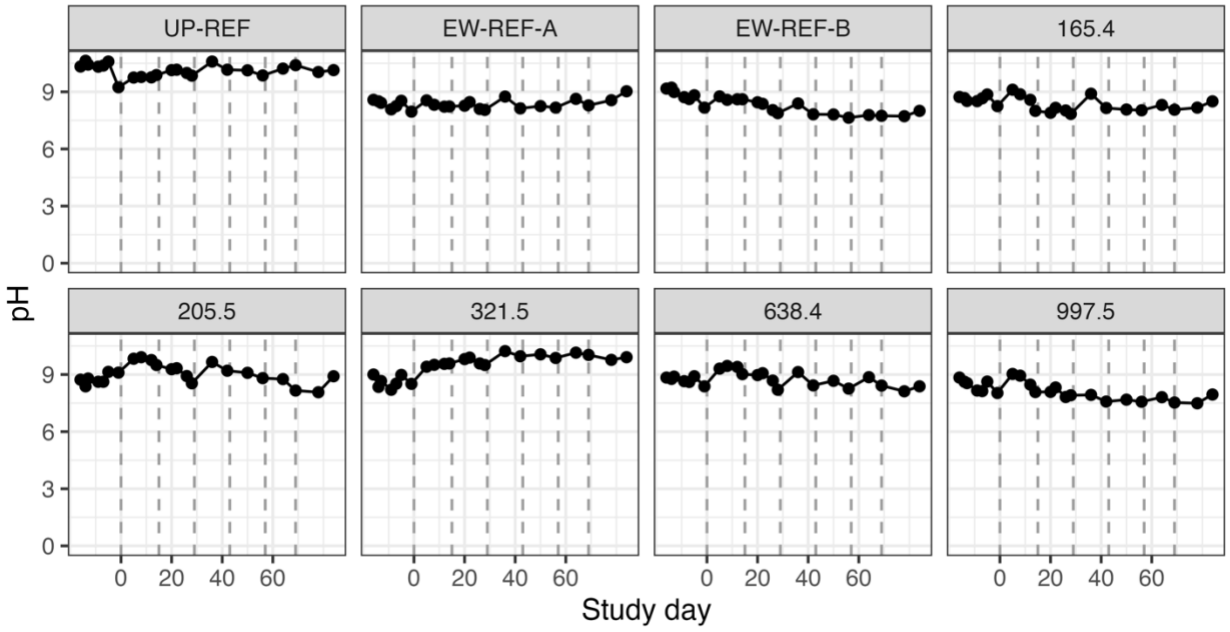

Figure A - 15. pH in EW mesocosm water. Graphical panels indicate total phosphorus loadings (as mg m^{-2}). Vertical dashed lines indicate aquaculture wastewater additions.

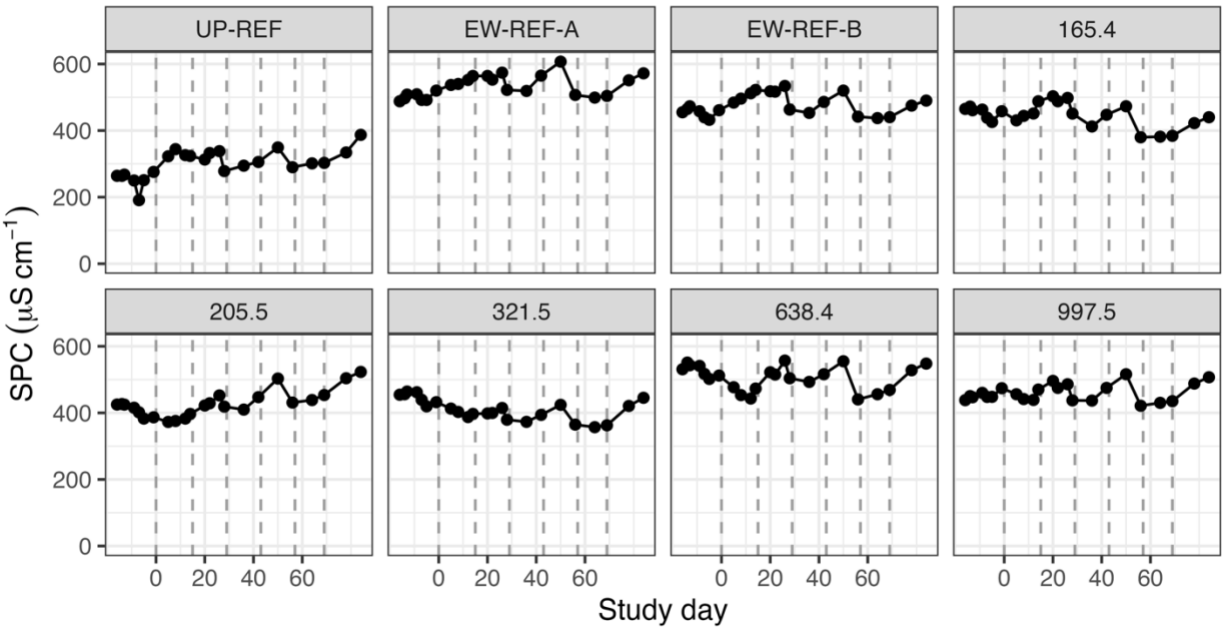

Figure A - 16. Specific conductance (SPC) in EW mesocosm water. Graphical panels indicate total phosphorus loadings (as mg m^{-2}). Vertical dashed lines indicate aquaculture wastewater additions.

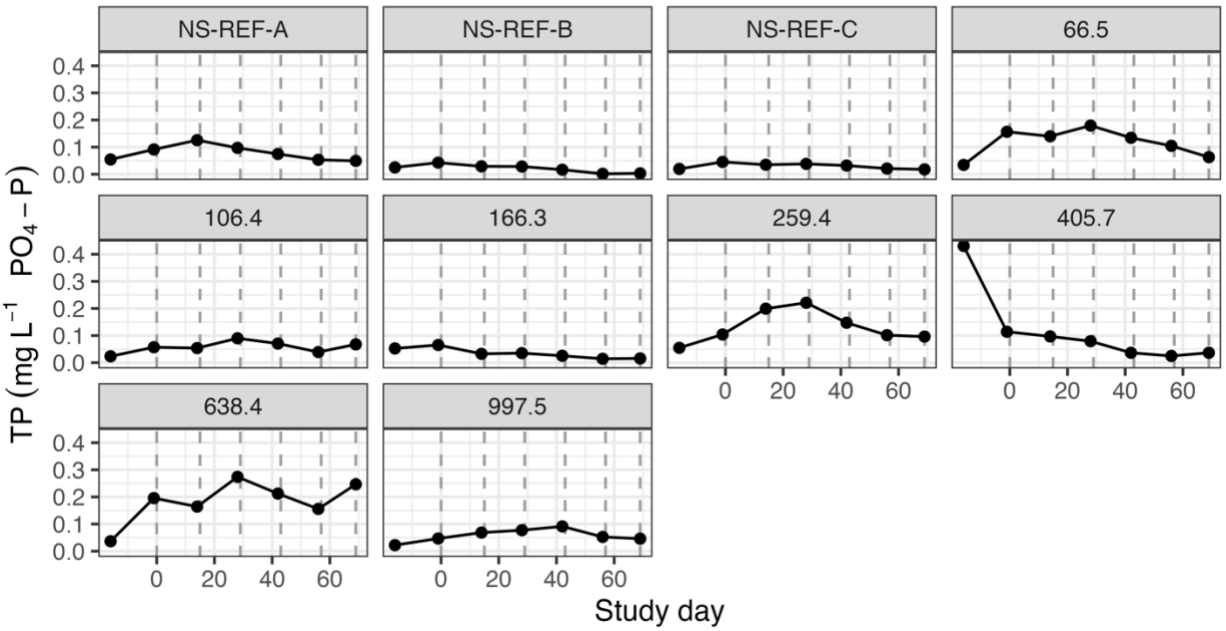

Figure A - 17. Total phosphorus (TP) in NS mesocosm water. Graphical panels indicate total phosphorus loadings (as mg m^{-2}). Vertical dashed lines indicate aquaculture wastewater additions.

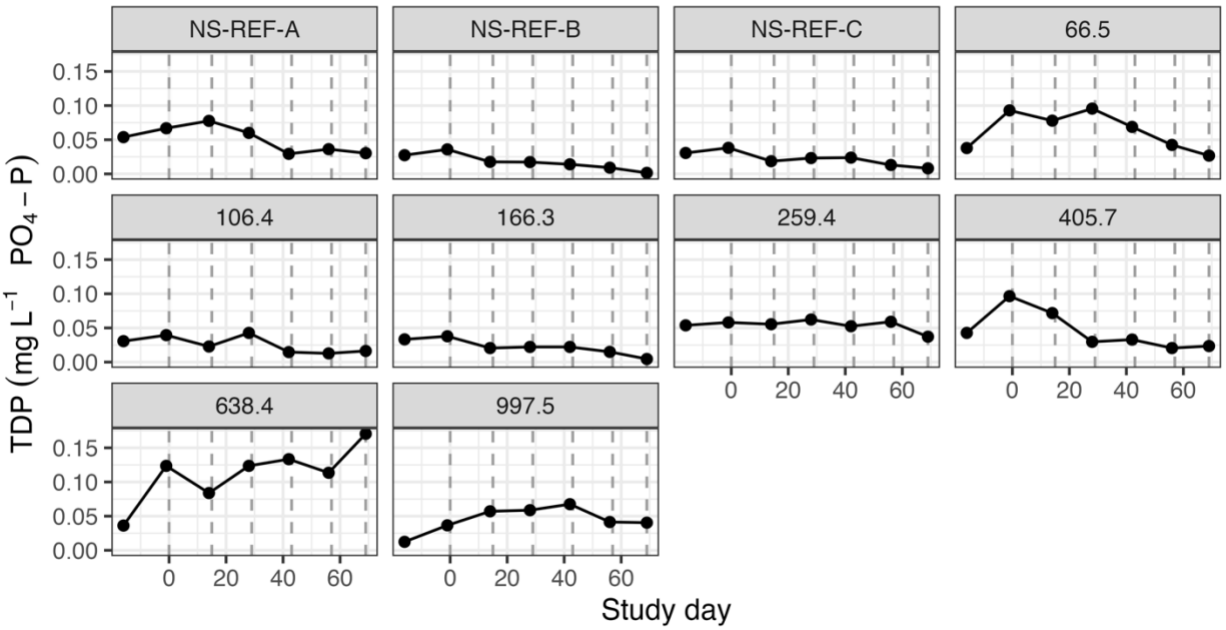

Figure A - 18. Total dissolved phosphorus (TDP) in NS mesocosm water. Graphical panels indicate total phosphorus loadings (as mg m^{-2}). Vertical dashed lines indicate aquaculture wastewater additions.

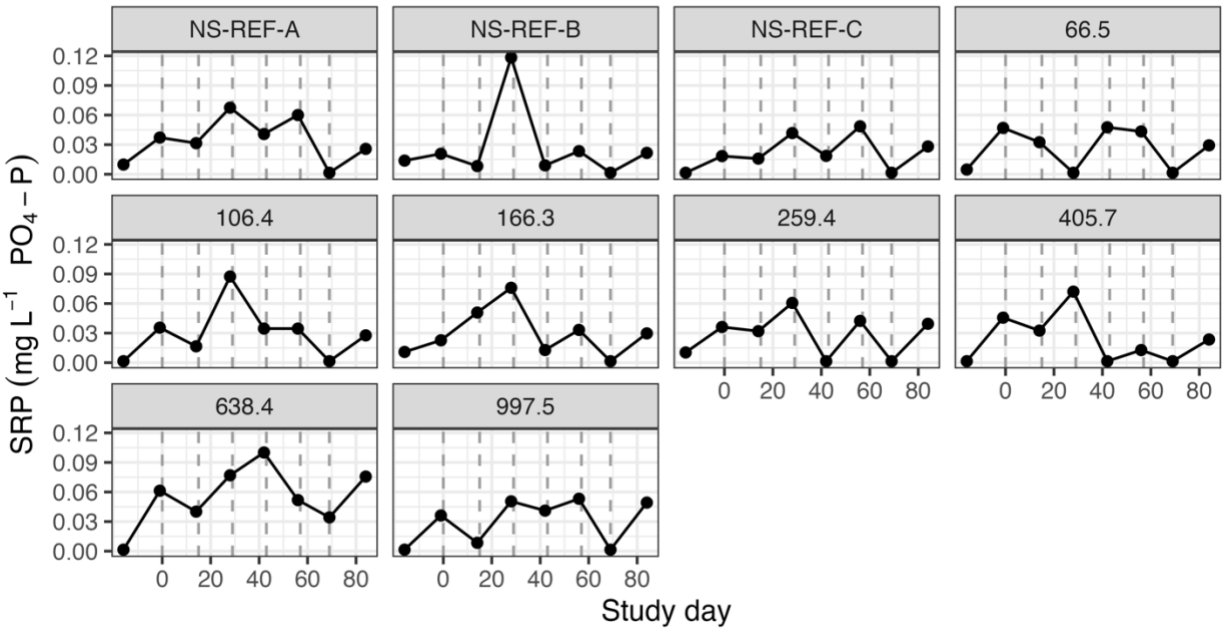

Figure A - 19. Soluble reactive phosphorus (SRP) in NS mesocosm water. Graphical panels indicate total phosphorus loadings (as mg m^{-2}). Vertical dashed lines indicate aquaculture wastewater additions.

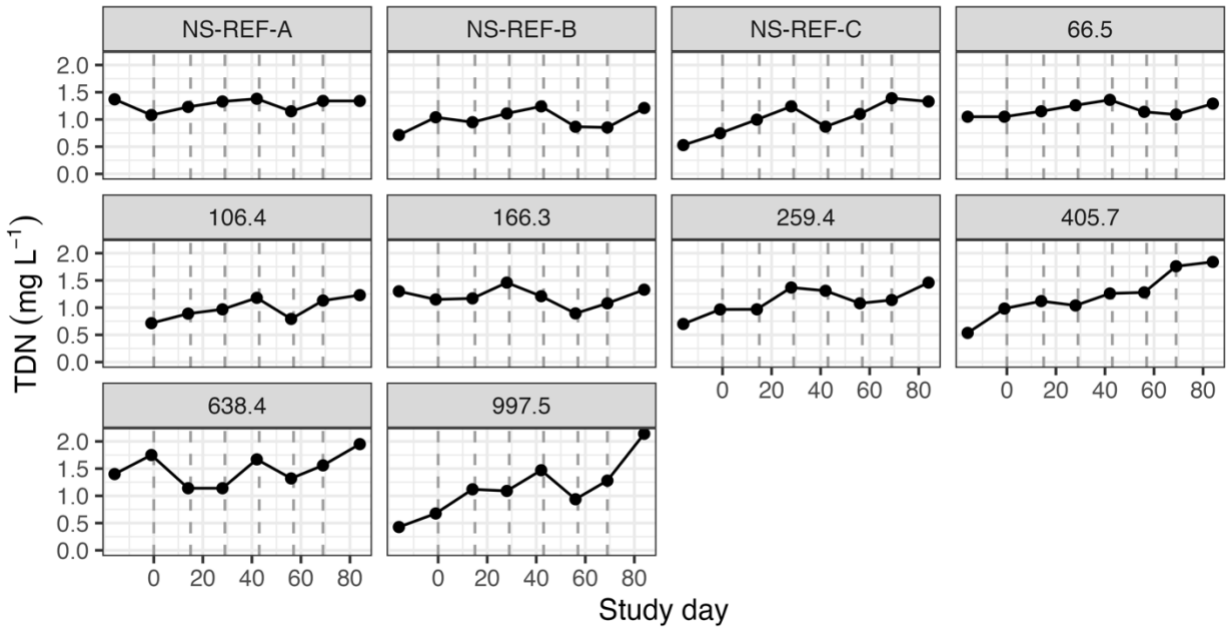

Figure A - 20. Total dissolved nitrogen (TDN) in NS mesocosm water. Graphical panels indicate total phosphorus loadings (as mg m^{-2}). Vertical dashed lines indicate aquaculture wastewater additions.

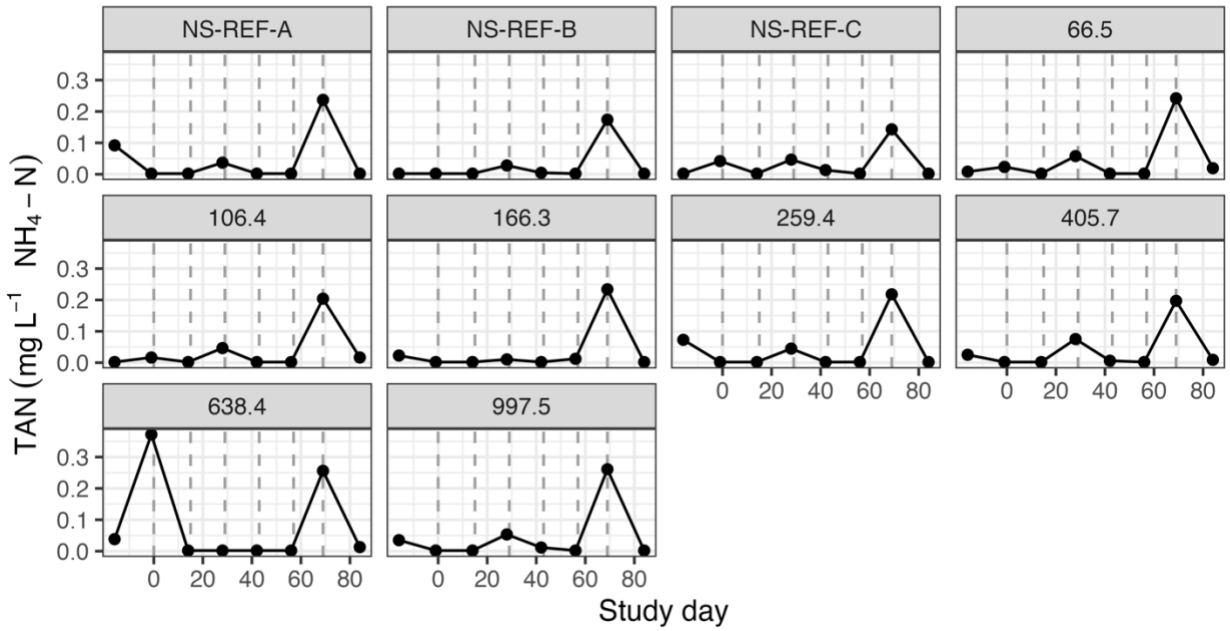

Figure A - 21. Total ammonia nitrogen (TAN) in NS mesocosm water. Graphical panels indicate total phosphorus loadings (as mg m^{-2}). Vertical dashed lines indicate aquaculture wastewater additions.

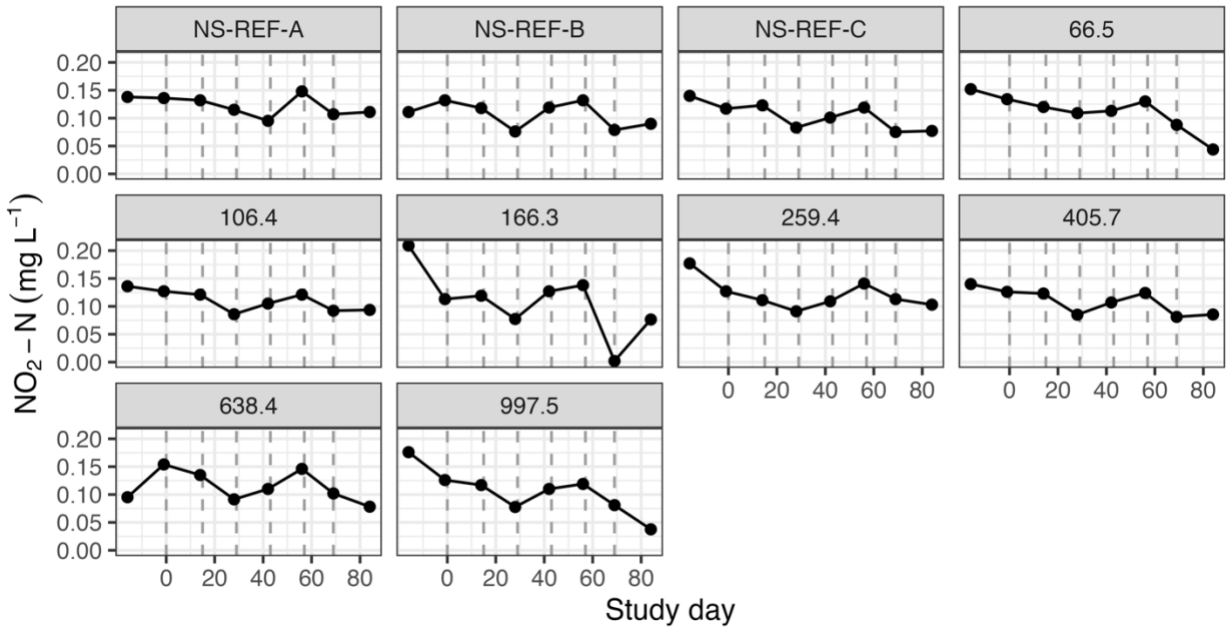

Figure A - 22. Nitrite nitrogen (NO_2–N) in NS mesocosm water. Graphical panels indicate total phosphorus loadings (as mg m^{-2}). Vertical dashed lines indicate aquaculture wastewater additions.

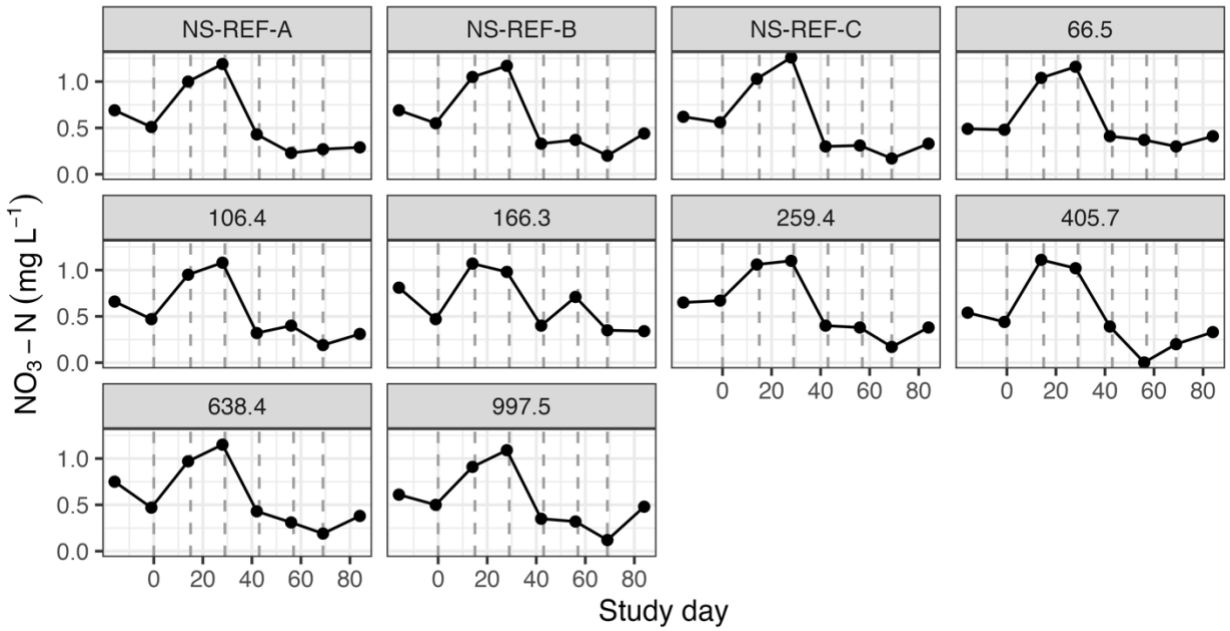

Figure A - 23. Nitrate nitrogen (NO_3–N) in NS mesocosm water. Graphical panels indicate total phosphorus loadings (as mg m^{-2}). Vertical dashed lines indicate aquaculture wastewater additions.

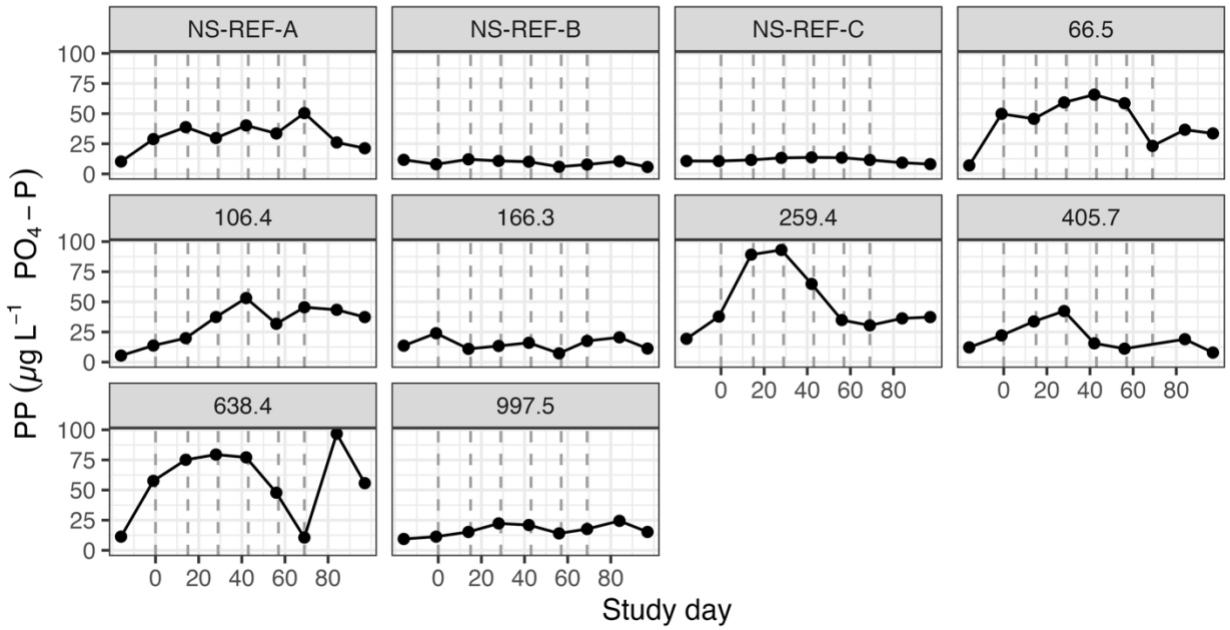

Figure A - 24. Particulate phosphorus (PP) in NS mesocosm water. Graphical panels indicate total phosphorus loadings (as mg m^{-2}). Vertical dashed lines indicate aquaculture wastewater additions.

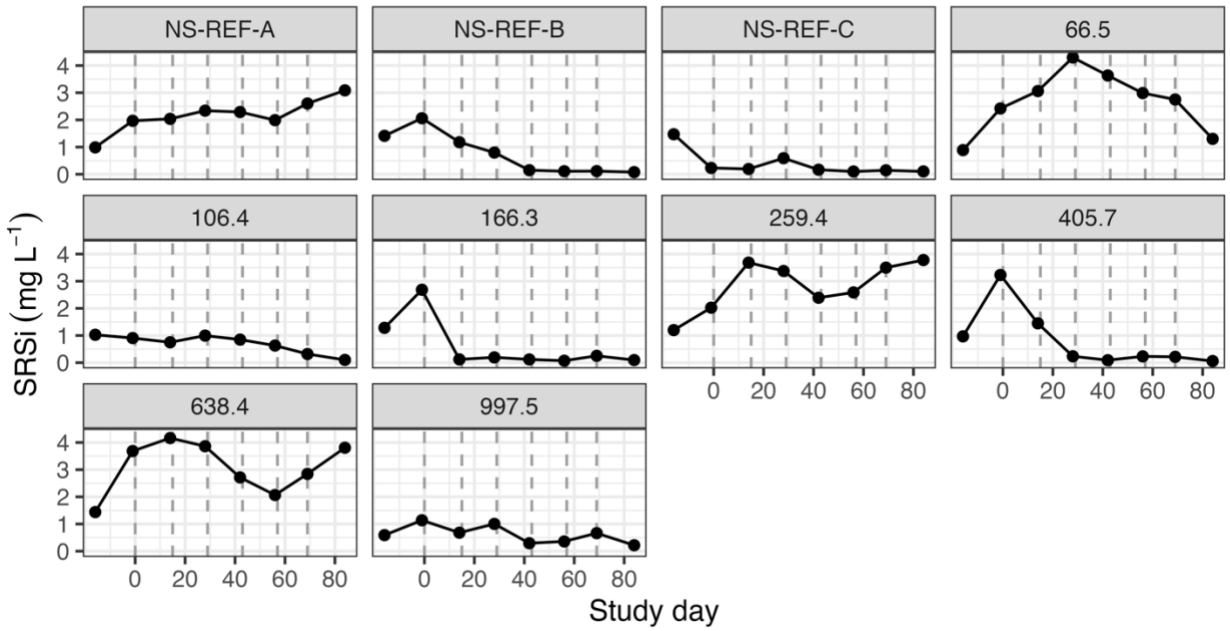

Figure A - 25. Soluble reactive silica (SRSi) in NS mesocosm water. Graphical panels indicate total phosphorus loadings (as mg m^{-2}). Vertical dashed lines indicate aquaculture wastewater additions.

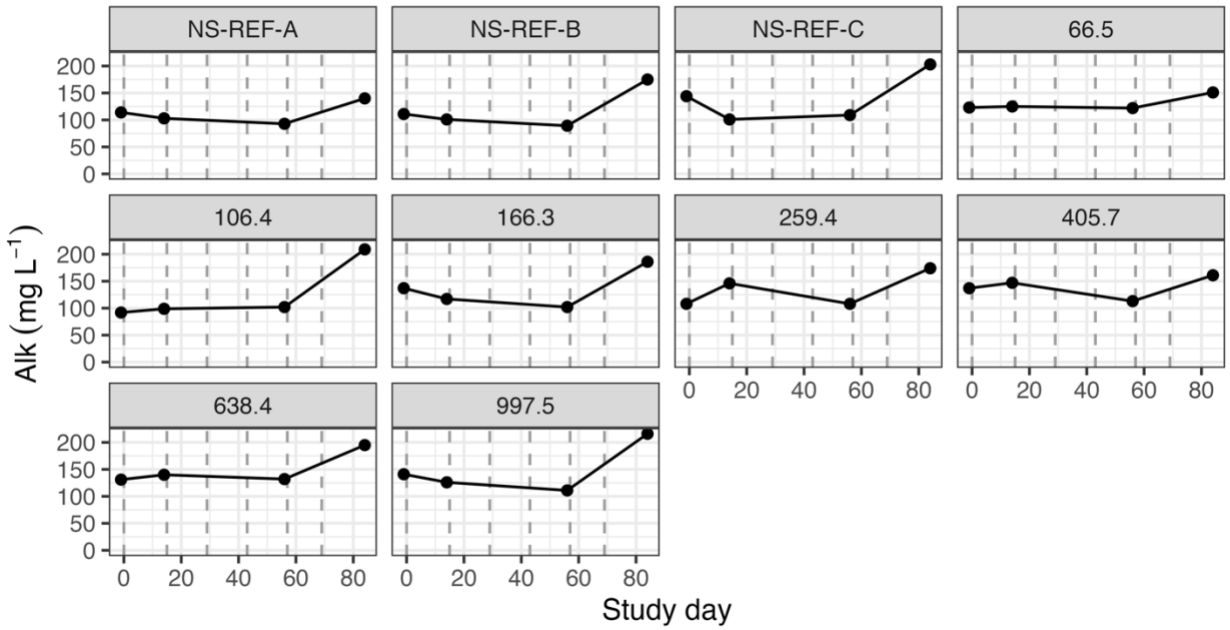

Figure A - 26. Total alkalinity (Alk) in NS mesocosm water. Graphical panels indicate total phosphorus loadings (as mg m^{-2}). Vertical dashed lines indicate aquaculture wastewater additions.

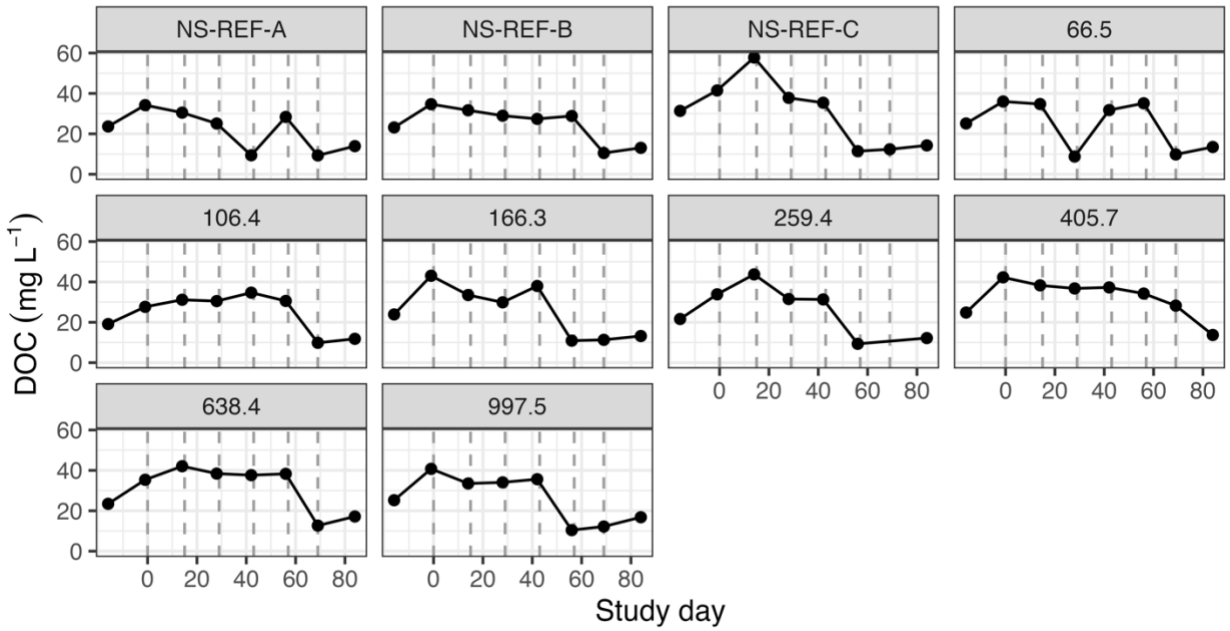

Figure A - 27. Dissolved organic carbon (DOC) in NS mesocosm water. Graphical panels indicate total phosphorus loadings (as mg m^{-2}). Vertical dashed lines indicate aquaculture wastewater additions.

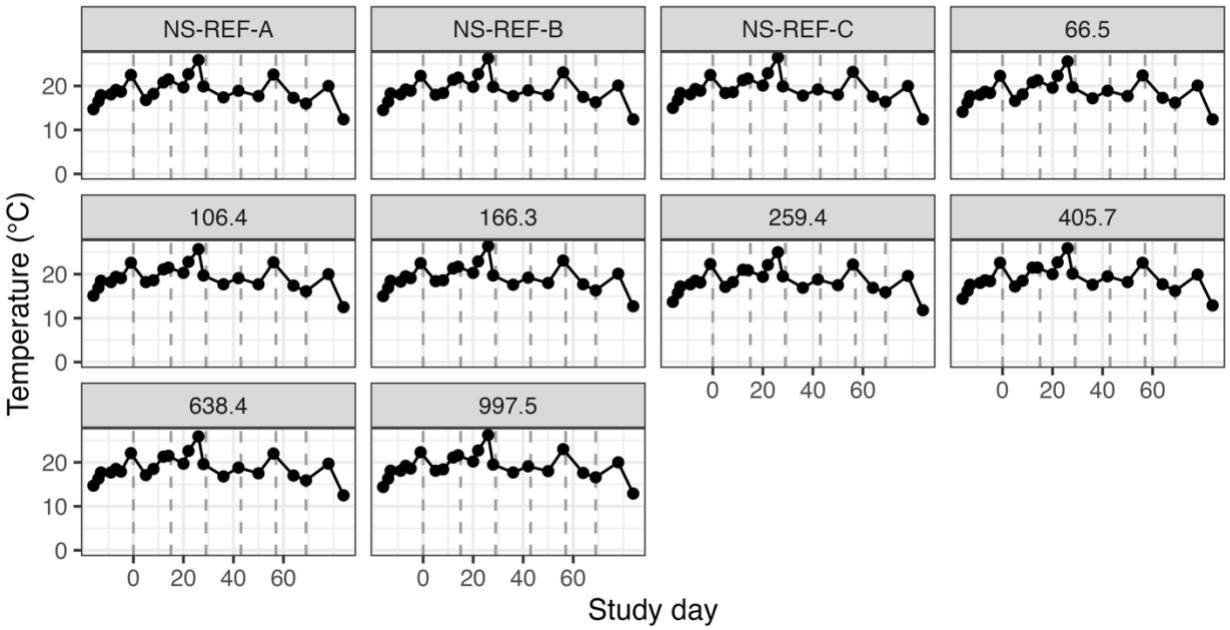

Figure A - 28. Temperature in NS mesocosm water. Graphical panels indicate total phosphorus loadings (as mg m^{-2}). Vertical dashed lines indicate aquaculture wastewater additions.

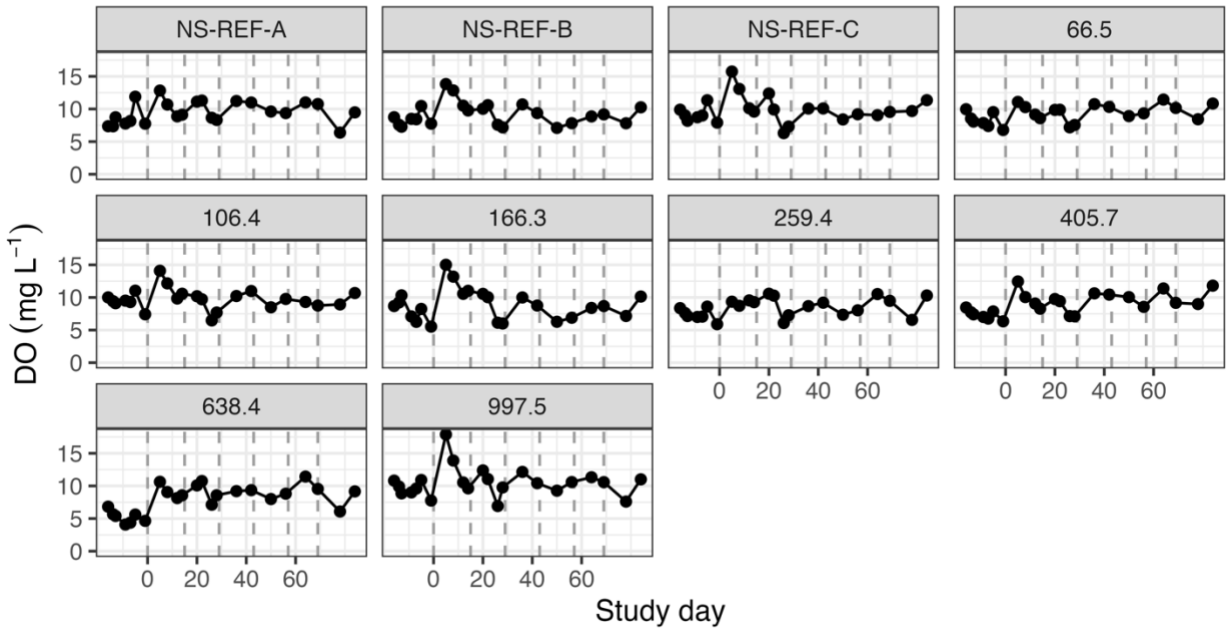

Figure A - 29. Dissolved oxygen (DO) in NS mesocosm water. Graphical panels indicate total phosphorus loadings (as mg m^{-2}). Vertical dashed lines indicate aquaculture wastewater additions.

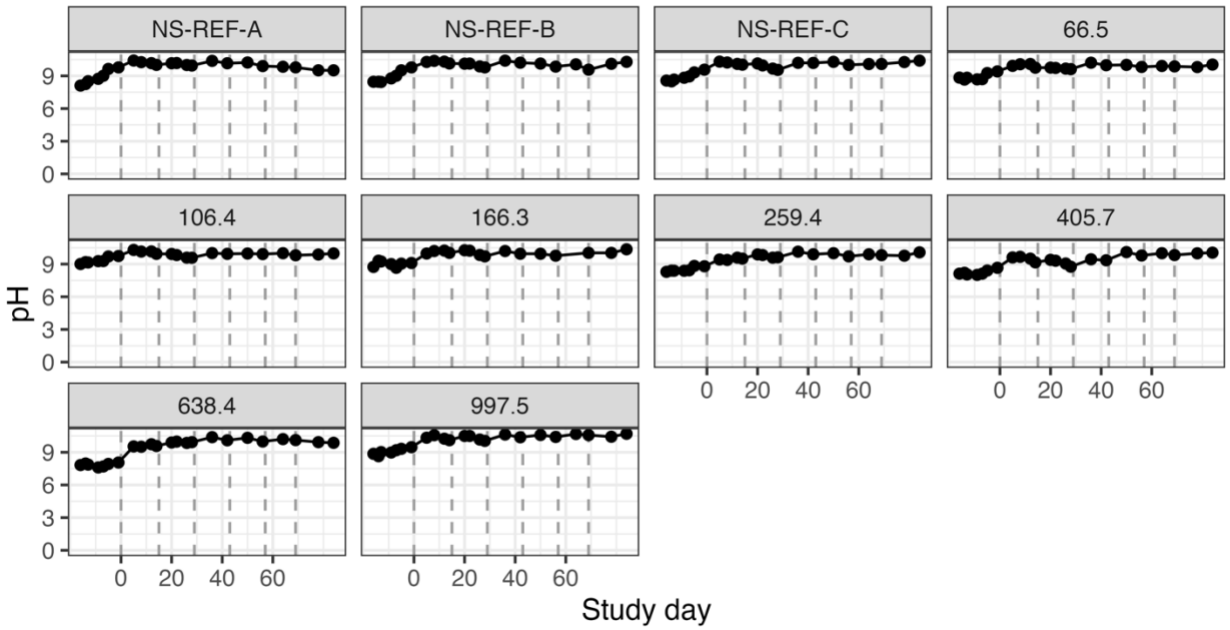

Figure A - 30. pH in NS mesocosm water. Graphical panels indicate total phosphorus loadings (as mg m^{-2}). Vertical dashed lines indicate aquaculture wastewater additions.

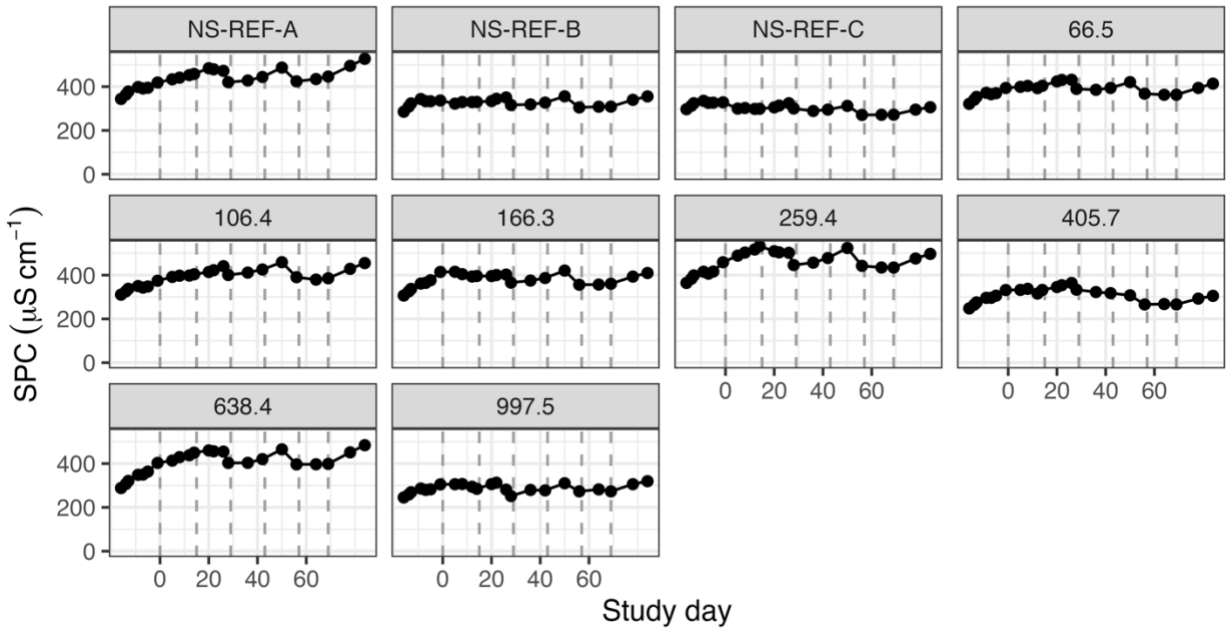

Figure A - 31. Specific conductance (SPC) in NS mesocosm water. Graphical panels indicate total phosphorus loadings (as mg m^{-2}). Vertical dashed lines indicate aquaculture wastewater additions.

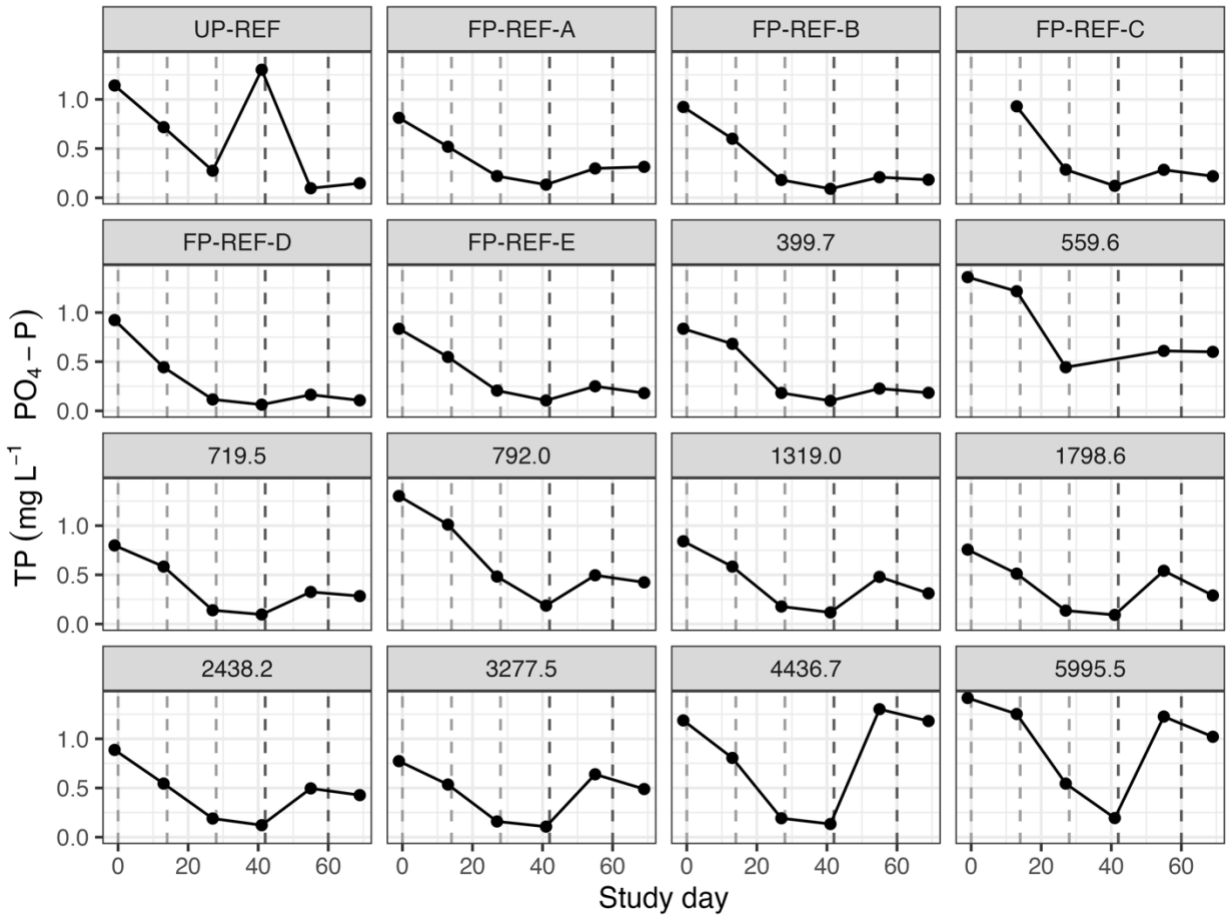

Figure A - 32. Total phosphorus (TP) in FP mesocosm water. Graphical panels indicate total phosphorus loadings (as mg m^{-2}). Vertical dashed lines indicate aquaculture wastewater (AWW) additions. The final two AWW addition events (dark dashed lines) were made with a different AWW source and twice the nominal volume of the first three addition events (light dashed lines).

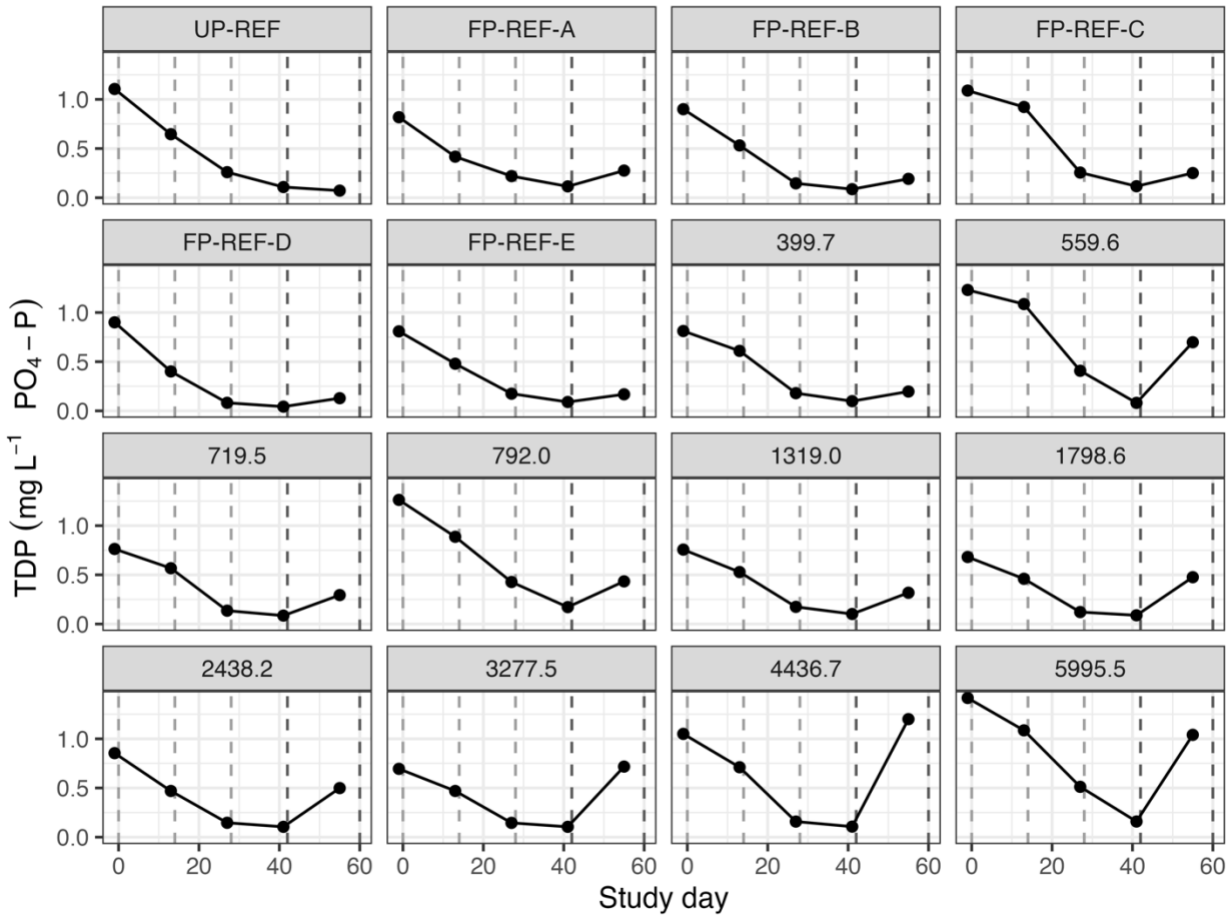

Figure A - 33. Total dissolved phosphorus (TDP) in FP mesocosm water. Graphical panels indicate total phosphorus loadings (as mg m^{-2}). Vertical dashed lines indicate aquaculture wastewater (AWW) additions. The final two AWW addition events (dark dashed lines) were made with a different AWW source and twice the nominal volume of the first three addition events (light dashed lines).

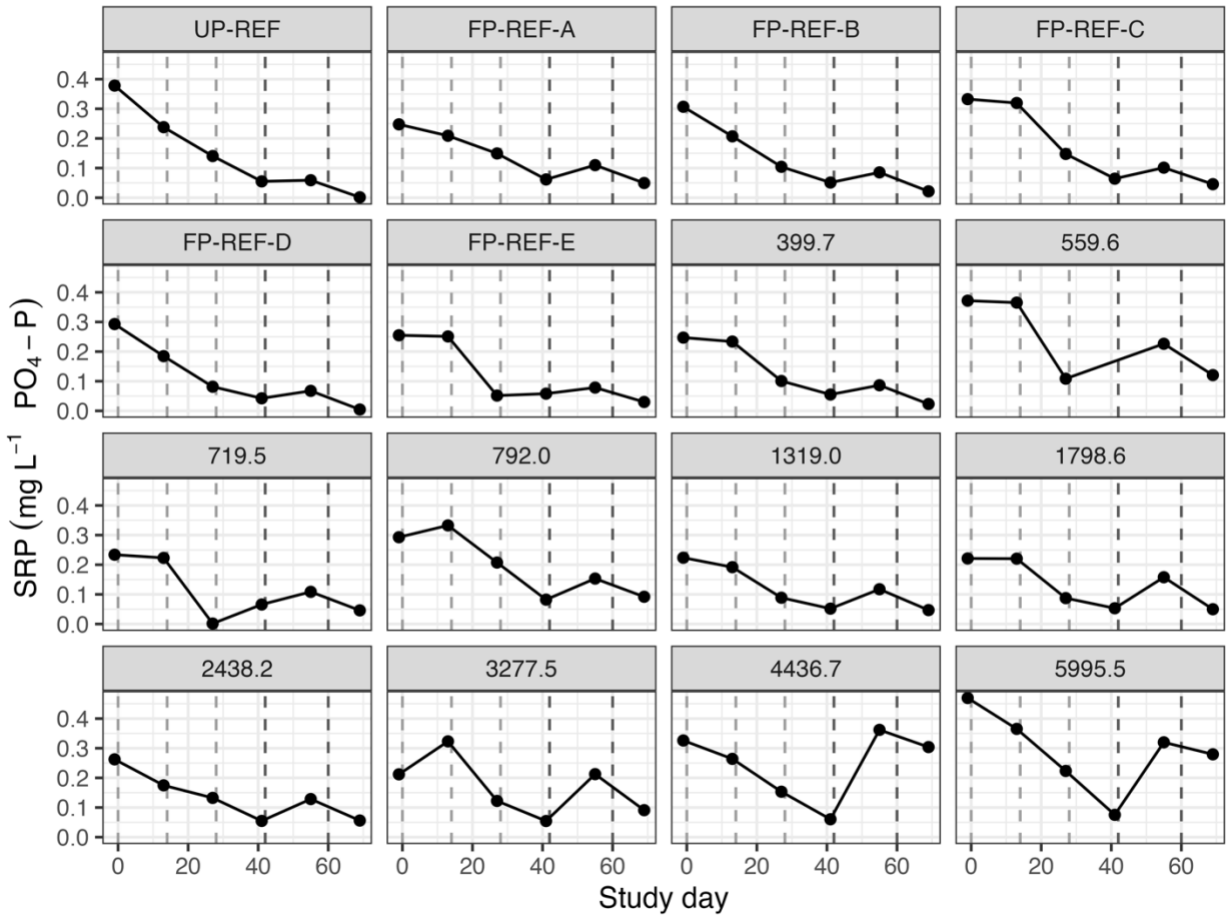

Figure A - 34. Soluble reactive phosphorus (SRP) in FP mesocosm water. Graphical panels indicate total phosphorus loadings (as mg m^{-2}). Vertical dashed lines indicate aquaculture wastewater (AWW) additions. The final two AWW addition events (dark dashed lines) were made with a different AWW source and twice the nominal volume of the first three addition events (light dashed lines).

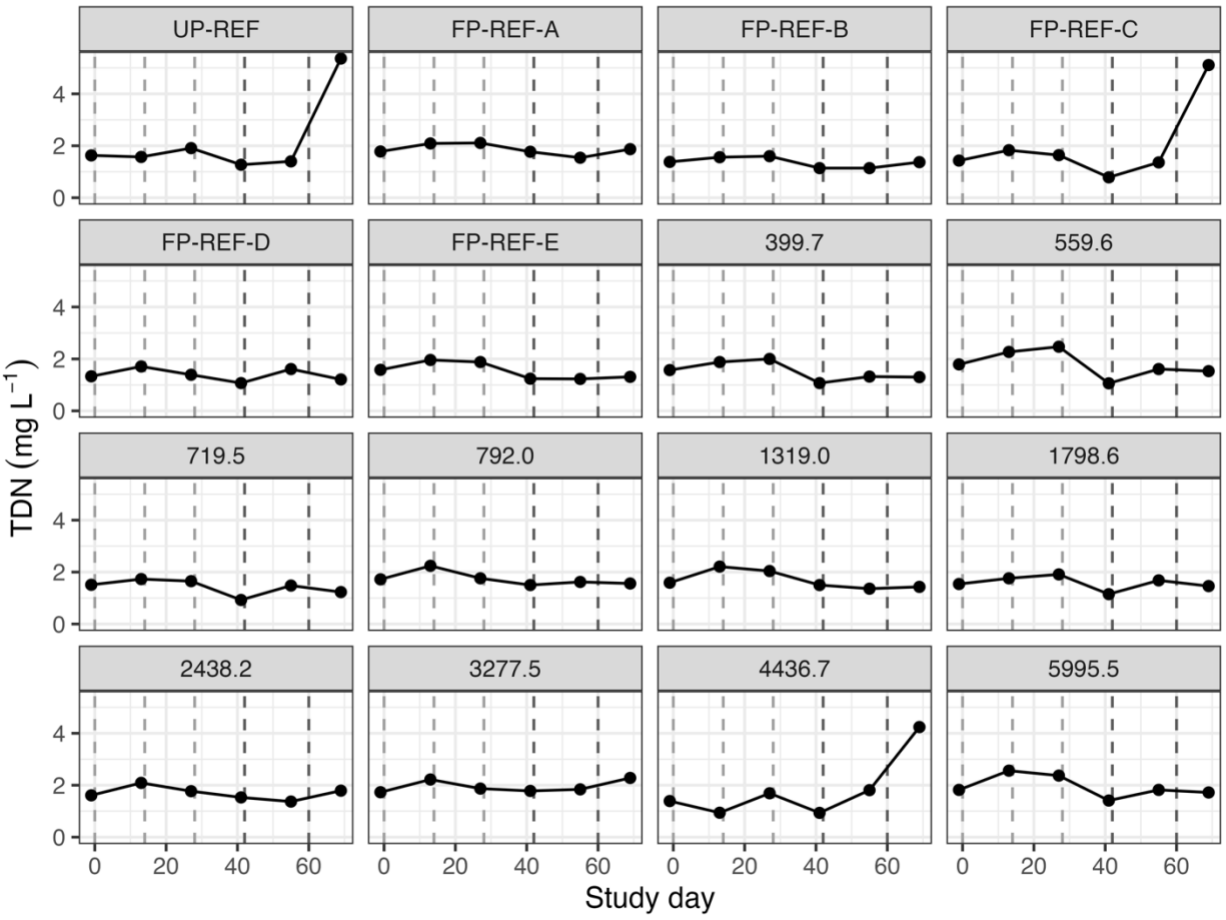

Figure A - 35. Total dissolved nitrogen (TDN) in FP mesocosm water. Graphical panels indicate total phosphorus loadings (as mg m^{-2}). Vertical dashed lines indicate aquaculture wastewater (AWW) additions. The final two AWW addition events (dark dashed lines) were made with a different AWW source and twice the nominal volume of the first three addition events (light dashed lines).

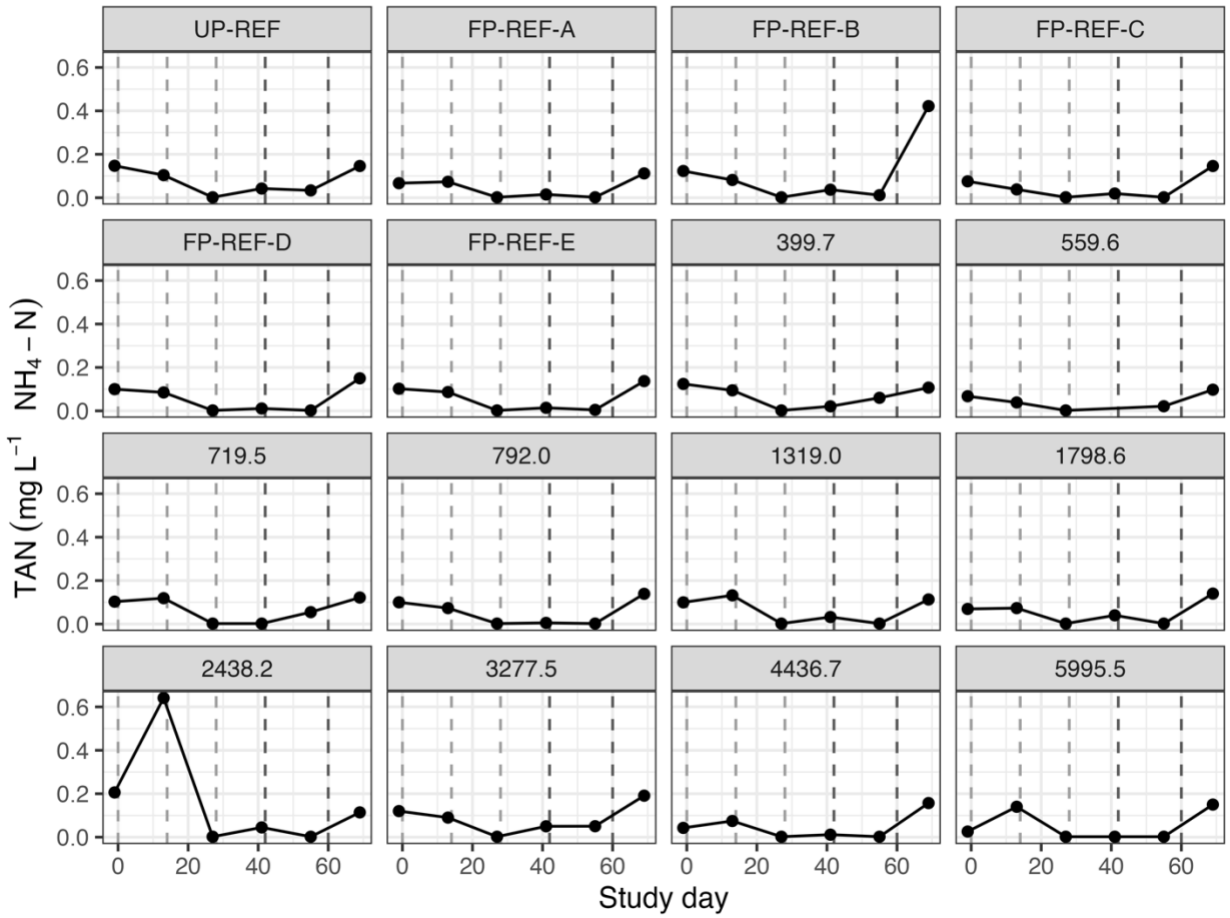

Figure A - 36. Total ammonia nitrogen (TAN) in FP mesocosm water. Graphical panels indicate total phosphorus loadings (as mg m^{-2}). Vertical dashed lines indicate aquaculture wastewater (AWW) additions. The final two AWW addition events (dark dashed lines) were made with a different AWW source and twice the nominal volume of the first three addition events (light dashed lines).

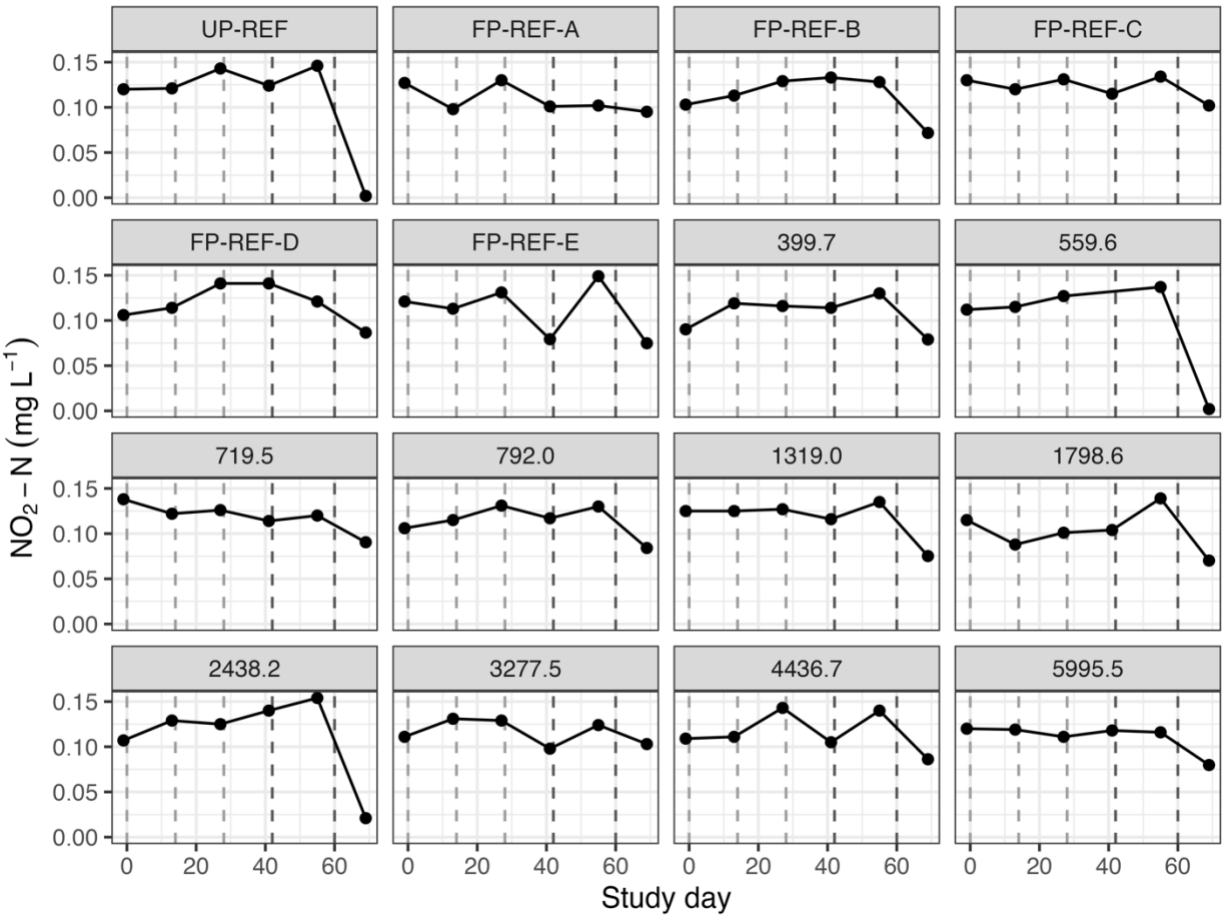

Figure A - 37. Nitrite nitrogen (NO_2–N) in FP mesocosm water. Graphical panels indicate total phosphorus loadings (as mg m^{-2}). Vertical dashed lines indicate aquaculture wastewater (AWW) additions. The final two AWW addition events (dark dashed lines) were made with a different AWW source and twice the nominal volume of the first three addition events (light dashed lines).

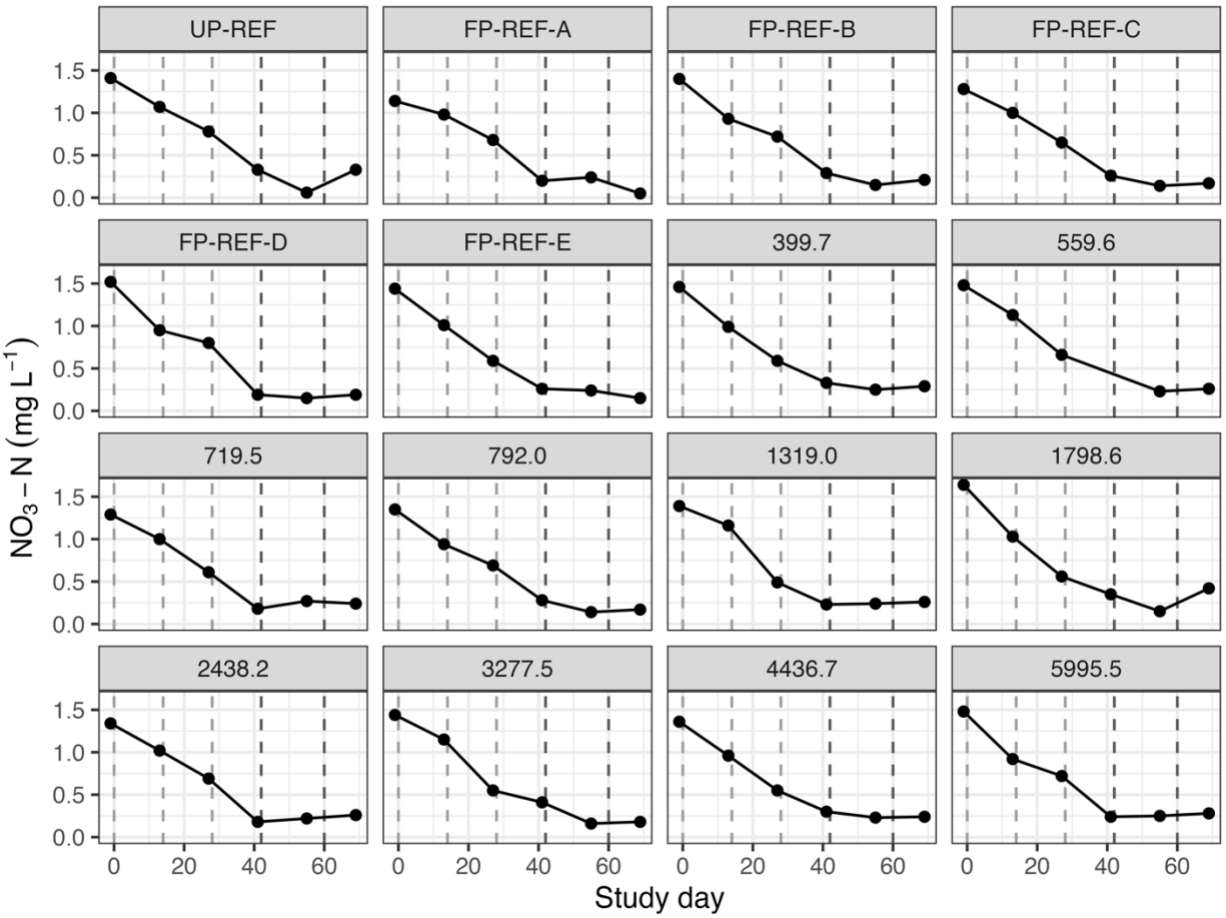

Figure A - 38. Nitrate nitrogen (NO_3–N) in FP mesocosm water. Graphical panels indicate total phosphorus loadings (as mg m^{-2}). Vertical dashed lines indicate aquaculture wastewater (AWW) additions. The final two AWW addition events (dark dashed lines) were made with a different AWW source and twice the nominal volume of the first three addition events (light dashed lines).

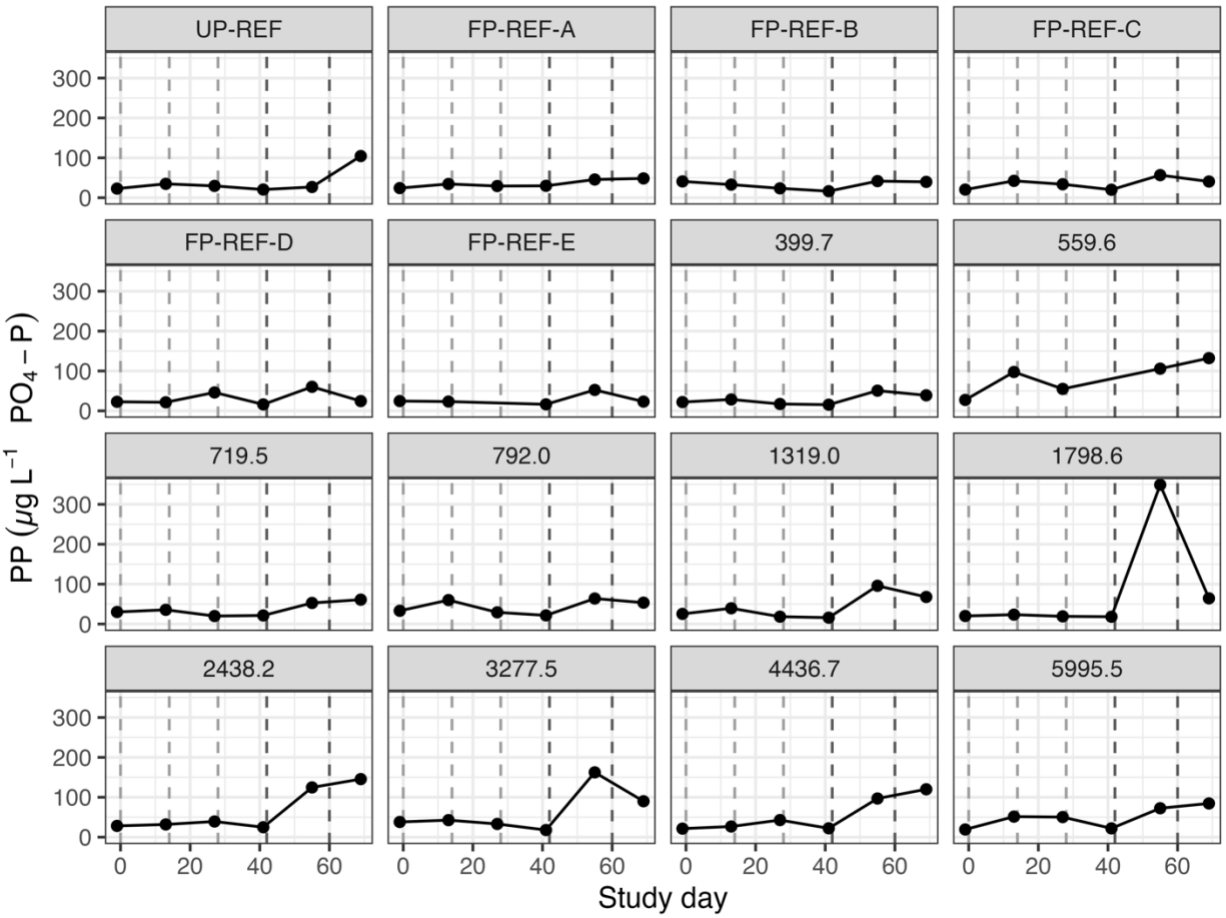

Figure A - 39. Particulate phosphorus (PP) in FP mesocosm water. Graphical panels indicate total phosphorus loadings (as mg m^{-2}). Vertical dashed lines indicate aquaculture wastewater (AWW) additions. The final two AWW addition events (dark dashed lines) were made with a different AWW source and twice the nominal volume of the first three addition events (light dashed lines).

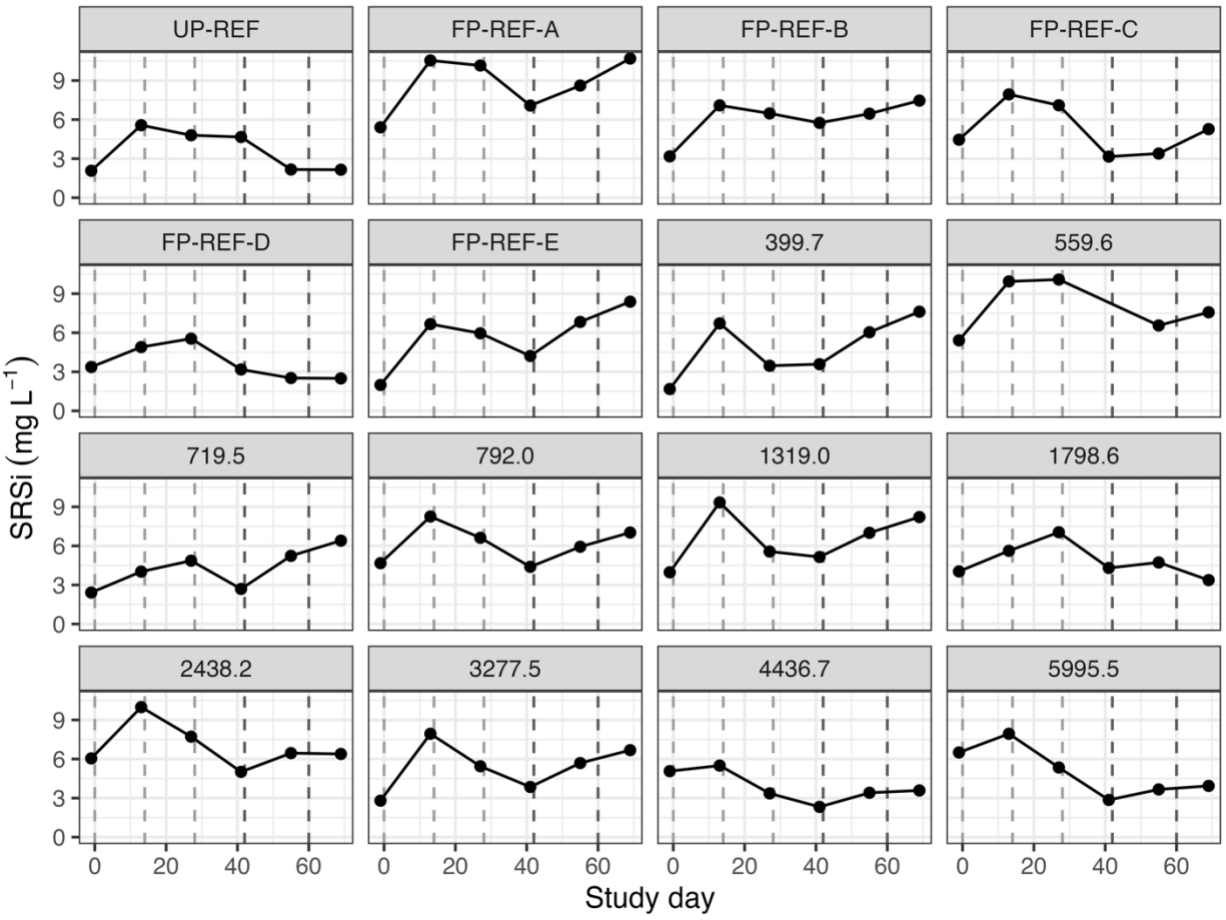

Figure A - 40. Soluble reactive silica (SRSi) in FP mesocosm water. Graphical panels indicate total phosphorus loadings (as mg m^{-2}). Vertical dashed lines indicate aquaculture wastewater (AWW) additions. The final two AWW addition events (dark dashed lines) were made with a different AWW source and twice the nominal volume of the first three addition events (light dashed lines).

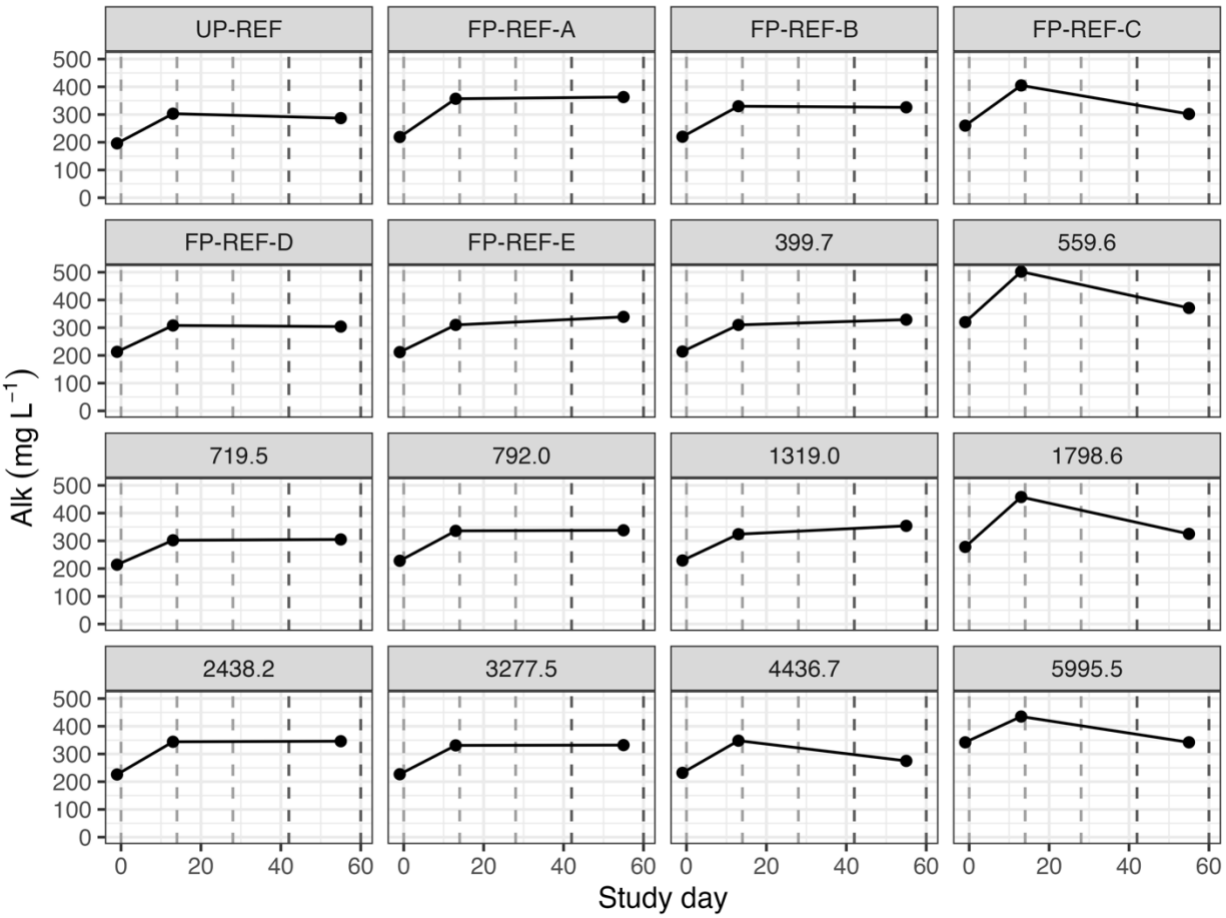

Figure A - 41. Total alkalinity (Alk) in FP mesocosm water. Graphical panels indicate total phosphorus loadings (as mg m^{-2}). Vertical dashed lines indicate aquaculture wastewater (AWW) additions. The final two AWW addition events (dark dashed lines) were made with a different AWW source and twice the nominal volume of the first three addition events (light dashed lines).

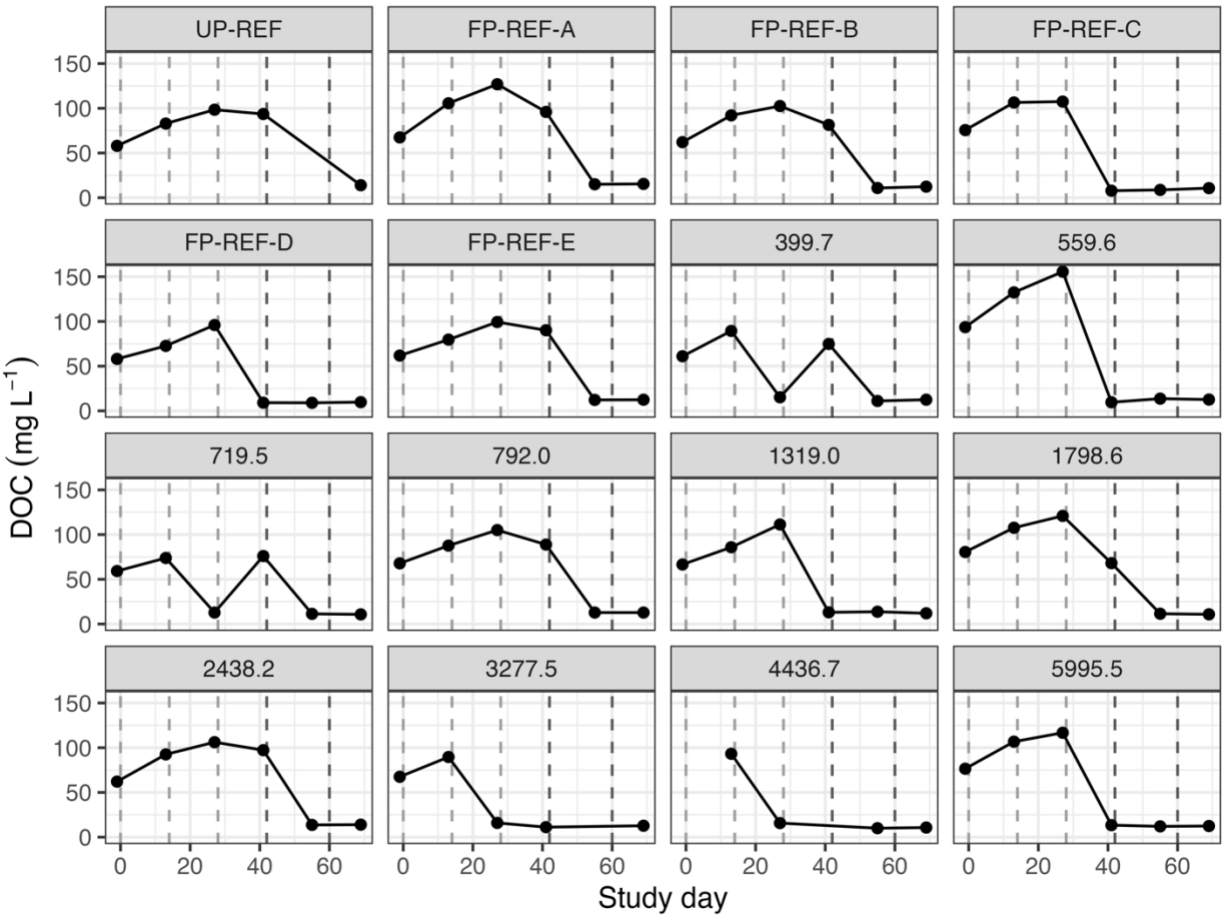

Figure A - 42. Dissolved organic carbon (DOC) in FP mesocosm water. Graphical panels indicate total phosphorus loadings (as mg m^{-2}). Vertical dashed lines indicate aquaculture wastewater (AWW) additions. The final two AWW addition events (dark dashed lines) were made with a different AWW source and twice the nominal volume of the first three addition events (light dashed lines).

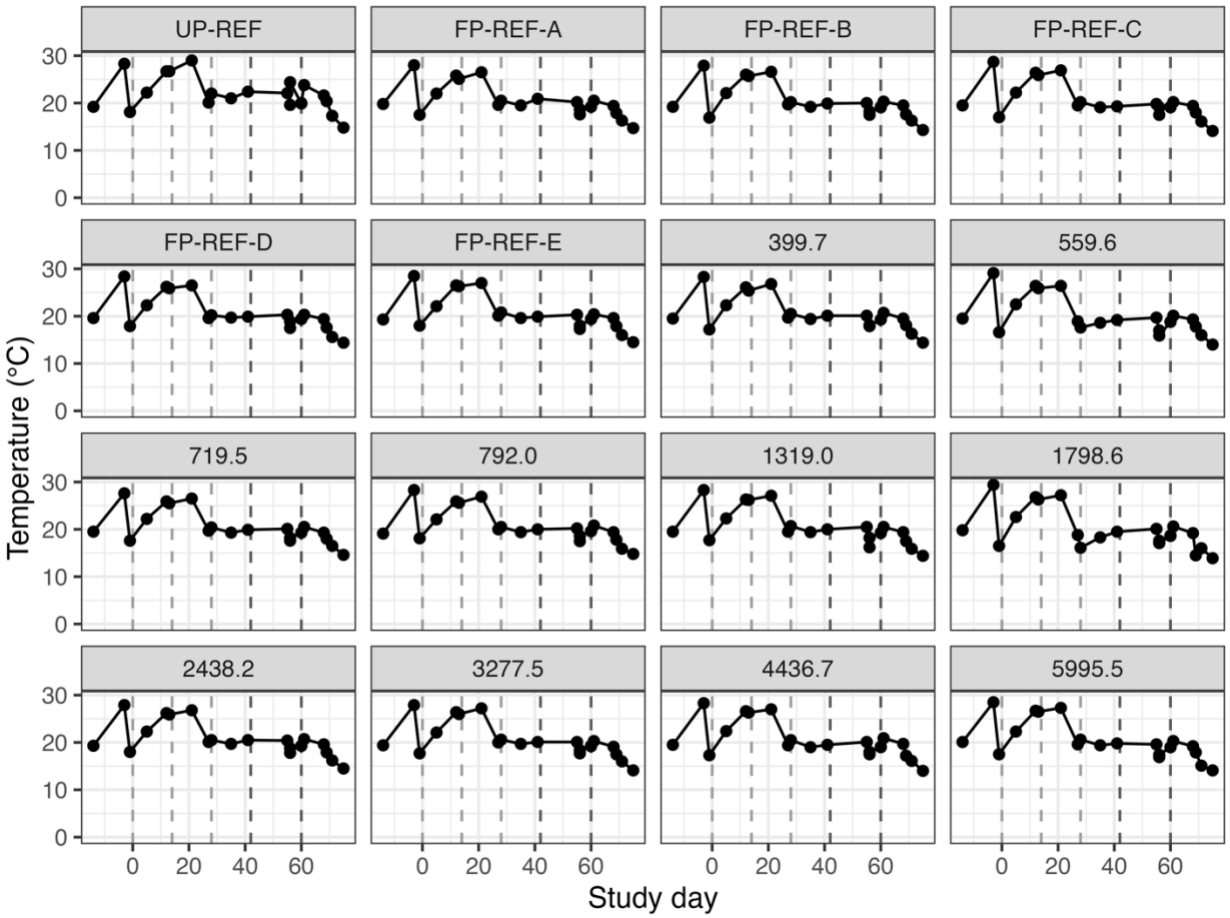

Figure A - 43. Temperature in FP mesocosm water. Graphical panels indicate total phosphorus loadings (as mg m^{-2}). Vertical dashed lines indicate aquaculture wastewater (AWW) additions. The final two AWW addition events (dark dashed lines) were made with a different AWW source and twice the nominal volume of the first three addition events (light dashed lines).

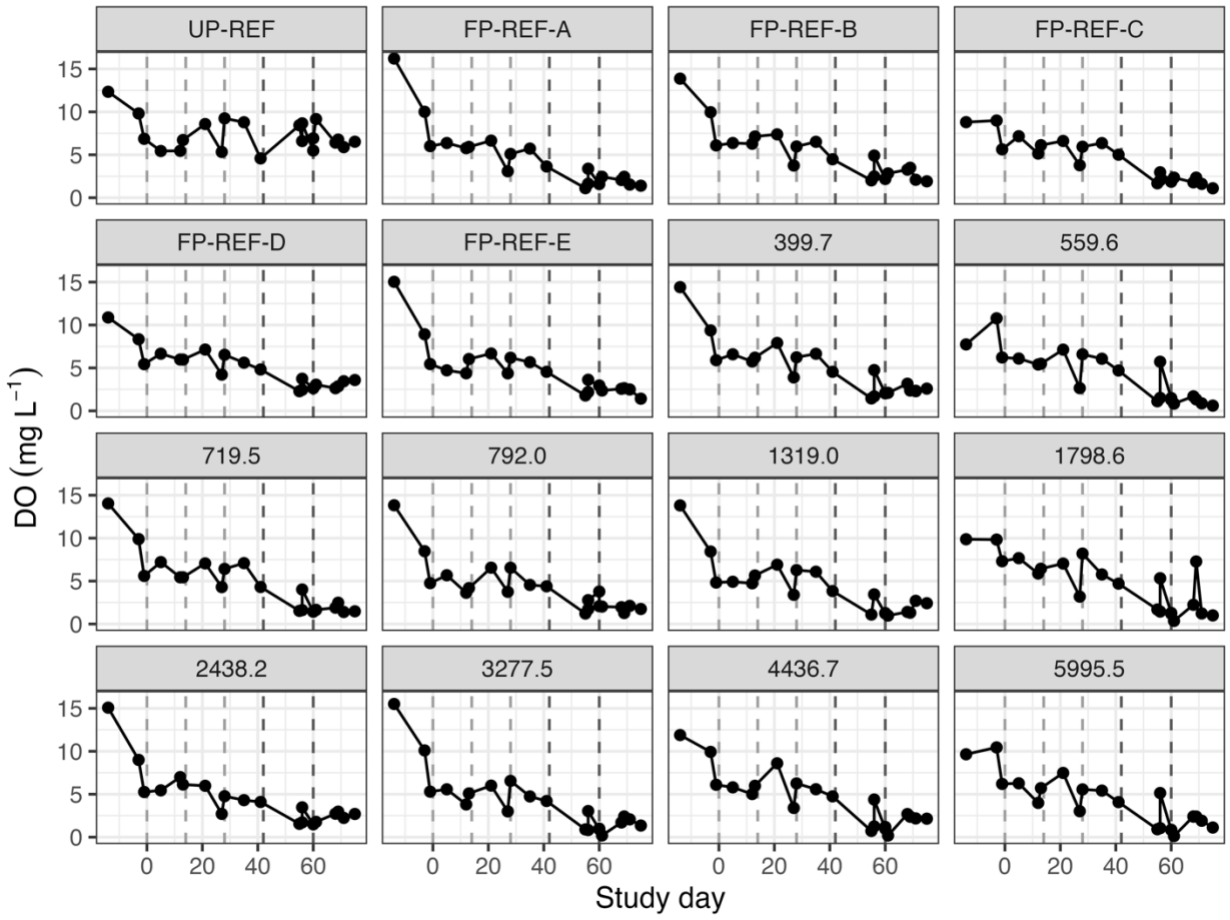

Figure A - 44. Dissolved oxygen (DO) in FP mesocosm water. Graphical panels indicate total phosphorus loadings (as mg m^{-2}). Vertical dashed lines indicate aquaculture wastewater (AWW) additions. The final two AWW addition events (dark dashed lines) were made with a different AWW source and twice the nominal volume of the first three addition events (light dashed lines).

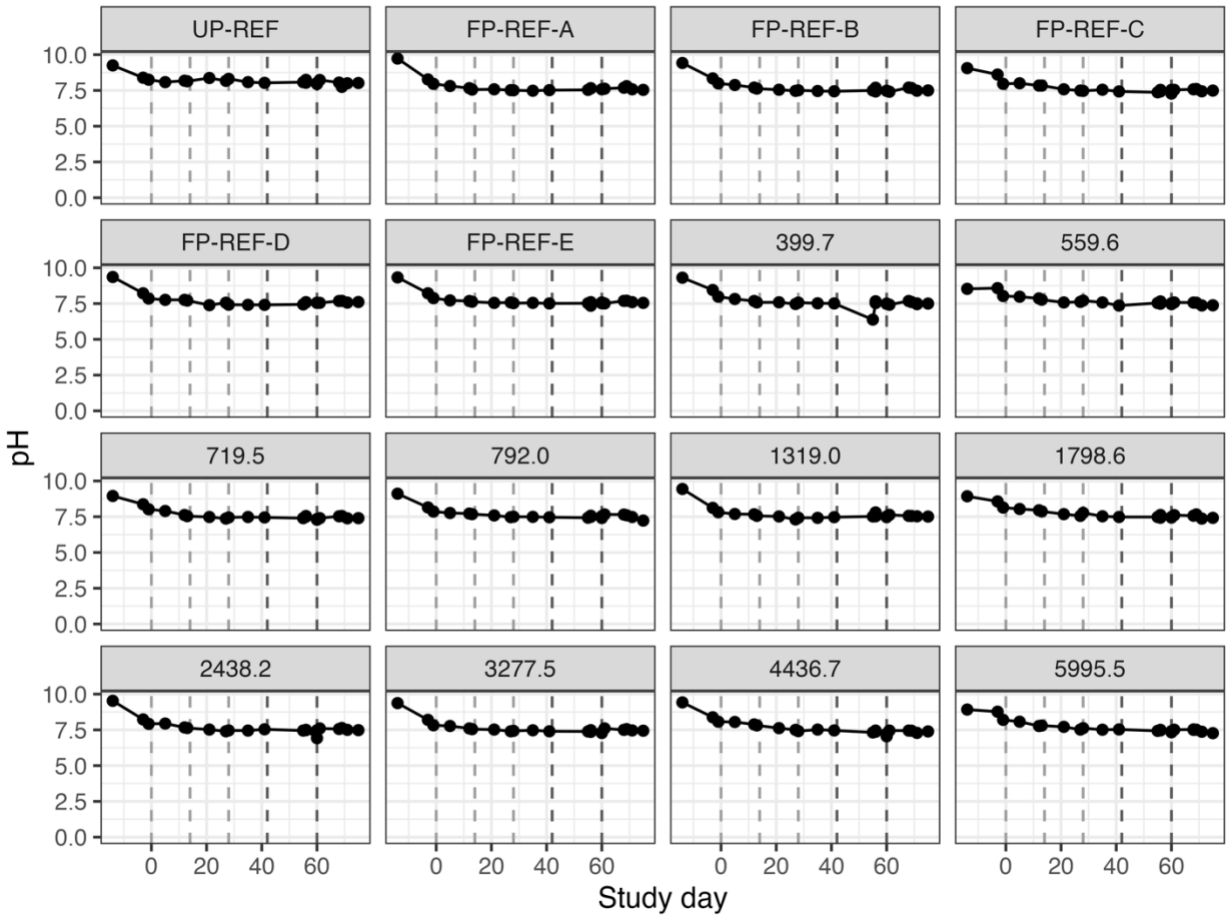

Figure A - 45. pH in FP mesocosm water. Graphical panels indicate total phosphorus loadings (as mg m^{-2}). Vertical dashed lines indicate aquaculture wastewater (AWW) additions. The final two AWW addition events (dark dashed lines) were made with a different AWW source and twice the nominal volume of the first three addition events (light dashed lines).

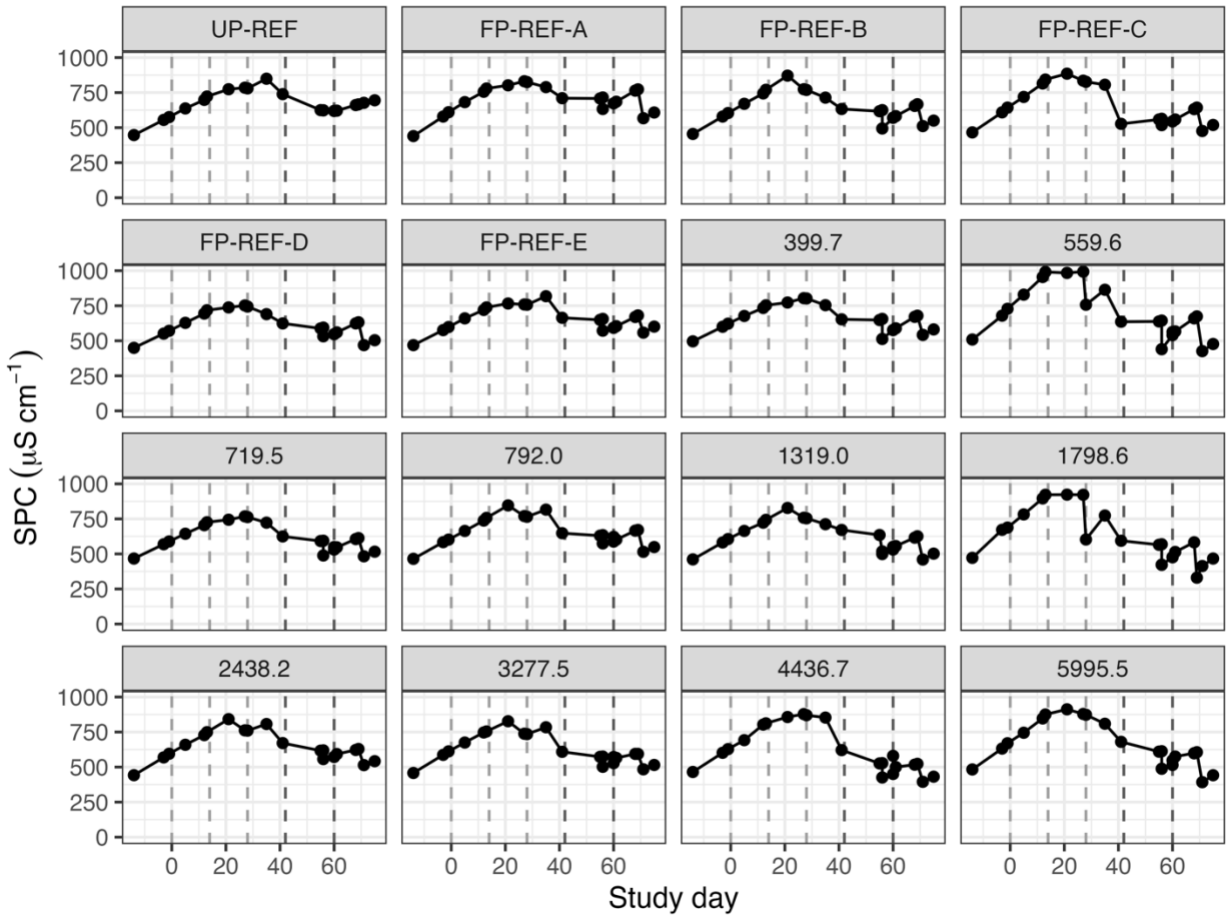

Figure A - 46. Specific conductance (SPC) in FP mesocosm water. Graphical panels indicate total phosphorus loadings (as mg m^{-2}). Vertical dashed lines indicate aquaculture wastewater (AWW) additions. The final two AWW addition events (dark dashed lines) were made with a different AWW source and twice the nominal volume of the first three addition events (light dashed lines).